

**FATE AND EFFECT OF QUATERNARY AMMONIUM
COMPOUNDS IN BIOLOGICAL SYSTEMS**

A Dissertation
Presented to
The Academic Faculty

by

Ulas Tezel

In Partial Fulfillment
of the Requirements for the Degree
Doctor of Philosophy in the
School of Civil and Environmental Engineering

Georgia Institute of Technology
May 2009

Copyright © 2009 by Ulas Tezel

**FATE AND EFFECT OF QUATERNARY AMMONIUM
COMPOUNDS IN BIOLOGICAL SYSTEMS**

Approved by:

Dr. Spyros G. Pavlostathis, Advisor
School of Civil and Environmental
Engineering
Georgia Institute of Technology

Dr. Patricia A. Sobecky
School of Biology
Georgia Institute of Technology

Dr. Ching-Hua Huang
School of Civil and Environmental
Engineering
Georgia Institute of Technology

Dr. Jim C. Spain
School of Civil and Environmental
Engineering
Georgia Institute of Technology

Dr. Joseph B. Hughes
School of Civil and Environmental
Engineering
Georgia Institute of Technology

Date Approved: January 5, 2009

ACKNOWLEDGEMENTS

I would like to thank my academic advisor, Dr. Spyros G. Pavlostathis, for his support and encouragement. His guidance and suggestions made this study and the time I spent in his lab a valuable learning experience for me. He treated me as a “partner” and trusted me truly, which made my voyage in his ship adventures, exciting and productive.

I would also like to express my gratitude to my committee members, Dr. Ching-Hua Huang, Dr., Joe Hughes, Dr. Patricia Sobecky and Dr. Jim Spain, for their review of the study and valuable recommendations. In particular, I would like to thank Dr. Sobecky for providing me the opportunity to work in her lab for the molecular biology experiments that I performed during my research.

I would like to thank the undergraduate students, Tram Dinh, Gretell Otano, Ainsley Cartwright, Andrew deRussy and Hamilton Giles, for helping me in various parts of my research. I deeply thank my colleagues, Dr. Rob Martinez and Dr. Madan Tandukar for their guidance and involvement in molecular biology experiments performed in this research. I also thank Dr. Zainab Ismail for her contribution to this study.

I would like to thank all the faculty and staff within the Environmental Engineering Program at the Georgia Institute of Technology. In particular, I am indebted to Dr. Guangxuan Zhu for lending me his expertise and support in instrumental analyses and to John Pierson for introducing me to sanitizers and leading the way to connect the outcomes of my study to real-life applications.

I would like to thank my friends, all past and present students of Dr. Pavlostathis' research group. In particular, I would like to give my special thanks to Jeongwoo Yang for his friendship during the late night lab performances.

I would like to express my gratitude to Dr. Goksel Demirer, Dr. Sibel Uludag-Demirer, Dr. Engin Guven and Dr. Tuba Erguder who made me start to walk on this road.

I am grateful to my family, Zuhail, Mehmet, Ceren Tezel, and Burcak Kaynak for all their true love and support.

I would like to acknowledge the Georgia Institute of Technology Library which I believe is a well-organized and extensive resource of information at Tech.

Finally, the State of Georgia/Food Processing Advisory Council (FoodPAC) is acknowledged for the partial financial support of this research.

TABLE OF CONTENTS

	Page
ACKNOWLEDGEMENTS	iii
LIST OF TABLES	xii
LIST OF FIGURES	xiv
SUMMARY	xxiii
CHAPTER 1. INTRODUCTION	1
CHAPTER 2. BACKGROUND	7
2.1. Quaternary Ammonium Compounds (QACs)	7
2.2. Applications and Implications of QACs	10
2.2.1. Demand and Consumption of QACs	10
2.2.2. Distribution of QACs in the Environment	15
2.2.3. Toxicity and Inhibitory Effects of QACs in Biological Systems	18
2.2.4. QAC Related Antimicrobial Resistance Mechanisms as a Challenge to Human Health	24
2.3. Biotransformation of QACs	32
2.3.1. Aerobic Biotransformation	32
2.3.2. Anaerobic Biotransformation	38

CHAPTER 3. MATERIALS AND METHODS	45
3.1. General Analytical Methods	45
3.1.1. pH	45
3.1.2. Oxidation-Reduction Potential (ORP)	45
3.1.3. Ammonia	45
3.1.4. Total and Soluble Chemical Oxygen Demand (tCOD and sCOD)	46
3.1.5. Dissolved Organic Carbon (DOC)	46
3.1.6. Total and Volatile Solids (TS and VS)	47
3.1.7. Total and Volatile Suspended Solids (TSS and VSS)	47
3.1.8. Total Gas Production	48
3.1.9. Gas Composition	48
3.1.10. Volatile Fatty Acids (VFAs)	49
3.1.11. Organic Acids, Alcohols and Carbohydrates	49
3.1.12. Anions	50
3.2. Analyses of QACs and Related Compounds	52
3.2.1. Chemicals	52
3.2.2. Disulfine Blue Pair-Ion Extraction Method (DSB-PIX)	54
3.2.3. Extraction of QACs from Biological Media	55
3.2.4. High Performance Liquid Chromatography of QACs	56

3.2.5. Liquid Chromatography-Mass Spectrometry of QACs	59
3.3. General Procedures	62
3.3.1. Methanogenic Culture Media	62
3.3.2. Aerobic Culture Media	63
CHAPTER 4. QUANTITATIVE STRUCTURE-ACTIVITY RELATIONSHIPS FOR QACs	66
4.1. Introduction	66
4.2. Materials and Methods	68
4.2.1. Target Compounds	68
4.2.2. Critical Micelle Concentration (CMC) Analysis	68
4.2.3. 1-Octanol/Water Partitioning (K_{ow}) Analysis	70
4.2.4. Biosolids Partitioning Assays	71
4.2.5. Microtox® Toxicity Assays	75
4.3. Results and Discussion	76
4.3.1. Critical Micelle Concentration	76
4.3.1.1. Effect of Alkyl Chain Length on CMC	80
4.3.1.2. Effect of Counter-ions on CMC	91
4.3.2. Assessment of Biosolids Partitioning of QACs	95
4.3.3. Assessment of QAC Toxicity	105
4.4. Summary	115

CHAPTER 5. BIOTRANSFORMATION OF BENZALKONIUM CHLORIDE UNDER AEROBIC CONDITIONS	117
5.1. Introduction	117
5.2. Materials and Methods	119
5.2.1. BAC Enrichment Culture	119
5.2.2. Energetics Calculations	120
5.2.3. Batch Biotransformation Assay	121
5.2.4. Phylogenetic Analysis of the BAC Enrichment Culture	122
5.3. Results and Discussion	124
5.3.1. Energetics of QAC Biodegradation	124
5.3.2. Biotransformation Kinetics and Pathway of C ₁₄ BDMA-Cl	128
5.3.3. Bacteria Community Composition Based on 16S rDNA Sequence Analyses	136
5.4. Summary	141
CHAPTER 6. BIOTRANSFORMATION POTENTIAL OF QACs IN A MIXED METHANOGENIC CULTURE UNDER FERMENTATIVE/METHANOGENIC CONDITIONS	142
6.1. Introduction	142
6.2. Materials and Methods	144
6.2.1. Target Compounds	144
6.2.2. Mixed Methanogenic Culture	144

6.2.3. Batch Inhibition Assay	145
6.2.4. QAC Phase Distribution Test	146
6.2.5. Inhibition Assay Using an Anaerobic Fed-Batch Reactor	147
6.3. Results and Discussion	149
6.3.1. Effect of QACs on Mixed Methanogenic Culture – Serum Bottle Assay	149
6.3.2. Phase Distribution of QACs	160
6.3.3. Effect of QACs on Mixed Methanogenic Culture – Fed-Batch Reactor Assay	164
6.3.4. QAC Phase Distribution, Inhibition and Recalcitrance	167
6.4. Summary	168
CHAPTER 7. BIOTRANSFORMATION POTENTIAL OF DIDECYL DIMETHYL AMMONIUM CHLORIDE AND BENZALKONIUM CHLORIDE IN A MIXED METHANOGENIC CULTURE UNDER NITRATE REDUCING CONDITIONS	170
7.1. Introduction	170
7.2. Materials and Methods	171
7.2.1. Target Compounds	171
7.2.2. Mixed Methanogenic Culture	171
7.2.3. Batch Inhibition Assay	171
7.2.4. Batch BAC Transformation Assays	173

7.2.5. Electron Equivalents Calculations	174
7.3. Results and Discussion	175
7.3.1. Didecyl Dimethyl Ammonium Chloride (DC ₁₀ DMA-Cl)	175
7.3.1.1. Effect of DC ₁₀ DMA-Cl on Nitrate Reduction	175
7.3.1.2. Effect of DC ₁₀ DMA-Cl on Electron Flow	178
7.3.1.3. Phase Distribution of DC ₁₀ DMA-Cl	181
7.3.2. Benzalkonium Chloride (C _n BDMA-Cl)	181
7.3.2.1. Effect of C _n BDMA-Cl on Nitrate Reduction	181
7.3.2.2. Effect of C _n BDMA-Cl on Electron Flow	186
7.3.2.3. Phase Distribution of C _n BDMA-Cl	190
7.3.2.4. C _n BDMA-Cl Transformation	192
7.3.2.5. Mechanism of C _n BDMA-Cl Transformation	199
7.4. Summary	207
CHAPTER 8. BIOTRANSFORMATION OF BENZALKONIUM CHLORIDE	209
UNDER FERMENTATIVE AND NITRATE REDUCING	
CONDITIONS	
8.1. Introduction	209
8.2. Materials and Methods	210
8.2.1. Batch C ₁₄ BDMA-Cl Biotransformation Assay	210
8.3. Results and Discussion	211

8.4. Summary	221
CHAPTER 9. CONCLUSIONS AND RECOMMENDATIONS	222
9.1. Conclusions	222
9.2. Potential Applications of the Study Outcomes	225
9.3. Recommendations	227
APPENDIX A: CALCULATION OF LOG K_{ow} VALUES OF QACS USING THE HANSCH AND LEO METHOD	229
APPENDIX B: GIBB'S FREE FORMATION ENERGY OF QACS	238
REFERENCES	247
VITA	262

LIST OF TABLES

	Page
Table 2.1. Representative QAC groups, their general structure and abbreviations used in this study	8
Table 2.2. Biocidal activity of alkyl (C ₁₂₋₁₆)benzyl dimethyl and didecyl (C ₁₀)dimethyl ammonium chlorides	13
Table 2.3. Multidrug efflux determinants of QAC resistance	28
Table 3.1. Chemicals used in this study	53
Table 3.2. Ethyl acetate extraction efficiency for C ₁₂ BDMA-Cl, C ₁₄ BDMA-Cl and C ₁₆ BDMA-Cl from biological media containing 2.5 g VS/L	58
Table 3.3. LC/MS monitored ions of target analytes	62
Table 3.4. Composition of media for the mixed methanogenic culture used in this study	64
Table 3.5. Composition of media for the mixed aerobic culture used in this study	65
Table 4.1. Characteristics of undiluted sludge samples used in the adsorption isotherm	73
Table 4.2. Critical micelle concentrations of target QACs determined in this study and reported in the literature at 298 °K	78
Table 4.3. 1-Octanol/water partitioning coefficients of target QACs determined in this study and reported in the literature at 298 °K	86
Table 4.4. log K _{ow} contribution of fragments and bond factors used in the Hansch and Leo method	92
Table 4.5. Freundlich adsorption isotherm constants for QAC phase distribution in municipal primary and waste activated sludges, as well as mesophilic and thermophilic digested sludges	100
Table 4.6. Comparison of sorption affinities of monoalkonium and benzalkonium chlorides for different sludge sorbents	102

Table 4.7	Results of the Microtox® acute toxicity assay (5- and 15-min) of monoalkonium, dialkonium and benzalkonium chlorides	105
Table 5.1.	QAC half-reactions and their Gibb's free energy at pH 7 and 298°K	125
Table 5.2.	QAC oxidation reactions and their Gibb's free energy at pH 7 and 298 °K	126
Table 5.3.	Representative bacterial clones sequenced from 16S rDNA clone library of the BAC enrichment culture	140
Table 6.1.	Feeding protocol of the fed-batch reactor used to assess the long-term effect of Vigilquat® on a mixed methanogenic culture	148
Table 6.2.	COD utilization and products at the end of the incubation in mixed methanogenic culture amended with D/P and different initial C _n BDMA-Cl concentrations (10-100 mg/L)	154
Table 6.3.	COD utilization and products at the end of the incubation in mixed methanogenic culture amended with D/P and different initial DC ₁₀ DMA-Cl concentrations (10-100 mg/L)	155
Table 6.4.	COD utilization and products at the end of the incubation in mixed methanogenic culture amended with D/P and different initial DC ₈ DMA-Cl concentrations (10-100 mg/L)	156
Table 6.5.	COD utilization and products at the end of the incubation in mixed methanogenic culture amended with D/P and different initial DC ₈₋₁₀ DMA-Cl concentrations (10-100 mg/L)	157
Table 6.6.	Freundlich adsorption isotherm constants for QAC phase distribution in a mixed methanogenic culture	162
Table 7.1.	Electron equivalents balance in C _n BDMA-Cl -free and C _n BDMA-Cl -amended mixed methanogenic culture series	187
Table 8.1.	Experimental matrix of culture series and controls used in the batch C ₁₄ BDMA-Cl biotransformation assay	212

LIST OF FIGURES

		Page
Figure 1.1.	General molecular structure of a QAC (R represents a functional group, X ⁻ represents a counter ion such as Cl ⁻ , Br ⁻ , or NO ₃ ⁻)	1
Figure 2.1.	Synthesis pathway of alkylbenzyl dimethyl ammonium chloride	7
Figure 2.2.	Distribution of QAC use in the market	11
Figure 2.3.	Schematic representation of QAC fluxes and expected QAC concentration levels in different compartments of engineered and natural systems calculated based on the global QAC consumption	19
Figure 2.4.	Histogram of reported EC ₅₀ values for monoalkonium, dialkonium and benzalkonium chlorides for aquatic organisms. Data obtained from the European Center for Ecotoxicology and Toxicology of Chemicals (ECETOC) and the U.S. EPA Ecotoxicology (ECOTOX) databases using the OECD Application ToolBox	23
Figure 2.5.	General structure of a Class 1 integron and a gene cassette and the mechanism of antibiotic resistance gene insertion into a Class 1 integron	30
Figure 2.6.	Two biotransformation pathways observed for tetradecyl benzyl dimethyl ammonium chloride under aerobic conditions	34
Figure 2.7.	Pathways of (A) hexadecane and (B) hexadecyl trimethyl ammonium biotransformation in a mixed aerobic culture	36
Figure 2.8.	Scheme of fumarate addition to toluene by benzylsuccinate synthase (Bss)	41
Figure 2.9.	Biotransformation of toluene by the fumarate addition mechanism under anoxic/anaerobic conditions	42
Figure 2.10.	Predicted biotransformation pathway of C ₁₄ BDMA by the fumarate addition mechanism using UM-BBD-PPS (annotations in parentheses represent the UM-BBD-PPS rules applicable to the corresponding reaction)	44

Figure 3.1.	Sample LC chromatogram of organic acids	51
Figure 3.2.	Extent of interference by protonated amines on the disulfine blue ion-pair extraction method (DSB-PIX) measurements	56
Figure 3.3.	Mechanisms involved in QAC recovery from biological media by liquid/liquid extraction	57
Figure 3.4.	Sample HPLC chromatogram of benzalkonium chlorides (dodecylbenzyl dimethyl ammonium chloride (C ₁₂ BDMA-Cl), tetradecylbenzyl dimethyl ammonium chloride (C ₁₄ BDMA-Cl), hexadecylbenzyl dimethyl ammonium chloride (C ₁₆ BDMA-Cl)), benzyl amine (BA), benzyl methyl amine (BMA), benzyl dimethyl amine (BDMA) and benzyl trimethyl ammonium chloride (BTMA-Cl). The bromide peak is given as the reference for a non-retained analyte	60
Figure 3.5.	Applied mobile phase gradient (A) and sample LC-MS chromatograms of 10 μM monoalkonium (B), dialkonium (C), benzalkonium (D) chlorides and alkyl dimethyl amines (E)	61
Figure 4.1.	Distribution of BZA tautomers (A) and corresponding enolic tautomer absorbance at different QAC concentrations (0.08-8.3 mM in the cuvette) (B)	69
Figure 4.2.	Normalized total QAC mass recovered from both the 1-octanol and water phase at the end of the partitioning assay	72
Figure 4.3.	Measured CMC values of monoalkonium, dialkonium and benzalkonium chlorides	79
Figure 4.4.	The effect of the alkyl chain length (n) on the CMC of (A) monoalkonium, (B) dialkonium and (C) benzalkonium chlorides	81
Figure 4.5.	Change in CMC with respect to the alkyl chain length (n) (A) and comparison of the number of carbon atoms in the alkyl chain that satisfies the same CMC for monoalkonium, dialkonium and benzalkonium chlorides	83
Figure 4.6.	Effect of the alkyl chain length (n) on K _{ow} of (A) monoalkonium, (B) dialkonium and (C) benzalkonium chlorides	88

Figure 4.7.	(A) Residual and (B) graphical comparison between measured and predicted log K_{ow} values of monoalkonium, dialkonium and benzalkonium chlorides (the Meylan and Howard method was used to obtain predicted log K_{ow} values)	89
Figure 4.8.	(A) Residual and (B) graphical comparison between measured and predicted log K_{ow} values of monoalkonium, dialkonium and benzalkonium chlorides (the Hansch and Leo method was used to obtain predicted log K_{ow} values)	93
Figure 4.9.	Relationship between CMC and (A) calculated K_{ow} values using the Meylan and Howard method, (B) calculated K_{ow} values using the Hansch and Leo method and (C) measured K_{ow} (Dashed lines represent 95% confidence intervals)	94
Figure 4.10.	Effect of (A) Cl^- , (B) NO_2^- , (C) Br^- , (D) CH_3COO^- and (E) NO_3^- on the CMC of benzalkonium chloride at concentrations up to 50 mM (Dashed lines represent 95% confidence intervals)	96
Figure 4.11.	Effect of counter-ion electro-negativity expressed by its retention time on ion chromatography (IC) and size on the CMC of benzalkonium chloride	97
Figure 4.12.	Freundlich adsorption isotherms for $C_{12}TMA-Cl$, $C_{12}BDMA-Cl$, $C_{16}TMA-Cl$ and $C_{16}BDMA-Cl$ at equilibrium with (A) thermophilic digested sludge and (B) mesophilic digested sludge at 1 g VS/L	99
Figure 4.13.	Relationship between CMC and adsorption affinity of monoalkonium and benzalkonium chlorides on (A) PS, (B) WAS, (C) TDS and (D) MDS (Dashed lines represent 95% confidence intervals)	103
Figure 4.14.	Effect of the alkyl chain length (n) on the adsorption affinity of monoalkonium and benzalkonium chlorides on different sludge sorbents	104
Figure 4.15.	The 5-minute acute toxicity EC_{50} values of monoalkonium, dialkonium and benzalkonium chlorides to the bioluminescent marine microorganism <i>Vibrio fischeri</i> obtained using the Microtox® assay (Error bars represent 95% confidence intervals)	107
Figure 4.16.	The 15-minute acute toxicity EC_{50} values of monoalkonium, dialkonium and benzalkonium chlorides to the bioluminescent marine microorganism <i>Vibrio fischeri</i> obtained using the Microtox® assay (Error bars represent 95% confidence intervals)	108

Figure 4.17.	Relationship between the CMC and EC ₅₀ values of monoalkonium, dialkonium and benzalkonium chlorides at (A) 5-minute, (B) 15-minute and (C) 1-day exposure time (Error bars represent 95% confidence intervals)	109
Figure 4.18.	The effect of 342 mM Br ⁻ , CH ₃ COO ⁻ and NO ₃ ⁻ on the toxicity of (1) C ₁₂ BDMA-Cl, (2) C ₁₄ BDMA-Cl and (3) C ₁₆ BDMA-Cl for (A) 5-minute and (B) 15-minute exposure times (Error bars represent 95% confidence intervals)	112
Figure 4.19.	The effect of NOM at different concentrations (10-100 mg/L) on the toxicity of (1) C ₁₂ BDMA-Cl, (2) C ₁₄ BDMA-Cl and (3) C ₁₆ BDMA-Cl for (A) 5-minute and (B) 15-minute exposure time (Error bars represent 95% confidence intervals)	113
Figure 4.20.	Relationship between NOM concentration and EC ₅₀ of (1) C ₁₂ BDMA-Cl, (2) C ₁₄ BDMA-Cl and (3) C ₁₆ BDMA-Cl for a (A) 5-minute and (B) 15-minute exposure time (Error bars represent 95% confidence intervals)	114
Figure 5.1.	Schematic showing the positions of CO ₂ /QAC and O ₂ /H ₂ O redox couples on the electron tower and the standard free energy upon complete oxidation of QACs to CO ₂ under oxic conditions (QACs represent monoalkonium, dialkonium and benzalkonium chlorides which have average half-reaction free energy equal to 28.9 ± 3.5 kJ/eeq)	127
Figure 5.2.	Time course of C ₁₄ BDMA-Cl transformation and formation and consumption of BDMA in the BAC enrichment culture amended with C ₁₄ BDMA-Cl	129
Figure 5.3.	Time course of C ₁₄ TMA-Cl transformation in the BAC enrichment culture amended with C ₁₄ TMA-Cl for the first time	129
Figure 5.4.	Time course of BTMA-Cl in the BAC enrichment culture amended with BTMA-Cl for the first time	130
Figure 5.5.	Time course of C ₁₄ BDMA-Cl transformation and formation and consumption of BDMA in a dilute BAC enrichment culture amended with C ₁₄ BDMA-Cl	130
Figure 5.6.	Time course of (A) BDMA, (B) BMA and (C) BA transformation in the BAC enrichment culture amended with BDMA, BMA and BA for the first time	131

Figure 5.7.	Time course of (A) C ₁₄ BDMA-Cl, (B) BDMA, (C) BMA and (D) BA biotransformation in BAC enrichment culture and simulation of sequential C ₁₄ BDMA-Cl, BDMA and BMA transformation as proposed by Patrauchan et al. (2003) (symbols represent the experimental data whereas lines represent model simulations)	133
Figure 5.8.	Time course and model simulations of C ₁₄ TMA-Cl transformation in the BAC enrichment culture	134
Figure 5.9.	Proposed pathway of C ₁₄ BTMA-Cl biotransformation by the BAC enrichment culture	136
Figure 5.10.	Rarefaction curve determined for different RFLP patterns of Bacteria 16S rDNA clones obtained from the BAC enrichment culture	137
Figure 5.11	Phylogenetic tree of relationships of 16S rDNA clone sequences, as determined by distance Jukes-Cantor analysis, from BAC enrichment culture to selected cultured isolates and environmental clones. Bootstrap values represent 5000 replicates and only values greater than 50% are reported. The scale bar represents 0.05 substitutions per nucleotide position. <i>Methanosarcina barkeri</i> was used as the out group	139
Figure 6.1	Schematic showing the positions of CO ₂ /QAC and CO ₂ /methane redox couples on the electron tower and the standard free energy upon complete oxidation of QACs to CO ₂ under methanogenic conditions (QACs represent monoalkonium, dialkonium and benzalkonium chlorides which have average half-reaction free energy equal to 28.9 ± 3.5 kJ/eeq)	143
Figure 6.2	Methane (A) and carbon dioxide (B) production profiles during the batch inhibition assay with Vigilquat® at different concentrations (0-100 mg/L)	150
Figure 6.3	Methane (A) and carbon dioxide (B) production profiles during the batch inhibition assay with (1) C _n BDMA-Cl, (2) DC ₁₀ DMA-Cl, (3) DC ₈ DMA-Cl, and (4) DC ₈₋₁₀ DMA-Cl at different concentrations (0-100 mg/L)	151
Figure 6.4	COD conversion profiles relative to the reference series during the batch inhibition assay with (A) Vigilquat®, (B) C _n BDMA-Cl, (C) DC ₁₀ DMA-Cl, (D) DC ₈ DMA-Cl, and (E) DC ₈₋₁₀ DMA-Cl at different concentrations (0-100 mg/L)	152

Figure 6.5	Phase distribution of Vigilquat®, C _n BDMA-Cl, DC ₁₀ DMA-Cl, DC ₈ DMA-Cl, and DC ₈₋₁₀ DMA-Cl in the mixed methanogenic culture (Error bars represent one standard deviation of the means; hollow and filled symbols represent total and liquid phase QAC concentrations, respectively)	161
Figure 6.6	Freundlich adsorption isotherms for Vigilquat®, C _n BDMA-Cl, DC ₁₀ DMA-Cl, DC ₈ DMA-Cl, and DC ₈₋₁₀ DMA-Cl at equilibrium (Error bars represents one standard deviation of the means; solid lines are model predictions)	163
Figure 6.7	Gas production (A), VFA (B) and VQ (C) profiles in the fed-batch reactor	165
Figure 7.1.	Schematic showing the positions of CO ₂ /QAC and NO ₃ ⁻ /N ₂ redox couples on the electron tower and the standard free energy upon complete oxidation of QACs to CO ₂ under nitrate reducing conditions (QACs represent monoalkonium, dialkonium and benzalkonium chlorides which have average half-reaction free energy equal to 28.9 ± 3.5 kJ/eeq)	172
Figure 7.2.	Production and consumption profiles of N oxides and N ₂ in mixed methanogenic culture series amended with 750 mg/L glucose and 70 mg nitrate-N/L (5 mmol N/L) at (A) 0 (nitrate reference), (B) 10, (C) 25, (D) 50, (E) 75, and (F) 100 mg/L DC ₁₀ DMA-Cl during 100 days of incubation (Error bars represent one standard deviation of the means; <i>n</i> = 3).	176
Figure 7.3.	Distribution of nitrogen species at the end of the incubation period in mixed methanogenic culture series amended with 750 mg/L glucose, 70 mg nitrate-N/L (5 mmol N/L) and different DC ₁₀ DMA-Cl concentrations (0-100 mg/L) (Error bars represent one standard deviation of the means; <i>n</i> = 3).	177
Figure 7.4.	Profiles of (A) methane production in glucose and nitrate reference cultures and 10 mg DC ₁₀ DMA-Cl amended culture and (B) VFAs production and consumption in the mixed methanogenic cultures amended with 750 mg/L glucose and 70 mg nitrate-N/L at different DC ₁₀ DMA-Cl concentrations (0-100 mg/L) (Error bars represent one standard deviation of the means).	180
Figure 7.5.	Phase distribution of DC ₁₀ DMA-Cl in mixed methanogenic culture series amended with DC ₁₀ DMA-Cl at different concentrations (0-100 mg/L) at the end of the incubation (Error bars represent one standard deviation of the means; <i>n</i> = 3).	182

Figure 7.6.	Production and consumption profiles of N oxides and N ₂ in mixed methanogenic culture series amended with 750 mg/L glucose and 70 mg nitrate-N/L (5 mmol N/L) at (A) 0 (nitrate reference), (B) 10, (C) 25, (D) 50, (E) 75, and (F) 100 mg/L C _n BDMA-Cl during 100 days of incubation (Error bars represent one standard deviation of the means; <i>n</i> = 3).	183
Figure 7.7.	Distribution of nitrogen species at the end of the incubation period in mixed methanogenic culture series amended with 750 mg/L glucose, 70 mg nitrate-N/L (5 mmol N/L) and different C _n BDMA-Cl concentrations (0-100 mg/L) (Error bars represent one standard deviation of the means; <i>n</i> = 3)	185
Figure 7.8.	Profiles of (A) methane production in glucose and nitrate reference cultures and the cultures amended with 10 and 25 mg C _n BDMA-Cl, and (B) VFAs production and consumption in the mixed methanogenic cultures amended with 750 mg/L glucose and 70 mg nitrate-N/L at different C _n BDMA-Cl concentrations (0-100 mg/L) (Error bars represent one standard deviation of the means)	189
Figure 7.9.	Phase distribution of C _n BDMA-Cl in mixed methanogenic culture series amended with C _n BDMA-Cl at different concentrations (0-100 mg/L) at the end of the incubation (Error bars represent one standard deviation of the means; <i>n</i> = 3)	191
Figure 7.10.	Concentrations of (A) C _n BDMA-Cl and (B) nitrogen species at the end of 100 days incubation, cycle 1 and cycle 2 (<i>See text</i> ; Error bars represent one standard deviation of the means; <i>n</i> = 3)	193
Figure 7.11.	(A) Profiles of C _n BDMA-Cl consumption and N ₂ O formation during the incubation period and (B) distribution of C _n BDMA-Cl homologues and alkyl dimethyl amines at the first and last day of incubation in a mixed methanogenic culture amended with 750 mg/L glucose and 70 mg nitrate-N/L (5 mmol N/L) at 100 mg C _n BDMA-Cl/L (Error bars represent one standard deviation of the means; <i>n</i> = 6)	195
Figure 7.12.	Profiles of (A) C _n BDMA-Cl in all test culture series and N oxides consumption and production in culture series amended with 100 mg/L C _n BDMA-Cl and 5 mmol N/L of (B) NO ₃ ⁻ , (C) NO ₂ ⁻ and (D) NO, respectively (Error bars represent one standard deviation of the means; <i>n</i> = 3)	197

Figure 7.13.	Profiles of (A) C _n BDMA-Cl in all abiotic controls and N oxides consumption and production in abiotic controls amended with 100 mg/L C _n BDMA-Cl and 5 mmol N/L of (B) NO ₃ ⁻ , (C) NO ₂ ⁻ and (D) NO, respectively (Error bars represent one standard deviation of the means; <i>n</i> = 3).	198
Figure 7.14.	Profiles of (A) C _n BDMA-Cl homologues and formation of alkyl dimethyl amines and mass spectra of total ion chromatograms of samples taken from the abiotic control amended with 5 mmol N/L of NO ₂ ⁻ and 100 mg/L BAC after (B) 1 day and (C) 42 days of incubation	200
Figure 7.15.	Reaction scheme of nucleophilic elimination and substitution reactions involving C _n BDMA-Cl	202
Figure 7.16.	Proposed C _n BDMA-Cl transformation mechanism	203
Figure 7.17.	Gas chromatogram and total mass spectrum of the compound detected in the samples in which BAC was transformed, and identified as benzonitrile	203
Figure 7.18.	Electrostatic potential charges of the atoms of C ₁₄ BDMA-Cl and DC ₁₀ DMA-Cl calculated by using Austin Model 1 (AM1) method of MOPAC, a semi-empirical molecular orbital estimation program. Closed shell (restricted) was used as the wave function and water was selected as the solvent. The size of the atoms represent the magnitude where as color indicates the sign of the charges (red (+) and blue (-))	206
Figure 8.1.	Profile of C ₁₄ BDMA-Cl in autoclaved culture media over the incubation period	212
Figure 8.2.	(A) Time course of fumarate metabolism and (B) distribution of organic acids in the fumarate-only culture at the beginning and the end of the incubation period	214
Figure 8.3.	Fumarate disproportionation pathway described previously by Zaunmuller et al. (2006)	215
Figure 8.4.	Time course of (A) nitrate reduction, (B) fumarate fermentation and (C) C ₁₄ BDMA transformation in the fumarate-control culture before (Cycle-1) and after (Cycle-2) nitrate (5 mM) addition	216
Figure 8.5.	Proposed mechanism of fumarate addition to C ₁₄ BDMA	217

Figure 8.6.	Profile of C ₁₄ BDMA in the C ₁₄ BDMA-control culture	217
Figure 8.7.	Profiles of (A) nitrate and (B) C ₁₄ BDMA in the nitrate-control culture	218
Figure 8.8.	Time course of (A) nitrate reduction, (B) fumarate fermentation and (C) C ₁₄ BDMA transformation in the test culture at three nitrate amendment cycles	219
Figure 8.9.	HPLC chromatograms showing the time course of C ₁₄ BDMA transformation in the BAC enrichment culture under nitrate reducing conditions	220

SUMMARY

Quaternary ammonium compounds (QACs) are organic molecules that are extensively used in domestic, agricultural, healthcare, and industrial applications as surfactants, emulsifiers, fabric softeners, disinfectants, pesticides, corrosion inhibitors, and personal care products. As a result, QACs are ubiquitous contaminants found worldwide in both engineered and natural systems. QACs are toxic to aquatic organisms and cause co-selection for antibiotic resistance, thus providing a reservoir of antibiotic-resistant bacteria, as well as antibiotic resistance genes in QAC-polluted environments. The objectives of the research presented here were to: a) systematically assess the fate and toxicity of QACs using quantitative structure-activity relationships (QSAR); b) evaluate the biotransformation potential of QACs under aerobic, anoxic and anaerobic conditions; and c) assess the potential toxicity of QACs biotransformation products. Nine QACs, belonging to three homologous groups -- monoalkonium, dialkonium and benzalkonium chlorides -- were the target QACs. The QACs critical micelle concentration (CMC) was determined. Then, the CMC was used as a descriptor to derive relationships between QAC structure and partitioning to biosolids as well as acute Microtox® toxicity. QACs with low CMCs had a relatively high adsorption affinity for biosolids and a lower toxicity than QACs with higher CMCs, which suggests that QACs that are more mobile and more (bio)available are more toxic. The biotransformation potential of benzalkonium chlorides (BAC) -- the most commonly used QACs found in engineered and natural biological systems -- under aerobic, methanogenic, nitrate reducing, and fermentative conditions was evaluated using bioenergetics and batch

bioassays. The aerobic BAC biotransformation involved sequential dealkylation and debenzylation steps resulting in the formation of benzyl dimethyl amine, and dimethyl amine, respectively. The bacterial community involved in the aerobic BAC degradation was mainly composed of species belonging to the *Pseudomonas* genus. All QACs tested were recalcitrant under methanogenic conditions and inhibited methanogenesis at and above 25 mg QAC/L. Under nitrate reducing and fermentative conditions, BAC was transformed to alkyldimethyl amines via an abiotic reaction known as *modified Hofmann degradation* and a biotic reaction known as *fumarate addition*, respectively. Both reactions are based on a mechanism known as *nucleophilic substitution*. The discovery of BAC transformation by the above mentioned two reactions is the first ever report to document QAC transformation under anoxic/anaerobic conditions and delineate the transformation pathway. This research contributes to a better understanding of the environmental and human health risks associated with QACs by providing systematic information on physical, chemical and biological processes that determine the fate and effect of QACs in engineered and natural systems.

CHAPTER 1

INTRODUCTION

Quaternary ammonium compounds (QACs) are organic compounds that contain four functional groups attached covalently to a central nitrogen atom (R_4N^+). These functional groups (R) include at least one long chain alkyl group and the rest are either methyl or benzyl groups. QACs are among the High Production Volume Chemicals (HPVs, i.e., chemicals manufactured in or imported in amounts equal to or greater than one million pounds per year) found on the lists of both the U.S. Environmental Protection Agency (U.S. EPA) and the Organization for Economic Co-operation and Development (OECD). QACs are extensively used in domestic, agricultural, healthcare and industrial applications as surfactants, emulsifiers, fabric softeners, disinfectants, pesticides, corrosion inhibitors and personal care products (Garcia et al., 1999; Steichen, 2001; Patrauchan and Oriel, 2003). The 2004 world-wide annual consumption of QACs was reported as 500,000 tons (CESIO, 2004) and was expected to reach or exceed 700,000 tons (Steichen, 2001).

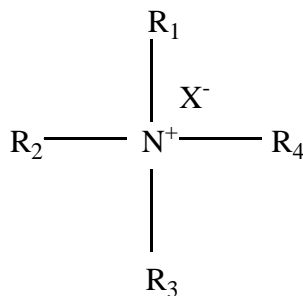


Figure 1.1. General molecular structure of a QAC (R represents a functional group, X^- represents a counter ion such as Cl^- , Br^- , or NO_3^-)

About 75% of the QACs consumed annually are released into wastewater treatment systems whereas the rest is directly discharged into the environment. As a result, QACs are ubiquitous contaminants found worldwide in sewage (Merino et al., 2003; Clara et al., 2007; Kreuzinger et al., 2007; Martinez-Carballo et al., 2007), industrial wastewater (Kreuzinger et al., 2007; Martinez-Carballo et al., 2007), effluents of laundries and hospitals (Kummerer et al., 1997; Kreuzinger et al., 2007; Martinez-Carballo et al., 2007), treated wastewater (Ding and Liao, 2001; Clara et al., 2007; Kreuzinger et al., 2007), sewage sludge (Martinez-Carballo et al., 2007; Sutterlin et al., 2007), surface waters (Ding and Liao, 2001; Ferrer and Furlong, 2001; Merino et al., 2003; Kreuzinger et al., 2007; Martinez-Carballo et al., 2007) and aquatic sediments (Ferrer and Furlong, 2002; Kreuzinger et al., 2007; Martinez-Carballo et al., 2007) at levels that may threaten biological treatment and environmental systems. Despite the fact that QACs are listed as HPV chemicals and consumed extensively in everyday applications, making them ubiquitous pollutants, crucial information on their toxicity and environmental fate does not exist.

QACs are toxic to aquatic organisms at environmentally relevant concentrations (Kummerer et al., 1997; Nalecz-Jawecki et al., 2003). The fate of QACs in aerobic biological systems has been studied. QACs are biodegradable in biological systems such as activated sludge systems, surface waters, soil and groundwater under aerobic conditions. The half-lives of aerobic degradation of QACs in such systems vary extensively from hours to months depending on the QAC concentration and structure, microbial acclimation and presence of QAC resistant/degrading microorganisms. Certain microorganisms that are resistant to QACs and capable of QAC degradation have been

isolated (van Ginkel et al., 1992; Nishihara et al., 2000; Patrauchan and Oriol, 2003; Takenaka et al., 2007). However, the aerobic QAC degradation mechanisms/pathways and the toxicity of the resulting products are not clear.

On the other hand, QACs rapidly and strongly sorb onto a wide variety of materials including biomass, sediments, clays, and minerals such as halides, sulfides, sulfates, and oxides. Indeed, sorption generally outcompetes biodegradation in aerobic compartments in the environment and therefore QACs are transferred to anoxic/anaerobic compartments such as anaerobic digesters and aquatic sediments (Boethling, 1994; Ying, 1999). It has been reported that QAC concentrations in municipal anaerobic digesters may range from 4,000 to 10,500 ppm (mg/kg dry solids) (ECETOC, 1993; Garcia et al., 1999; Ying, 1999) and their concentrations in sediments typically exceed an enrichment factor of 500 (Valls, 1989; Fernandez et al., 1991; Sun et al., 2003; Martinez-Carballo et al., 2007). So far, there is no evidence of biotransformation of QACs, except the esterquats (QACs with ester bonds, i.e., O=C-OC) and natural QACs such as choline, under anaerobic/anoxic conditions (Battersby and Wilson, 1989; Federle and Schwab, 1992; Garcia et al., 1999; Garcia et al., 2000; Tezel et al., 2006; Tezel et al., 2007), most likely because of the highly reduced nature of the QAC structure. Moreover, QACs are inhibitory to anaerobic microbial processes such as methanogenesis. In spite of the fact that QACs are present in anoxic/anaerobic biological systems, their fate and effect under these conditions have been largely unexplored to date.

The bactericidal properties of QACs are well established and microorganisms which are resistant to QACs and can utilize them as energy source under aerobic conditions have been isolated. QAC utilizing bacterial species such as *Pseudomonas*

fluorescens and *Aeromonas hydrophila* contain QAC resistance genes (e.g., *qacE*) which occur on the same mobile genetic elements, such as Class 1 integrons and plasmids, known to confer antibiotic resistance (Gaze et al., 2005; Schluter et al., 2007). Hence, selection for QAC resistance may cause co-selection for antibiotic resistance, providing a reservoir of antibiotic-resistant bacteria, as well as antibiotic resistance genes in QAC-polluted environments. The spread of antibiotic resistance is an alarming, continuing problem worldwide (WHO, 2000; Josephson, 2006; Pruden et al., 2006; Singer et al., 2006; Weber et al., 2007; Smith et al., 2008), and a critical human health challenge (Maillard, 2007). Therefore, the fate and effect of chemicals such as QACs, which have the potential to persist in the environment, cause toxicity and induce antibiotic resistance genes and facilitate the transfer of antibiotic resistance in the environment, must be thoroughly investigated.

The overall objectives of the research presented here were to (1) supply systematic information on the fate and toxicity of QACs using quantitative structure-activity relationships, and (2) evaluate the biotransformation potential of QACs under aerobic, anoxic and anaerobic conditions as well as the toxicity of biotransformation products.

The specific objectives and the approach followed in this research were:

(1) Assessment of fate and toxicity of QACs in biological systems by using quantitative structure-activity relationships (QSAR) approach.

Approach: A global structure-specific descriptor was identified and used to evaluate the biosolids partitioning and toxicity of QACs with different structures.

(2) Evaluation of biotransformation potential of QACs in biological systems, identification of QAC biotransformation pathways, and assessment of the potential toxicity of the resulting compounds.

Approach (three steps):

Step 1: Bioenergetic calculations were used to evaluate the biotransformation potential and the pathway of QACs under aerobic, anoxic and anaerobic conditions.

Step 2: Biotransformation experiments were performed to evaluate the biotransformation potential and pathway of QACs under aerobic, anoxic and anaerobic conditions.

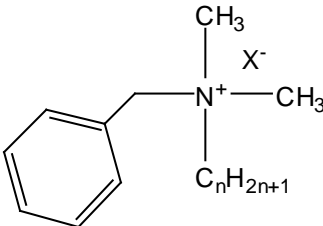
Step 3: The Microtox[®] toxicity assay was performed to evaluate the toxicity of QACs and their biotransformation products.

The research commenced with the selection of representative QACs to be used in this study based on their consumption rate, frequency of occurrence in engineered and natural biological systems, and molecular structure. Nine QACs, belonging to three groups -- monoalkonium, dialkonium and benzalkonium chlorides -- were selected as the target QACs. The critical micelle concentration (CMC) of these QACs was determined. Then, the CMC was used as a descriptor to derive relationships between QAC structure and partitioning to biosolids as well as toxicity. The effect of environmental constituents, such as anions and natural organic matter, on the QAC toxicity was also evaluated. The biotransformation potential of QACs under aerobic, methanogenic, nitrate reducing and fermentative conditions was evaluated using bioenergetics and tested in batch biotransformation experiments. In addition, the inhibitory effect of QACs under methanogenic and nitrate reducing conditions was systematically investigated. QAC

transforming biotic and abiotic conditions, as well as the transformation pathways (at least the initial, activation steps) and products were identified to the extent possible.

This research contributes to a better understanding of the environmental and human health risks associated with QACs by providing systematic information on physical, chemical and biological processes that determine the fate of QACs in engineered and natural systems. Therefore, it may facilitate the development of strategies to mitigate adverse effects of QACs and to aid industry, as well as state and federal regulatory agencies in the development of sound policies and risk assessment strategies.

Table 2.1. Representative QAC groups, their general structure and abbreviations used in this study (X is a halide counter-ion)

QAC Group	Molecular Structure	Abbreviation
Monoalkonium halides	$ \begin{array}{c} \text{CH}_3 \\ \\ \text{CH}_3 - \text{N}^+ - \text{CH}_3 \\ \\ \text{C}_n\text{H}_{2n+1} \\ \text{X}^- \end{array} $	$\text{C}_n\text{TMA-X}$
Dialkonium halides	$ \begin{array}{c} \text{CH}_3 \\ \\ \text{CH}_3 - \text{N}^+ - \text{C}_n\text{H}_{2n+1} \\ \\ \text{C}_n\text{H}_{2n+1} \\ \text{X}^- \end{array} $	$\text{DC}_n\text{DMA-X}$
Benzalkonium halides		$\text{C}_n\text{BDMA-X}$

QACs are large molecules having molecular weights typically between 300 and 400 g/mole and are composed of two distinctly different moieties: hydrophobic alkyl groups and a hydrophilic, positively charged central N atom, which retains its cationic character at all pH values. The two moieties affect the QACs' physical and chemical properties (Boethling, 1994).

QACs have distinct physical/chemical properties, which are conferred by their substituents, mainly the alkyl chain length. QACs may be freely soluble or insoluble in water. The aqueous solubility of QACs decreases as the hydrophobicity or the alkyl chain length of the molecule increases. For instance, the aqueous solubility of DC₈DMA-Cl, DC₁₀DMA-Cl, DC₁₂DMA-Cl, DC₁₄DMA-Cl, DC₁₈DMA-Cl is 8100, 700, 77, 12 and 2.7 mg/L, respectively (Boethling, 1994). Likewise the critical micelle concentration (CMC) of QACs, which affects the efficiency of many surfactant-related applications, decreases as the alkyl chain length of the molecule increases. For example, the CMC of C₁₂BDMA-Cl, C₁₄BDMA-Cl, C₁₆BDMA-Cl is 3, 2 and 0.5 mM, respectively (Garcia et al., 2006). Other physical/chemical properties that can affect the fate of QACs in the environment, such as octanol-water and organic carbon-water partitioning, are influenced by the molecular structure of the QACs. The sorption of QACs on organic surfaces, such as biomass and sediment, increases as the alkyl chain length increases. On the contrary, as the alkyl chain length of the molecule decreases, ionic interactions become dominant and favor the sorption of QACs onto ionic surfaces, such as clay minerals.

The physical and chemical properties of QACs strongly affect not only their fate but also their toxicity and biodegradability in both engineered and natural systems. In fact, large quantities of QACs with different molecular structures are consumed and

released into the environment. Therefore, methodical assessment of the environmental risk associated with each QAC molecule is extensively difficult. For that reason, development of quantitative structure-activity relationships for QACs is desirable and is one of the objectives of this study. Hereafter, an extensive review on the occurrence of QACs, mainly monoalkonium, dialkonium and benzalkonium salts, their inhibitory effects and toxicity to living organisms, and their biodegradation potential in engineered and natural systems is presented in the sections that follow.

2.2. Applications and Implications of QACs

2.2.1. Demand and Consumption of QACs

QACs are designated as the ultimate work-horse of the surfactant industry. They are on the High Production Volume Chemicals list of the USEPA. The world-wide annual consumption rate of QACs was reported as 0.5 million metric tons in the 6th World Surfactants Congress held in Germany (CESIO, 2004) and this rate was expected to reach 0.7 million metric tons (Steichen, 2001). While the demand for QACs is usually found to be 10% of the total surfactant demand, they nevertheless represent an irreplaceable category of surfactants for over two centuries (Steichen, 2001).

QACs possess surface-active properties, self-assembly characteristics, detergency and antimicrobial properties. The unique physical/chemical properties of QACs have resulted in a variety of uses and a high level of popularity in domestic and industrial applications as surfactants, emulsifiers, fabric softeners, disinfectants, pesticides, phase-transfer catalysts and corrosion inhibitors (Figure 2.2) (Boethling, 1994).

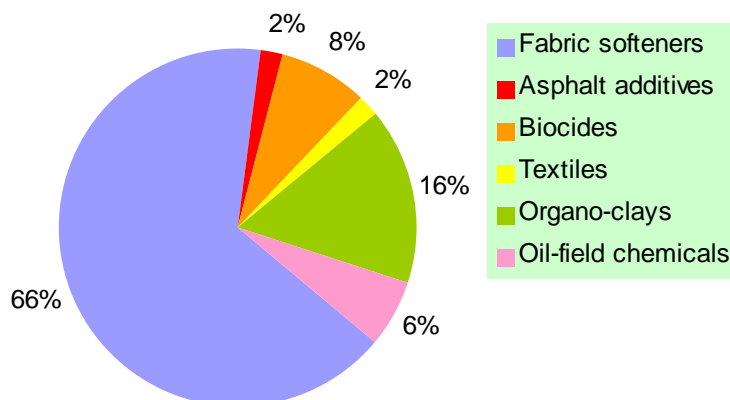


Figure 2.2. Distribution of QAC use in the market (Boethling, 1994)

QACs are the major active ingredient of fabric softeners (20-30 wt %). The most common softener active ingredients that are commercially viable in today's marketplace are (i) dialkonium salts, (ii) diethylenetriamide compounds and (iii) ester quaternary salts. The first group has the highest demand in the market, however ester quaternary salts are good substitutes for the dialkonium salts since they are readily biodegradable and less toxic than the dialkonium salts. QACs are also utilized for fabric softening and soil removal purposes in laundry detergents. Laundry detergents that also provide fabric softening utilize relatively simple QACs such as monoalkonium salts with an alkyl chain length of 12 to 18 carbons (Zachvieja, 2001).

QACs reduce surface and interfacial tension by sorbing to a surface or an interface such as hair and skin. The adsorption ability of QACs onto organic surfaces makes the use of QACs extremely important in the personal care industry. Skin care products and hair conditioners contain mainly alkyl QACs (including mono-, di- and tri-

alkonium salts), ethoxylated and ester QACs in their formulations (Tang, 2001).

QACs are also used in paper processing to produce tissue paper or fluff pulp, which are used in diapers, toweling, napkins and facial and toilette tissue products. It is known that QACs, such as dialkylammonium salts are effective chemical debonding agents in paper. QACs interact with the natural fiber-to-fiber bonding that occurs during the paper-making process. The hydrophobic and hydrophilic moieties of the QACs interact with the fiber surface, reduce the inter-fiber bonding, and form a thin lubricant layer. This reduction of the inter-fiber bonding, together with the lubricating effect, gives a soft feel to the paper. In the mechanical fluff pulp process, QACs protect the fibers against damage and reduce the defibration energy needed (Bergstrom, 2001).

QACs are extensively used as bioactive agents. They exhibit a broad spectrum of antimicrobial activity over a wide range of pH and are used in domestic, industrial, agricultural and medical applications as wood preservatives, pesticides, fungicides, sanitizers/disinfectants, and hard-surface cleansers. They are effective against a variety of bacteria, fungi and viruses at very low concentrations (Table 2.2). When QACs are used as disinfectants, the applied concentration is typically between 400 and 500 ppm and almost always below 1000 ppm (e.g., 0.1% w/v in Lysol®) (Tiedink, 2001).

The use of QACs as biocides in wood preservation formulations is a common application. QACs are used either by themselves or in combination with other modern biocides, such as fungicides, bactericides or insecticides. The most commonly used QACs are dialkylammonium and benzalkonium chlorides (Tiedink, 2001).

Table 2.2. Biocidal activity of alkyl (C₁₂₋₁₆)benzyl dimethyl and didecyl (C₁₀)dimethyl ammonium chlorides

Microorganism	Minimum Bactericidal Concentration (ppm)	
	C ₁₂₋₁₆ BDMA-Cl	DC ₁₀ DMA-Cl
<i>Enterococcus faecium</i>	30	10
<i>Staphylococcus aureus</i>	40	10
<i>Escherichia coli</i>	100	25
<i>Pseudomonas aeruginosa</i>	700	250
<i>Salmonella typhimurium</i>	150	40
<i>Proteis mirabilis</i>	300	200
<i>Campylobacter jejuni</i>	45	4
<i>Legionella pneumophila</i>	80	30
<i>Listeria monocytogenes</i>	25	5

QACs are used in agricultural formulations as biocides and adjuvants. The consumption of C₁₂₋₁₆BDMA-Cl, DC₁₀DMA-Cl, DC₈₋₁₀DMA-Cl and DC₈DMA-Cl as biocides in the State of California in 2003 was 3394, 1176, 157 and 79 kg, respectively (www.pesticideinfo.org). Many pesticides are insoluble in water and not active as they applied individually, however QACs (as adjuvants) enhance the solubility, rain fastness and penetration of pesticides as they are applied together with the pesticides. Typical QAC concentrations in agrochemical tank-mixed sprays range from 0.05 to 0.5% v/v (Gustavsson, 2001).

QACs are used in the production of organoclays. Organoclays are produced by the displacement of the inorganic cations on a clay mineral (i.e., morillonite or hectorite) by organic cations. The organic cations used in the manufacturing of organoclays are QACs such as dialkylammonium and benzalkonium salts. Organoclays are used in a number of different formulations such as oil-based drilling fluids, printing inks, oil based paints, latex polymers and nail polishers (Hoey, 2001). Organoclays are able to adsorb organic molecules from both aqueous systems and air and are used in landfill liners, groundwater remediation (Boyd et al., 1988) and in air filters. The annual demand for organophilic clays, which typically contain 40% by weight of QACs, is around 16% of the QAC market (Figure 2.2).

Oil-field applications of QACs include anti-swelling/clay stabilization, foaming, silt suspension, corrosion inhibition, biocides and demulsification (Witco Corporation, 1995; Akzo Chemicals Inc., 1998).

One of the new applications for QACs is phase-transfer catalysis. Many organic syntheses are carried out in which one reactant is dissolved in an aqueous solution and

the other in a hydrophobic organic phase. QACs act as phase-transfer catalysts and mediate the reaction at the interface between the two phases or after one of the solutes has passed through the interface and entered the other phase. QACs are believed to show better selectivity, greater rate increase, and cost less than other types of phase transfer catalysts. Benzalkonium and monolakonium salts are used extensively as phase transfer catalysts (Boethling, 1994).

2.2.2. Distribution of QACs in the Environment

QACs have been extensively used in many industrial, domestic and agricultural applications over two centuries. Their production and consumption rates are increasing as they find new applications. On the other hand, QACs are inevitably released into the environment at the production stage or at the end of the consumption of the QAC-bearing products. QACs are, therefore, ubiquitous contaminants. Moreover, available data suggest that QACs are extensively accumulated in aquatic sediments, however, information on residues of QACs in aquatic sediments near sites of industrial or domestic effluent discharge are scarce. The concentration of QACs in domestic wastewater, effluent wastewater, sewage sludge and surface water has been reported as 0.5, 0.05, 3000, and 0.04 ppm, respectively (Schmitt, 1994).

Random samples of sewage from treatment plants in Switzerland, which have various inputs from metallurgical processes or textile industry, had QAC levels ranging from 0.04 to 0.45 ppm (Michelsen, 1978). Huber (1979) and Kupfer (1982) described monitoring studies in Germany, and Wee (1984) determined the levels of dialkonium chlorides in untreated sewage and final effluent from a plant in the United States. The QAC concentrations in the influent and effluent sewage ranged from 0.05 to 1.3 ppm and

0.01 to 0.2 ppm, respectively. The concentrations of monoalkonium chlorides were monitored in composite sewage samples in England and Germany. The total monoalkonium chloride concentration in the influent and effluent sewage was 0.13 ppm and 0.03 ppm, respectively. A recent study conducted in Austria to survey QAC concentrations in influents of five different wastewater treatment plants reported QAC concentrations ranging from 1 to 170 ppb (Martinez-Carballo et al., 2007). On the contrary, the QAC concentrations would be higher in the effluents of specific industrial facilities, such as paper processing, textile and food processing (1-40 ppm, based on the data obtained during a screening study for a poultry processing facility in Georgia), than the influents of municipal wastewater treatment plants. Kummerer et al. (1997) analyzed benzalkonium chlorides in highly complex effluent samples from different sized European hospitals. The measured concentrations were between 0.05 and 6.03 ppm. Although the reported QAC concentrations are low in the wastewater, many studies delineating the effect and biodegradability of QACs in wastewater treatment systems have worked at concentrations ranging from 10 to 100 mg/L. Therefore, one would expect high QAC concentrations in the wastewater treatment systems or surface waters receiving influents from industrial applications that use QACs extensively.

Levels of QACs in receiving waters are typically in the low microgram per liter range. Huber (1979) reported QAC concentrations of 5 to 20 ppb in the Main River in Germany. Schneider and Levsen (1983) found that the concentrations of dialkonium chlorides in sewage and surface water samples collected in Germany were 0.35 to 0.48 ppm and 6 to 12 ppb, respectively. Likewise, 5 to 30 ppb of monoalkonium chloride concentration was reported in the random samples collected from several rivers in the

United States (Wee and Kennedy, 1982; Wee, 1984). Lewis and Wee (1983) subsequently conducted a follow-up study, in which samples were collected at various distances downstream from wastewater treatment facilities. Mean dialkonium chloride levels were <2, 24, 17, and 33 ppb for Millers River (MA), Otter River (MA), Blackstone River (MA) and Rapid Creek (SD). The concentration of DC_nDMA-Cl in the samples collected at distances from 4.4 to 55 miles downstream from the wastewater treatment plants ranged from 191 to 100 ppb.

QACs adsorb strongly on suspended solids such as minerals, biomass and inorganic particles and are transferred to anaerobic digesters or aquatic sediments. For instance, mean concentrations of DC_nDMA-Cl's in anaerobically stabilized sludge samples from five different municipal sewage treatment plants in Switzerland were 3670, 960, 470, and 210 ppm (mg/kg-dry) in 1991, 1992, 1993, and 1994, respectively (Fernandez et al., 1996), whereas, ppb levels were found in the sewage as discussed above. It was also reported that QAC concentrations in anaerobic digesters may range from 4000 to 10,500 ppm (mg/kg-dry solids). Lewis and Wee (1983) obtained sediment samples from Rapid Creek at distances from 0.8 to 88 km downstream from a sewage outfall. DC_nDMA-Cl levels averaged 23 ppm over 18 samples. Fernandez et al. (1991) found that DC_nDMA-Cl was a ubiquitous contaminant in coastal sediments collected near Barcelona, Spain (Fernandez et al., 1991). Utsunomiya et al. (1989) reported the levels of QACS in river water and sediment samples from Japan. Levels of QACs in influent sewage, river water and sediment were 0.10 to 0.15, 0.05 and 6.2 to 69 ppm, respectively. Sun et al. (Sun et al., 2003) studied the fate of QACs in a river running through Toyama City, Japan. They found that total influx of QACs into the river was 1.4 g/min, and the

concentration was between 0.01 and 0.02 ppm. The QACs in the sediment samples were 500 times higher than that found in the river water. In another study, it was reported that DC_nDMA-Cl was present at 0.63 ppm in surface water and 9.7 ppm (0 to 0.6 m depth) and 7.4 ppm (0.6 to 1.2 m depth) in the sediment at a pond that had been receiving untreated wastewater from a laundromat since 1962 (Federle and Schwab, 1992). Dialkonium chlorides were also detected in drinking water samples derived from river water and groundwater in England.

Based on the information presented above, QAC fluxes and expected QAC concentrations in engineered and natural systems are shown in Figure 2.3.

2.2.3. Toxicity and Inhibitory Effects of QACs in Biological Systems

As mentioned above, QACs are used extensively in domestic and industrial applications. About 75% of QACs consumed end up in wastewater treatment plants (Figure 2.3). The EC₅₀ values for C₁₆TMA-Br and C₁₂BDMA-Cl obtained from a respirometric assay conducted with activated sludge ranged between 10 and 40 mg/L (Reynolds et al., 1987). The EC₅₀ of C₁₄₋₁₈TMA-Cl for unacclimated sludge determined based on the inhibition of [¹⁴C]glucose uptake was 28 mg/L (Larson and Schaeffer, 1982). Another study showed that DC₁₀DMA-Cl inhibited the COD removal in a rotating biological contactor at concentrations above 20 mg/L and the biofilm was totally eliminated at 160 mg/L. Overall, these studies suggest that QACs are unlikely to manifest significant toxicity in wastewater treatment at the levels normally expected. However, sudden discharges of QACs resulting in temporarily high levels in treatment plants could upset plant function. Microorganisms that have resistance to QACs and utilize them as the energy source at high concentrations have been identified (e.g., *Pseudomonas* spp.).

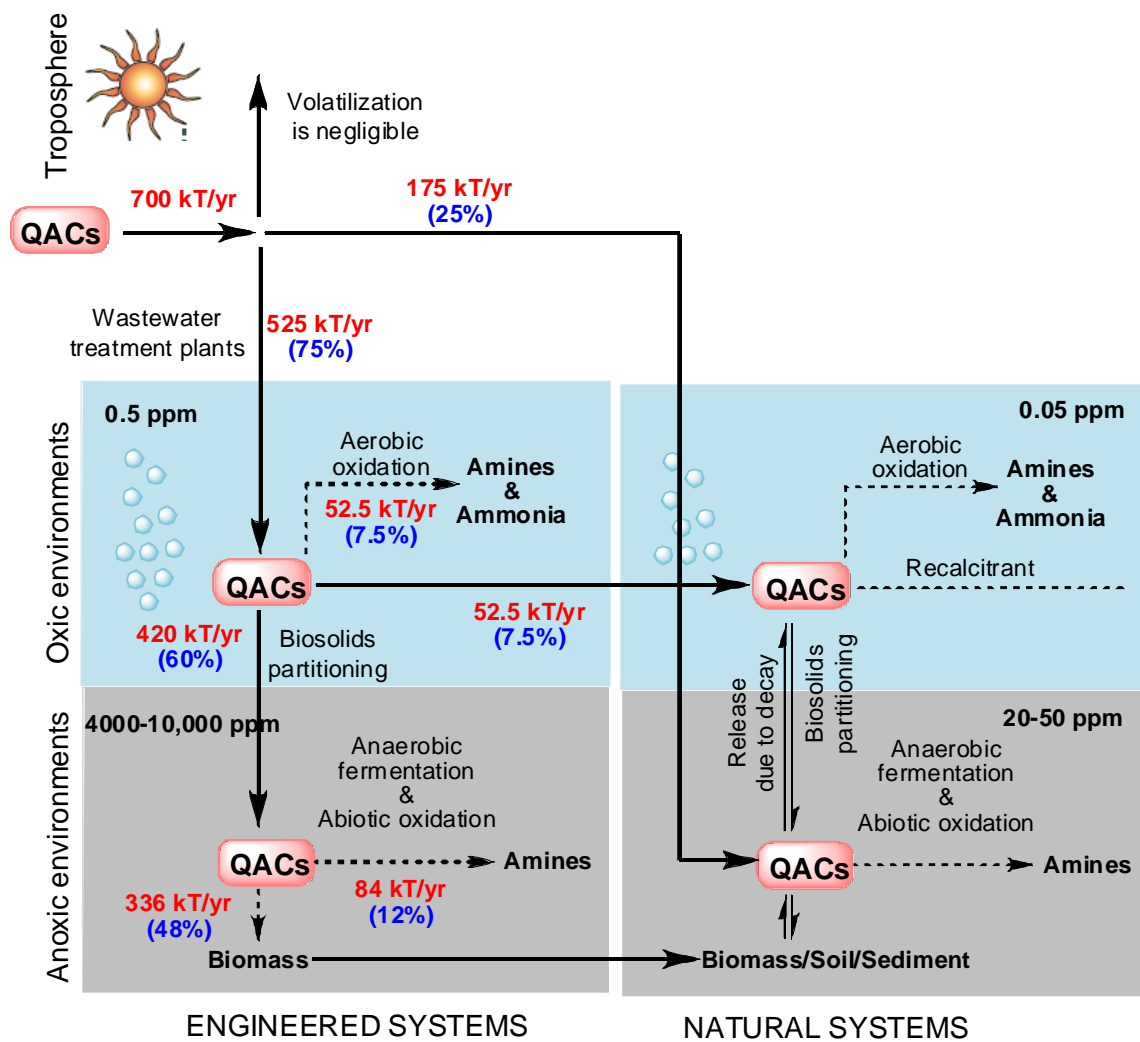


Figure 2.3. Schematic representation of QAC fluxes and expected QAC concentration levels in different compartments of engineered and natural systems calculated based on the global QAC consumption

On the other hand, many wastewater treatment plants practice biological nutrient removal and they use anaerobic, anoxic and aerobic biological units. A variety of physiologically different microorganisms participate in the wastewater treatment process, therefore the response of each species to QAC inhibition is expected to be different. For instance, QACs are particularly toxic to nitrifiers. Benzalkonium chloride was inhibitory to a mixed nitrifying culture at 10 to 15 mg/L with a non-competitive inhibition coefficient equal to 1.5 mg/L (Yang, 2007).

QACs have high affinity to adsorb onto (bio)solids. Generally, adsorption outcompetes biodegradation in aerobic biological treatment systems and therefore QACs are transferred to anaerobic digesters as part of the primary and waste activated sludge (Boethling, 1994). It was reported that QAC concentrations may reach up to 50 mg/L in anaerobic digesters of sewage treatment plants (ECETOC, 1993; Garcia et al., 1999). QAC concentrations may exceed these levels in biological treatment systems of industrial facilities, such as food processing, that extensively use QACs. Under anaerobic conditions, there is no evidence of mineralization of QACs that contain alkyl or benzyl groups (Battersby and Wilson, 1989; Federle and Schwab, 1992; Garcia et al., 1999, 2000), most likely because of the highly reduced nature of these substituent groups. Moreover, QACs are inhibitory to anaerobic microbial processes such as methanogenesis (Battersby and Wilson, 1989; Garcia et al., 1999, 2000). Tezel et al. (2006) investigated the effect of four QACs – DC₈DMA-Cl, DC₈₋₁₀DMA-Cl, DC₁₀DMA-Cl and C₁₂₋₁₆BDMA-Cl – on a mixed mesophilic methanogenic culture. It was reported that all QACs tested in this study had short- or long-term inhibitory effects on the mixed methanogenic culture at 25 mg/L and above. Methanogenesis was more sensitive to QAC

inhibition than acidogenesis. The inhibitory impact of the individual QACs on the methanogenic activity decreased according to the following series: DC₈DMA-Cl > DC₈₋₁₀DMA-Cl > C₁₂₋₁₆BDMA-Cl > DC₁₀DMA-Cl. Thus, QACs with the shorter alkyl chain length are the most inhibitory QACs. Moreover, it was concluded that the inhibitory effect of QACs was inversely proportional to their adsorption affinity on the biomass or their hydrophobicity (Tezel et al., 2006; Tezel et al., 2007). Similar results were reported by Garcia et al. (1999).

About 25% of QACs consumed are discharged into the environment (Figure 2.3). The effect of monoalkonium and dialkonium QACs on the aquatic microbial communities in a lake ecosystem was investigated and the results showed that QACs elicit ecologically significant responses at concentrations below 1 mg/L and mainly heterotrophic bacterial activity was affected (Ventullo and Larson, 1986). Tubing and Admiraal (1991) examined the effect of DC₁₈DMA-Cl on natural populations of bacteria and phytoplankton from the lower River Rhine and reported significant decreases in the growth rate of bacterioplankton and in the photosynthetic rate of phytoplankton at a nominal DC₁₈DMA-Cl concentration 0.03 to 0.1 mg/L (Tubbing and Admiraal, 1991). Nye et al. (1994) investigated the heterotrophic activity in a soil ecosystem treated with C₁₆TMA-Br. Addition of C₁₆TMA-Br to the soil resulted in increased lag periods and decreased rates and extends of mineralization of ¹⁴C-labeled organic compounds as a result of toxicity toward Gram-negative soil microorganisms (Nye et al., 1994).

QACs are toxic at ppm levels and lower to aquatic organisms including algae, fish, mollusks, barnacles, rotifers, starfish, shrimp, and others. Toxicity of 15 QACs (with molecular weights ranging between 313.5 and 547.0 g/mole) were investigated in four

bioassays, such as *Microtox*, *Spirotox*, *Protoxkit F* and *Artotoxkit M*, comprising a bacterium (*Vibrio fischeri*), two ciliated protozoa (*Spirostomum ambiguum* and *Tetrahymena thermophila*), and an anostracean crustacean (*Artemia franciscana*). The Microtox® assay acute toxicity EC₅₀ values for tested QACs ranged between 0.6 to 50 µM (0.24 to 21.5 mg/L at the average QAC molecular weight of 430.25 g/mole). The results indicated that QACs had high toxicity against the bioindicators tested and were toxic not only to bacteria, but also to non-target protozoa and crustacea. It was also stated that the toxicity of QACs decreases as the alkyl chain length increases, since the hydrophobicity of QACs with longer alkyl chain length increases resulting in low bioavailability and high partitioning with organic or negative charged surfaces (Nalecz-Jawecki et al., 2003).

Algae represent a group of organisms which appears to be very sensitive to QACs. The EC₅₀ values of C_nTMA-Br and C_nTMA-Cl for algae range between 0.03 and 0.38 mg/L. On the other hand, EC₅₀ values for dialkonium QACs range between 0.05 and 18 mg/L, therefore the toxicity of dialkonium QACs is less than the toxicity of monoalkonium QACs (Lewis, 1991; Utsunomiya et al., 1997). Benzalkonium QACs are toxic to aquatic organisms below 1 mg/L.

The toxicity of QACs to fish and invertebrates has also been studied. It was reported that all QACs are acutely toxic to aquatic invertebrates and fish as indicated by EC/LC₅₀ values below 1 mg/L by affecting the reproduction and larval growth and development (Lewis, 1991; Boethling, 1994; Utsunomiya et al., 1997). The no observed effect concentration (NOEC) for *Daphnia* exposed to DC₁₈DMA-Cl and C₁₂TMA-Cl in river water was 0.38 and 0.065 mg/L, respectively (Lewis, 1991). According to

Kummerer and co-workers (1997), the LC₅₀ of C_nBDMA-Cl to fish is between 0.5 and 5.0 ppm, and the toxicity to daphnids is even higher, with an LC₅₀ from 0.1 to 1.0 ppm (Kummerer et al., 1997). Data retrieved from the European Center for Ecotoxicology and Toxicology of Chemicals (ECETOC) and U.S. EPA Ecotoxicology (ECOTOX) databases using the OECD Application ToolBox (OECD, 2008) showed that monoalkonium, dialkonium and benzalkonium chlorides are toxic to aquatic organisms, i.e., bacteria, algae, fish, invertebrates, etc. The minimum, maximum and median of reported EC₅₀ values are 37 pg/L, 58 mg/L and 0.5 mg/L, respectively (Figure 2.4).

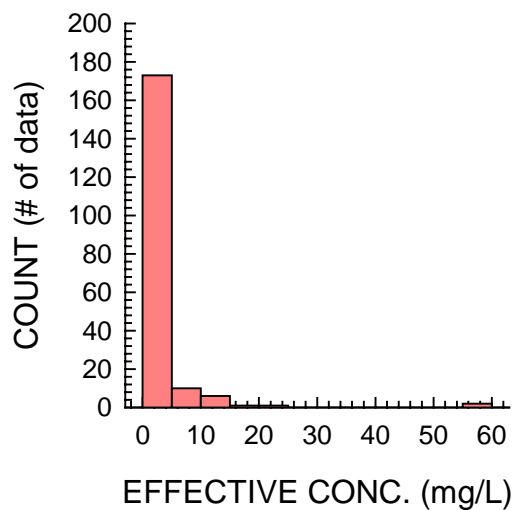


Figure 2.4. Histogram of reported EC₅₀ values for monoalkonium, dialkonium and benzalkonium chlorides for aquatic organisms. Data obtained from the European Center for Ecotoxicology and Toxicology of Chemicals (ECETOC) and the U.S. EPA Ecotoxicology (ECOTOX) databases using the OECD Application ToolBox

QACs are widely distributed in the environment and are detected in drinking water. They are the main active ingredients of many household products and cosmetics. As a result of these widespread uses, humans are exposed to them with almost all body surfaces and cavities and QACs have the potential to be adsorbed, inhaled, and ingested.

In general, the acute (single-dose) toxicity of QACs is characterized, at lethal doses, by peripheral paralysis and central nervous system stimulant-like effects. In chronic (multiple-dose) studies, the toxic effects of QACs commonly consist of adverse effects on body weight or growth, reduced food consumption, dehydration, and increased mortality (Drobeck, 1994). Several human fatalities due to exposure to benzalkonium QACs have been reported over the years. Xue et al. (2004) investigated the distribution and disposition of C_nBDM-Cl following oral administration (PO) and intravascular jugular vein (W), femoral artery (FA), femoral vein (FV) and jugular artery (JA) administration in rats along with pathological examinations. In this study, toxic doses of 250 and 15 mg/kg of C_nBDM-Cl were used for PO and intravascular administration, respectively. The fatal effects of C_nBDM-Cl appeared soon in JV-, FV- or JA-rats, but took hours in PO or FA-rats. No rat receiving benzalkonium chloride via FA survived longer than 1 day. The PO-rats that aspirated benzalkonium chlorides into their lungs had some systemic symptoms and higher blood and tissue concentrations of benzalkonium chloride. The blood benzalkonium chloride levels and kinetics were similar among the different routes of intravascular administration, but the lung and kidney levels were higher in JV-rats. Pathological examinations confirmed severe congestion and edema in the lungs and kidneys (Xue et al., 2004).

2.2.4. QAC Related Antimicrobial Resistance Mechanisms as a Challenge to Human Health

QACs have been actively deployed as antimicrobial agents since the 1930s in many clinical, industrial and domestic applications. As a result, bacterial resistance to QACs has become a serious problem. Many aerobic and facultative microbial species that

acquire resistance to QACs and co-resistance to many other disinfectants, antibiotics, solvents and metals have been isolated not only in hospitals and food processing facilities but also in environments polluted with QACs (Maillard, 2007).

The mode of action of QACs against bacterial cells involves perturbation of lipid bilayer of the bacterial cytoplasmic membrane and the outer membrane of Gram-negative bacteria. Such action leads to a progressive leakage of cytoplasmic components out of the cell. Low concentrations of QACs bind to anionic sites found on the membrane surface, cause cells both to lose osmotic regulation capability and to leak potassium ions and protons. Intermediate levels of QACs inhibit membrane-located processes such as respiration, solute transport, and cell wall biosynthesis. The high concentrations kill cells by disintegration of the membranes and release of cytoplasmic contents and coagulation of proteins and nucleic acids. At the molecular level, action involves the association of the cationic quaternary nitrogen with the head groups of the acidic-phospholipids within the membrane due to ionic interactions. The hydrophobic tail (alkyl groups) then integrates into the lipid core with hydrophobic interactions. Such interactions increase the surface pressure in the exposed layer of the membrane and decrease membrane fluidity. The membrane undergoes a transition from fluid to liquid crystalline state and loses its osmoregulatory and physiological functions. As a result, QACs penetrate into the cell and reach their target sites of action (Maillard, 2002; Gilbert and Moore, 2005). QACs are also involved in the inhibition of respiratory enzymes and the dissipation of proton motive force (PMF) which affect the microbial metabolism, active transport, oxidative phosphorylation and ATP synthesis in bacteria (Knox et al., 1949; Maillard, 2002).

Many aerobic and facultative microorganisms acquire resistance to QACs by

changing the composition of their outer membrane proteins (Loughlin et al., 2002; Tabata et al., 2003), fatty acids (increase in saturated fatty acids) (Guerin-Mechin et al., 1999; Guerin-Mechin et al., 2000; Dubois-Brissonnet et al., 2001), lipids (Loughlin et al., 2002), lipopolysaccharide, cell wall surface hydrophobicity and the zeta potential of the cell surface or the acquisition or hyperexpression of certain multidrug efflux pumps (Poole, 2002). These QAC resistance mechanisms are very similar to resistance mechanisms to hydrocarbons (Sikkema et al., 1995; Van Hamme et al., 2003), metals and antibiotics (Poole, 2002; Poole, 2005).

The efflux-mediated QAC resistance mechanism has gained significant interest since it has a genetic origin and is transferable among unrelated microbial species. The efflux-mediated resistance to QACs generally confers the co-resistance to multiple antimicrobials such as antibiotics and is facilitated by multidrug efflux pumps. Multidrug efflux pumps mediate the transfer of a biocide from inside to the outside of the cell. Multidrug efflux systems are categorized into one of five classes, small multidrug resistance family (SMR), drug/metabolite transporter (DMT) superfamily, the major facilitator superfamily (MFS), the ATP-binding cassette (ABC) family, the resistance-nodulation-division (RND) family, and the multidrug and toxic compound extrusion (MATE) family (Putman et al., 2000). Several QAC efflux determinants have been identified and the majority of these determinants are plasmid-encoded such as QacC/D, QacE Δ 1, QacG, QacH, QacJ and QacA/B (Poole, 2005).

Multidrug efflux determinants of QAC resistance in Gram-positive bacteria include QacA/B, NorA (a multidrug transporter implicated in fluoroquinolone resistance), NorB and MdeA which are MFS efflux systems; EmrE, QacE Δ 1, QacG,

QacH and QacJ which are SMR efflux systems; and MepA which is a MATE family efflux system (Table 2.3). A study conducted on methicillin-resistant *Staphylococcus aureus* (MRSA) strains isolated between 1999 and 2004 in Japan revealed that MRSA contains the *qacA/B* gene and over expression of this gene reduces the susceptibility of this organism to QACs. The *qacA/B* gene has been detected also on plasmids bearing β -lactamases and heavy metals resistance determinants in clinical isolates. Studies of clinical *S. aureus* isolates showing reduced susceptibility to C_nBDMA-CIs have demonstrated enhanced expression of the NorA multidrug exporter in some of these, with a significant increase in fluoroquinolone resistance. Moreover, QAC-resistant *S. aureus* often showed cross-resistance to fluoroquinolones as a result of increased *norA* expression, in deed QACs seemed to more effectively select NorA-expressing mutants than did fluoroquinolones. Another MFS multidrug transporter, MdeA, has been identified in *S. aureus* and again QAC-resistant laboratory isolates overproducing this protein showed a modest cross-resistance to several antibiotics (Huang et al., 2004).

Efflux systems able to accommodate biocides, including QACs, in Gram-negative bacteria are also multidrug transporters (Table 2.3). Efflux determinants in Gram-negative bacteria are generally chromosomally-encoded (except *qacE*, *qacEΔ1*, *qacF* and *qacG*) in contrast to that of Gram-positive bacteria. *qacE*, *qacEΔ1*, *qacF* and *qacG* are associated with potentially mobile integron elements (Class 1 integrons) which are recombination and expression systems that capture genes as a part of a genetic element known as gene cassette. Many cassettes with known functions confer antibiotic or QAC resistance. Especially, *qacEΔ1* is widely distributed among both Gram-negative and positive bacteria, however a correlation between this determinant and QAC resistance is

Table 2.3. Multidrug efflux determinants of QAC resistance

Efflux Determinant	Organism
Gram-positive	
QacA	<i>Staphylococcus aureus</i>
QacB	<i>Staphylococcus aureus</i>
Smr	<i>Staphylococcus aureus</i>
QacEΔ1	<i>Staphylococcus aureus</i> , <i>Enterococcus faecelis</i>
QacG	<i>Staphylococcus aureus</i>
QacH	<i>Staphylococcus aureus</i>
QacJ	<i>Staphylococcus</i> spp.
MdeA	<i>Staphylococcus aureus</i>
NorA	<i>Staphylococcus aureus</i>
NorB	<i>Staphylococcus aureus</i>
MepA	<i>Staphylococcus aureus</i>
Gram-negative	
QacE	<i>Klebsiella pneumoniae</i> , <i>Pseudomonas aeruginosa</i> <i>P. aeruginosa</i> , <i>P. fluorescens</i> , <i>Pseudomonas</i> spp. <i>P. vulgaris</i> , <i>P. stuartii</i> , <i>Escherichia coli</i> , <i>K. pneumoniae</i> , <i>S. enterica</i> , <i>H. pylori</i> , <i>S. marcescens</i> , <i>Vibrio</i> spp., <i>Campylobacter</i> spp., <i>E. cloacae</i> , <i>S. maltophilia</i> , <i>C. freundii</i> , <i>Aeromonas</i> spp., <i>M. morgani</i> .
QacEΔ1	
QacF	<i>E. aerogenes</i> , <i>E. cloacae</i>
QacG	<i>P. aeruginosa</i> , <i>A. salmonicida</i>
EmeA	<i>E. faecalis</i>
EmrE	<i>E. coli</i>
EvgA	<i>E. coli</i>
MdfA	<i>E. coli</i>
NorM	<i>Neisseria meningitidis</i> , <i>N. gonorrhoeae</i>
PmpM	<i>P. aeruginosa</i>
SugE	<i>E. coli</i>
YhiUV-TolC	<i>E. coli</i>
AcrAB-TolC	<i>E. coli</i>
CmeABC	<i>Campylobacter jejuni</i>
CmeDEF	<i>C. jejuni</i>
SdeXY	<i>S. marcescens</i>

not clear yet. A number of the MATE (NorM of *Neisseria* spp., PmpM of *P. aeruginosa*), and RND (AcrAB-TolC, AcrEF-TolC and YhiUV-TolC pumps of *E. coli*; SdeXY pump of *S. marcescens*) family multidrug transporters implicated in antibiotic resistance have been shown to contribute to QAC resistance. The RND family exporter, MexCD-OprJ, a significant determinant of fluoroquinolone resistance in laboratory and clinical isolates, is inducible by QACs. The strains of *E. coli*, including *E. coli* O157:H7 adapted to C_nBDMA-Cl_s *in vitro* show a multiple antibiotic-resistant mutants expressing the RND family AcrAB-TolC exporters (Poole, 2005). It was reported that QAC resistant *E. coli* mutant OW66 is resistant to multiple QACs (Paraquat, cetyl pyridinium chloride, C_nBDMA-Cl_s), antibiotics (ampicillin, amoxicillin, kanamycin, etc.) heavy metals (Co, Cu) and hydrocarbons (dodecane, decane, cyclohexane etc.), although the actual resistance determinant was not determined (Ishikawa et al., 2002). The SMR family EmrE multidrug exporter of *E. coli* also accommodates QACs (Poole, 2005). A *Pseudomonas fluorescens* isolate contaminating a batch solution of C_nBDMA-Cl_s and showing high-level resistance to multiple QACs has been reported (Nagai et al., 2003). The same type pseudomonad containing *qacE* and *qacEΔI* on its class 1 integron has been isolated from a QAC polluted site of a textile mill (Gaze et al., 2005).

Among the multidrug efflux genes, *qacEΔI* has attracted significant interest since it is widespread in Gram-negative bacteria due to its presence in the 3' conserved segment of most Class 1 integrons and usually co-exists with other efflux genes in the same integron. Class 1 integrons (Figure 2.5) consist of a 5' conserved region consisting of an integrase gene, *int1*, encoding a site-specific recombinase, an *attI* site where cassettes are integrated, and a promoter, P_{ant}, that regulates the expression of gene

cassettes. The antibiotic resistance genes that integrons capture are located on gene cassettes. Gene cassettes contain a protein coding region and a recombination site known as a 59-be site, *attC*, which is responsible for the orientation of integration (Figure 2.5). The cassettes exist as free, circular DNA but cannot be replicated or transcribed in this form.

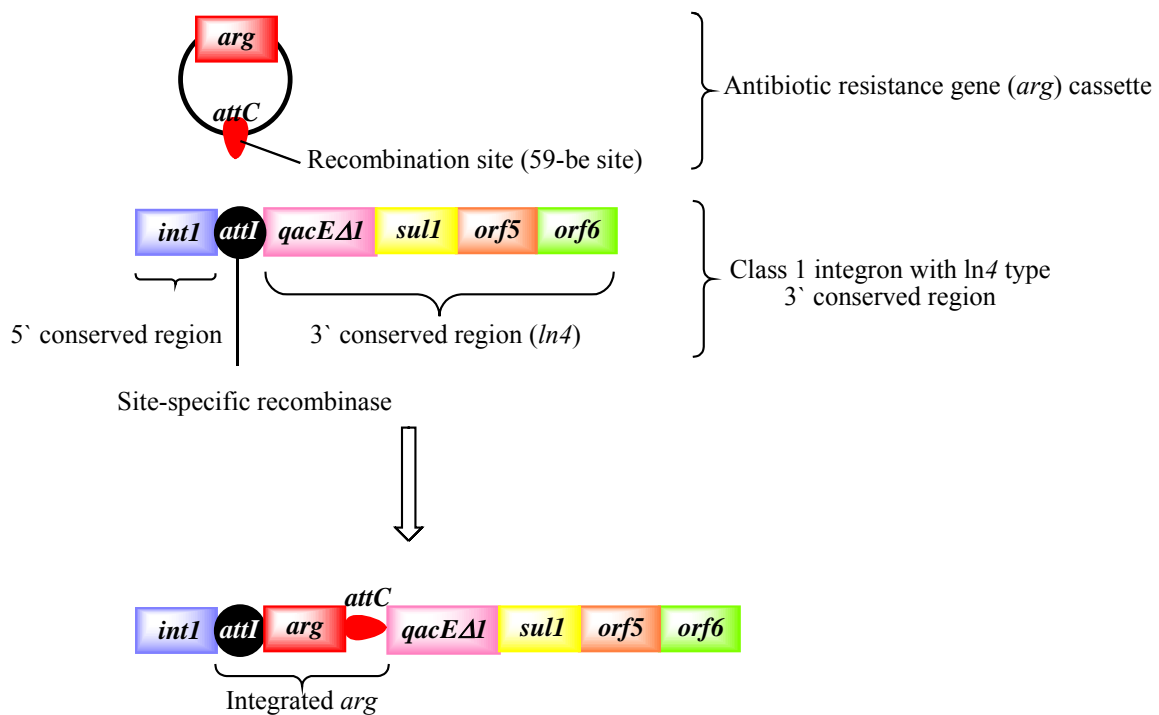


Figure 2.5. General structure of a Class 1 integron and a gene cassette and the mechanism of antibiotic resistance gene insertion into a Class 1 integron

A recombination event occurs between *attI* and *attC*, integrating the cassette into the integron (Figure 2.5). The gene on the cassette is then bound by the *attI* site on the 5' conserved region and by *attC* on the 3' conserved region. The 3' conserved region of an integron may have one of three backbone structures. The first backbone type consists of a

Tn402 (In16)-like arrangement consisting of a *tni* module containing three transposition genes and a resolvase gene. The second, In5 type consists of *qacEΔ1*, *sul1* (sulfonamide resistance gene), *orf5*, *orf6* (open reading frames), and a partial *tni* module, *tniΔ*, consisting of two transposition genes. The third, In4 type carries just *qacEΔ1*, *sul1*, *orf5* and *orf6* (Partridge et al., 2002; Gaze et al., 2005).

A Class 1 integron may contain more than one *args* belonging to different gene cassettes at the same time and these *args* may confer resistance to a wide variety of antibiotics/biocides such as β-lactams (e.g., *blaP*, *oxa*), streptomycin and spectinomycin (e.g., *aadA*), aminoglycosides (e.g., *aadB*, *aacA*, *aacC*), chloramphenicol (e.g., *catB*, *cmlA*), trimethoprim (e.g., *dfrA*, *dfrB*) and disinfectants (*qacE*) (Hall and Collis, 1998).

Recently, several bacterial species including *Pseudomonas fluorescens*, *Pseudomonas* spp., *Aeromonas hydrophila*, *Enterobacteriaceae*, *Serratia proteamaculans* and *Serratia* spp. that contain *qacEΔ1* have been isolated from a QAC polluted environment near a textile mill. This study is an important example that shows antibiotic resistance may not reside in only clinical species but spread in the environmental systems and QACs seems to be the major facilitator of antibiotic resistance in the environment. Again recently, but more striking, clinical and environmental isolates of *Vibrio cholerae* and *V. parahaemolyticus* that were isolated between 1991 and 1996 in different provinces of Angola were reported to be resistant to ampicillin, chloramphenicol, trimethoprim, sulfamethoxazole, and tetracycline. They also contained a large conjugative plasmid (p3iANG) with a set of three class 1 integrons harboring *dfrA15*, *blaP1*, and *qacH-aad48* cassettes, which code for resistance to trimethoprim, β-lactams, quaternary ammonium compounds, and aminoglycosides, clustered in a 19-kb region

(Ceccarelli et al., 2006). These two studies indicate that class 1 integrons are indicative of antibiotic and QAC resistance and contribute to the circulation of these multiple-drug resistance genes in the environment among various bacteria. For that reason presence of QACs in the environment possess a high level risk for human health.

2.3. Biotransformation of QACs

2.3.1. Aerobic Biotransformation

Most uses of QACs lead to their release into wastewater treatment systems or directly into the environment. The fate of QACs in aerobic biological treatment systems and receiving waters has been studied and the results of these studies have been reviewed extensively (Boethling, 1994; van Ginkel, 1996). These studies indicated that QACs are degraded under aerobic conditions and up to 90% of QAC removal by means of biodegradation is reported in engineered and natural systems. In fact, the half-lives for aerobic ultimate degradation of QACs vary extensively from hours to months depending on the QAC concentration, structure, microbial acclimation and presence of QAC resistant/degrading microorganisms. The alkyl chain length not only determines the physical/chemical properties of the QACs, but also may have a decisive role in the fate and effects of these compounds in the environment. Under aerobic conditions, the biodegradability of QACs generally decreases with the number of alkyl groups as $R_4N^+ < R_3MeN^+ < R_2Me_2N^+ < RMe_3N^+ < Me_4N^+$. Moreover, substitution of a methyl group with a benzyl group can decrease biodegradability further (Ying, 2006). A comparison of the degradation rates of benzalkonium chlorides and monoalkonium bromides under aerobic conditions was undertaken. The rate of degradation of $C_{12}BDMA-Cl$, $C_{14}BDMA-Cl$ and $C_{16}BDMA-Cl$, and $C_{12}TMA-Br$, $C_{14}TMA-Br$ and $C_{16}TMA-Br$ was inversely related to

the length of alkyl group (C_n) and substitution of benzyl group decreased the rate as well. Indeed, C_{16} BDMA-Cl was found to be the most recalcitrant of the tested compounds, with a plateau at only 30% degradation after 10 days. Likewise, it was reported that the aerobic degradation of QACs was dependent on the length of the alkyl group; however the number alkyl groups had a more pronounced effect on biodegradability. For example, dialkonium QACs were degraded five times more slowly than monoalkonium QACs (van Ginkel and Kolvenbach, 1991).

Certain microorganisms that are capable of QAC degradation have been isolated. These microorganisms are *Xanthomonas* (Dean-Raymond and Alexander, 1977), *Pseudomonas* B1 (van Ginkel et al., 1992), *Pseudomonas fluorescens* TN4 (Nishihara et al., 2000), *Aeromonas hydrophila* sp.K (Patrauchan and Oriel, 2003), and *Pseudomonas* spp. strain 7-6 (Takenaka et al., 2007) which were isolated from either sewage or soil.

Two biotransformation pathways, which are different from each other in terms of initial attack on alkyl chain, have been observed for monoalkonium, dialkonium and benzalkonium chlorides (Figure 2.6): (1) hydroxylation of terminal C (ω -hydroxylation) which is not adjacent to central N, followed by multiple β -oxidations, progressing toward the hydrophilic moiety, resulting in liberation of two carbons in each β -oxidation cycle from the alkyl chain of a QAC and (2) hydroxylation of C that is adjacent to central N (α -hydroxylation) followed by the central fission of the molecule resulting in separation of the hydrophobic from the hydrophilic moiety. The microbial attack to a QAC starts on the alkyl chain. Activation of the alkyl chain is commenced with NADH-dependent hydroxylation of either ω - or α -carbon of the alkyl group by a monooxygenase enzyme in the presence of oxygen. Activation of the alkyl chain of a QAC is very similar to the

activation of alkanes under aerobic conditions. A comparative pathway of hexadecane

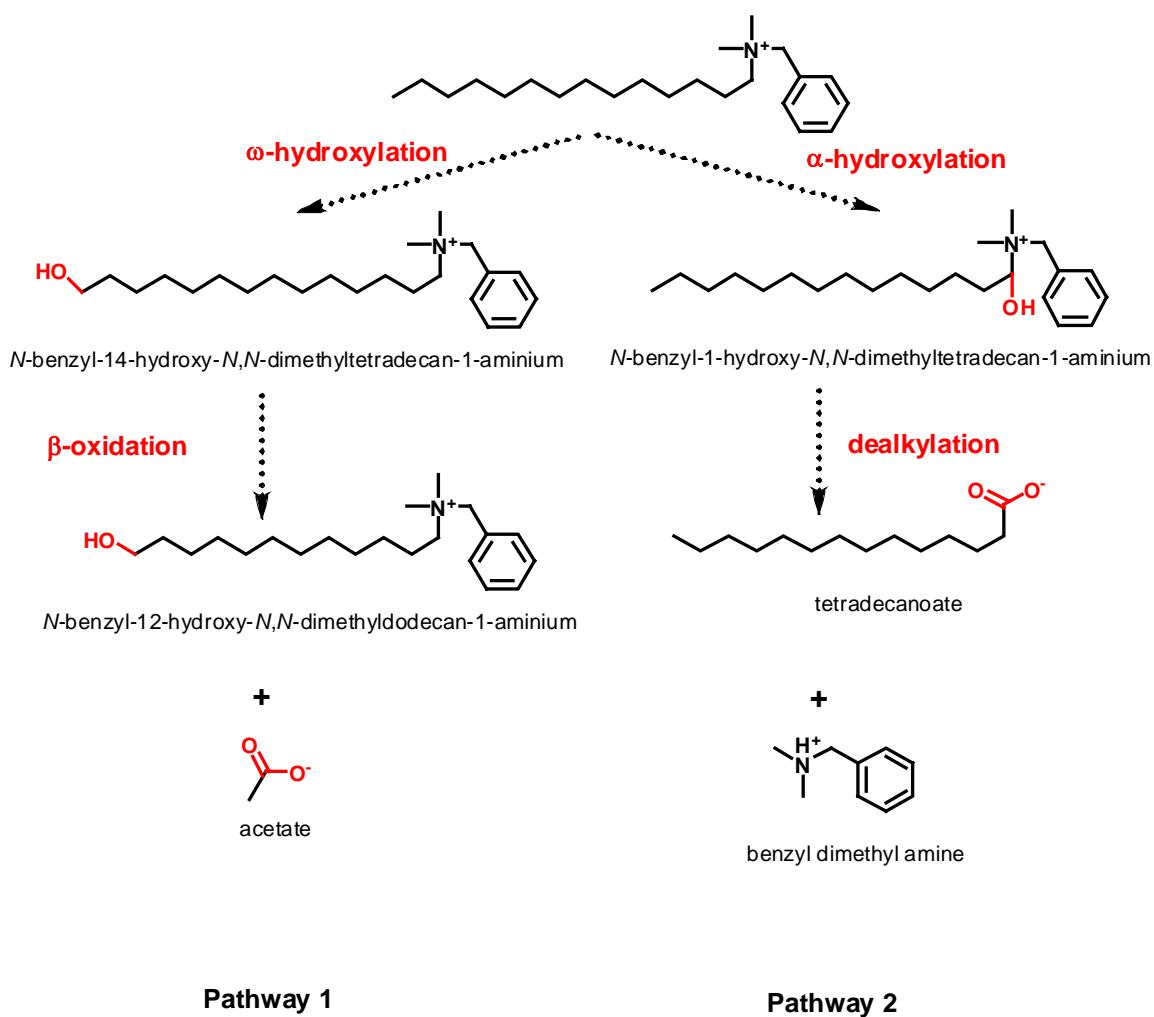


Figure 2.6. Two biotransformation pathways observed for tetradecyl benzyl dimethyl ammonium chloride under aerobic conditions

and hexadecyl trimethyl ammonium degradation is given in Figure 2.7.

A bacterium, *Xanthomonas* sp., capable of utilizing the monoalkonium QAC C₁₀TMA-Br as the sole carbon and energy source was isolated (Dean-Raymond and Alexander, 1977). The products of C₁₀TMA-Br biotransformation were identified as 9-carboxynonyl and 7-carboxyheptyl trimethyl ammoniums. Identification of these carboxyalkyl trimethyl ammonium salts verifies that the metabolism of C₁₀TMA-Br includes ω -hydroxylation followed by β -oxidation of the alkyl moiety (Pathway 1). In another study, a bacterium, tentatively identified as *Pseudomonas* sp. that grows on monoalkonium chlorides with alkyl chain lengths ranging from C₁₂ to C₁₈ was obtained through enrichment in a continuous culture inoculated with activated sludge. Growth on monoalkonium chlorides resulted in the production of trimethylamine. The transformation of monoalkonium chlorides therefore is proposed to follow NADH dependent α -hydroxylation of the alkyl moiety followed by a central fission of the C_{alkyl}-N bond (dealkylation) (Pathway 2, Figure 2.7.B) (van Ginkel et al., 1992). The aldehyde formed as a result of the chemical hydrolysis of the C_{alkyl}-N bond was converted into an alkanoate which underwent successive β -oxidation resulting in the complete oxidation of the alkyl chain. However, the biotransformation of trimethylamine has not been achieved with this strain. Another demonstration of the C_{alkyl}-N fission as the first degradation step of monoalkonium QACs with a mixed culture of microorganisms was presented by Nishiyama et al. (Nishiyama et al., 1995). In contrast to the previous findings, however, a recent study proposed the degradation of monoalkonium QACs, i.e., C₁₂TMA-Br, by *Pseudomonas* sp. strain 7-6, isolated from a wastewater treatment plant, via dual pathways. Besides the fission of the C_{alkyl}-N bond, *Pseudomonas* sp. strain 7-6 initiates

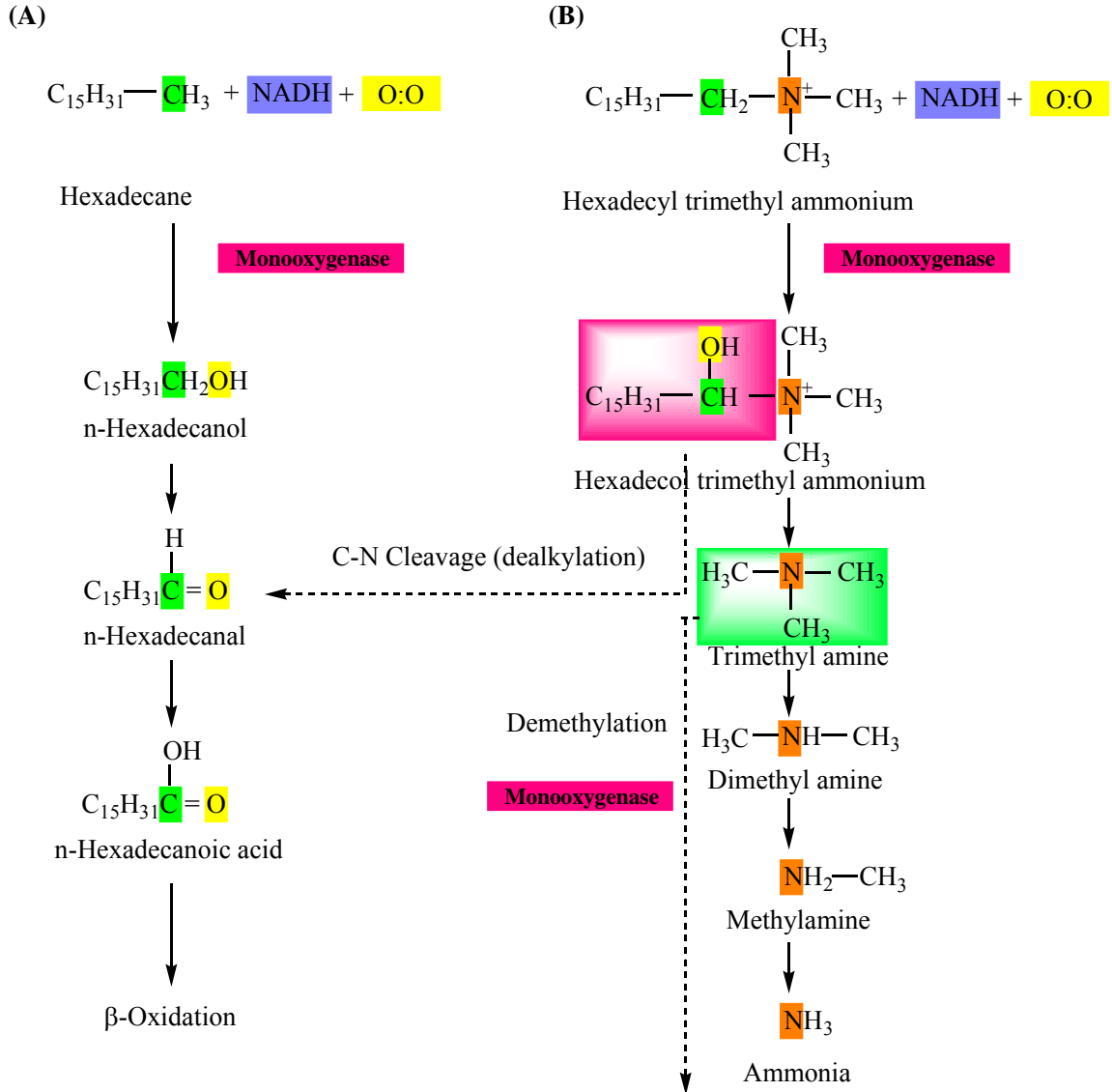


Figure 2.7. Pathways of (A) hexadecane and (B) hexadecyl trimethyl ammonium biotransformation in a mixed aerobic culture

the degradation via hydroxylation of the methyl group and cleavage of the C_{methyl}-N bond (demethylation).

The biotransformation of dialkonium QACs by *Pseudomonas fluorescens* TN4 (Nishihara et al., 2000) and *Achromobacter* sp. (van Ginkel, 2004) was found to occur in a similar fashion, by two consecutive dealkylations resulting in the formation of dimethyl amine as the end product.

None of the isolates described above was able to grow on the non-alkyl containing amines such as trimethyl amine and dimethyl amine after dealkylation, most probably due to the lack of methylmonooxygenases. In fact, symbiosis of at least two species is necessary for a complete mineralization of monoalkonium and dialkonium QACs to ammonia and carbon dioxide under aerobic conditions (Kim et al., 2001; Kroon and van Ginkel, 2001).

A biotransformation pathway of benzalkonium chlorides by *Aeromonas hydrophila* sp. K was recently reported (Patrauchan and Oriel, 2003). This pathway is similar to that of mono and dialkonium chlorides and commenced with a dealkylation step resulting in the formation of benzyl dimethyl amine (BDMA) as the first intermediate. This bacterium is also capable of growing on benzyl dimethyl amine as sole carbon and energy source and converts it to benzyl methyl amine, benzyl amine and ammonium by following two demethylations and a debenzylation, respectively. On the other hand, van Ginkel (2004) demonstrated an alternative benzalkonium chloride biotransformation pathway in a mixed culture. Based on his findings, benzalkonium chlorides are transformed into benzyl dimethyl amine, dimethyl amine and ammonia following consecutive dealkylation, debenzylation and demethylation steps which

involve three microorganisms that utilize the alkyl chain, the aromatic moiety and the dimethyl amine, respectively (van Ginkel, 2004).

Overall, the biotransformation pathways of QACs indicate that biotransformation is mostly commenced with the cleavage of C_{alkyl}-N bond irrespective of the type of QACs and the degradation of the produced alkanals proceeds via β -oxidation for complete mineralization. Once the alkyl chain is removed from a QAC, the QAC loses its toxicity. On the other hand, hydrophilic compounds such as trimethyl amine, dimethyl amine and benzyl dimethyl amine, formed after the dealkylation are utilized by other microorganisms. Obtaining sustainable microbial consortia that can mineralize a QAC to ammonium and carbon dioxide is difficult because QACs are biocides and are very toxic to microorganisms that are not capable of resisting them. QAC degraders are generally resistant to QACs and the ones that degrade the biotransformation products may not be. However, many studies performed with mixed cultures showed the ultimate degradation of QACs whereas none of them investigated the community structure of a QAC degrading consortium.

2.3.2. Anaerobic Biotransformation

QACs are rapidly and strongly sorbed onto a wide variety of materials of environmental relevance such as biomass, sediment, clay, and minerals. Indeed, sorption generally outcompetes biodegradation in aerobic environments and therefore, QACs are transferred to anoxic/anaerobic compartments such as anaerobic digesters, as part of the primary and waste activated sludge, and aquatic sediments (Boethling, 1994). Under anaerobic conditions, there is no evidence of mineralization of QACs that contain alkyl or benzyl groups (Battersby and Wilson, 1989; Federle and Schwab, 1992; Garcia et al.,

1999, 2000), most likely because of the highly reduced nature of these substituent groups. Moreover, QACs are inhibitory to anaerobic microbial processes such as methanogenesis (Battersby and Wilson, 1989; Garcia et al., 1999, 2000; Tezel et al., 2006, 2007).

On the other hand, diethylester dimethyl ammonium chloride (DEEDMA-Cl), a recent analog of dialkonium chlorides was completely degraded by anaerobic digester sludge in a standard test based on biogas formation (Giolando et al., 1995). DEEDMA-Cl differs structurally from dialkonium chlorides by the inclusion of two ester linkages between the ethyl and alkyl chains. These ester linkages allow DEEDMA-Cl to be rapidly and completely degraded in standard laboratory screening tests and a range of environmental media such as sludge, soil and river water with half-lives ranging from 0.8 to 18 days. Likewise, it is known that natural QACs such as choline and betaine can be ultimately degraded under anoxic/anaerobic conditions (Neill et al., 1978; King, 1984). As a result, QACs in which the hydrophobic moieties are linked to the head group with ester bonds (esterquats), choline, betaine (natural QACs), and those in which alkyl chains are linked directly to N^+ have a different fate under anoxic/anaerobic conditions. The latter are recalcitrant under these conditions.

QACs possess alkyl, benzyl and/or methyl functional groups. As discussed above, the initial step in QAC biotransformation is very similar to that of the hydrocarbon degradation under aerobic conditions. Moreover, similar types of microorganisms participate in the biotransformation of both types of compounds under aerobic conditions. Relatively recently it was discovered that both aliphatic and aromatic hydrocarbons can be degraded under anoxic/anaerobic conditions by the fumarate addition mechanism (Heider et al., 1998; Spormann and Widdel, 2000; Van Hamme et al., 2003; Suflita et al.,

2004; Davidova et al., 2005; Callaghan et al., 2006; Heider, 2007; Washer and Edwards, 2007; Winderl et al., 2007; Callaghan et al., 2008; Grundmann et al., 2008). Under this pathway, biotransformation of hydrocarbons involves the integration of a fumarate molecule to the alkyl group of alkylbenzenes or to the subterminal C atom of alkanes. The enzymes that catalyze the fumarate addition to hydrocarbons are *benzylsuccinate synthase* (*Bss*) and *alkylsuccinate synthase* (*Ass*). These enzymes are glycyl radical enzymes that are grouped in the *pyruvate-formate lyase* (*Pfl*) superfamily and have catalytic subunits with a strong homology to *Pfl* (Coschigano et al., 1998; Krieger et al., 2001; Callaghan et al., 2008; Grundmann et al., 2008). The fumarate addition to toluene catalyzed by *Bss* is given in Figure 2.8 (Widdel and Rabus, 2001; Himo, 2002; Himo, 2005) and follows: (1) the glycyl radical (-NH-•CH-CO-) of *Bss* acquires a hydrogen atom from a neighboring cysteine residue (-SH) creating a thiyl radical (-S•); (2) the thiyl radical abstracts a hydrogen atom from toluene and creates a toluyl radical; (3) this radical attacks the double bond of fumarate producing a benzylsuccinyl radical intermediate; (4) a hydrogen atom is transferred to benzylsuccinyl radicals from cysteine yielding benzylsuccinate, and (5) glycine is converted to glycyl radical by transferring a hydrogen to thiyl and the enzyme is reactivated.

Following this unusual addition reaction, the C-skeleton of the hydrocarbon is reorganized and goes into β -oxidation metabolism (Figure 2.9). Such biotransformation pathways have been observed to take place under Fe(III)-reducing, denitrifying, sulfate reducing and methanogenic conditions.

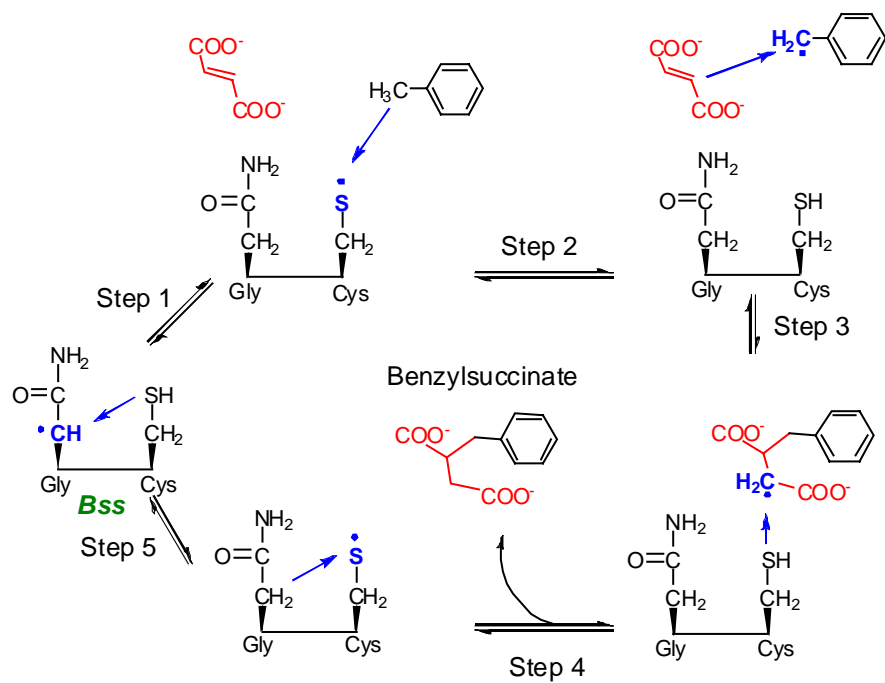


Figure 2.8. Scheme of fumarate addition to toluene by benzylsuccinate synthase (Bss)

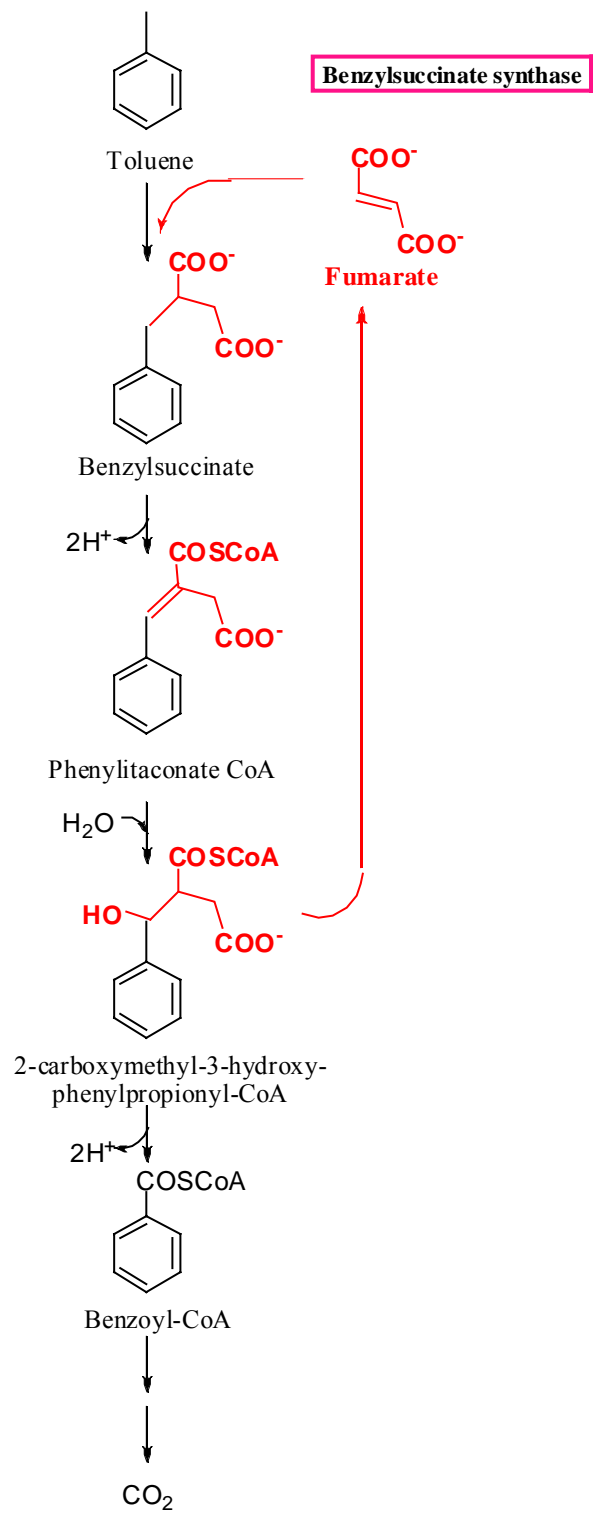


Figure 2.9. Biotransformation of toluene by the fumarate addition mechanism under anoxic/anaerobic conditions

Other terminal electron acceptors shown to be used during anaerobic hydrocarbon metabolism include manganese oxides, soil humic acids, anthraquinone-2,6-disulfonate and fumarate.

QACs may be completely mineralized through fumarate addition mechanism under anoxic/anaerobic conditions. For instance, complete mineralization of a benzalkonium chloride, C₁₄BDMA-Cl, was successfully simulated using the University of Minnesota-Biocatalysis/Biodegradation Database-Pathway Prediction System (UM-BBD-PPS) (<http://umbbd.msi.umn.edu/predict/>) (Wackett and Ellis, 1999; Ellis et al., 2000; Hou et al., 2003) (Figure 2.10). According to this pathway, fumarate is added to a methylene carbon that connects the benzene ring to the quaternary nitrogen of C₁₄BDMA. The resulting product, which is fumarate added C₁₄BDMA or (2R)-2-((dimethyl(tetradecyl)ammonio) (phenyl)methyl)succinate (abbreviated as C₁₄BDMA^{*}, hereafter), is activated by coenzyme A (CoA), followed by rearrangement of the C₁₄BDMA^{*} skeleton. The rearrangement results in the separation of the benzyl group from the C₁₄BDMA^{*} yielding tetradecyldimethyl amine (C₁₄DMA) and benzalsuccinylCoA (BS-CoA). Then, C₁₄DMA and BS-CoA are utilized as carbon and energy source via β -oxidation after further metabolized through consecutive fumarate addition and benzoyl-CoA pathways, respectively (Heider et al., 1998; Boll et al., 2002; Gibson and Harwood, 2002; Davidova et al., 2005). Although the fumarate addition mechanism is a promising pathway of QAC degradation under anoxic/anaerobic conditions, no attempt has yet been made to delineate the biotransformation potential of QACs via this mechanism.

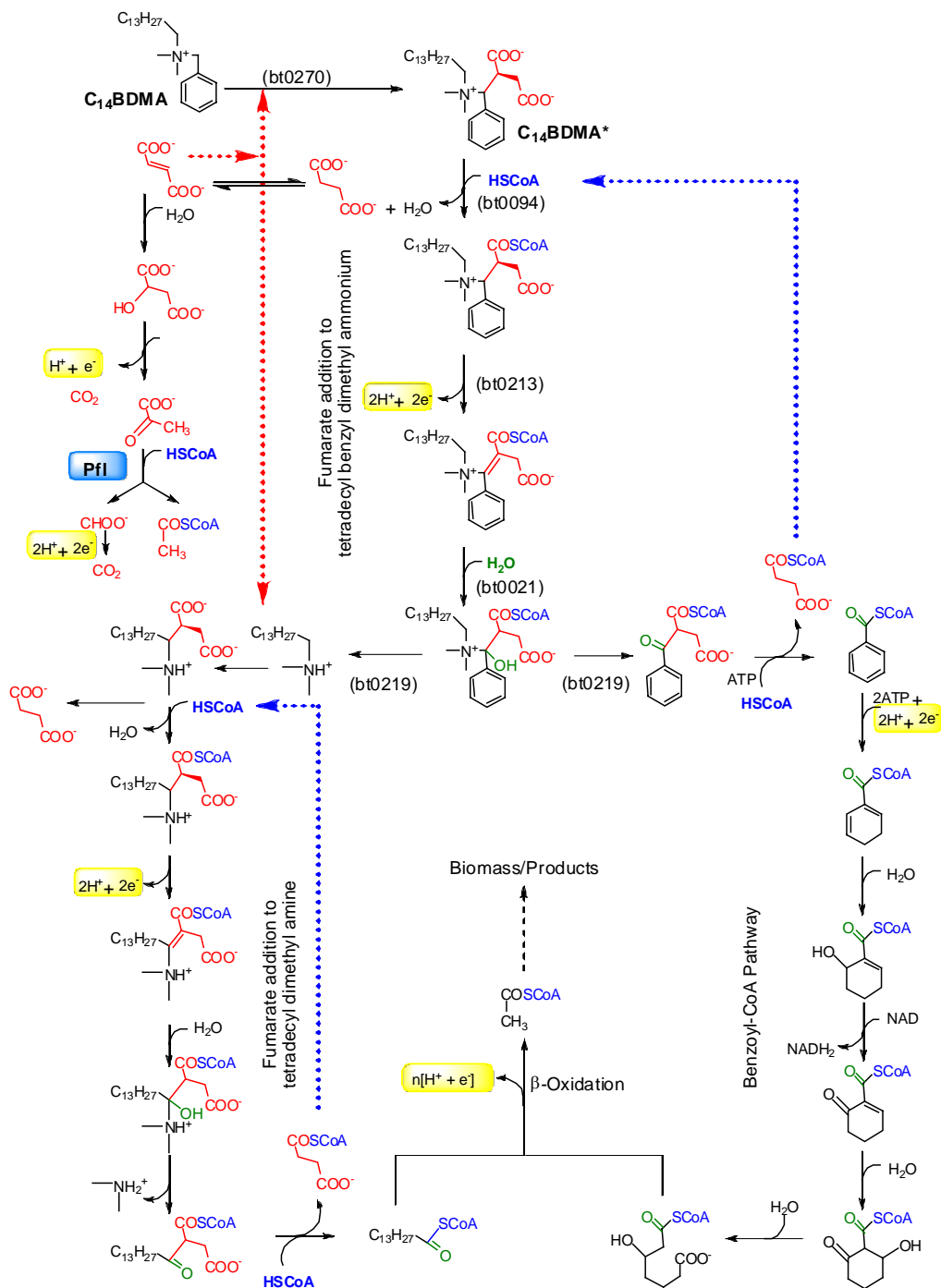


Figure 2.10. Predicted biotransformation pathway of C₁₄BDMA by the fumarate addition mechanism using UM-BBD-PPS (annotations in parentheses represent the UM-BBD-PPS rules applicable to the corresponding reaction)

CHAPTER 3

MATERIALS AND METHODS

3.1. General Analytical Methods

3.1.1. pH

All pH measurements were performed using the potentiometric method with a ATI Orion Model 370 digital pH meter (Orion Research Inc., Boston, MA) and a gel-filled combination pH electrode (VWR International, West Chester, PA). The meter was calibrated weekly with pH 4.0, 7.0, and 10.0 standard buffer solutions (Fisher Scientific, Pittsburg, PA).

3.1.2. Oxidation-Reduction Potential (ORP)

ORP measurements were performed using an ATI Orion Model 370 millivolt meter and a Sensorex combination ORP electrode (Sensorex Co., Garden Grove, CA) which is a platinum electrode with an Ag/AgCl reference electrode in a 3.5 M KCl gel. The meter and electrode output were periodically checked using saturated quinhydrone solutions prepared in pH 4.0, 7.0, and 10.0 buffers. To obtain ORP values with reference to the standard hydrogen electrode, a correction factor of +220 mV was added to the instrument reading values.

3.1.3. Ammonia

Ammonia concentration was measured using the distillation method described in *Standard Methods* (Eaton et al., 2005). The samples were centrifuged at 12,000 rpm for 15 minutes and filtered through a 0.2 μm nitrocellulose membrane filter (Fisher

Scientific, Pittsburgh, PA). The ammonia distillation was performed using a Labconco distillation apparatus (Labconco Corp., Kansas City, MO). The distillate then was titrated with 0.2 N H₂SO₄ and the ammonia was quantified.

3.1.4. Total and Soluble Chemical Oxygen Demand (tCOD and sCOD)

COD was measured using the closed reflux, colorimetric method as described in *Standard Methods* (Eaton et al., 2005). An aliquot of 3 mL digestion solution composed of 4.9 g K₂Cr₂O₇, 6 g HgSO₄, 6 g Ag₂SO₄ and 500 mL H₂SO₄ was transferred to HACH COD digestion vials (HACH Company, Loveland, CO) and then 2 mL of sample was added to the vial. After tumbling the vial for 4-8 times, the content in the vials was digested at 150°C for 2 hours and then cooled down to room temperature. The absorbance was measured at 620 nm with a Hewlett-Packard Model 8453 UV/Visible spectrophotometer (Hewlett-Packard Co., Palo Alto, CA) equipped with a diode array detector, deuterium and tungsten lamps and a 1 cm path length. Samples were centrifuged and filtered through a 0.2 µm nitrocellulose membrane filter if the sCOD was measured, otherwise well-mixed samples were used after appropriate dilution for tCOD measurements. All samples were prepared in triplicates and a calibration curve was prepared using 1 g/L standard solution of potassium hydrogen phthalate (KHP).

3.1.5. Dissolved Organic Carbon (DOC)

DOC measurements were performed using a Shimadzu TOC-5050A Total Organic Carbon Analyzer (Shimadzu Scientific Instruments Inc., Columbia, MD) equipped with a non-dispersive infrared detector for the analysis of total, organic and inorganic carbon of liquid samples. Liquid samples were filtered through 0.2 µm PVDF filters, acidified below pH 2.0 using a 0.2 N HCl solution and purged with CO₂-free air

for 2 minutes. Triplicate measurements were performed for each sample using 25 μL injection volume. Carbon analysis was based on catalytic combustion of the sample at 680°C. A calibration curve was prepared using 1g C/L standard solution of KHP.

3.1.6. Total and Volatile Solids (TS and VS)

Total solids content of samples were determined according to procedures outlined in *Standard Methods* (Eaton et al., 2005). Samples were weighed in pre-ignited (550°C) and cooled ceramic crucibles using an Ohaus AP250D Analytical Balance (precise to ± 0.02 mg up to 52 g, and to ± 0.1 mg between 52 and 210 g). The samples were then dried at 105°C for 24 hours in a Fisher Isotemp Model 750G oven. After drying, the crucibles were transferred to a desiccator until cooled, and then the dry weight was measured. If VS were to be determined, the crucibles were transferred to a Fisher Isotemp Model 550-126 muffle furnace and ignited at 550°C for 20 minutes. After ignition, the samples were cooled in a desiccator and the remaining solids weight was measured. TS and VS were then calculated using the equations below.

$$\text{TS (mg/L)} = \frac{(\text{Crucible weight after } 105^{\circ}\text{C (mg)}) - (\text{Crucible tare weight (mg)})}{\text{Sample volume (L)}}$$

$$\text{VS (mg/L)} = \frac{(\text{Crucible weight after } 105^{\circ}\text{C (mg)}) - (\text{Crucible weight after } 550^{\circ}\text{C (mg)})}{\text{Sample volume (L)}}$$

3.1.7. Total and Volatile Suspended Solids (TSS and VSS)

TSS and VSS were determined according to procedures described in *Standard Methods* (Eaton et al., 2005). Whatman GF/C glass fiber filters (47 mm diameter and 1.2

µm nominal pore size; Whatman, Florham Park, NJ) were washed with deionized (DI) water and ignited at 550°C for 20 minutes in a Fisher Isotemp Model 550-126 muffle furnace before use. The filters were then cooled in a desiccator and weighed. Samples of known volume were filtered through the glass fiber filters. The filters were then rinsed with 10 mL DI water to remove dissolved organics and inorganic salts. The filters containing the samples were dried at 105°C for 90 minutes. After cooling in a desiccator, the dry weight was recorded and the filters containing the dry samples were ignited at 550°C for 20 minutes. After ignition, the samples were cooled down in a desiccator and the weight was measured. TSS and VSS concentrations were then calculated using the equations below.

$$\text{TSS (mg/L)} = \frac{(\text{Filter weight after } 105^{\circ}\text{C (mg)}) - (\text{Filter tare weight (mg)})}{\text{Sample volume (L)}}$$

$$\text{VSS (mg/L)} = \frac{(\text{Filter weight after } 105^{\circ}\text{C (mg)}) - (\text{Filter weight after } 550^{\circ}\text{C (mg)})}{\text{Sample volume (L)}}$$

3.1.8. Total Gas Production

Total gas production in closed assay bottles and large volume reactors was measured by either the gas-water displacement method or with a VWR Pressure/Vacuum transducer (resolution –1 atm to 1.974 atm with an accuracy of 0.002 atm).

3.1.9. Gas Composition

The gas composition was determined by a gas chromatography (GC) unit (Agilent Technologies, Model 6890N; Agilent Technologies, Inc., Palo Alto, CA) equipped with

two columns and two thermal conductivity detectors. Methane (CH₄) and dinitrogen (N₂) were separated with a 15 m HP-Molesieve fused silica, 0.53 mm i.d. column (Agilent Technologies, Inc.). Carbon dioxide (CO₂), nitric oxide (NO) and nitrous oxide (N₂O) were separated with a 25 m Chrompac PoraPLOT Q fused silica, 0.53 mm i.d. column (Varian, Inc., Palo Alto, CA). Helium was used as the carrier gas at a constant flow rate of 6 mL/min. The 10:1 split injector was maintained at 150°C, the oven was set at 40°C and the detector temperature was set at 150°C. All gas analyses were performed by injecting a 100 µL gas sample. The minimum detection limits for CH₄, CO₂, NO, N₂O and N₂ was 500, 800, 500, 7 and 50 ppmv, respectively.

3.1.10. Volatile Fatty Acids (VFAs)

VFAs (C₂ to C₇, i.e. acetic, propionic, iso-butyric, n-butyric, iso-valeric, n-valeric, iso-caproic, n-caproic and heptanoic acids) were measured after acidification of filtered samples with a 2.5% H₃PO₄ solution containing 1.5 g/L acetoin as the internal standard (sample:acid, 2:1 volume ratio) using an Agilent 6890 Series GC unit equipped with a flame ionization detector and a 35-m Stabilwax-DA, 0.53-mm I.D. column (Restek, Bellefonte, PA). Samples used for the measurement of VFAs were prepared by centrifugation at 10,000 rpm for 30 minutes and filtration through 0.22-µm PVDF membrane filters before acidification. The minimum detection limit for each acid mentioned above was 0.25, 0.10, 0.03, 0.02, 0.10, 0.08, 0.02, 0.02, 0.05 mM, respectively.

3.1.11. Organic Acids, Alcohols and Carbohydrates

Non-flame ionizable organic acids (formic, oxalic, citric, malic, pyruvic, lactic, succinic and fumaric acids), alcohols (methanol, ethanol, and buthanol), and

carbohydrates (glucose) were measured with a HP 1100 Series HPLC (Hewlett Packard, Palo Alto, CA) unit equipped with an Aminex HPX-87H ion exclusion column (300 × 7.8 mm)(Bio-Rad, Richmond, CA) and an Agilent 1100 Series UV/visible diode array and refractive index detectors (Agilent Technologies, New Castle, DE). A 0.01 N H₂SO₄ solution was used as the mobile phase with a flow rate of 0.6 mL/min and the column was maintained at 65°C. The samples were centrifuged and the supernatant was acidified with 0.2 N H₂SO₄ in a 1:1 ratio, and filtered through 0.2 μm membrane filters before the analyses. Organic acids were detected by the UV detector at 210 nm wavelength, whereas detection of alcohols and carbohydrates was achieved by the refractive index detector. A sample chromatogram of organic acids is given in Figure 3.1.

3.1.12. Anions

Chloride (Cl⁻), nitrite (NO₂⁻), bromide (Br⁻), nitrate (NO₃⁻), phosphate (PO₄³⁻), and sulfate (SO₄²⁻) anion concentrations were determined using a Dionex DX-100 ion chromatography unit (Dionex Corporation, Sunnyvale, CA) equipped with a suppressed conductivity detector, a Dionex IonPac AG14A (4x50mm) precolumn, and a Dionex IonPac AS14A (4x250 mm) analytical column. The unit was operated in autosuppression mode with 1mM NaHCO₃/8mM Na₂CO₃ eluent and a flow rate of 1 mL/min. All samples were filtered through 0.2 μm membrane filters prior to injection. The minimum detection limit for each anion listed above was 0.03, 0.02, 0.03, 0.04, 0.02 and 0.05 mM, respectively.

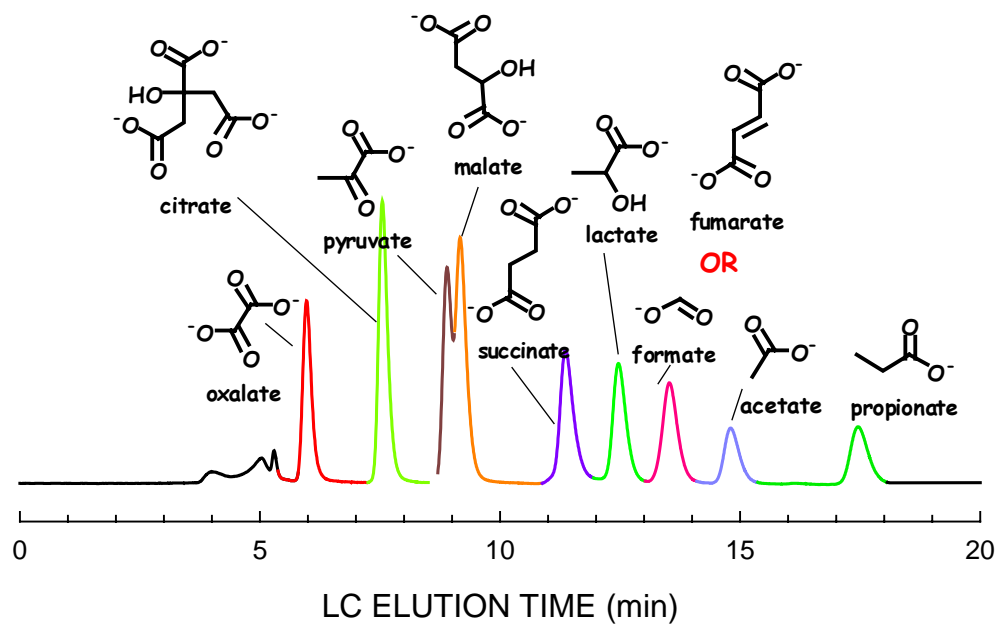


Figure 3.1. Sample LC chromatogram of organic acids

3.2. Analyses of QACs and Related Compounds

Analytical methods to quantify QACs and their potential transformation products such as benzyl amines and alkyl amines developed during this study are summarized in this section.

3.2.1. Chemicals

Benzalkonium chlorides (C_n BDMA-Cl: 32% C_{12} BDMA-Cl, 40% C_{14} BDMA-Cl, 8% C_{16} BDMA-Cl, 10% ethanol and 10% water (% w/w)), didecyl dimethyl ammonium chloride (80% DC₁₀DMA-Cl, 10% ethanol and 10% water (% w/w)), dioctyl dimethyl ammonium chloride (80% DC₈DMA-Cl, 10% ethanol and 10% water (% w/w)) and octyl decyl dimethyl ammonium chloride (80% DC₈₋₁₀DMA-Cl, 10% ethanol and 10% water (% w/w)) were obtained from Lonza Inc. (Williamsport, PA). Dodecyl benzyl dimethyl ammonium (C_{12} BDMA-Cl, $\geq 99\%$), tetradecyl benzyl dimethyl ammonium (C_{14} BDMA-Cl, $\geq 99\%$) and hexadecyl benzyl dimethyl ammonium (C_{16} BDMA-Cl, $\geq 97\%$) chlorides, benzyl methyl amine (BMA, $\geq 97\%$), benzyl amine (BA, $\geq 99.5\%$), tetradecyl dimethyl amine (C_{14} DMA, $\geq 95\%$) and hexadecyl dimethyl amine (C_{16} DMA $\geq 95\%$) were obtained from Fluka (St. Louis, MO). Benzyl dimethyl amine (BDMA, $\geq 99\%$) and dodecyl dimethyl amine (C_{12} DMA, $\geq 95\%$) were purchased from Aldrich Chemical Company (St. Louis, MO) and Acros Organics (Morris Plains, NJ), respectively. Dodecyl trimethyl ammonium (C_{12} TMA-Cl, $>99\%$), tetradecyl trimethyl ammonium (C_{14} TMA-Cl, $>99\%$) and hexadecyl trimethyl ammonium chlorides (C_{16} TMA-Cl, $>99\%$) were acquired from TCI Chemicals (Tokyo Chemical Industry Co., Ltd., Tokyo, Japan). Molecular structures, formulas and weights are given in Table 3.1.

Table 3.1. Chemicals used in this study

Quaternary Ammonium Compounds	Formula	Molecular Weight g mole ⁻¹
Monoalkonium Chlorides (CnTMA-Cl)		
$\begin{array}{c} \text{C}_{12}\text{H}_{25}-\text{N}^+- \\ \\ \text{Cl}^- \\ \text{Dodecyl trimethyl ammonium chloride} \end{array}$	C ₁₅ H ₃₄ NCl	263.9
$\begin{array}{c} \text{C}_{14}\text{H}_{29}-\text{N}^+- \\ \\ \text{Cl}^- \\ \text{Tetradecyldimethyl amine} \end{array}$	C ₁₇ H ₃₈ NCl	291.9
$\begin{array}{c} \text{C}_{16}\text{H}_{33}-\text{N}^+- \\ \\ \text{Cl}^- \\ \text{Hexadecyldimethyl amine} \end{array}$	C ₁₉ H ₄₂ NCl	320.0
Dialkonium Chlorides (DCnDMA-Cl)		
$\begin{array}{c} \text{C}_8\text{H}_{17}-\text{N}^+- \\ \quad \\ \text{Cl}^- \quad \text{C}_8\text{H}_{17} \\ \text{Diocetyl dimethyl ammonium chloride} \end{array}$	C ₁₈ H ₄₀ NCl	306.0
$\begin{array}{c} \text{C}_8\text{H}_{17}-\text{N}^+- \\ \quad \\ \text{Cl}^- \quad \text{C}_{10}\text{H}_{21} \\ \text{Octyl decyl dimethyl ammonium chloride} \end{array}$	C ₂₀ H ₄₄ NCl	334.0
$\begin{array}{c} \text{C}_{10}\text{H}_{21}-\text{N}^+- \\ \quad \\ \text{Cl}^- \quad \text{C}_{10}\text{H}_{21} \\ \text{Didecyl dimethyl ammonium chloride} \end{array}$	C ₂₂ H ₄₈ NCl	362.1
Benzalkonium Chlorides (CnBDMA-Cl)		
$\begin{array}{c} \text{C}_{12}\text{H}_{25}-\text{N}^+- \\ \quad \\ \text{Cl}^- \quad \text{C}_6\text{H}_5 \\ \text{Dodecyl benzyl dimethyl ammonium chloride} \end{array}$	C ₂₁ H ₃₈ NCl	340.0
$\begin{array}{c} \text{C}_{14}\text{H}_{29}-\text{N}^+- \\ \quad \\ \text{Cl}^- \quad \text{C}_6\text{H}_5 \\ \text{Tetradecyl benzyl dimethyl ammonium chloride} \end{array}$	C ₂₃ H ₄₂ NCl	368.0
$\begin{array}{c} \text{C}_{16}\text{H}_{33}-\text{N}^+- \\ \quad \\ \text{Cl}^- \quad \text{C}_6\text{H}_5 \\ \text{Hexadecyl benzyl dimethyl ammonium chloride} \end{array}$	C ₂₅ H ₄₆ NCl	396.1

Table 3.1 (Continued)

Amines	Formula	Molecular Weight g mole ⁻¹
$\begin{array}{c} \\ \text{C}_{12}\text{H}_{25}-\text{N} \\ \\ \text{Dodecyl dimethyl amine} \end{array}$	$\text{C}_{14}\text{H}_{31}\text{N}$	213.4
$\begin{array}{c} \\ \text{C}_{14}\text{H}_{29}-\text{N} \\ \\ \text{Tetradecyl dimethyl amine} \end{array}$	$\text{C}_{16}\text{H}_{35}\text{N}$	241.5
$\begin{array}{c} \\ \text{C}_{16}\text{H}_{33}-\text{N} \\ \\ \text{Hexadecyl dimethyl amine} \end{array}$	$\text{C}_{18}\text{H}_{39}\text{N}$	269.5
$\begin{array}{c} \text{H}_2\text{N} \\ \\ \text{C}_6\text{H}_5 \\ \text{Benzyl amine} \end{array}$	$\text{C}_7\text{H}_9\text{N}$	107.2
$\begin{array}{c} \text{HN} \\ \\ \text{C}_6\text{H}_5 \\ \text{Benzyl methyl amine} \end{array}$	$\text{C}_8\text{H}_{11}\text{N}$	121.2
$\begin{array}{c} \\ \text{N} \\ \\ \text{C}_6\text{H}_5 \\ \text{Benzyl dimethyl amine} \end{array}$	$\text{C}_9\text{H}_{13}\text{N}$	135.2

3.2.2. Disulfine Blue Pair-Ion Extraction Method (DSB-PIX)

Routine, non-specific quantification of QACs in whole and centrifuged culture samples was performed using a previously reported and modified disulfine blue pair-ion extraction method (HMSO, 1981). According to this method, an anionic dye-QAC ion pair is formed, which is then solvent extracted, and the color intensity in the solvent phase is measured spectrophotometrically. Analyses were carried out in 25-mL test tubes by adding 5 mL of acetate buffer, 2 mL of dye solution and 2 mL of the sample. The acetate buffer included 115 g anhydrous sodium acetate and 35 mL glacial acetic acid in 1 L DI water. The dye solution was prepared by dissolving 0.16 g of Patent Blue VF (Acros Organics, N.J., USA) in 2 mL ethanol and diluting to 250 mL with DI water.

Addition of 10 mL of methylene chloride to the 25-mL test tube resulted in the formation of a biphasic solution that was tumbled for 24 hours in order to achieve complete transfer of the dye-QAC ion pair into the solvent phase. The bottom solvent layer was then transferred into 2-mL clear glass vials and the color intensity measured with a UV/Vis HP model 8453 spectrophotometer equipped with a diode array detector (Hewlett-Packard Co., Palo Alto, CA, USA). The QAC concentration was quantified based on sample absorbance at the characteristic maximum wavelength of 628 nm and previously prepared calibration curves for each individual QAC at a concentration range 0 to 30 mg/L. Methylene chloride was used as the blank for all spectrophotometric analyses. The minimum method detection limit was 0.2 mg/L. Culture samples without any QACs, and DI water were analyzed using the same procedure and the resulting spectra did not have any background interference. Major QAC transformation products reported so far include tertiary and secondary amines which are positively charged at neutral pH (discussed in Chapter 2). Interference of these compounds with the quantification of QACs with the DSB-PIX method is insignificant (Figure 3.2).

3.2.3. Extraction of QACs from Biological Media

Extraction of QACs from biological media is challenging since QACs bind to organic material by both ionic and hydrophobic interactions. Therefore, both interactions have to be overcome. The extraction method described here therefore was designed to achieve a high degree of recovery of analytes from biological media by (1) elimination of hydrophobic interactions between QAC and biosolids with a water miscible solvent such as acetonitrile; (2) elimination of ionic interaction between QAC and biosolids through cation exchange; (3) forming a counter-ion (an anion) mediated hydrophobic ion-pair;

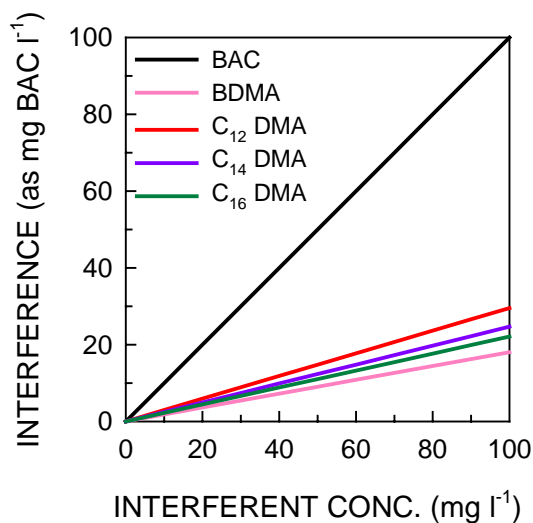


Figure 3.2. Extent of interference by protonated amines on the disulfine blue ion-pair extraction method (DSB-PIX) measurements.

and (4) transferring this ion-pair into a polar solvent (ethyl acetate) (Figure 3.3).

QACs and alkyl amines in 2.5 mL samples were extracted with a mixture of 1 mL of 100 mM AgNO₃, 1.5 mL of acetonitrile and 2.5 mL of ethylacetate. The recovery of each analyte by this method is between 97 and 102%. The ethyl acetate extraction efficiency for benzalkonium chlorides by using different salt combinations and no salt and acetonitrile is given in Table 3.2. The maximum extraction efficiency without any interference was obtained by using AgNO₃ and acetonitrile as the extraction mixture, therefore this mixture was used throughout the study.

3.2.4. High Performance Liquid Chromatography of QACs

Benzalkonium chlorides as well as benzyl dimethyl amine (BDMA), benzyl methyl amine (BMA) and benzyl amine (BA), which are possible BAC transformation products, were measured using a HP 1100 Series HPLC (Hewlett Packard, Palo Alto,

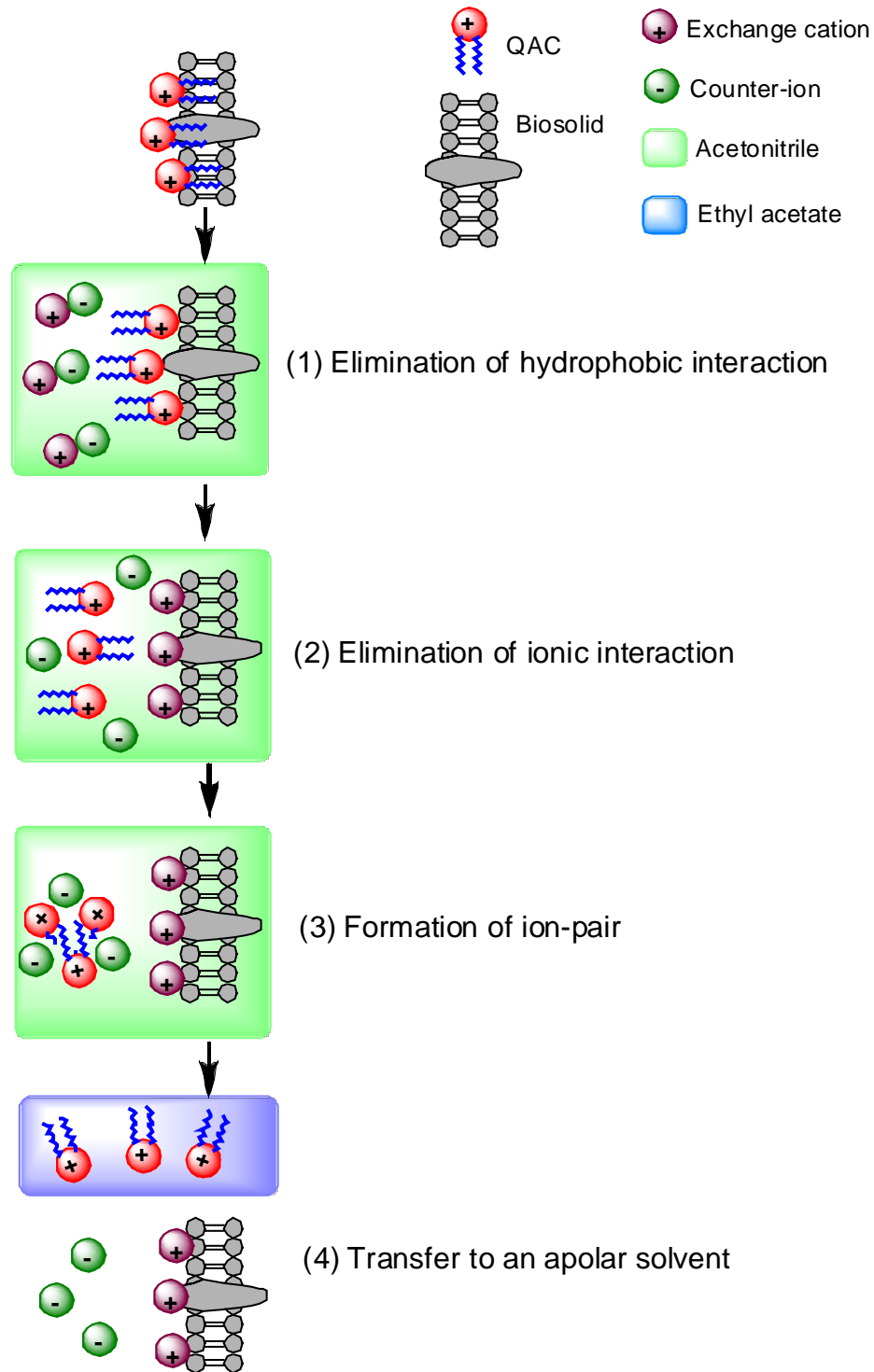


Figure 3.3. Mechanisms involved in QAC recovery from biological media by liquid/liquid extraction

Table 3.2. Ethyl acetate extraction efficiency for C₁₂BDMA-Cl, C₁₄BDMA-Cl and C₁₆BDMA-Cl from biological media containing 2.5 g VS/L

Modifier	C₁₂BDMA-Cl	C₁₄BDMA-Cl	C₁₆BDMA-Cl	Interference
No ACN/No Salt	0.0±0.0	0.0±0.0	0.0±0.0	+
ACN Only	92.3±2.5	91.2±2.5	96.7±3.0	+
100 mM AgNO ₃	73.4±2.0	80.4±2.1	119.2±2.1	-
100 mM KH ₂ PO ₄ +ACN (40:60)	95.0±2.7	97.5±2.7	96.8±2.9	+
100 mM KNO ₃ +ACN (40:60)	97.6±1.9	98.7±1.8	98.6±1.7	+
100 mM NaNO ₃ +ACN (40:60)	97.9±0.7	99.1±0.8	97.9±1.5	+
100 mM NH ₄ NO ₃ +ACN (40:60)	98.3±1.9	99.5±1.8	98.3±1.8	+
50 mM Co(NO ₃) ₂ +ACN (40:60)	96.4±1.3	98.3±1.2	90.9±3.7	+
100 mM AgNO₃+ACN (40:60)	97.4±1.9	99.0±1.8	97.5±2.2	-
100 mM HNO ₃ +ACN (40:60)	97.6±1.9	98.5±1.9	97.6±2.3	+

CA) unit equipped with a Phenomenex Luna SCX column (250 x 4.6 mm, 5 μ) (Phenomenex, Inc., Torrance, CA) followed by a Polaris C₁₈A column (50 x 4.6 mm, 3.2 μ) (MetaChem Technologies Inc., Torrance, CA). A Phenomenex SCX SecurityGuard cartridge (4 x 3.0 mm) was used as a precolumn. A 60:40 (v/v) mixture of acetonitrile and 50 mM phosphate buffer (pH 2.5) was used as the mobile phase at a flow rate of 1.0 ml/min and the columns were maintained at 35°C. Detection was achieved with a HP 1100 series UV-Vis diode array detector at a wavelength of 210 nm. The molar response factor for each analyte at 210 nm was 21.8 \pm 1.2 area unit/ μ M. The minimum detection limit for C₁₂BDMA-Cl, C₁₄BDMA-Cl, C₁₆BDMA-Cl, BA, BMA, and BDMA was 1.57, 2.55, 4.36, 1.13, 1.46 and 1.21 μ M, respectively. An example HPLC chromatogram of 10 μ M analytes is given in Figure 3.4.

3.2.5. Liquid Chromatography-Mass Spectrometry of QACs

Monoalkonium and dialkonium chlorides, and alkyl dimethyl amines, such as dodecyl (C₁₂DMA), tetradecyl (C₁₄DMA) and hexadecyl (C₁₆DMA) dimethyl amines, along with the benzalkonium chlorides were measured using an Agilent 1100 Series LC unit equipped with a Polaris C₁₈A column (50 x 4.6 mm, 3.2 μ) and an Agilent 1100 Series LC/MSD mass spectrometry (MS) detector. A gradient elution was applied using 0.01% (v/v) formic acid in DI water (A) and 0.01% formic acid in acetonitrile (B) as mobile phases at a flow rate of 1.0 mL/min (Figure 3.5(A)). The column was maintained at 35°C. MS analysis was conducted by electrospray ionization in positive mode at 70 eV fragmentation voltage with a mass scan range of m/z 50-500. The drying gas (nitrogen) flow was 13 L/min at 350°C, the nebulizer pressure was 50 psig, and the capillary voltage was 4000 V. Sample LC-MS chromatograms showing each analyte elution order and its

retention time are given in Figure 3.5 (B-E). The monitored ions of the target analytes are presented in Table 3.3.

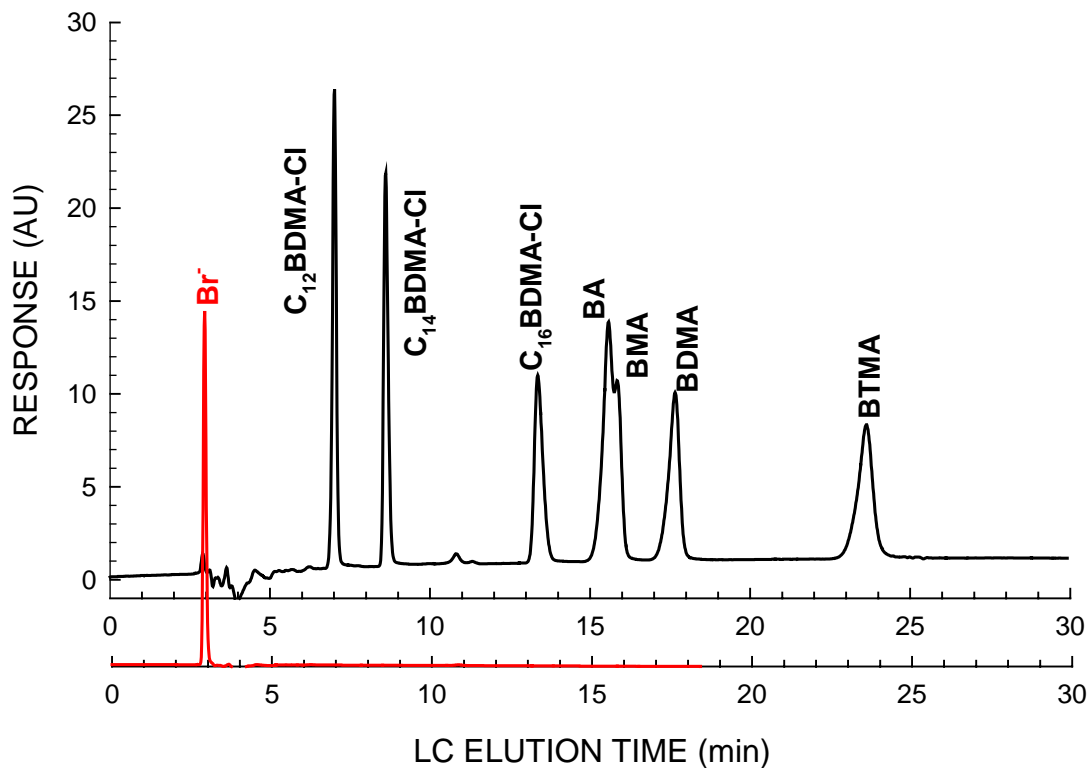


Figure 3.4. Sample HPLC chromatogram of benzalkonium chlorides (dodecylbenzyl dimethyl ammonium chloride (C₁₂BDMA-Cl), tetradecylbenzyl dimethyl ammonium chloride (C₁₄BDMA-Cl), hexadecylbenzyl dimethyl ammonium chloride (C₁₆BDMA-Cl)), benzyl amine (BA), benzyl methyl amine (BMA), benzyl dimethyl amine (BDMA) and benzyl trimethyl ammonium chloride (BTMA-Cl). The bromide peak is given as the reference for a non-retained analyte.

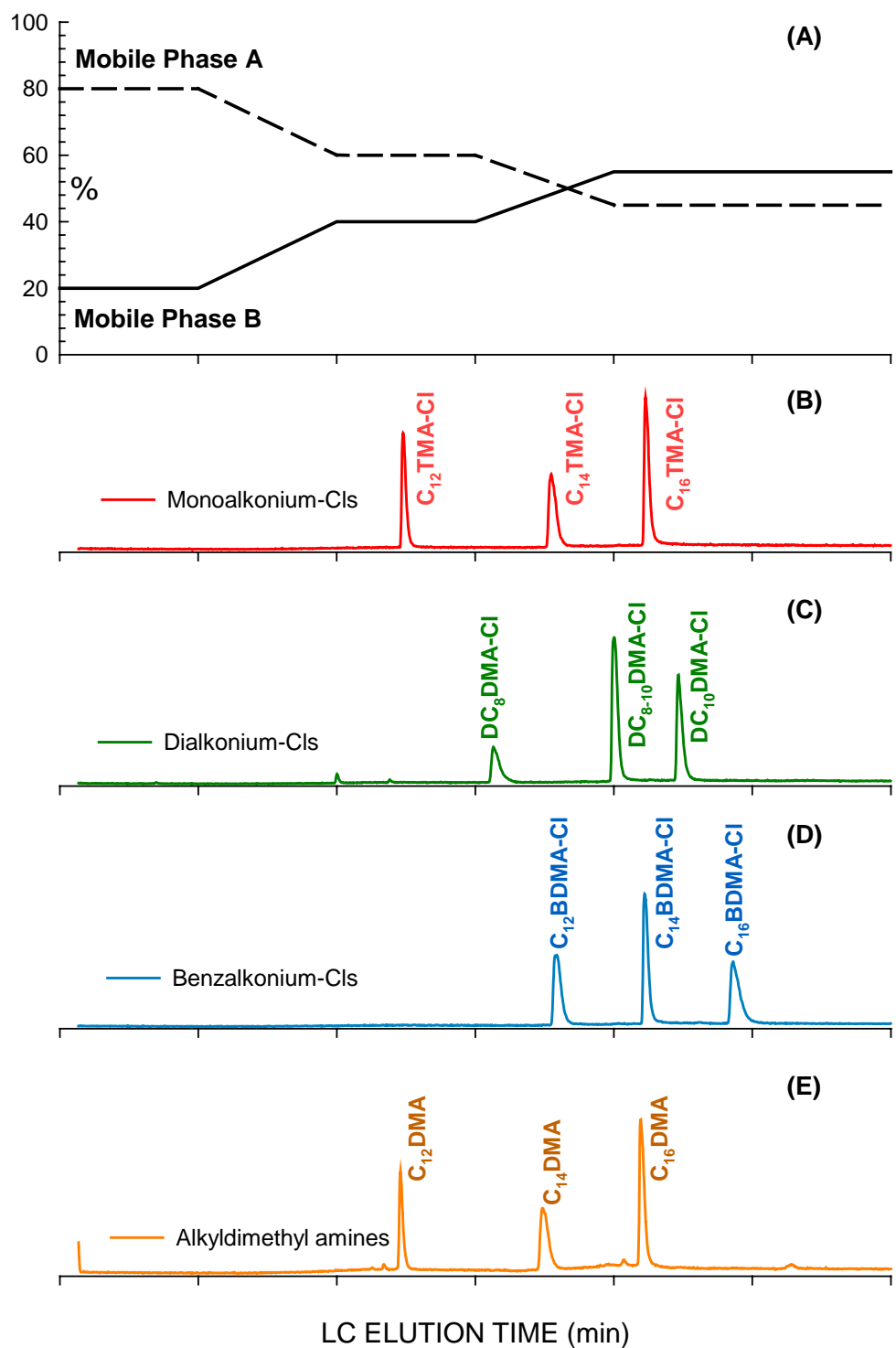


Figure 3.5. Applied mobile phase gradient (A) and sample LC-MS chromatograms of 10 μ M monoalkonium (B), dialkonium (C), benzalkonium (D) chlorides and alkyl dimethyl amines (E)

Table 3.3. LC/MS monitored ions of target analytes

Analyte	m/z parent ion
C ₁₂ TMA-Cl	228.3
C ₁₄ TMA-Cl	256.3
C ₁₆ TMA-Cl	284.3
DC ₈ DMA-Cl	270.3
DC ₈₋₁₀ DMA-Cl	298.3
DC ₁₀ DMA-Cl	326.4
C ₁₂ BDMA-Cl	304.3
C ₁₄ BDMA-Cl	332.3
C ₁₆ BDMA-Cl	360.4
C ₁₂ DMA	214.2
C ₁₄ DMA	242.3
C ₁₆ DMA	270.3

3.3. General Procedures

3.3.1. Methanogenic Culture Media

A mixed methanogenic culture used in this study was sustained in medium which supplied necessary nutrients, trace metals, and vitamins. The composition of the culture media is shown in Table 3.4. Resazurin was used as a redox indicator (ORP < -110 mV) (Gerhardt et al., 1994).

Culture media were prepared by adding the first six ingredients in Table 3.4 to 8 L DI water in 9-L Pyrex serum bottles. The bottles were then autoclaved at 250°F (121°C) and 21 psi (1.43 atm) for 45 minutes. After autoclaving, the bottles contents were purged with helium for 1.5 hours in order to strip oxygen from the media. After purging, and while the media were still warm, the rest of the ingredients listed in Table 3.4 were

added.

3.3.2. Aerobic Culture Media

Aerobic cultures used in this study were sustained in growth media shown in Table 3.5. The media was utilized without autoclaving.

Table 3.4. Composition of media for the mixed methanogenic culture used in this study

Compound/Solution	Concentration
K ₂ HPO ₄	0.9 g/L
KH ₂ PO ₄	0.5 g/L
NH ₄ Cl	0.5 g/L
MgCl ₂ ·6H ₂ O	0.2 g/L
Trace metal stock solution	1 mL/L
1 g/L resazurin stock	2 mL/L
Vitamin stock solution	1 mL/L
CaCl ₂ ·2H ₂ O	0.1 g/L
FeCl ₂ ·4H ₂ O	0.1 g/L
NaHCO ₃	3.5 g/L
Na ₂ S·9H ₂ O	0.5 g/L
Trace metal stock solution	Concentration
ZnCl ₂	0.5 g/L
MnCl ₂ ·4H ₂ O	0.3 g/L
H ₃ BO ₃	3.0 g/L
CoCl ₂ ·6H ₂ O	2.0 g/L
CuCl ₂ ·2H ₂ O	0.1 g/L
NiSO ₄ ·6H ₂ O	0.2 g/L
Na ₂ MoO ₄ ·2H ₂ O	0.3 g/L
Vitamin stock solution	Concentration
Biotin	0.2 g/L
Folic Acid	0.2 g/L
Pyridoxine hydrochloride	1.0 g/L
Riboflavin	0.5 g/L
Thiamine	0.5 g/L
Nicotinic Acid	0.5 g/L
Pantothenic Acid	0.5 g/L
Vitamin B12	0.01 g/L
p-Aminobenzoic Acid	0.5 g/L
Thioctic Acid	0.5 g/L

Table 3.5. Composition of media for the mixed aerobic culture used in this study

Compound	Concentration
K ₂ HPO ₄	600 mg/L
KH ₂ PO ₄	335 mg/L
CaCl ₂ ·2H ₂ O	67.5 mg/L
MgCl ₂ ·6H ₂ O	135 mg/L
MgSO ₄ ·7H ₂ O	267.5 mg/L
FeCl ₂ ·4H ₂ O	67.5 mg/L
Trace metal stock solution	0.67 mL/L
Trace metal stock solution	Concentration
ZnCl ₂	0.5 g/L
MnCl ₂ ·4H ₂ O	0.3 g/L
H ₃ BO ₃	3.0 g/L
CoCl ₂ ·6H ₂ O	2.0 g/L
CuCl ₂ ·2H ₂ O	0.1 g/L
NiSO ₄ ·6H ₂ O	0.2 g/L
Na ₂ MoO ₄ ·2H ₂ O	0.3 g/L

CHAPTER 4

QUANTITATIVE STRUCTURE-ACTIVITY RELATIONSHIPS FOR QACS

4.1. Introduction

Predictive quantitative structure-activity relationship (QSAR) analysis was developed to predict the biological activity of a variety of chemicals by using their physical and chemical properties defined by the molecular structure (e.g., functional groups) (Hansch et al., 1995). A descriptor which reflects the physical and chemical properties of a certain compound is identified and used to define relationships between the structure and the magnitude of its biological activity. For this reason, a descriptor has to be a comprehensive parameter which represents electronic, steric, and hydrophobic properties of a chemical, which in turn determine its (re)activity. The magnitude of the descriptor and the activity of a group of chemicals that contains a limited number of homologues are determined by either experiments or models and the relationship between the descriptor and the activity is generally analyzed by using linear regression. The correlation between the descriptor and the activity is then interpreted to estimate the activity of different chemicals for which the descriptor magnitude is known. QSAR is therefore a useful method to obtain information on the activity of a wide set of chemicals by using the information that is obtained for a limited set of chemicals. After the QSAR technique was introduced in 1962, it has been deployed for many applications such as drug discovery, adsorption, phase distribution, metabolism and excretion (ADME) evaluation of pharmaceuticals, evaluation of mutagenesis and carcinogenesis,

toxicity/ecotoxicity, and environmental fate of a wide variety of chemicals (Hansch et al., 1995).

Sustainable development became a key concept in the world as the consumption of the world's limited natural resources and environmental pollution significantly increased since the industrial revolution. Given the environmental and human health impacts of anthropogenic chemicals and formulations, management of raw materials, production and formulation, consumption and disposal of these formulations as well as understanding their environmental impact with a "cradle-to-grave" approach is a must. Therefore, QSAR is a simple and useful tool that can be pursued in the exploitation of chemicals as well as in determining their environmental impact and risk.

QACs are a group of compounds which contain homologues with a relatively high structural variety (Chapter 2). Tones of QACs with different molecular structures are consumed and released into engineered and natural systems. Each QAC structure has its own fate in these systems, therefore a comprehensive assessment of environmental risk associated with QACs is difficult. In turn, using QSAR is a promising approach to understand the fate and impact of the QACs in both engineered and natural systems.

The high affinity of QACs to sorb on biological matrices and their biocidal activity are major factors that determine their fate and impact in biological systems. However, until recently, there has been limited work on QSAR modeling of biosolids partitioning and toxicity of QACs (Garcia et al., 2001; Roberts and Costello, 2003; Garcia et al., 2004) and these works are not comprehensive and conclusive.

The objectives of the research reported in this chapter were to (a) define and evaluate a structural descriptor for QACs; and (b) develop relationship between the

identified descriptor and biosolids partitioning of QACs on different municipal wastewater sludges and toxicity for QACs using Microtox® toxicity assay.

4.2. Materials and Methods

4.2.1. Target compounds

Monoalkonium, dialkonium and benzalkonium chlorides were used. Homologues within each of these QACs groups differ in terms of alkyl chain length. The QACs used in this part of the study were dodecyl (C_{12} TMA-Cl), tetradecyl (C_{14} TMA-Cl) and hexadecyl (C_{16} TMA-Cl) trimethyl ammonium chloride, dioctyl (DC_8 DMA-Cl), octyldecyl (DC_{8-10} DMA-Cl) and didecyl (D_{10} DMA-Cl) dimethyl ammonium chloride, and dodecyl (C_{12} BDMA-Cl), tetradecyl (C_{14} BDMA-Cl) and hexadecyl (C_{16} BDMA-Cl) benzyl dimethyl ammonium chloride (see Chapter 3 for their description).

4.2.2. Critical Micelle Concentration (CMC) Analysis

The critical micelle concentration (CMC) of each QAC in DI water was measured by using a method described by Dominguez et al. (1997) which is based on the tautomerism of benzoylacetone (BZA) (Dominguez et al., 1997). According to this method, BZA exists as a mixture of ketonic and enolic tautomers (Figure 4.1) in aqueous solutions which have characteristic wavelengths at 250 and 315 nm, respectively.

The concentration of enolic tautomer increases in the solution when a surfactant concentration reaches its CMC value and above since the enolic form is taken up by the surfactant micelles, the reaction proceeds forward (Figure 4.1). When the concentration of the enolic tautomer is plotted against the logarithm of the QAC concentration, the

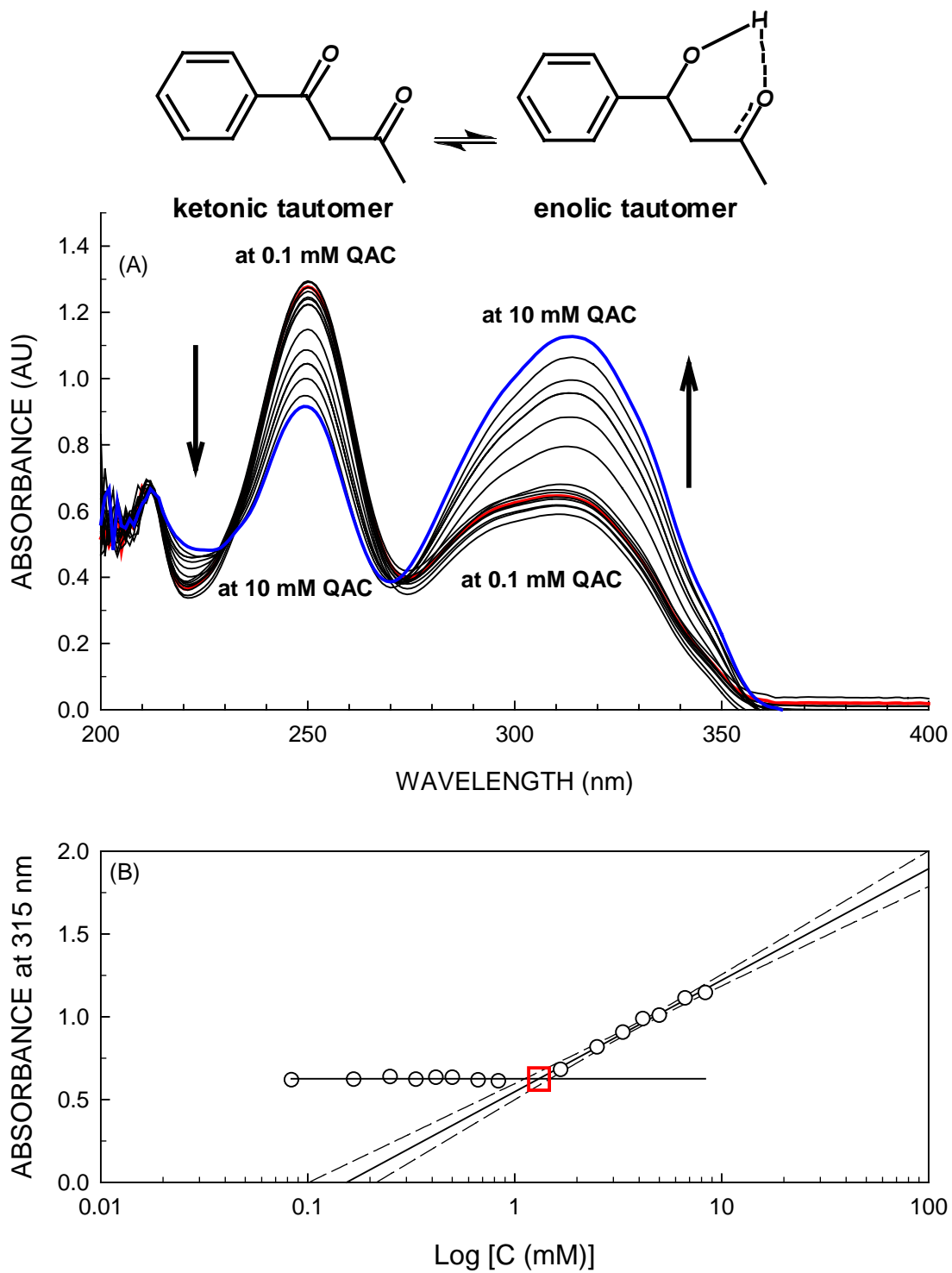


Figure 4.1. Distribution of BZA tautomers (A) and corresponding enolic tautomer absorbance at different QAC concentrations (0.08-8.3 mM in the cuvette) (B)

break-point of the line signifies the QAC concentration at which the micelles start to form, which in turn defines the CMC value (Figure 4.1B).

CMC analyses were performed in 2.5-mL, 1-cm UV-Vis cuvettes. Aliquots of 0.4 mL of aqueous BZA solution (0.7 mM) prepared by diluting a 30 mM BZA solution (in dioxane) in DI water were added to each cuvette. Then, 2 mL of a QAC solution at a concentration range from 0.1 to 100 mM (0.08-83 mM in the cuvette) were added. The cuvettes were sealed with caps and gently agitated for 2 minutes. When the mixture in the cuvettes reached equilibrium after 10 minutes at room temperature, the concentration of the enolic tautomer was quantified based on sample absorbance at the characteristic maximum wavelength of 315 nm after running blank samples prepared for every QAC concentration, which contained 0.4 mL of DI water in place of aqueous BZA solution. The sample absorbance at 315 nm was plotted against the logarithm of QAC concentration, and the break-point of the line which corresponds to the CMC value of each QAC was determined.

4.2.3. 1-Octanol/Water Partitioning (K_{ow}) Analysis

The 1-octanol/water partitioning coefficient of each QAC was determined by using the tumble-tube method developed in our laboratory based on OECD Test No.123 method (OECD, 2006). The test was performed in 25-mL serum tubes, which received 20 mL 1-octanol saturated DI water containing 10 μ M of a QAC and 4 mL DI water saturated 1-octanol. The tubes were then sealed with Teflon-lined butyl stoppers and aluminum caps. The content in each tube was agitated by tumbling at 6 revolutions per minute for either 1 or 6 days in the dark at 22°C in order to reach equilibrium of QACs between the two phases. At the end of each agitation period, 1.5 mL of sample from each

layer was transferred to 1.8-mL amber glass HPLC vials and the QAC concentration was determined by the LC-MS method described in Chapter 3. The K_{ow} value was then calculated using the following equation.

$$K_{ow} = \frac{[QAC]_{1\text{-octanol}}}{[QAC]_{\text{water}}} \quad (\text{Equation 4.1})$$

In order to quantify the QAC recovery from both the water and 1-octanol phase, the QAC concentration in each phase was multiplied by the phase volume and summed up. The so obtained QAC mass was then normalized to the QAC mass in a control which contained the same QAC concentration in 20 mL DI water. The mean total mass recovery for all QACs was $107 \pm 15\%$ ($n = 54$) (Figure 4.2). Equilibrium between the two phases was reached in 1 day of agitation since the K_{ow} values obtained after 1 and 6 days of agitation were very similar having an average coefficient of variation of $5 \pm 6\%$ ($n = 48$).

4.2.4. Biosolids Partitioning Assays

Partitioning of C_{12} TMA-Cl, C_{16} TMA-Cl, C_{12} BDMA-Cl and C_{16} BDMA-Cl on different types of municipal sludge (i.e., primary (PS), waste activated sludge (WAS), mesophilic digested sludge (MDS), and thermophilic digested sludge (TDS)) was evaluated in a shake-flask adsorption isotherm assay. The PS, WAS, and MDS were obtained from the South Cross Bayou Water Reclamation Facility in Pinellas County, Florida, whereas the TDS was acquired from the Regional Plant 1, operated by the Inland Empire Utilities Agency (IEUA) located in Ontario, California. The characteristics of the sludge samples used in this study are given in Table 4.1. Dilute sludge samples with 1 g/L VS concentration were prepared with tap water in 4 L glass bottles. The pH of each sludge sample was adjusted to 7.0. In order to inhibit any biological activity and prevent

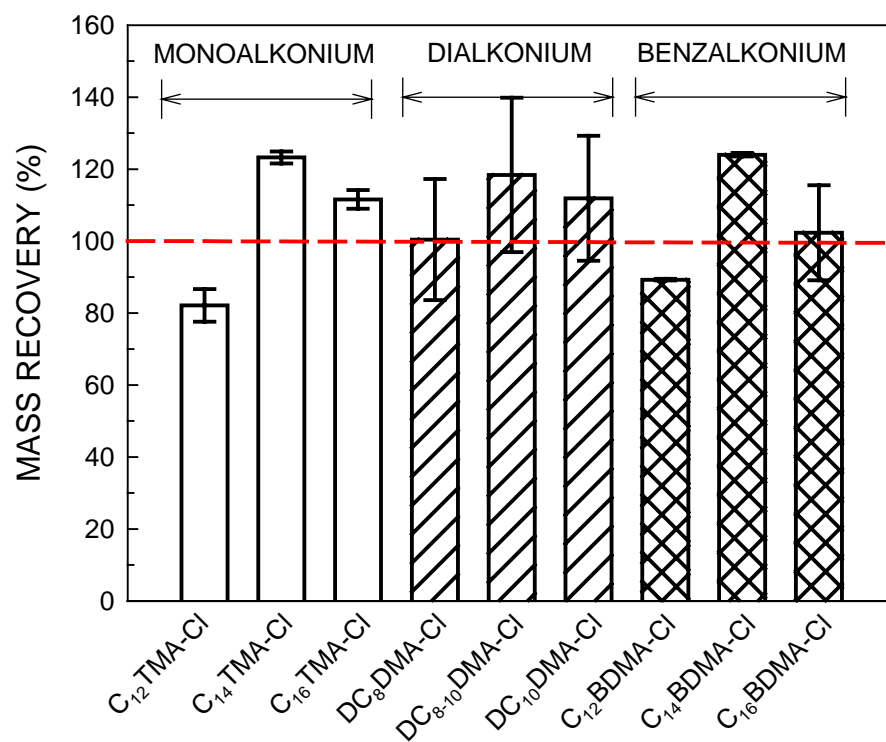


Figure 4.2. Normalized total QAC mass recovered from both the 1-octanol and water phase at the end of the partitioning assay

Table 4.1. Characteristics of undiluted sludge samples used in the adsorption isotherm

Parameter	PS	WAS	MDS	TDS
pH	5.55	6.61	6.95	7.30
TS, g/kg wet sample	25.0	67.0±1	33.8±0.1	32.8±0.1
VS, g/kg wet sample	19.7	44.0±1	22.0±0.1	20.4±0.1
VS/TS, %	78.8	65.7	65.1	62.2
Total COD, g/g VS	2.3	1.9	1.8	1.8
Soluble COD, g/L	4.56	2.5±0.1	0.60	1.50
VFAs, mg COD/L	1,400	567	50±5	75±7
Carbohydrate, g/g VS	0.39	0.48	0.38	0.49
Protein, g/g VS	0.30	0.46	0.47	0.43
Total fat, g/g VS	0.31	0.06	0.15	0.07
Total Kjeldahl nitrogen (TKN), g N/g VS	0.06	0.08	0.10	0.10
Ammonia, mg N/L	243	460±13	495±16	719±58
Total phosphorus, g P/g VS	0.04	0.11	0.11	0.12

Abbreviations: PS, primary sludge; WAS, waste activated sludge; MDS, mesophilic digested sludge; TDS, thermophilic digested sludge

possible biotransformation of the QACs, sodium azide (NaN_3) was added to all sludge samples to a final concentration of 200 mg/L. Each bottle was sealed with a rubber stopper, and then flushed with helium gas for 15 min. The partitioning assays were performed in 250-mL Erlenmeyer flasks. Seven sets of flasks for each QAC and sludge sample were prepared by mixing 145 mL of diluted sludge having a fixed VS concentration, with 5 mL of QAC solutions at 1.5, 2.25, 3.0, 4.5, 6.0, 7.5 or 9.0 g QAC/L, respectively. The initial QAC concentration in each flask was 50, 75, 100, 150, 200, 250 and 300 mg/L, respectively. All initial QAC concentrations were below their respective CMC values. The flasks were sealed with rubber stoppers and agitated on a orbital shaker at a rate of 190 rpm in the dark at 22°C for 24 hours. The total and liquid phase QAC concentration was measured at the end of 24 hours by the DSB-PIX method described in Chapter 3. The mass of QACs on the sludge solids was calculated by subtracting the liquid phase QAC concentration from the total QAC concentration. The liquid-phase QAC concentrations were plotted against the solid-phase QAC concentrations, and the resulting data points were fitted to the Freundlich isotherm equation given below.

$$q = K_F C^n \quad (\text{Equation 4.2})$$

In equation 4.2, q is the equilibrium QAC concentration on the sludge solids (mg QAC/g VS), C is the equilibrium QAC concentration in the liquid phase (mg QAC/L), K_F is the capacity factor ((mg/g VS)(L/mg) ^{n}), and n is the Freundlich exponent. The two adsorption constants (K_F and n) were determined by non-linear regression based on equation 4.2.

4.2.5. Microtox® Toxicity Assays

The acute toxicity of the selected QACs was assessed using the standard Microtox® test. The Microtox® system consists of the Azur Environmental M500 Analyzer with Microtox® Omni Software (Strategic Diagnostics Inc., Newark, DE). The acute toxicity is measured by determining the change in luminescence of *Vibrio fischeri*, a marine bacterium that naturally emits luminescent light, at different toxicant concentrations. All QAC samples were adjusted to 2% NaCl before analysis in order to maintain the proper osmotic pressure (ionic strength of 342 mM) for *Vibrio fischeri*. Different sample dilutions ranging from 1 to 2⁷ were tested for 5 and 15 minutes exposure times. The luminescence emitted at different QAC concentrations was compared to that of the control, which consisted of 2% NaCl in DI water (pH 6.5-7.0) having no QACs. The effective concentration of a toxicant (QAC) that causes the bacteria to emit light at 50% of the control is the EC₅₀ concentration. The 95% confidence range and r² values were calculated by linear regression of the data (x-axis: log of QAC concentration; y-axis: log of the fractional change in fluorescence after the sample was added and incubated for 5 or 15 minutes taking into account the change of fluorescence in the control).

The Microtox® assays performed to assess the effect of different anions (counter-ions) on QAC toxicity followed the same procedure described above. However, a 342 mM counter-ion salt solution was used to maintain the same osmotic pressure instead of NaCl.

The effect of natural organic matter (NOM) (Aldrich humic acid, Aldrich Chemical Company, St. Louis, MO) on QAC toxicity was tested by using the standard

Microtox® assay. Every assay vial, including the control, received NOM at a target concentration along with 2% NaCl.

4.3. Results and Discussion

4.3.1. Critical Micelle Concentration

QACs are cationic surfactants and as all surfactants do, QACs form micelles. Micelle formation is triggered by the coexistence of polar and hydrophobic moieties in the same molecule. In a polar solvent such as water, the polar moiety tends to interact with the solvent, whereas the hydrophobic moiety is repelled. When the surfactant concentration increases in a solution, the attraction between the hydrophobic moieties of the surfactant molecules prevails and results in the formation of bi-phasic aggregates called micelles. Therefore, a micelle contains a hydrophilic region that faces and interacts with the surrounding polar solvent, and a hydrophobic region, which is protected from the solvent. The affinity of a surfactant to form micelle is defined by a parameter called critical micelle concentration (CMC), which is the threshold surfactant concentration at which micellization begins. Micelle formation results in abrupt changes in the physical properties of a solution, such as surface tension, electrical conductivity and detergency. The CMC of a surfactant is defined by its electronic, steric and hydrophobic properties given by the molecular structure. Given the fact that CMC is related with the physical and chemical properties of a surfactant molecule, it is a promising descriptor to be used in QSAR modeling for surfactants as described above.

All QACs possess a polar head group containing a cationic nitrogen. In fact, the hydrophobic regions containing long-chain alkyl and benzyl groups are different in each QAC molecule and this difference gives a specificity to a QAC molecule. In this section,

the CMCs of nine QACs belonging to three QAC groups were measured and are given in Table 4.2.

The CMC values of the target QACs covered a wide range from 0.58 to 21.13 mM with a median of 2.55 mM ($n = 9$) (Figure 4.3). The measured CMCs were consistent with previously reported values which were determined utilizing conductivity and surface tension methods (Table 4.2). The lowest CMC in each QAC group was found for the QACs which have the longest alkyl chain length within the homologous group (Figure 4.4). These values are for C₁₆TMA-Cl (1.31 mM), DC₁₀DMA-Cl (1.50 mM) and C₁₆BDMA-Cl (0.58 mM) which belong to monoalkonium, dialkonium and benzalkonium chlorides, respectively. On the other hand, the highest CMC in each QAC group was for the QACs which have the shortest alkyl chain length within the group (Figure 4.4). These values are for C₁₂TMA-Cl (21.13 mM), DC₈DMA-Cl (16.48 mM) and C₁₂BDMA-Cl (3.8 mM) which belong to monoalkonium, dialkonium and benzalkonium chlorides, respectively. The dependence of CMC on the alkyl chain length suggests that the hydrophobicity of the QACs has a significant effect on the CMC.

The CMCs of benzalkonium chlorides were significantly lower than the CMCs of monoalkonium chlorides with the same alkyl chain length (Table 4.2 and Figure 4.3). Given this fact, not only the alkyl chain length but also the addition of a benzyl group to the polar head results in the decrease of CMC, most probably due to the electron withdrawing property of the benzene ring which in turn reduces the polarity and the hydration sphere of the head group and facilitates the micelle formation (Rodriguez et al., 2002).

Table 4.2. Critical micelle concentrations of target QACs determined in this study and reported in the literature at 298 °K

QACs	CMC (mM) ^a
Monoalkonium Chlorides	
C ₁₂ TMA-Cl	21.13 (20.00 ^b)
C ₁₄ TMA-Cl	5.62 (4.50 ^b)
C ₁₆ TMA-Cl	1.31 (1.40 ^b)
Dialkonium Chlorides	
DC ₈ DMA-Cl	16.48 (NA) ^c
DC ₈₋₁₀ DMA-Cl	2.55 (NA)
DC ₁₀ DMA-Cl	1.50 (1.85 ^d)
Benzalkonium Chlorides	
C ₁₂ BDMA-Cl	3.80 (8.1 ^e)
C ₁₄ BDMA-Cl	1.72 (2.0 ^e)
C ₁₆ BDMA-Cl	0.58 (0.5 ^e)

^a Previously reported values in parenthesis

^b (Jalali-Heravi and Konouz, 2003)

^c NA, not available

^d (Lianos et al., 1983)

^e (Gonzalez-Perez et al., 2001)

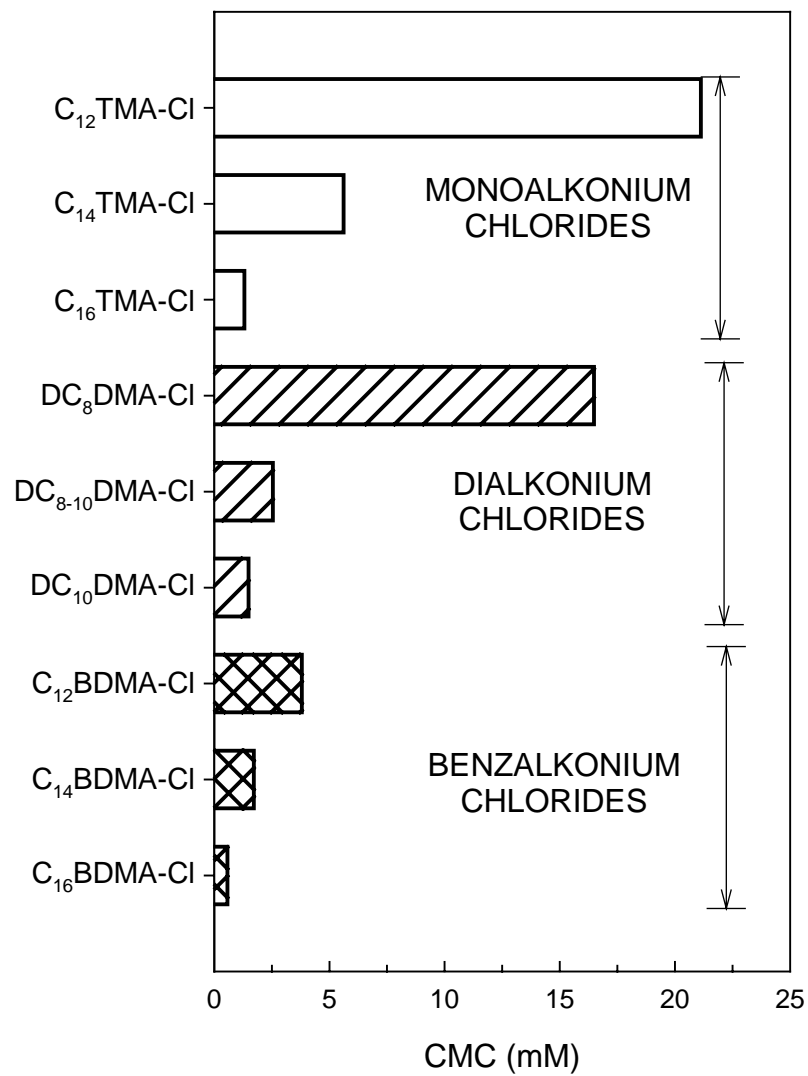


Figure 4.3. Measured CMC values of monoalkonium, dialkonium and benzalkonium chlorides

4.3.1.1. Effect of Alkyl Chain Length on CMC

The micelle formation is enhanced by the hydrophobicity of the surfactant. In an homologous series of surfactants, the affinity for micellization increases and the CMC decreases with an increase of the alkyl chain length. As a general rule, the CMC decreases by a factor of ca. 2 on adding one methylene group (-CH₂-) to the alkyl chain. Alkyl chain branching, double bonds, aromatic groups or some other polar character in the hydrophobic region produce sizable changes in the CMC (Hiemenz and Rajagopalan, 1997).

At constant temperature, the effect of addition of a methylene group to the alkyl chain on CMC can be expressed using the Stauff-Klevens empirical formula (Gonzalez-Perez et al., 2001) as follows.

$$\log \text{CMC} = A - Bn \quad (\text{Equation 4.3})$$

where n is the total number of carbon atoms in the unbranched alkyl chain and A and B are empirical regression constants. A is dependent on the polarity of the headgroup, whereas B represents the magnitude of CMC decrease per added methylene group to the alkyl chain (Gonzalez-Perez et al., 2001). The empirical regression constants for monoalkonium, dialkonium and benzalkonium chlorides were determined by using linear regression analysis (Figure 4.4). A and B values obtained for monoalkonium, dialkonium and benzalkonium chlorides were 1.96 and 0.30, 2.29 and 0.26, and 0.05 and 0.21, respectively (Figure 4.4). These values are consistent with previously reported values (Kopecky, 1996). Benzalkonium chlorides have lower CMCs than monoalkonium chlorides with the same alkyl chain length. In order to reach the same CMC as that of benzalkonium chlorides, monoalkonium chlorides have to have more carbons on the alkyl

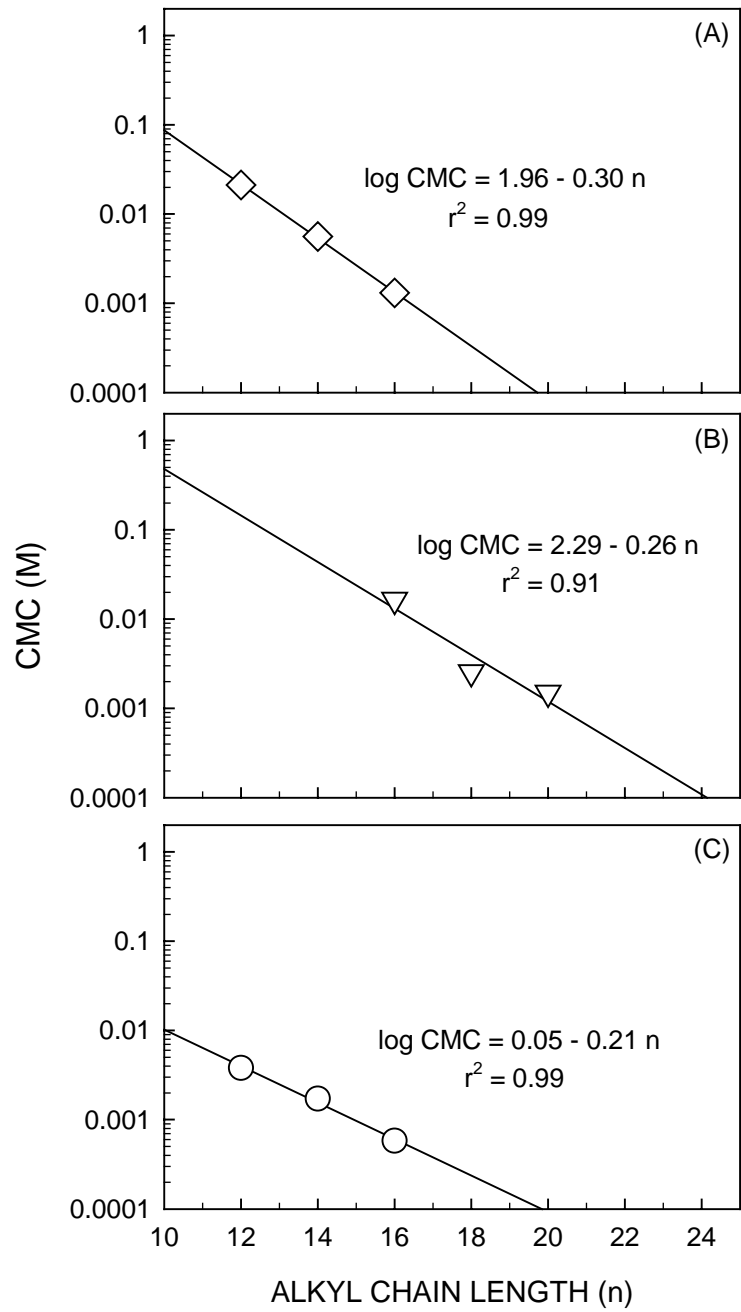


Figure 4.4. The effect of the alkyl chain length (n) on the CMC of (A) monoalkonium, (B) dialkonium and (C) benzalkonium chlorides

chain (Figure 4.5) because of the presence of the benzyl group in the benzalkonium chlorides. The benzyl group accounts for, on average, two extra carbons in the alkyl chain length for benzalkonium chlorides when the alkyl chain length is longer than 5 and shorter than 18 carbons (Figure 4.5) (Kopecky, 1996). However the benzyl group effect on the CMC decreases as the chain length increases and the CMC becomes the same for benzalkonium and monoalkonium chlorides at a 21-carbons chain length. On the other hand, dialkonium chlorides have higher CMCs than monoalkonium chlorides with the same alkyl chain length. In order to reach the same CMC, dialkonium chlorides have to have an average of four more carbons on the alkyl chain (Figure 4.5) because the carbons on the dialkonium chlorides are located in two alkyl chains which have lower chain lengths than the total carbon number, which in turn makes the molecule less hydrophobic.

The benzalkonium chlorides have the lowest A value among all QACs (Table 4.2), which indicates that their head group is less hydrophilic than the ones of other QACs because of the benzene ring effect as explained above. The constant B in the Stauff-Klevens relation accounts for the free energy for the methylene group to transfer from the aqueous phase to the micellar micro-phase and can be defined by using the equations given below (Hiemenz and Rajagopalan, 1997).

$$\Delta G_{\text{mic}}^0 = (n - 1)\Delta G_{\text{CH}_2} + \Delta G_{\text{CH}_3} + \Delta G_{\text{polar head}} \quad (\text{Equation 4.4})$$

$$\ln \chi_{\text{cmc}} = \frac{(n - 1)\Delta G_{\text{CH}_2}}{RT} + A' \quad (\text{Equation 4.5})$$

where ΔG_{mic}^0 (J/mol) is the Gibb's free energy of micellization, ΔG_{CH_2} , ΔG_{CH_3} and $\Delta G_{\text{polar head}}$ (J/mol) is the Gibb's free energy of methylene, methyl and polar head transfer from the aqueous phase to the micelle, respectively. The χ_{cmc} is the critical micelle

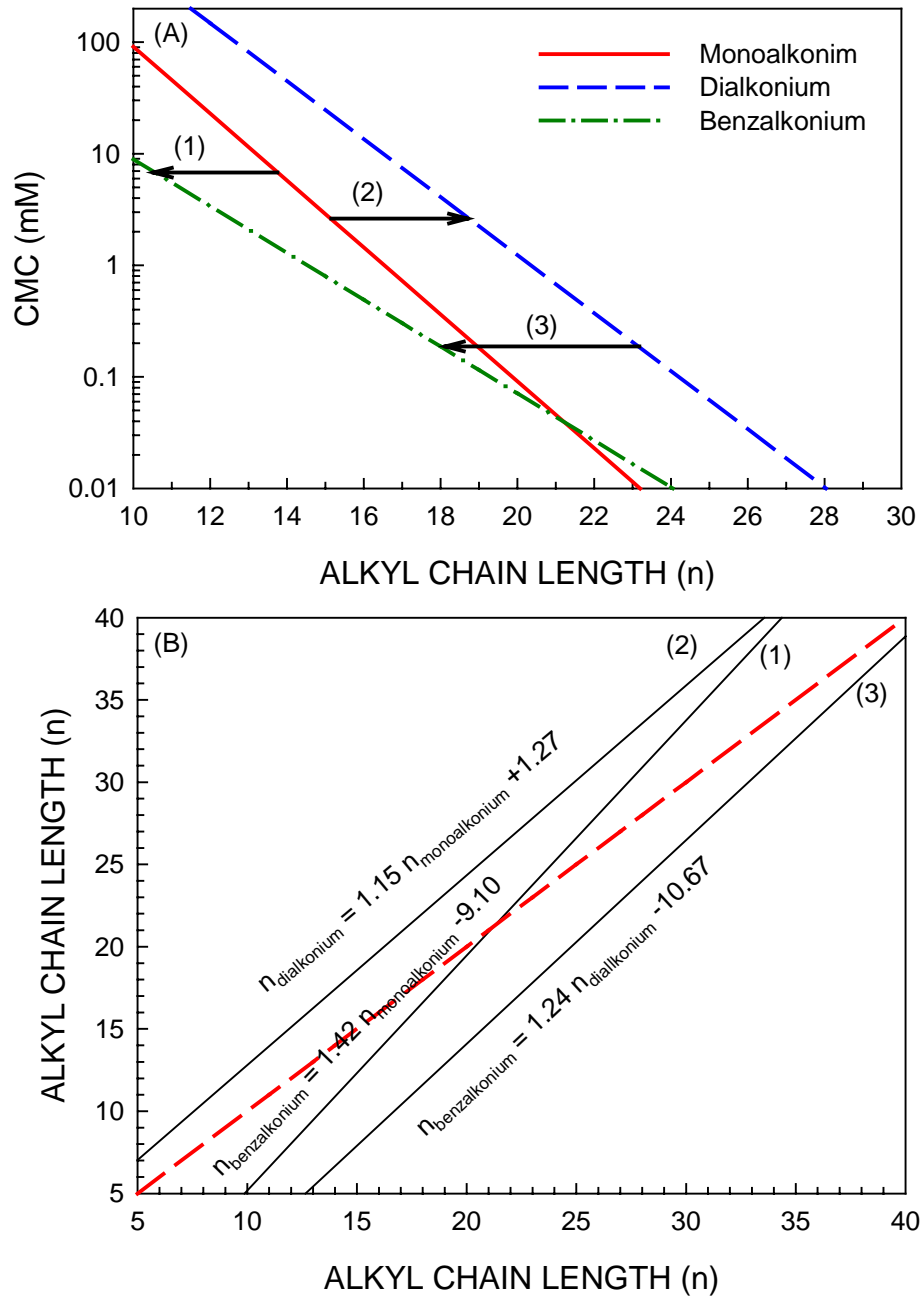


Figure 4.5. Change in CMC with respect to the alkyl chain length (n) (A) and comparison of the number of carbon atoms in the alkyl chain that satisfies the same CMC for monoalkonium, dialkonium and benzalkonium chlorides

concentration expressed in terms of molar fraction ($\chi_{\text{cmc}} = \text{CMC}/55.5$, where 55.5 is the molar concentration of 1L water assuming a specific gravity of water equal to 1 at 298.15 °C). R (J/mole·°K) is the ideal gas constant and T (°K) is the absolute temperature. The constant A' can be defined by using the equation below.

$$A' = \frac{\Delta G_{\text{CH}_3}}{RT} + \frac{\Delta G_{\text{polar head}}}{RT} = -2.303B + 2.303A - 4.02 \quad (\text{Equation 4.6})$$

The constants A and B were previously defined in Equation 4.3. By using Equation 4.5, the Gibb's free energy to transfer one methylene (ΔG_{CH_2}) from the aqueous solution to the monoalkonium chloride micelle is -1.71 kJ/mole which is very close to a previously reported value of -1.72 kJ/mole (Hiemenz and Rajagopalan, 1997). On the other hand, the Gibb's free energy to transfer one methylene (ΔG_{CH_2}) from the aqueous solution to the dialkonium and benzalkonium chloride micelles is -1.48 and -1.20 kJ/mole, respectively. Transfer of one methylene to either dialkonium or benzalkonium chloride micelles is more difficult than to transfer it to a monoalkonium chloride micelle. This is because of the steric effects exerted by the presence of two hydrophobic hydrocarbons attached on the quaternary nitrogen in dialkonium and monoalkonium chlorides. As a result, addition of two carbons to monoalkonium chlorides leads to a more pronounced CMC decrease than the addition of two carbons to dialkonium and benzalkonium chlorides (Figure 4.4 and Table 4.2).

The major driving force of micellization of QACs is the hydrophobic interaction between their alkyl groups (Kopecky, 1996). The hydrophobicity of a compound is well defined by its 1-octanol/water partitioning coefficient (K_{ow}). K_{ow} is also widely used in QSAR modeling of biosolids partitioning, bioaccumulation and toxicity for a variety of organic compounds. Because of this reason, we examined the effect of hydrophobicity on

CMC of QACs and evaluated the extent of CMC dependence on hydrophobicity in order to assess the potential use of CMC in QSAR instead of K_{ow} .

The K_{ow} values of QACs were either determined experimentally or calculated using two different atom/fragment contribution methods developed by Meylan and Howard and Hansch and Leo (Hansch and Leo, 1979; Meylan and Howard, 1995). Comparison between the experimentally determined and calculated K_{ow} values was done in order to determine if the current K_{ow} estimation methods are appropriate to derive QSAR models.

The log K_{ow} values of the target QACs ranged from 0.28 to 2.97 with a median of 1.50 ($n = 9$) (Table 4.3). The measured log K_{ow} values are consistent with previously reported values (Table 4.3). The highest log K_{ow} in each QAC group was found for the QACs which have the longest alkyl chain length within each homologous group. These are C_{16} TMA-Cl (1.50 ± 0.06), DC_{10} DMA-Cl (2.56 ± 0.01) and C_{16} BDMA-Cl (2.97 ± 0.03) which belong to monoalkonium, dialkonium and benzalkonium chlorides, respectively. On the other hand, the lowest log K_{ow} in each QAC group was found for the QACs which have the shortest alkyl chain length within each homologous group. These are C_{12} TMA-Cl (0.36 ± 0.07), DC_8 DMA-Cl (0.28 ± 0.22) and C_{12} BDMA-Cl (0.59 ± 0.04) which belong to monoalkonium, dialkonium and benzalkonium chlorides, respectively.

As discussed above, B in Equation 4.3 correlates with the Gibb's free energy for the transfer of one methylene from water to the QAC micellar core. Equation 4.3 can be used to determine the Gibb's free energy for the transfer of one methylene from water to 1-octanol. Addition of a methylene to the alkyl chain of QACs has a more pronounced effect on K_{ow} than on the CMC since the B value for K_{ow} ranges between 0.3 and 0.6

Table 4.3. 1-Octanol/water partitioning coefficients of target QACs determined in this study and reported in the literature at 298 °K

QACs	log K_{ow} ^a
Monoalkonium Chlorides	
C ₁₂ TMA-Cl	0.36±0.07
C ₁₄ TMA-Cl	0.70±0.05
C ₁₆ TMA-Cl	1.50±0.06 (1.81 ^b)
Dialkonium Chlorides	
DC ₈ DMA-Cl	0.28±0.22 (NA) ^c
DC ₈₋₁₀ DMA-Cl	1.54±0.06 (NA)
DC ₁₀ DMA-Cl	2.56±0.01 (NA)
Benzalkonium Chlorides	
C ₁₂ BDMA-Cl	0.59±0.04 (0.95 ^d)
C ₁₄ BDMA-Cl	1.67±0.02 (1.81 ^d)
C ₁₆ BDMA-Cl	2.97±0.03 (2.11 ^d)

^a Previously reported values in parenthesis

^b (Ying, 2006)

^c NA, not available

^d (Hansch et al., 1995)

(Figure 4.6), whereas B is between 0.2 and 0.3 for CMC (Figure 4.4). Such results suggest a less hydrophobic and a more polar nature of the QAC micelle core than the octanol medium (Kopecky, 1996). Noting a better correlation between alkyl chain length and the $\log K_{ow}$ than between alkyl chain length and the \log CMC (Figure 4.4 and Figure 4.6), suggests that other interactions apparently contribute to QAC micellization besides the hydrophobicity, such as ionic interactions associated with the polar head of QACs. In fact, K_{ow} is limited in representing overall interactions which are significant in QSAR modeling of biosolids partitioning and toxicity of QACs.

The most popular environmental QSAR tools, such as the EPISuite and the OECD Application Toolbox (OECD, 2008; Syracuse Research Corporation, 2007) utilize $\log K_{ow}$ values calculated using the atom/fragment contribution method developed by Meylan and Howard (Meylan and Howard, 1995) and are integrated into KOWWIN® (version 1.06) (Syracuse Research Corporation, 2007) to predict the toxicity and bioconcentration factor of chemicals as well as their distribution in environmental compartments. In fact, this method overpredicted the $\log K_{ow}$ values of the target QACs (Figure 4.7B). The difference between the predicted and measured $\log K_{ow}$ values was constant and equal to ca. 1.76 which suggests that the error is systematic but non-specific for the target QACs. The residual, which is the difference between the predicted and measured $\log K_{ow}$ values for a particular QAC used in this study, ranges from 0.9 to 2.4 ($n = 9$) (Figure 4.7A). The residual for monoalkonium chlorides was less than that for dialkonium and benzalkonium chlorides, which suggests that all carbons, no matter how close to the polar head or how they are aligned in the molecule, are treated in a same way

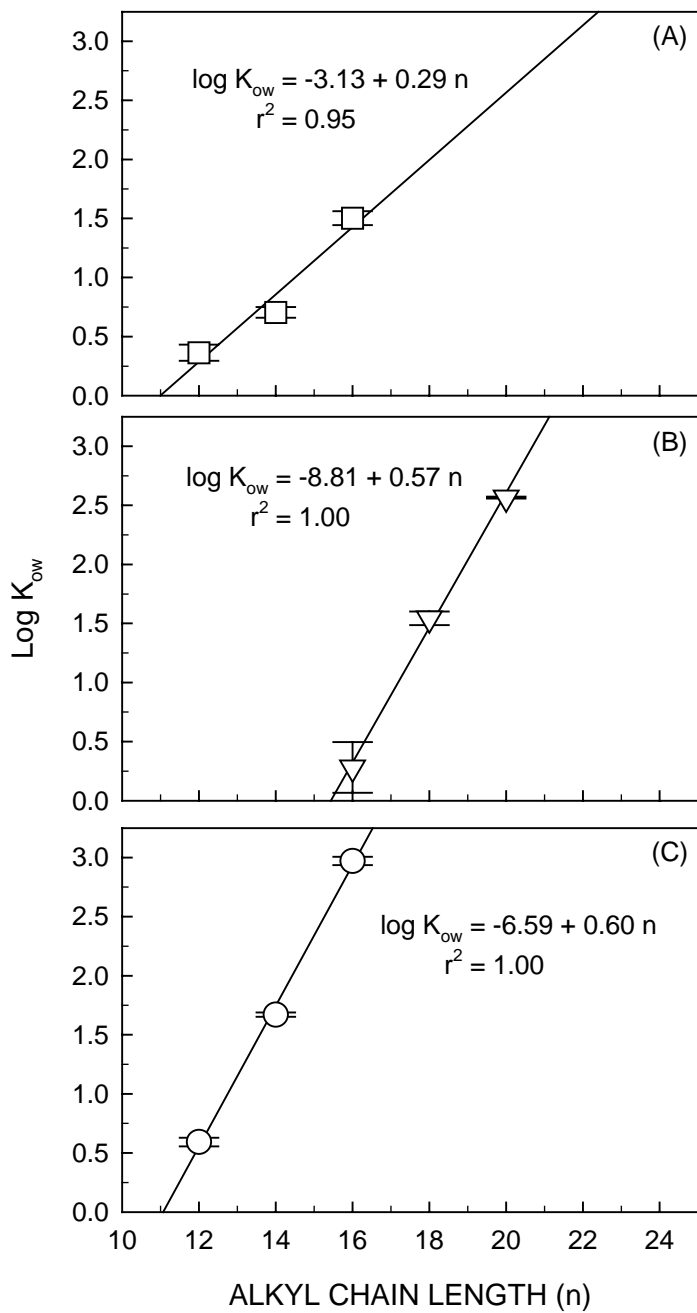


Figure 4.6. Effect of the alkyl chain length (n) on K_{ow} of (A) monoalkonium, (B) dialkonium and (C) benzalkonium chlorides

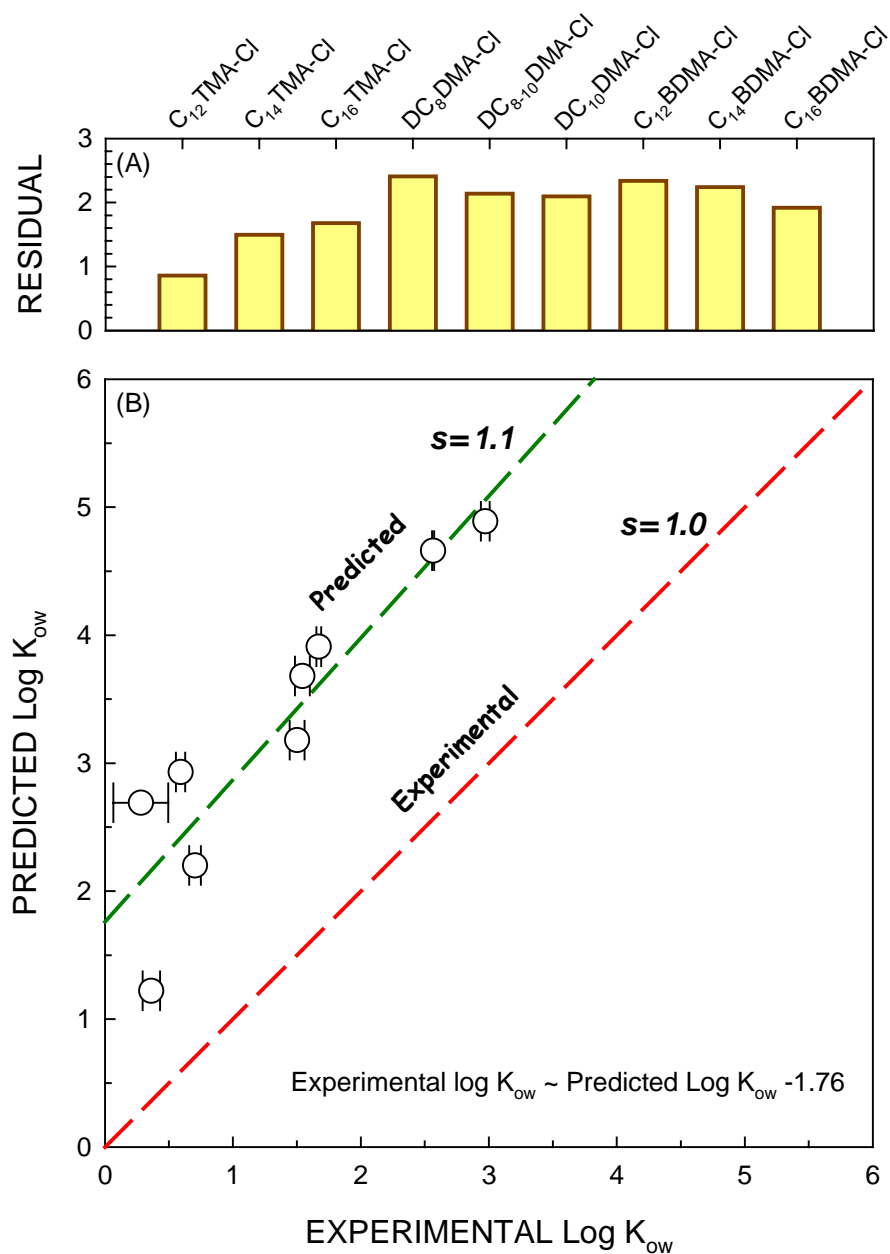


Figure 4.7. (A) Residual and (B) graphical comparison between measured and predicted log K_{ow} values of monoalkonium, dialkonium and benzalkonium chlorides (the Meylan and Howard method was used to obtain predicted log K_{ow} values)

and the effect of the polar head on the hydrophobic groups of a QAC molecule is not taken into account by this method.

In search for the best available $\log K_{ow}$ estimation method, a method developed by Hansch and Leo (1979) was identified as the most precise one. According to this method, $\log K_{ow}$ values are calculated conceptually by breaking the molecule down into its simplest fragments (i.e., $-\text{CH}_3$, $-\text{CH}_2-$, $-\text{C}_7\text{H}_7$, $>\text{N}^+<$, etc.), summing their partial $\log K_{ow}$ values (referred to as f) and applying factors F to allow for variation in how the fragments are combined together in the whole molecule. Based on this, the overall $\log K_{ow}$ equation can be written as follows:

$$\log K_{ow} = \sum_1^i a_i f_i + \sum_1^j b_j F_j \quad (\text{Equation 4.7})$$

where “a” is the number of occurrence of fragment “i” and “b” is the number of applications of factor “j”. Hansch and Leo (1979) defined specific bond factors (F) for ionic organics, specifically for protonated amines and quaternary ammonium compounds, by taking the effect of the polar head on the hydrophobicity of the attached alkyl chain into account. Therefore, the values of F were determined depending on the position of the carbon atom in the alkyl chain.

This complex method not only accounts for the hydrophobicity exerted by each carbon fragment but also includes the effect of the polar head on the hydrophobicity of carbons depending on their locations nearby the polar head. Such interactions are not accounted for in the previously described method. The overall equation to estimate the $\log K_{ow}$ values of QACs is given below.

$$\begin{aligned} \log K_{ow} = & f_{\text{N}^+} + f_{\text{Cl}^-} + a_{\text{CH}_3} f_{\text{CH}_3} + a_{\text{CH}_2} f_{\text{CH}_2} + a_{\text{C}_7\text{H}_7} f_{\text{C}_7\text{H}_7} + b_1 F_1 + b_2 F_2 + b_3 F_3 \\ & + b_4 F_4 + b_5 F_5 + b_{\geq 6} F_{\geq 6} \end{aligned} \quad (\text{Equation 4.8})$$

The contributions of each fragment and bond factor to $\log K_{ow}$ of QACs are given in Table 4.4.

The $\log K_{ow}$ values calculated using the Hansch and Leo method had a better agreement with the measured $\log K_{ow}$ values (Figure 4.8B) than the ones calculated using the Meylan and Howard method (Figure 4.7B). All residuals were less than 0.5 units (expressed as absolute value) (Figure 4.8A). The close agreement verified the importance of the polar head group on the chemical properties of QACs.

Good correlations between CMC, measured, and calculated K_{ow} values were achieved, which verifies the dependence of CMC on hydrophobicity (Figure 4.9). The relationship between CMC and K_{ow} can be expressed as follows:

$$\log \text{CMC} = C - D \log K_{ow} \quad (\text{Equation 4.9})$$

where C is the intercept and D is the slope of the regression line. D correlates with the partitioning intensity of QACs between 1-octanol and water. The correlation between CMC and $\log K_{ow}$ values calculated using the Hansch and Leo method and measured $\log K_{ow}$ values is better than the $\log K_{ow}$ values calculated using the Meylan and Howard method.

4.3.1.2. Effect of Counter-ions on CMC

The presence of an anion (counter-ion with respect to the positive charge of the QACs) in an aqueous solution of QACs almost always facilitates the micellization and leads to a lower CMC value. The high affinity of anions to bind on the polar head of

Table 4.4. log K_{ow} contribution of fragments and bond factors used in the Hansch and Leo method

Fragment/Bond Factor	Contribution (Unitless)
f_{N^+}	-3.40
f_{Cl^-}	0.06
f_{CH_3}	0.89
f_{CH_2}	0.66
$f_{C_7H_{17}}$	2.51
F_1	-0.90
F_2	-0.60
F_3	-0.45
F_4	-0.35
F_5	-0.30
$F_{\geq 6}$	-0.27

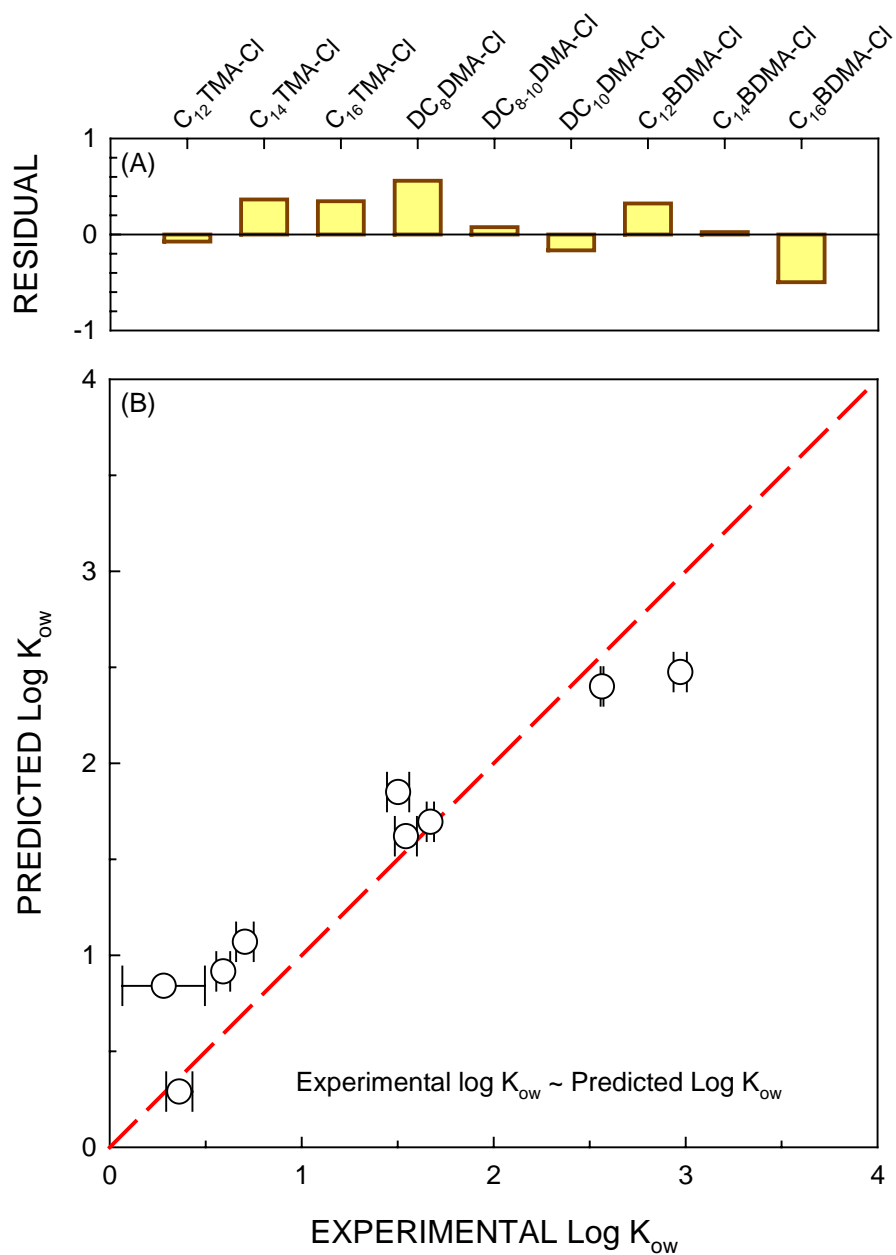


Figure 4.8. (A) Residual and (B) graphical comparison between measured and predicted log K_{ow} values of monoalkonium, dialkonium and benzalkonium chlorides (the Hansch and Leo method was used to obtain predicted log K_{ow} values)

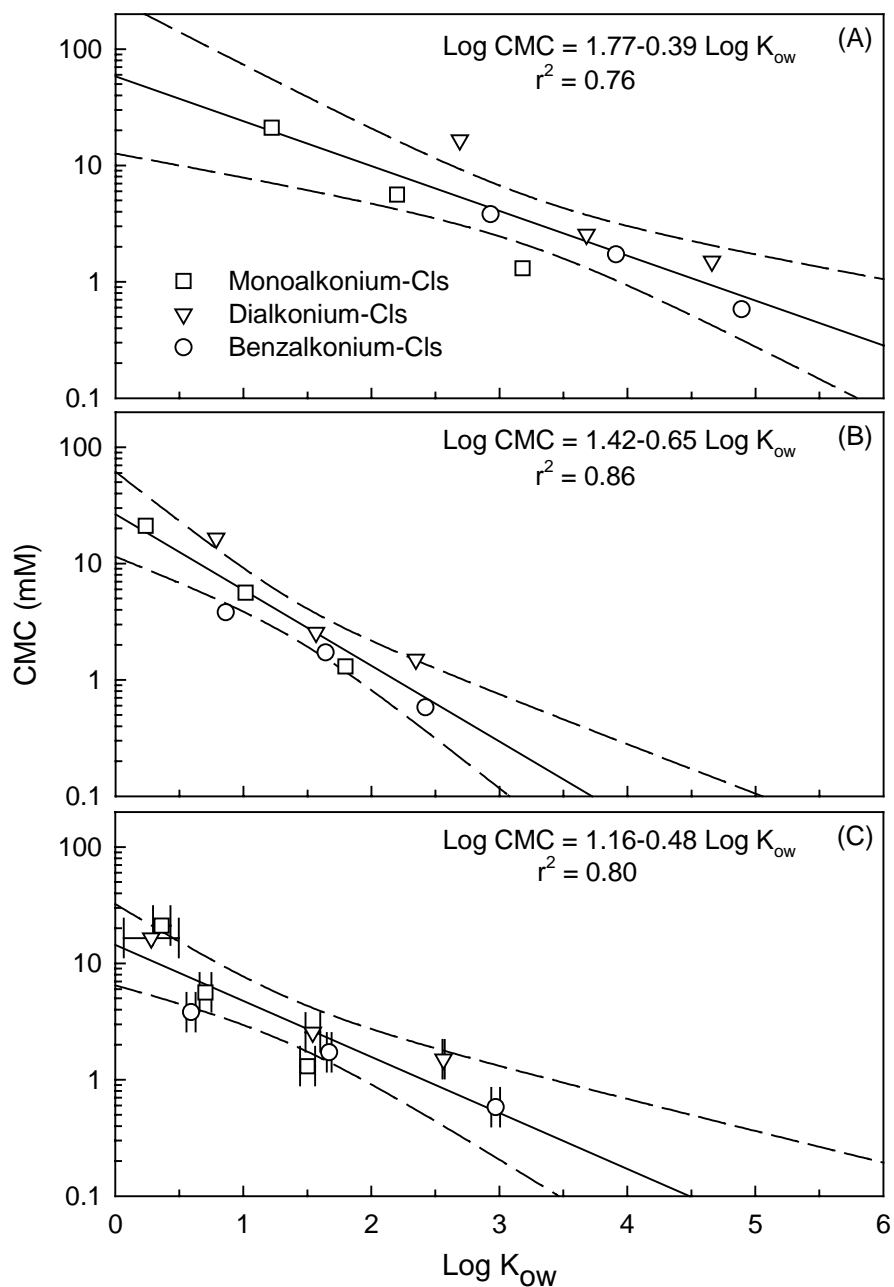


Figure 4.9. Relationship between CMC and (A) calculated K_{ow} values using the Meylan and Howard method, (B) calculated K_{ow} values using the Hansch and Leo method and (C) measured K_{ow} (Dashed lines represent 95% confidence intervals)

QACs results in a decrease of its polarity and an increase in its hydrophobicity.

Thermodynamically, addition of a counter-ion in a QAC solution decreases the Gibb's free energy for the transfer of the polar head from the aqueous solution to the QAC micelle ($\Delta G_{\text{polar head}}$, as expressed in Equation 4.4). The effect of counter ions on the CMC of QACs can therefore be expressed by an equation similar to Equation 4.3 as follows (Gaillon et al., 1999).

$$\log \text{CMC} = E - \beta' \log C_{\text{counter-ion}} \quad (\text{Equation 4.10})$$

where E is the intercept and β' is the slope of the linear regression line which correlates with the degree of association of the micelle with counter ions.

The effect of four monovalent inorganic (i.e., Cl^- , NO_2^- , Br^- and NO_3^-) and an organic (i.e., acetate, CH_3COO^-) counter-ion on the CMC of benzalkonium chloride (a mixture of $\text{C}_{12}\text{BDMA-Cl}$, $\text{C}_{14}\text{BDMA-Cl}$ and $\text{C}_{16}\text{BDMA-Cl}$) was tested at concentrations up to 50 mM and the results are given in Figure 4.10. The log CMC decreased at a rate of 0.108, 0.179, 0.211, 0.228 and 0.261 per 10 mM of Cl^- , NO_2^- , Br^- , CH_3COO^- and NO_3^- , respectively (Figure 4.10). These results and the trend were comparable with the ones reported by Gaillon et al. (1999) for monoalkonium chlorides. The results suggest that not only the concentration but also the type of counter-ion affect the CMC. The order of counter ion binding to the positive micelles was as follows: $\text{Cl}^- > \text{NO}_2^- > \text{Br}^- > \text{CH}_3\text{COO}^- > \text{NO}_3^-$; that is, larger anions that are more polarizable bind to QACs more effectively and result in the decrease of CMC (Figure 4.11) (Hiemenz and Rajagopalan, 1997).

4.3.2. Assessment of Biosolids Partitioning of QACs

Biosolids are mainly composed of lipids, carbohydrates and proteins which have ionic and hydrophobic properties. Therefore, QACs have a high affinity to accumulate on

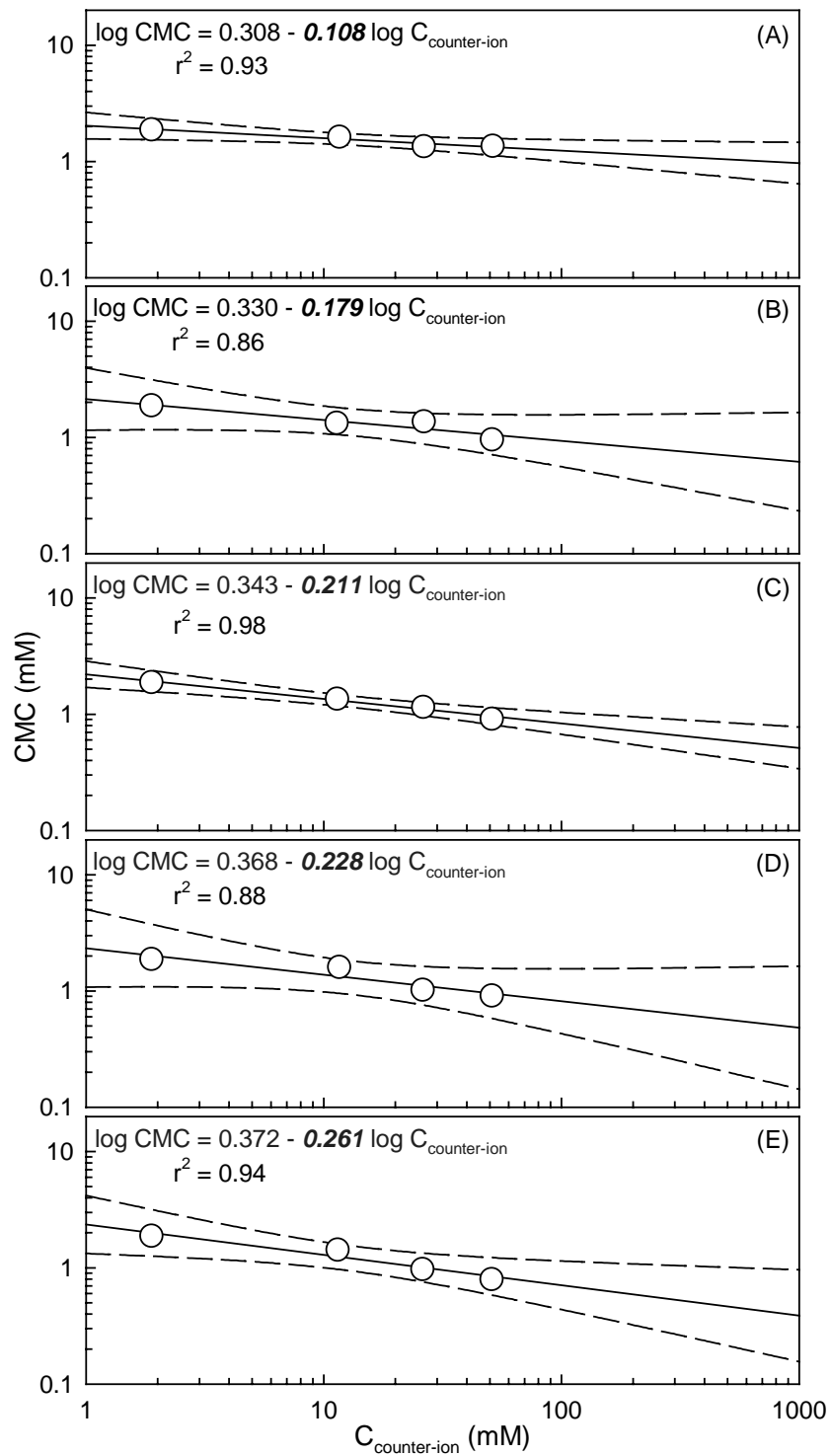


Figure 4.10. Effect of (A) Cl^- , (B) NO_2^- , (C) Br^- , (D) CH_3COO^- and (E) NO_3^- on the CMC of benzalkonium chloride at concentrations up to 50 mM (Dashed lines represent 95% confidence intervals)

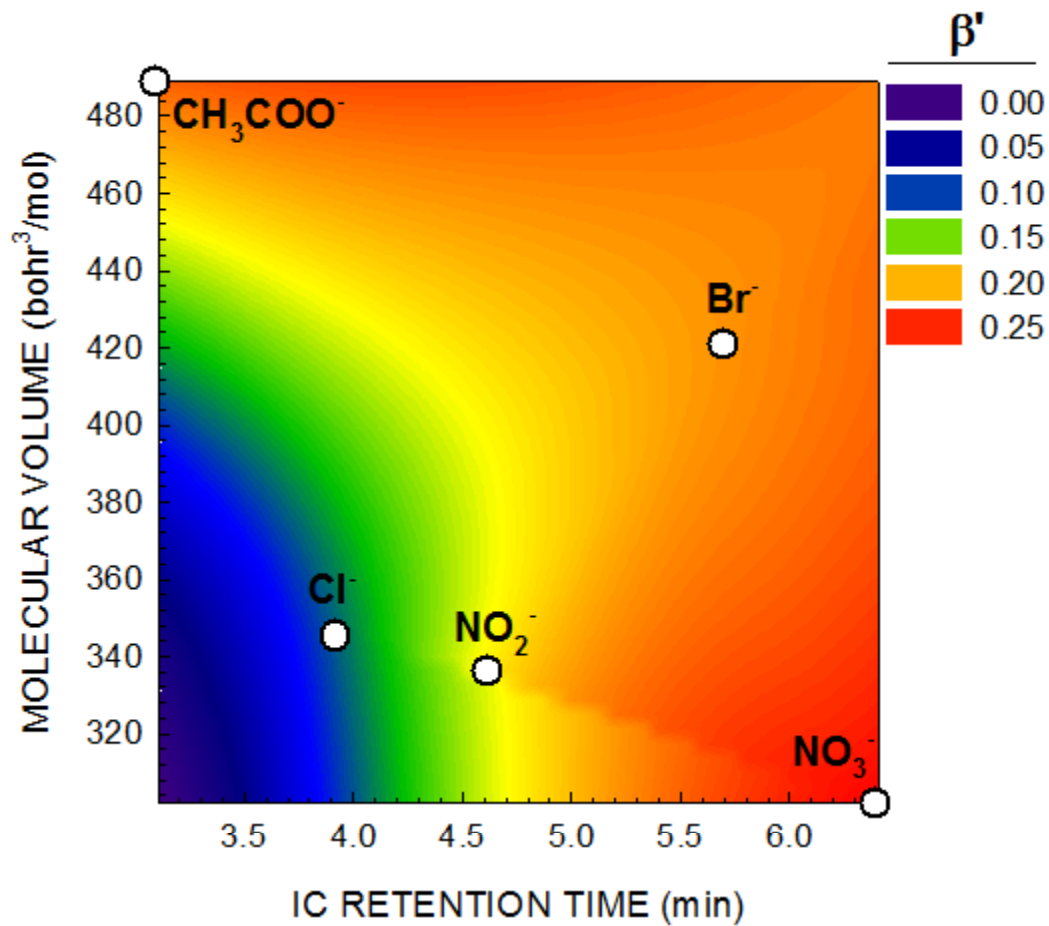


Figure 4.11. Effect of counter-ion electro-negativity expressed by its retention time on ion chromatography (IC) and size on the CMC of benzalkonium chloride

biomolecules via both ionic and hydrophobic interactions. These interactions define the fate of QACs in engineered and natural biological systems.

Adsorption of four QACs, representing the least and the most hydrophobic QACs among those used in this study, belonging to monoalkonium and benzalkonium chlorides (i.e., C₁₂TMA-Cl, C₁₆TMA-Cl, C₁₂BDMA-Cl and C₁₆BDMA-Cl), on primary (PS), waste activated (WAS), mesophilic digested (MDS) and thermophilic digested sludge

(TDS) biosolids was investigated at QAC concentrations up to 300 mg/L (< CMC). Preliminary adsorption kinetic assays showed that equilibrium was reached in more than 3 hours, but less than 24 hours for all sludge types and QACs used in this study (Ismail et al., 2008). Freundlich adsorption isotherms and the estimated parameter values (K_F , capacity factor/sorption affinity and n , Freundlich exponent) are given in Figure 4.12 and Table 4.5, respectively. The Freundlich isotherm model represented well the QAC adsorption on municipal sludge biosolids since the regression coefficients of the non-linear fits were above 90% (Table 4.5). In all cases, the value of n was less than 1 which indicates that at higher and higher QAC concentrations, adsorption free energy becomes weaker and weaker so that it becomes more and more difficult for additional QAC molecules to sorb. This occurs in cases where sorbent adsorption sites are occupied instantly at low sorbate concentrations and the remaining binding sites are less accessible to the sorbate molecules. Such isotherms are encountered in adsorption processes that involve hydrophobic (e.g., sorption to activated carbon) and/or ionic (e.g., sorption to clay mineral) interactions between sorbate and sorbent which is the case in QAC sorption to biosolids (Schwarzenbach et al., 2003). In fact, n values showed some variability between the sludges although the composition (lipid, carbohydrate and protein fractions of VS) of all sludges is relatively similar (Table 4.1). The n values for PS (0.71 ± 0.10) and WAS (0.75 ± 0.08) were higher than the n values for MDS (0.56 ± 0.02) and TDS (0.56 ± 0.09), which indicates that the adsorption sites of PS and WAS solids are more homogeneous than the sites of MDS and TDS solids. Therefore QAC sorption to PS and WAS is a continuum, whereas active sorption sites of MDS and TDS are occupied at very low QAC concentrations. This argument is true since sludge digestion results in more

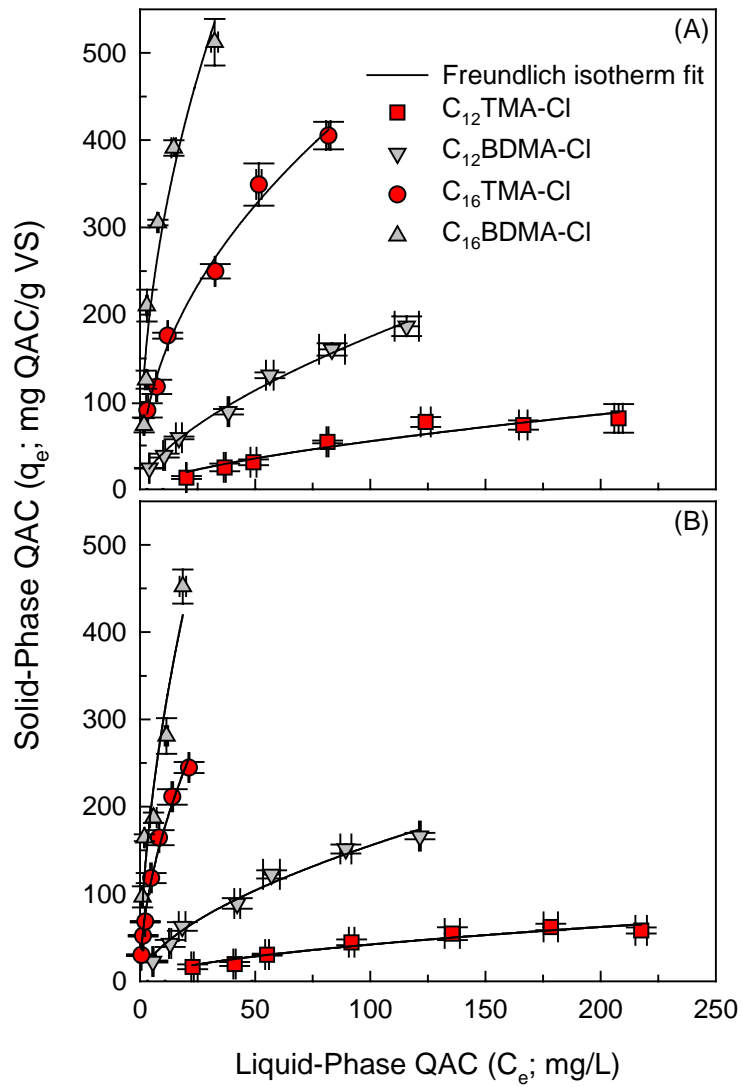


Figure 4.12. Freundlich adsorption isotherms for C_{12} TMA-Cl, C_{12} BDMA-Cl, C_{16} TMA-Cl and C_{16} BDMA-Cl at equilibrium with (A) thermophilic digested sludge and (B) mesophilic digested sludge at 1 g VS/L

Table 4.5. Freundlich adsorption isotherm constants for QAC phase distribution in municipal primary and waste activated sludges, as well as mesophilic and thermophilic digested sludges^a

QAC	K_F (mg/g VS)(L/mg) ⁿ	n	r ²
<i>Primary Sludge</i>			
C ₁₂ TMA-Cl	1.28 ± 0.24 ^b	0.64 ± 0.03	0.992
C ₁₆ TMA-Cl	28.90 ± 3.29	0.61 ± 0.03	0.992
C ₁₂ BDMA-Cl	4.73 ± 0.86	0.83 ± 0.04	0.993
C ₁₆ BDMA-Cl	20.73 ± 1.90	0.76 ± 0.03	0.996
<i>Waste Activated Sludge</i>			
C ₁₂ TMA-Cl	0.95 ± 0.15	0.70 ± 0.03	0.995
C ₁₆ TMA-Cl	21.19 ± 3.32	0.69 ± 0.05	0.986
C ₁₂ BDMA-Cl	3.81 ± 0.67	0.86 ± 0.04	0.994
C ₁₆ BDMA-Cl	18.89 ± 2.16	0.74 ± 0.04	0.993
<i>Mesophilic Digested Sludge</i>			
C ₁₂ TMA-Cl	3.14 ± 1.29	0.56 ± 0.08	0.932
C ₁₆ TMA-Cl	48.36 ± 4.21	0.54 ± 0.03	0.983
C ₁₂ BDMA-Cl	10.76 ± 2.09	0.58 ± 0.05	0.989
C ₁₆ BDMA-Cl	82.03 ± 24.13	0.56 ± 0.12	0.922
<i>Thermophilic Digested Sludge</i>			
C ₁₂ TMA-Cl	2.86 ± 1.49	0.64 ± 0.11	0.923
C ₁₆ TMA-Cl	49.88 ± 6.24	0.48 ± 0.03	0.989
C ₁₂ BDMA-Cl	9.76 ± 1.44	0.63 ± 0.03	0.992
C ₁₆ BDMA-Cl	99.66 ± 20.85	0.48 ± 0.07	0.936

^a At 24 h adsorption equilibration period.

^b Mean ± standard error (number of data points = 8).

loamy and colloidal solids which have heterogeneous structure that also results in poor sludge settleability. n values of QACs, in fact, were similar for a specific sludge sorbent which indicates that n depends mainly on sorbent properties and less on the sorbate.

The adsorption capacity factors were expressed in terms of molar QAC concentration (K_F) in order to better compare the K_F values obtained in this study to those previously reported (Table 4.6). The K_F values for both monoalkonium and benzalkonium chlorides increased with increasing alkyl chain length for each municipal sludge. In turn, benzyl containing homologues had higher K_F values than non-benzyl containing QACs. According to these results, the affinity of individual QACs to adsorb on municipal biosolids forms the following series in descending order: C₁₆BDMA-Cl, C₁₆TMA-Cl, C₁₂BDMA-Cl and C₁₂TMA-Cl. The adsorption affinity of a particular QAC, in fact, was similar for every municipal sludge tested in this study and comparable with previously reported values (Garcia et al., 2004; Garcia et al., 2006) (Table 4.6). These results suggest that adsorption affinity is mainly dependent on the QAC structure and less on the sorbent type/composition when the QAC affinity is normalized to the VS concentration.

A satisfactory correlation between CMC and K_F was obtained for each sludge sorbent used in this study (Figure 4.13). The relation between CMC and K_F was expressed using an equation similar to Equation 4.9 as follows:

$$\log K_F = F - g \log \text{CMC} \quad (\text{Equation 4.11})$$

where F is the intercept and g is the slope of the regression line. The reciprocal of g correlates with the adsorption intensity. Noticing that the F and g values for all sludges were similar, indicates the significance of the sorbate on adsorption affinity rather than

Table 4.6. Comparison of sorption affinities of monoalkonium and benzalkonium chlorides for different sludge sorbents

Sludge sorbents	K_F (mmol/g)(1/mM) ^a			
	C ₁₂ TMA-Cl	C ₁₆ TMA-Cl	C ₁₂ BDMA-Cl	C ₁₆ BDMA-Cl
PS	0.17±0.03	3.05±0.35	1.76±0.32	4.93±0.45
WAS	0.18±0.03	3.55±0.56	1.69±0.30	3.99±0.46
AS	0.32 ^a	6.89 ^a	1.59 ^b	6.44 ^b
MDS	0.28±0.11	3.48±0.30	0.93±0.18	5.83±1.71
TDS	0.38±0.20	2.47±0.31	1.11±0.16	4.52±0.95

^a (Garcia et al., 2004); bromide salts of monoalkonium chlorides were used

^b (Garcia et al., 2006)

the sludge type. On the other hand, when Equations 4.9 and 4.11 are compared, the D and 1/g values had to be the same if the adsorption is driven solely by hydrophobicity.

However, the 1/g value (ca. 1) is higher than the D value (ca. 0.5). This result indicates that other processes such as ionic interaction between the QAC polar head and ionic sites of biosolids are also included in the QAC sorption mechanism besides the hydrophobic interactions. On the other hand, the pattern of K_F dependence on alkyl chain length (Figure 4.14) for monoalkonium and benzalkonium chlorides is similar to the pattern of CMC dependence on alkyl chain length (Figure 4.4). According to these results, the adsorption affinity increases with increasing alkyl chain length. The benzyl group further enhances the adsorption affinity but the benzyl group effect diminishes as the total carbon number of the alkyl chain increases. For all practical purposes, the adsorption affinity of monoalkonium and benzalkonium chlorides becomes the same when the alkyl chain contains 18 or more carbons. The same observation was made while the effect of the

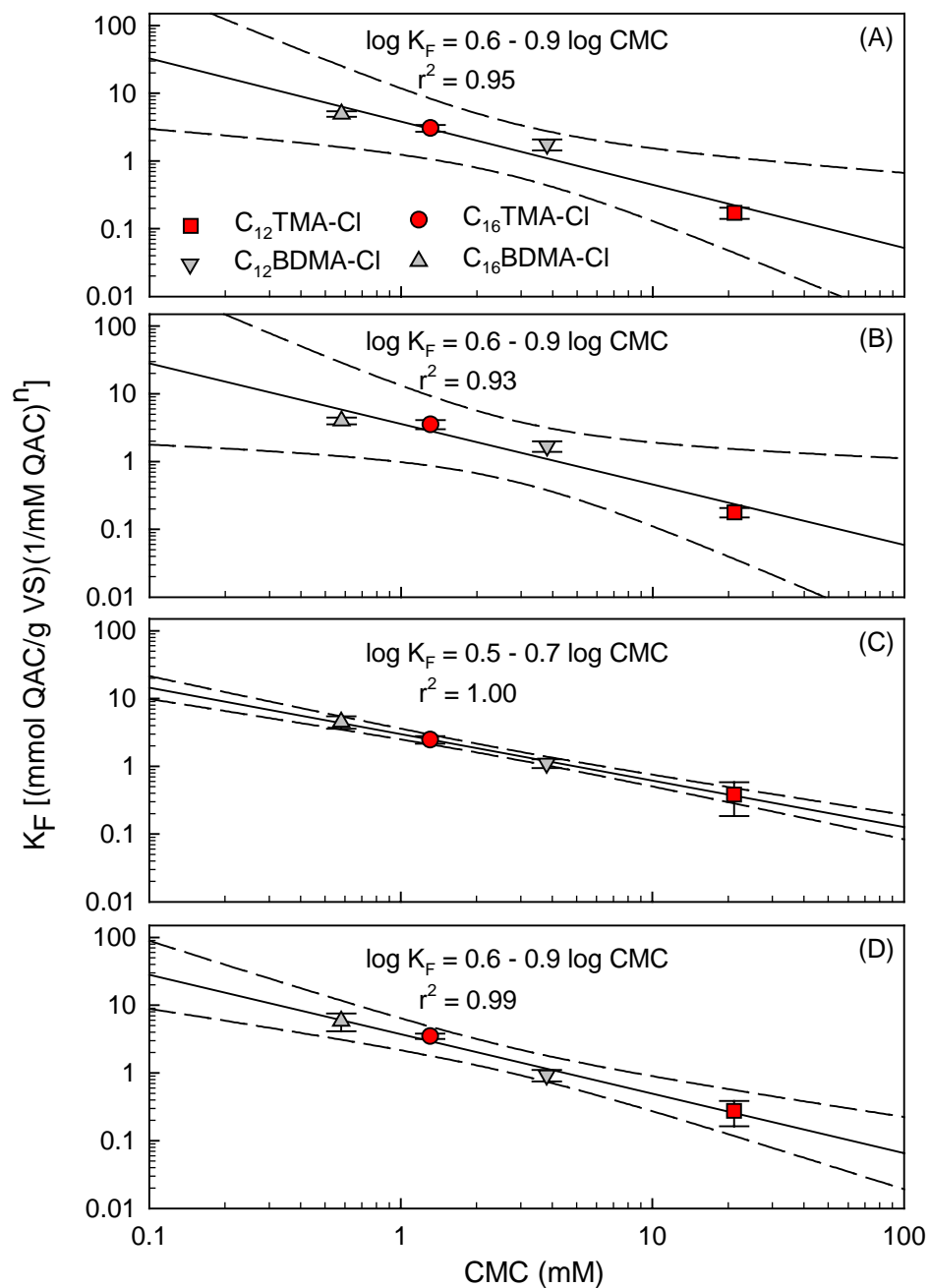


Figure 4.13. Relationship between CMC and adsorption affinity of monoalkonium and benzalkonium chlorides on (A) PS, (B) WAS, (C) TDS and (D) MDS (Dashed lines represent 95% confidence intervals)

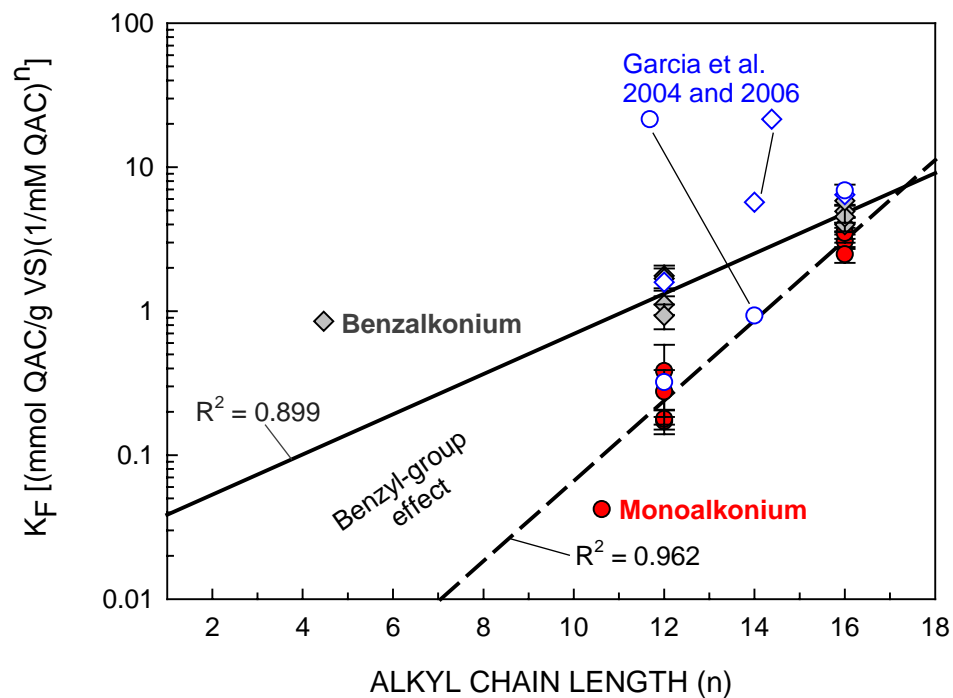


Figure 4.14. Effect of the alkyl chain length (n) on the adsorption affinity of monoalkonium and benzalkonium chlorides on different sludge sorbents

alkyl chain length on the CMC was considered in previous sections of this chapter (see Figure 4.5).

In conclusion, QACs have a high sorption affinity for municipal biosolids. The affinity depends mainly on the QAC structure rather than the sludge composition. QACs with a longer alkyl chain adsorb more than QACs with a shorter alkyl chain. The benzyl group enhances adsorption. The mechanism of QAC sorption on biosolids is complex, but both hydrophobic and ionic interactions are probably in effect. The CMC represents both hydrophobic and ionic properties of QACs and is thus an effective descriptor for QSAR modeling of biosolids partitioning of QACs.

4.3.3. Assessment of QAC Toxicity

The 5- and 15-minute acute toxicity of monoalkonium, dialkonium and benzalkonium chlorides to the bioluminescent marine microorganism *Vibrio fischeri* was investigated and the results are given in Table 4.7.

Table 4.7. Results of the Microtox® acute toxicity assay (5- and 15-min) of monoalkonium, dialkonium and benzalkonium chlorides

Compound	5 min-EC ₅₀ (mg/L)	15 min-EC ₅₀ (mg/L)
Monoalkonium Chlorides		
C ₁₂ TMA-Cl	0.26 [0.25-0.33] ^a	0.19 [0.16-0.23]
C ₁₄ TMA-Cl	0.90 [0.87-0.94]	0.40 [0.38-0.43]
C ₁₆ TMA-Cl	1.22 [1.08-1.37]	0.56 [0.38-0.83]
Dialkonium Chlorides		
DC ₈ DMA-Cl	0.20 [0.16-0.27]	0.12 [0.08-0.17]
DC ₈₋₁₀ DMA-Cl	0.28 [0.21-0.36]	0.17 [0.12-0.23]
DC ₁₀ DMA-Cl	0.49 [0.48-0.51]	0.25 [0.18-0.35]
Benzalkonium Chlorides		
C ₁₂ BDMA-Cl	0.19 [0.14-0.27]	0.14 [0.09-0.21]
C ₁₄ BDMA-Cl	0.38 [0.31-0.48]	0.27 [0.20-0.36]
C ₁₆ BDMA-Cl	0.92 [0.73-1.16]	0.66 [0.50-0.86]

^a Values in parenthesis are 95% confidence intervals

The 5-min EC₅₀ values of the target QACs ranged from 0.19 to 1.22 mg/L with a median at 0.38 mg/L (n=9) whereas the 15-min EC₅₀ values were between 0.12 and 0.66 mg/L with a median at 0.25 mg/L (n=9). These results show that the toxicity of QACs increases as the exposure time increases, meaning that a certain exposure time is

necessary for QACs to reach the target sites. Noting that as discussed above, QAC adsorption reaches equilibrium after 3 hours, the exposure time is important if the mode of toxicity is related to adsorption to and dissociation of cell membrane. The EC_{50} values obtained in this study are consistent with previously reported values obtained using the same toxicity assay (Leal et al., 1994; Garcia et al., 2001; Nalecz-Jawecki et al., 2003; Sutterlin et al., 2008). The lowest EC_{50} , which indicates the highest toxicity, in each QAC group was found to be QACs with the shortest alkyl chain length within an homologous group. These are C_{12} TMA-Cl, DC_8 DMA-Cl and C_{12} BDMA-Cl which belong to monoalkonium, dialkonium and benzalkonium chlorides, respectively. On the other hand, the highest EC_{50} values in each QAC group was found to be QACs which have the longest alkyl chain length within an homologous group. These are C_{16} TMA-Cl, DC_8 DMA-Cl and C_{12} BDMA-Cl which belong to monoalkonium, dialkonium and benzalkonium chlorides, respectively (Figure 4.15 and Figure 4.16). According to these results, the toxicity of QACs forms the following series in descending order: C_{12} BDMA-Cl > DC_8 DMA-Cl > C_{12} TMA-Cl > DC_{8-10} DMA-Cl > C_{14} BDMA-Cl > DC_{10} DMA-Cl > C_{14} TMA-Cl > C_{16} BDMA-Cl > C_{16} TMA-Cl, at 5 minute exposure time. However, the order changed as the exposure time increased and became as follows: DC_8 DMA-Cl > C_{12} BDMA-Cl > DC_{8-10} DMA-Cl > C_{12} TMA-Cl > DC_{10} DMA-Cl > C_{14} BDMA-Cl > C_{14} TMA-Cl > C_{16} TMA-Cl > C_{16} BDMA-Cl. The correlation between CMC and toxicity was poor for a 5-minute exposure time with an r^2 equal to 0.19, but became better for a 15-minute exposure time (Figure 4.17). In both cases, QACs with a higher CMC value were more toxic than the ones with a lower CMC value. The mode of action of QACs against bacteria involves perturbation of cytoplasmic membrane, inhibition of respiratory

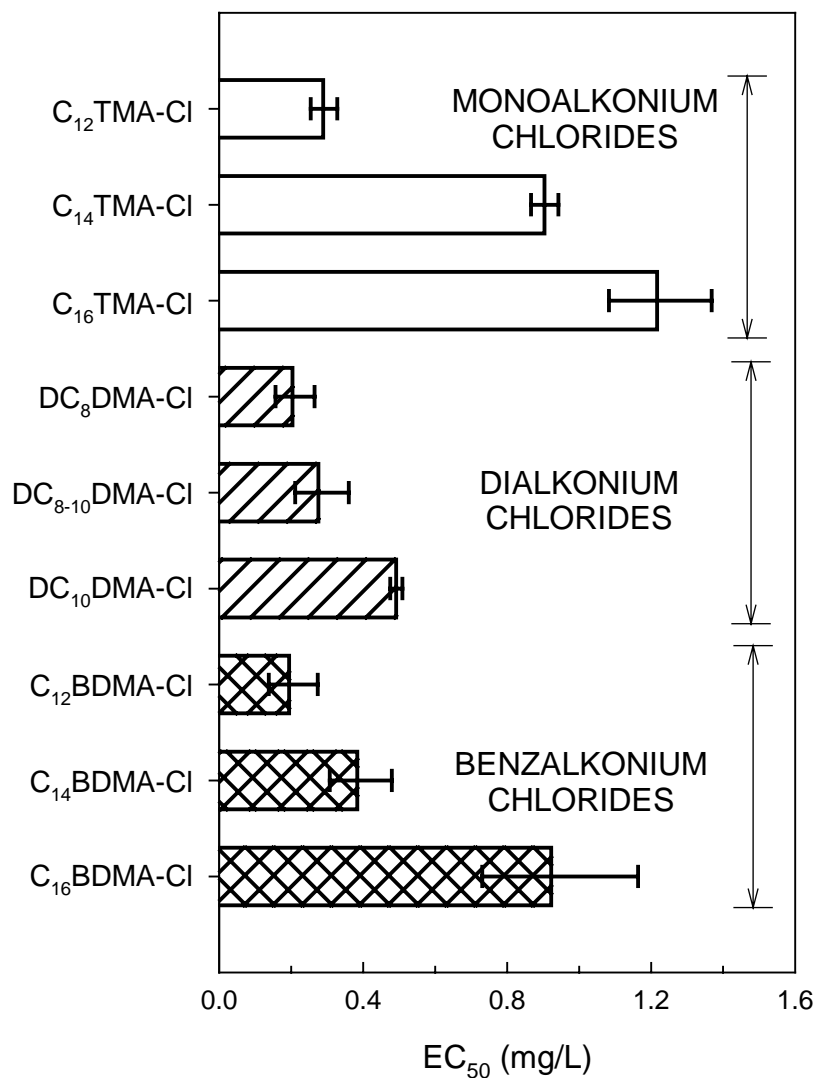


Figure 4.15. The 5-minute acute toxicity EC₅₀ values of monoalkonium, dialkonium and benzalkonium chlorides to the bioluminescent marine microorganism *Vibrio fischeri* obtained using the Microtox® assay (Error bars represent 95% confidence intervals)

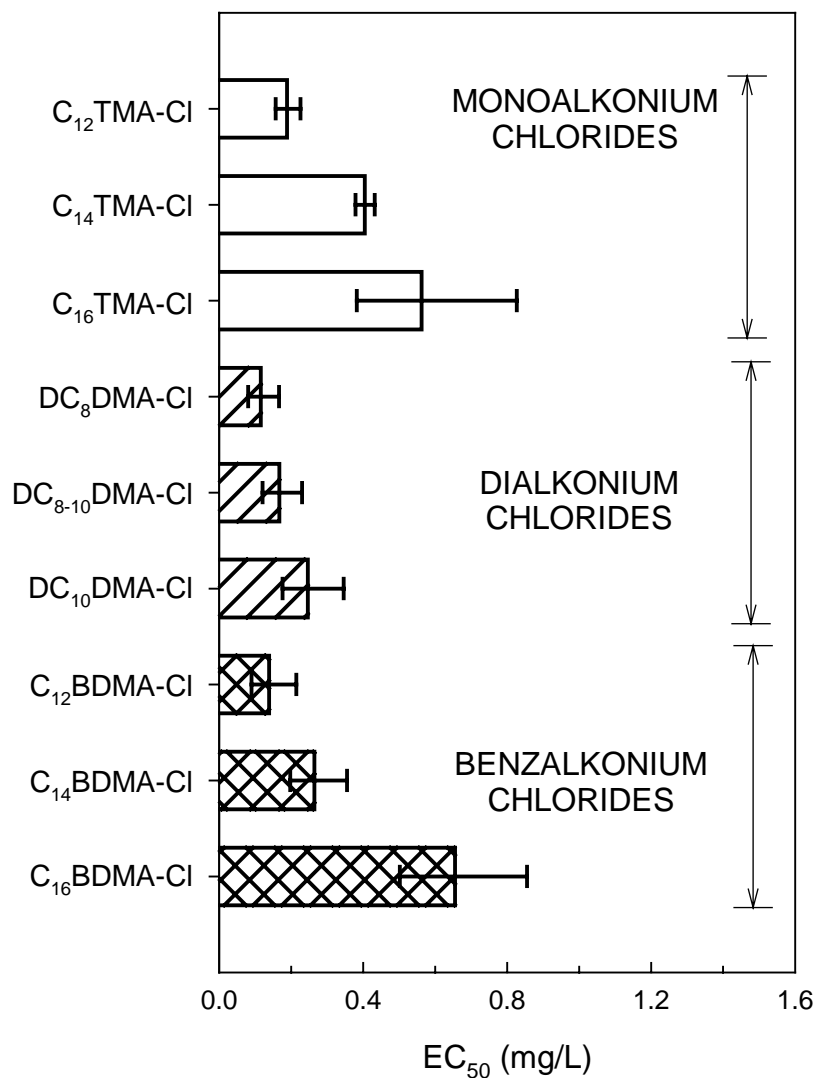


Figure 4.16. The 15-minute acute toxicity EC₅₀ values of monoalkonium, dialkonium and benzalkonium chlorides to the bioluminescent marine microorganism *Vibrio fischeri* obtained using the Microtox® assay (Error bars represent 95% confidence intervals)

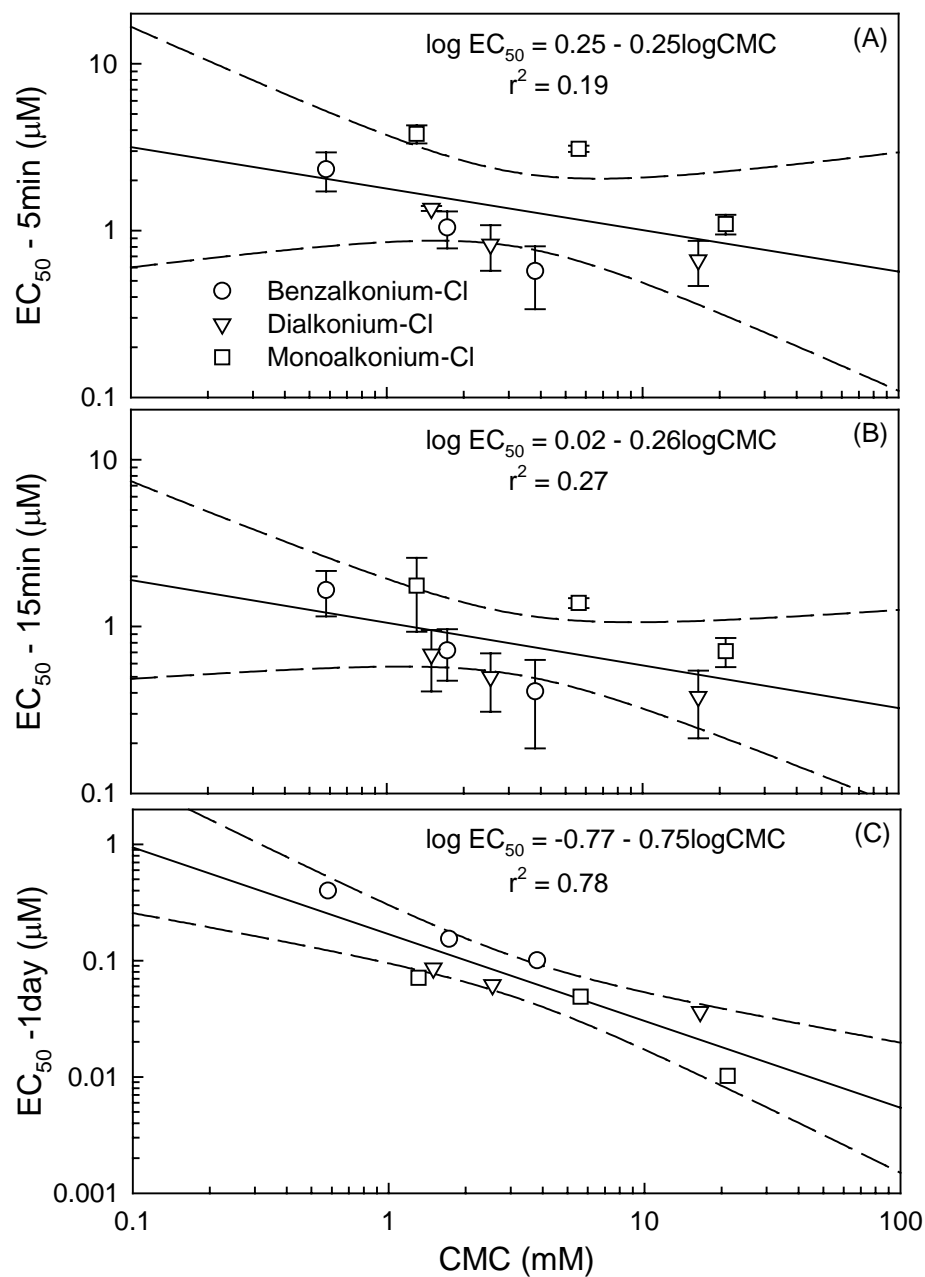


Figure 4.17. Relationship between the CMC and EC₅₀ values of monoalkonium, dialkonium and benzalkonium chlorides at (A) 5-minute, (B) 15-minute and (C) 1-day exposure time (Error bars represent 95% confidence intervals)

enzymes and dissipation of proton motive force (Maillard, 2002). Which one predominates may depend on the QAC structure as well as the exposure time. The observed effect of exposure time on QAC toxicity, therefore, is attributed to the difference between the mode of toxicity that each QAC structure exerted.

The EC_{50} values obtained for 5 and 15-minutes exposure times were extrapolated to obtain EC_{50} values for 1-day exposure time for each QAC by using a modified Chick-Watson equation as follows:

$$(EC_{50}^n)(t_{\text{exposure}}) = 0.5 \quad (\text{Equation 4.12})$$

The value of 0.5 indicates the 50 percent viable cells which in turn was defined as a constant since EC_{50} was used. The toxicity of QACs at 1-day exposure time forms the following series: $C_{12}\text{TMA-Cl} > \text{DC}_8\text{DMA-Cl} > C_{14}\text{TMA-Cl} > \text{DC}_{8-10}\text{DMA-Cl} > C_{16}\text{TMA-Cl} > \text{DC}_{10}\text{DMA-Cl} > C_{12}\text{BDMA-Cl} > C_{14}\text{BDMA-Cl} > C_{16}\text{BDMA-Cl}$. The correlation between the CMC and EC_{50} for a 1-day exposure time was better than the previous ones with an r^2 equal to 0.78 (Figure 4.17), indicating that chronic toxicity can be modeled more accurately by using CMC than the acute toxicity.

The (bio)available QAC concentration reaches a maximum at the CMC. Any agent or factor that decreases the CMC also diminishes the available QAC concentration. As the available QAC concentration decreases so does the biocidal activity. It was demonstrated that anions decrease the CMC of QACs by reducing the polarity of the head group and in turn increase the hydrophobicity of the overall molecule as they form ion pairs with the QACs. The effect of counter-ions, such as Br^- , NO_3^- and acetate, on the toxicity of benzalkonium chlorides was investigated at 342 mM counter-ion

concentration by using the Microtox® assay (the maximum achievable counter ion concentration that does not affect the performance of the Microtox® assay).

None of the counter-ions tested significantly affected the toxicity of the benzalkonium chlorides at each exposure time ($p > 0.05$) (Figure 4.18). This result indicates that QACs are toxic at such low concentrations that counter-ions do not affect their (bio)availability. Sutterlin et al. (2008) also reported no effect of anionic surfactants which are stronger electrolytes than the inorganic anions, to the toxicity of benzalkonium chloride using the *Vibrio fischeri* as the test organism (Sutterlin et al., 2008). Accounting. Considering that inorganic anions are present in both natural and engineered biological systems, their contribution to QAC toxicity is negligible.

Natural organic matter (NOM) is another major constituent in engineered and natural systems. NOM is known to chelate cationics and decrease their bioavailability (Schwarzenbach et al., 2003). Given the cationic nature of QACs, the effect of NOM on the toxicity of benzalkonium chlorides was tested at concentrations up to 100 mg/L.

NOM decreased the toxicity of benzalkonium chlorides for both 5- and 15-minute exposure time (Figure 4.19). The toxicity is linearly and negatively correlated with the NOM concentration. That is, as the NOM concentration increases the toxicity of benzalkonium chlorides decreases. The toxicity decreases at a rate of 0.007, 0.009 and 0.150 per mg NOM/L for a 5-minute exposure time and 0.004, 0.006, and 0.07 per mg NOM/L for a 15-minute exposure time (Figure 4.20). The most pronounced effect was found for the C₁₆BDMA-Cl, which is the most hydrophobic QAC among the benzalkonium chlorides tested. These results suggest that not only ionic interactions between QACs and NOM that cause chelation of QAC by the NOM, but also

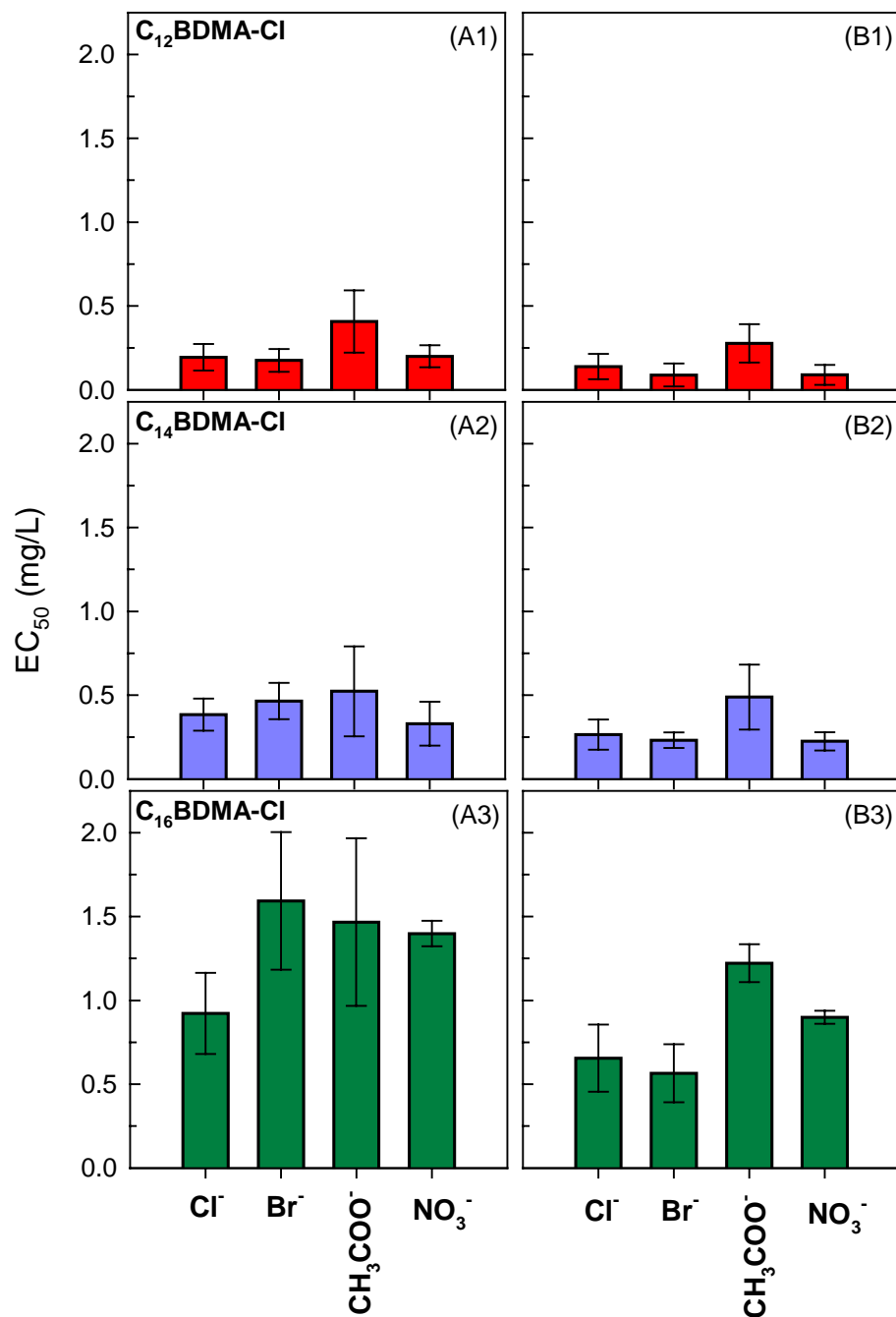


Figure 4.18. The effect of 342 mM Br⁻, CH₃COO⁻ and NO₃⁻ on the toxicity of (1) C₁₂BDMA-Cl, (2) C₁₄BDMA-Cl and (3) C₁₆BDMA-Cl for (A) 5-minute and (B) 15-minute exposure times (Error bars represent 95% confidence intervals)

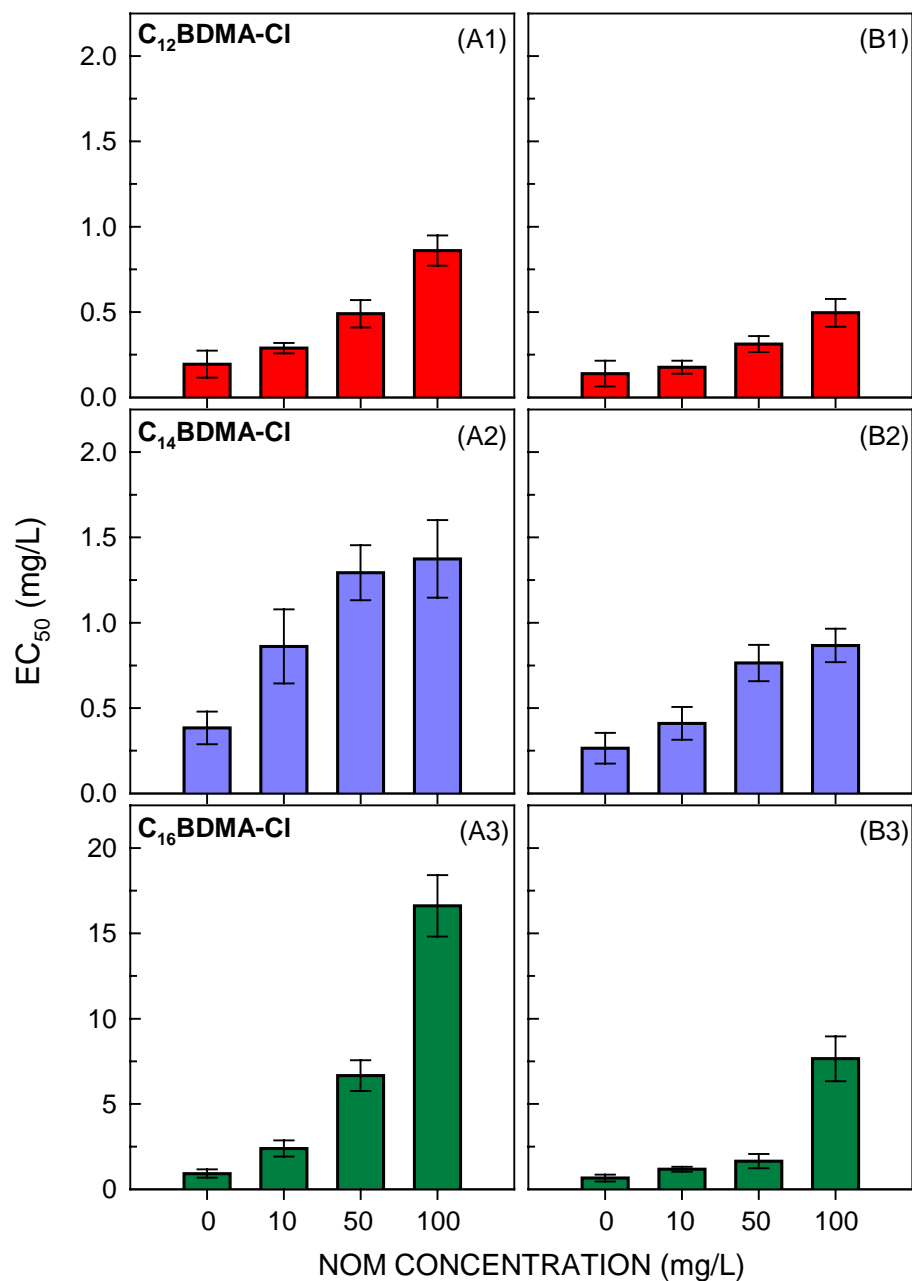


Figure 4.19. The effect of NOM at different concentrations (10-100 mg/L) on the toxicity of (1) C₁₂BDMA-Cl, (2) C₁₄BDMA-Cl and (3) C₁₆BDMA-Cl for (A) 5-minute and (B) 15-minute exposure time (Error bars represent 95% confidence intervals)

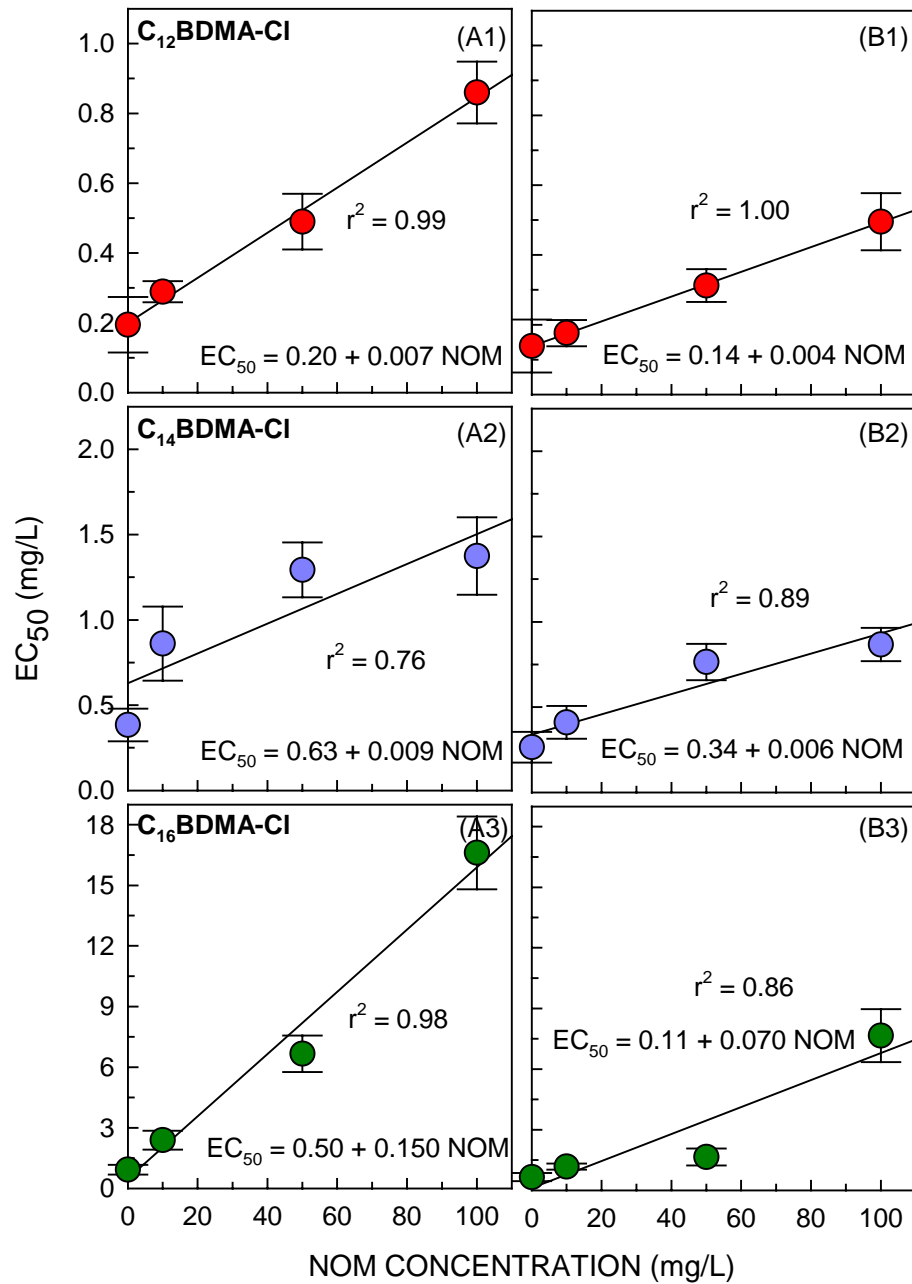


Figure 4.20. Relationship between NOM concentration and EC₅₀ of (1) C₁₂BDMA-Cl, (2) C₁₄BDMA-Cl and (3) C₁₆BDMA-Cl for a (A) 5-minute and (B) 15-minute exposure time (Error bars represent 95% confidence intervals)

hydrophobic interactions, such as adsorption of QAC to dissolved NOM, affect the (bio)availability of QACs, especially the most hydrophobic ones.

4.4. Summary

The critical micelle concentration of nine QACs belonging to three QAC groups was determined. The factors that affect the CMC, such as alkyl chain length, hydrophobicity and counter-ions were identified and their impact on CMC was quantified. The QACs tested had different CMCs ranging from 0.58 to 21.13 mM. In general, QACs with longer alkyl chain lengths had lower CMCs than the ones with shorter alkyl chain lengths. The length of alkyl chain affected mainly the hydrophobicity of the QACs. As a result, the CMC correlated well with the $\log K_{ow}$ which was either measured or calculated using the Hansch and Leo method. Micellization was positively correlated not only with the alkyl chain length and hydrophobicity, but also with the counter-ion concentration. The presence of counter-ions, such as Br^- , NO_2^- , CH_3COO^- and NO_3^- , decreased the CMC of QACs to some extent. The order of counter-ion binding to the QAC micelles was as follows: $Cl^- > NO_2^- > Br^- > CH_3COO^- > NO_3^-$; that is, the larger anions that are more polarizable bind to QACs more effectively and result in a decrease of the CMC.

The CMC was used as a descriptor in QSAR modeling of biosolids partitioning and toxicity, which are two important end-points that determine the fate and impact of QACs in engineered and natural biological systems. The adsorption affinity of monoalkonium and benzalkonium chlorides to four different municipal sludges with different characteristics, i.e., primary, waste activated, mesophilic digested and

thermophilic digested sludges, was tested. The acute toxicity of QACs was determined using the Microtox® assay.

The QACs tested in this study had a high sorption affinity for biosolids and their affinity depended mainly on the QAC structure rather than the biosolids chemical composition. QACs with lower CMCs had a higher adsorption affinity for biosolids than QACs with higher CMCs. This result suggests that QACs with high CMCs are more mobile in engineered and natural systems than the ones with lower CMCs. On the contrary, QACs with a high CMC were more toxic than the ones with low CMCs. The combination of these two facts brings out a detrimental environmental impact associated with QACs, that is, QACs which are more mobile and (bio)available are more toxic. The presence of anions has no significant effect on the toxicity. On the other hand, NOM decreases the toxicity of QACs. Quantitative sorption and toxicity information obtained, along with the QSAR approach developed in this study, would help to better determine the environmental impact of QACs.

CHAPTER 5

BIOTRANSFORMATION OF BENZALKONIUM CHLORIDE

UNDER AEROBIC CONDITIONS

5.1. Introduction

Biotransformation of monoalkonium, dialkonium and benzalkonium chlorides mainly commences with the cleavage of the bond between the alkyl group and the quaternary nitrogen. The monooxygenase catalyzed degradation of the produced alkyl aldehydes proceeds via β -oxidation for the complete mineralization, whereas the hydrophilic amines, such as trimethyl amine, dimethyl amine, and benzyl dimethyl amine, formed after the dealkylation of monoalkonium, dialkonium and benzalkonium chlorides, respectively, are converted to ammonium and carbon dioxide. Once the alkyl chain is removed, the toxicity is reduced and the resulting products are more bioavailable.

The microorganisms that are capable of using QACs as carbon and energy source are mainly classified in the genus *Pseudomonas* (Dean-Raymond and Alexander, 1977; Geftic et al., 1979; van Ginkel et al., 1992; Nishihara et al., 2000; Kaech and Egli, 2001; Nishiyama and Nishihara, 2002; Takenaka et al., 2007; Liffourrena et al., 2008). Other species that can catabolize various QACs are *Xanthomonas* sp. (Dean-Raymond and Alexander, 1977) and *Aeromonas* sp. (Patrauchan and Oriel, 2003).

Benzalkonium chlorides (BAC) are a group of QACs that are extensively used in various domestic and industrial applications (U.S. Environmental Protection Agency, 2006) and are the most predominant QACs found in engineered and natural systems (Kummerer et al., 1997; Clara et al., 2007; Kreuzinger et al., 2007; Martinez-Carballo et

al., 2007; Martinez-Carballo et al., 2007). Until recently, few studies had focused on the biotransformation/biodegradation of BAC (Patrauchan and Oriol, 2003; Qin et al., 2005). The biotransformation pathway of benzalkonium chlorides by a pure culture of *Aeromonas hydrophila* sp. K was recently reported (Patrauchan and Oriol, 2003). According to the results of this study, BAC biotransformation commences with the fission of the alkyl group from the quaternary nitrogen resulting in the formation of benzyl dimethyl amine as the first intermediate. This bacterium is capable of growing on benzyl dimethyl amine and converts it sequentially to benzyl methyl amine, benzyl amine and ammonia by following two demethylations and a debenzylation. In contrast, van Ginkel (2004) demonstrated an alternative BAC biotransformation pathway in a mixed culture. Based on this pathway, BAC is transformed into benzyl dimethyl amine, dimethyl amine and ammonia as a result of dealkylation, debenzylation and demethylation, which hypothetically involves three microorganisms that utilize the alkyl chain, the benzyl group and the dimethyl amine, respectively (van Ginkel, 2004). However, the microbial community capable of BAC degradation according to the above pathway was not described in that study. On the other hand, Kummerer et al. (2002) demonstrated that members of genus either *Acinetobacter* or *Pseudomonas* were selected in an activated sludge microcosm upon exposure to BAC (Kummerer et al., 2002). In another example, as a response to application of a nonionic surfactant in a hydrocarbon contaminated soil, a *Pseudomonas* population, which could utilize both hydrocarbons and the surfactant dominated (Colores et al., 2000). *Pseudomonas* was also the predominant genus among the microbial community isolated from a QAC-contaminated environment (Gaze et al., 2005).

The objectives of the research reported in this chapter were to: (a) assess the biotransformation mechanism and kinetics of C₁₄BDMA-Cl, which is the most common and predominant BAC detected in engineered and natural systems, by using bioenergetic calculations and biotransformation experiments; and (b) elucidate the microbial community structure of a mixed culture maintained using C₁₄BDMA-Cl as the sole carbon and energy source.

5.2. Materials and Methods

5.2.1. BAC Enrichment Culture

A suspended growth mixed, aerobic culture was developed using as inoculum a contaminated sediment sample collected at the Bayou d' Inde, a tributary of the Calcasieu River, near Lake Charles, Louisiana. The bayou and adjacent marshes are contaminated by hazardous substances, including polycyclic aromatic hydrocarbons (PAHs), metals, polychlorinated biphenyls (PCBs), dioxins/furans, and other hazardous compounds released from chemical manufacturing and petroleum refining facilities (http://www.darrp.noaa.gov/southeast/bayou_dinde/index.html). The culture was initially developed using a mixture of dextrin/peptone in order to sustain a diverse heterotrophic microbial community (Yang, 2007) and was fed-batch with 50 mg/L of BAC. Subsequently, using the mixed culture as inoculum, another BAC-degrading culture was enriched which has been maintained for almost two years using the benzalkonium chloride mixture as the sole carbon/energy source supplemented with stoichiometric levels of NH₄NO₃ as the nitrogen source (referred to as BAC enrichment culture).

The BAC enrichment culture has been maintained in a 2-L Pyrex® reactor with a total liquid volume of 1.6 L, a residence time of 14 days, fed once a week with media and

200 mg BAC/L (in the feed solution). The steady-state pH and VSS concentration of this culture was 6.9 and 137.6 mg/L ($2.41 \pm 0.31 \times 10^9$ cells/mL, measured by using DAPI staining).

5.2.2. Energetics Calculations

The standard Gibb's free energies of formation ($\Delta G_f^{0'}$) of QACs have not been published. A group contribution method developed by Mavrovouniotis (1990) was used to calculate $\Delta G_f^{0'}$ values of QACs and potential QAC transformation products using Equation 5.1.

$$\Delta G_f^{0'} = \sum_1^i a_i \Delta G_{f,i}^{0'} \quad (\text{Equation 5.1})$$

where, a is the number of occurrence of group i and $\Delta G_{f,i}^{0'}$ is the standard Gibb's free energy of formation of group i . The calculated $\Delta G_{f,i}^{0'}$ values are given in Appendix B. $\Delta G_f^{0'}$ values of other compounds involved in reactions of interest were obtained from the literature (Thauer et al., 1977; Rittmann and McCarty, 2001). The standard Gibb's free energies of half-reactions ($\Delta G^{0'}$) and oxidation-reduction reactions ($\Delta G_{\text{reac}}^{0'}$) without cell synthesis were calculated by using Equation 5.2 according to the method described by Rittmann and McCarty (2001).

$$\Delta G^{0'} \text{ (or } \Delta G_{\text{reac}}^{0'}) = \sum_1^j p_j \Delta G_{f,p_j}^{0'} - \sum_1^k r_k \Delta G_{f,r_k}^{0'} \quad (\text{Equation 5.2})$$

where, p is the molar fraction of product j and r is the molar fraction of reactant k whereas $\Delta G_{f,p}^{0'}$ and $\Delta G_{f,r}^{0'}$ are the standard Gibb's free energies of formation of products and reactants, respectively.

5.2.3. Batch Biotransformation Assay

A batch assay was performed to delineate the biotransformation potential and kinetics of C₁₄BDMA-Cl as well as its potential biotransformation products reported by Patrauchan et al. (2003), i.e., benzyl dimethyl amine (BDMA), benzyl methyl amine (BMA) and benzyl amine (BA), and two other QACs which were C₁₄TMA-Cl and benzyl trimethyl ammonium chloride (BTMA). The latter compounds are homologues of C₁₄BDMA-Cl having either no benzyl (C₁₄TMA-Cl) or long-chain alkyl group (BTMA). The assay was performed in 250-mL Erlenmeyer flasks. A sample of 1.5 L BAC enrichment culture, collected at the end of 7-day feeding cycle, was centrifuged at 10,000 xg and the pellet was washed and resuspended in an equal volume (1.5 L) fresh autoclaved culture media with a composition given in Chapter 3. The pH of the resuspended culture was adjusted to 7.0 with sodium bicarbonate.

Six culture series, used to determine the biotransformation kinetics of the individual compounds given above, were prepared by transferring 99 mL of resuspended culture along with 1 mL of 10 mM solution of an individual compound into each flask. The initial concentration of each compound in the corresponding culture was about 100 µM. The VSS concentration in all cultures was 78.7±5.3 mg/L. The cultures were agitated at 190 rpm on a rotary shaker and incubated at room temperature (22-23°C) over night. The cultures in which the compounds were depleted, were re-amended with the corresponding compound at the same initial concentration. The time course concentration of each compound in the corresponding culture was monitored.

A dilute culture was prepared by using 40 mL of inoculum and 59 L culture media in a 250-mL Erlenmeyer flask and was amended with 1 mL of 10 mM C₁₄BDMA-

Cl. The VSS concentration of the dilute culture was 31.5 ± 2.8 mg/L. This culture was used to elucidate the mechanism of C₁₄BDMA-Cl biotransformation. All the biotransformation experiments were performed without replicates.

5.2.4. Phylogenetic Analysis of the BAC Enrichment Culture

A sample of 30 mL BAC enrichment culture was centrifuged at 10,000 rpm and the pellet was resuspended in 250 μ L sterile 0.85% NaCl solution. DNA of the culture suspension was extracted using the UltraCleanTM Soil DNA Isolation Kit according to the manufacturer's instructions (MoBio Laboratories Inc., Solana Beach, CA), which includes a bead-beating and a spin-column purification step. Extracted DNA was confirmed by gel electrophoresis and quantified using NanoDrop Spectrophotometer (NanoDrop Technologies, Wilmington, DE). *Bacteria* 16S rDNA of extracted DNA was amplified by PCR using TaKaRa Ex TaqTM Kit (TaKaRa Bio USA, Madison, WI). The final concentrations of each chemical in the reaction mixture were: TaKaRa Ex Taq polymerase (1 unit), Ex Taq Buffer (1x), dNTPs (0.25mM each), DNA template (30 ng or 1 μ L), 27F forward primer (27F: 5'-AGAGTTTGATCCTGGCTCAG-3') (0.2 μ M), and 1522R reverse primer (1522R: 5'-AAGGAGGTGATCCARCCGCA-3') (0.2 μ M). PCR conditions included an initial denaturation at 95°C for 2 min and 60°C for 2 min, followed by 35 cycles at 95°C (1min), 52°C (1min) and 72°C (1min), with a final extension at 72°C for 10 min. Amplified 16S rDNA was electroporated on 0.7% agarose gel (SeaKem LE Agarose, Lonza Inc., Williamsport, PA), stained with ethidium bromide, UV-illuminated (GelDOC2000, Biorad, CA) and purified using Qiaquick Gel Extaction Kit (Qiagen Inc., Valencia, CA).

Purified 0.2 µg of 16S rDNA was ligated into a TOPO TA cloning vector pCR2.1 (Invitrogen Corporation, Carlsbad, CA) and the vector was electroporated into electrocompetent *E.coli* cells. The cells were spread on LB plates containing 50 µL/mL ampicillin and 64 µg/mL X-gal and incubated at 37°C overnight. White colonies grown on the plates were transferred onto new LB plates containing 50 µL/mL ampicillin and were incubated at 37°C overnight. Individual colonies were picked and then transferred into 100 µL of sterilized DI water and boiled at 100°C for 15 minutes (boil-preps). The 16S rDNA insert in each clone was amplified by PCR using 1 µL of boil-prep as the DNA template, and M13F (5'-GTAAAACGACGGCCAG-3') and M13R (5'-CAGGAAACAGCTATGAC-3') primers, as described above. PCR conditions included an initial denaturation at 95°C for 2 min, followed by 25 cycles at 95°C (1min), 52°C (1 min) and 72°C (1 min), with a final extension at 72°C for 7 min. A 5 µL of PCR amplicon of each clone was analyzed on 0.7% agarose gel as described above in order to verify the right insertion of the 16S rDNA. The amplicons with the right inserts were selected and digested with MspI restriction enzyme. Restriction fragment length polymorphism (RFLP) band pattern of each amplicon was analyzed on 2% agarose gel and the clones with unique band patterns were grouped. Based on the grouping, a rarefaction curve with 95% confidence intervals was generated by using EstimateS v8.0 software package (Corwell, 2006). The 16S rDNA of each unique clone was sequenced at the Washington University Genome Sequencing Center (St. Louis, MO). The nucleotide sequences of individual inserts were trimmed, edited and assembled with CLC Main Workbench v.4.0 (CLC Bio, Denmark). Sequences were initially aligned using the BLASTN suite (Zhang et al., 2000) available through the National Center for Biotechnology Information.

Sequences were checked for chimeras using Chimera Check v.2.07 from Ribosomal Database Project II (Cole et al., 2003). Sequences from this study and their three closest neighbor sequences identified in Small Subunit Reference (SSURef) datasets were subsequently aligned using CLUSTAL W (Higgins et al., 1994). At least 640 nucleotides were included in the phylogenetic analyses of bacterial clones. A bootstrapped neighbor-joining tree with 5000 samplings was created in MEGA v4.0 software package (Tamura et al., 2007) using the Jukes-Cantor Model (Jukes and Cantor, 1969).

5.3. Results and Discussion

5.3.1. Energetics of QAC Biodegradation

The standard Gibb's free energies of half-reactions and oxidation reactions for monoalkonium, dialkonium and benzalkonium chlorides are given in Table 5.1 and 5.2. The Gibb's free energy of the QAC half-reactions is between 28.8 and 29.1 kJ/eeq, which is close to the $\Delta G^{0'}$ of acetate, and the difference in $\Delta G^{0'}$ within a group was minor (Figure 5.1). On the other hand, the free energy of QAC oxidation was between -9704 and -15239 kJ/mol QAC. Therefore, biodegradation of all QACs is energetically feasible under aerobic conditions and complete QAC mineralization should yield an average energy of 107.5 kJ per electron equivalent (eeq). Recalling that the mean electron equivalent of monoalkonium, dialkonium and benzalkonium chlorides is 102, 120 and 130 eeq/mol, biodegradation of benzalkonium chlorides is energetically more feasible than the biodegradation of dialkonium and monoalkonium chlorides. In fact, the presence of other hydrophobic groups along with the alkyl group, such as benzyl and another alkyl group, is known to decrease the biodegradability of QACs because of the steric hindrance exerted by these functional groups (Ying, 2006). The highly reduced structure of QACs,

their high adsorption affinity/low bioavailability and toxicity are other factors that limit QAC biodegradation in engineered and natural biological systems.

Table 5.1. QAC half-reactions and their Gibb's free energy at pH 7 and 298 °K

Half-Reactions	ΔG^0, kJ/eq
<i>Monoalkonium Chlorides</i>	
$C_{12}TMA: \frac{15}{90}CO_2 + \frac{1}{90}NH_4^+ + H^+ + e^- \leftrightarrow \frac{1}{90}C_{15}H_{34}N^+ + \frac{30}{90}H_2O$	29.1
$C_{14}TMA: \frac{17}{102}CO_2 + \frac{1}{102}NH_4^+ + H^+ + e^- \leftrightarrow \frac{1}{102}C_{17}H_{38}N^+ + \frac{34}{102}H_2O$	29.0
$C_{16}TMA: \frac{19}{114}CO_2 + \frac{1}{114}NH_4^+ + H^+ + e^- \leftrightarrow \frac{1}{114}C_{19}H_{42}N^+ + \frac{38}{114}H_2O$	28.8
<i>Dialkonium Chlorides</i>	
$DC_8DMA: \frac{18}{108}CO_2 + \frac{1}{108}NH_4^+ + H^+ + e^- \leftrightarrow \frac{1}{108}C_{18}H_{40}N^+ + \frac{36}{108}H_2O$	28.9
$DC_{8-10}DMA: \frac{20}{120}CO_2 + \frac{1}{120}NH_4^+ + H^+ + e^- \leftrightarrow \frac{1}{120}C_{20}H_{44}N^+ + \frac{40}{120}H_2O$	28.8
$DC_{10}DMA: \frac{22}{132}CO_2 + \frac{1}{132}NH_4^+ + H^+ + e^- \leftrightarrow \frac{1}{132}C_{22}H_{48}N^+ + \frac{44}{132}H_2O$	28.7
<i>Benzalkonium Chlorides</i>	
$C_{12}BDMA: \frac{21}{118}CO_2 + \frac{1}{118}NH_4^+ + H^+ + e^- \leftrightarrow \frac{1}{118}C_{21}H_{38}N^+ + \frac{42}{118}H_2O$	28.7
$C_{14}BDMA: \frac{23}{130}CO_2 + \frac{1}{130}NH_4^+ + H^+ + e^- \leftrightarrow \frac{1}{130}C_{23}H_{42}N^+ + \frac{46}{130}H_2O$	28.6
$C_{16}BDMA: \frac{25}{142}CO_2 + \frac{1}{142}NH_4^+ + H^+ + e^- \leftrightarrow \frac{1}{142}C_{25}H_{46}N^+ + \frac{50}{142}H_2O$	28.6

Table 5.2. QAC oxidation reactions and their Gibb's free energy at pH 7 and 298 °K

Oxidation Reactions	ΔG^0 , kJ/mol QAC
<i>Monoalkonium Chlorides</i>	
C ₁₂ TMA: C ₁₅ H ₃₄ N ⁺ + 22.5O ₂ ↔ 15CO ₂ + NH ₄ ⁺ + 15H ₂ O	-9704
C ₁₄ TMA: C ₁₇ H ₃₈ N ⁺ + 25.5O ₂ ↔ 17CO ₂ + NH ₄ ⁺ + 17H ₂ O	-10987
C ₁₆ TMA: C ₁₉ H ₄₂ N ⁺ + 28.5O ₂ ↔ 19CO ₂ + NH ₄ ⁺ + 19H ₂ O	-12257
<i>Dialkonium Chlorides</i>	
DC ₈ DMA: C ₁₈ H ₄₀ N ⁺ + 27O ₂ ↔ 18CO ₂ + NH ₄ ⁺ + 18H ₂ O	-11567
DC ₈₋₁₀ DMA: C ₂₀ H ₄₄ N ⁺ + 30O ₂ ↔ 20CO ₂ + NH ₄ ⁺ + 20H ₂ O	-12902
DC ₁₀ DMA: C ₂₂ H ₄₈ N ⁺ + 33O ₂ ↔ 22CO ₂ + NH ₄ ⁺ + 22H ₂ O	-14179
<i>Benzalkonium Chlorides</i>	
C ₁₂ BDMA: C ₂₁ H ₃₈ N ⁺ + 29.5O ₂ ↔ 21CO ₂ + NH ₄ ⁺ + 17H ₂ O	-12676
C ₁₄ BDMA: C ₂₃ H ₄₂ N ⁺ + 32.5O ₂ ↔ 23CO ₂ + NH ₄ ⁺ + 19H ₂ O	-13952
C ₁₆ BDMA: C ₂₅ H ₄₆ N ⁺ + 35.5O ₂ ↔ 25CO ₂ + NH ₄ ⁺ + 21H ₂ O	-15239

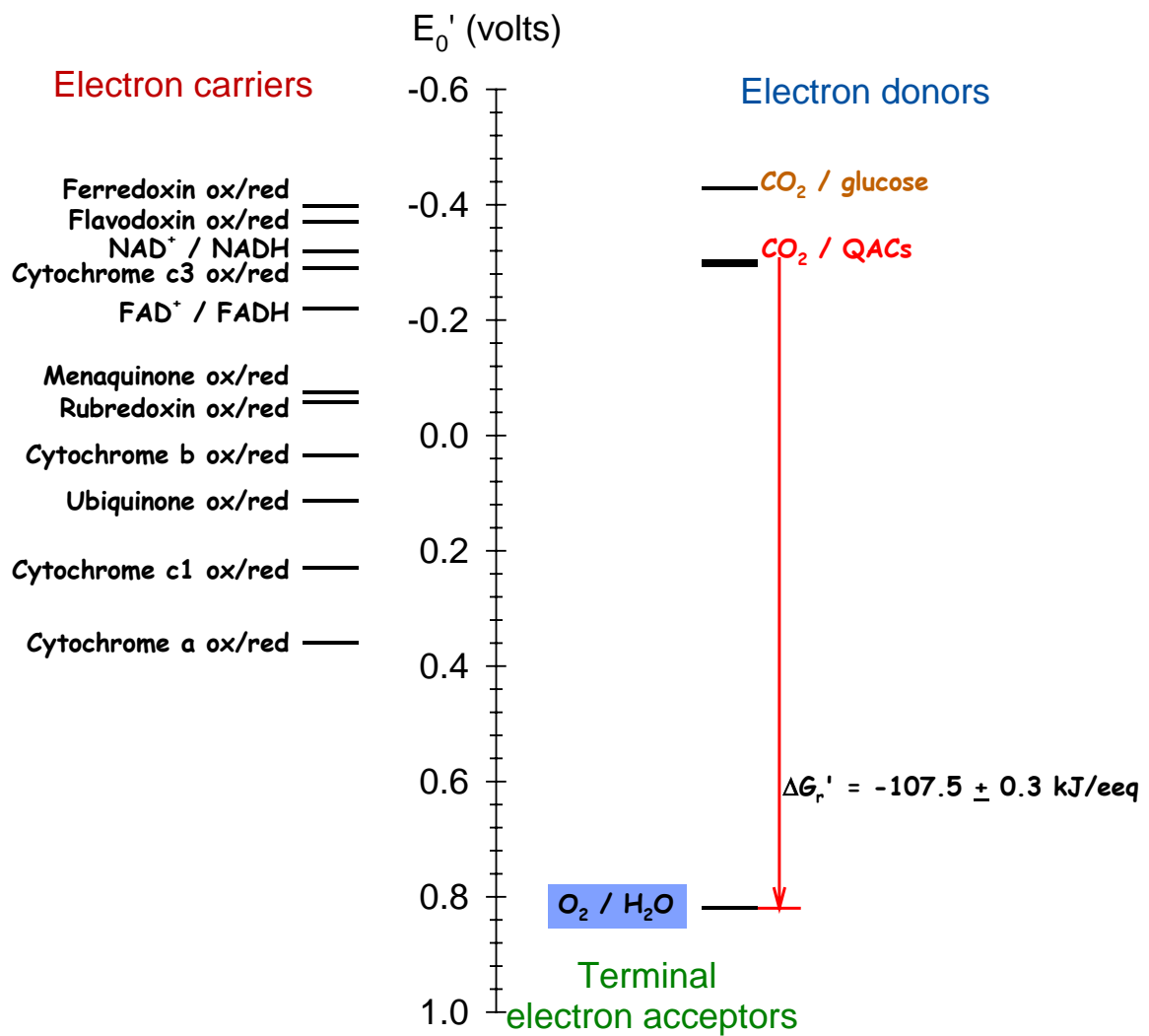


Figure 5.1. Schematic showing the positions of CO₂/QAC and O₂/H₂O redox couples on the electron tower and the standard free energy upon complete oxidation of QACs to CO₂ under oxic conditions (QACs represent monoalkonium, dialkonium and benzalkonium chlorides which have average half-reaction free energy equal to $28.9 \pm 3.5 \text{ kJ/eeq}$)

5.3.2. Biotransformation Kinetics and Pathway of C₁₄BDMA-Cl

C₁₄BDMA-Cl was utilized completely resulting in transient BDMA in the time course of the first incubation without experiencing a lag-phase (Figure 5.2). C₁₄TMA-Cl, the non-benzyl containing homologue of the C₁₄BDMA-Cl was utilized without a lag phase within 24 hours as well (Figure 5.3). The transformation of this compound yielded trimethyl amine which was qualitatively verified by the extensive fishy smell produced during the C₁₄TMA-Cl biotransformation. Trimethyl amine formation from monoalkonium chloride transformation was previously reported (van Ginkel et al., 1992). In contrast, BTMA, the non-alkyl containing homologue of the C₁₄BDMA-Cl, was not degraded throughout the incubation period (Figure 5.4). The recalcitrance of BTMA under aerobic conditions has been previously reported (Bayer Corporation, 2003). These results suggest that the alkyl moiety is the site for the first catabolic attack on a QAC molecule resulting in the cleavage of the C_{alkyl}-N bond which liberates the alkyl moiety as an aldehyde and forms a tertiary amine compound such as BDMA (Figure 5.2). The absence of an alkyl group may result in the recalcitrance of a QAC molecule.

The assay performed with a dilute culture showed that BDMA was the first product of C₁₄BDMA-Cl transformation and formed at equimolar concentration of C₁₄BDMA-Cl degraded (Figure 5.5). The BDMA transformation started after a 30 hours lag in the dilute culture having 31.5 mg VSS/L. On the other hand, the lag was about 10 hours in the culture series having 78.7 mg VSS/L (Figure 5.6A). Taking the effect of biomass concentration into account, the lag reported above for the two culture series was similar. Observing a considerable lag for the BDMA biotransformation while an active C₁₄BDMA-Cl degradation was progressing, suggests that C₁₄BDMA-Cl and BDMA

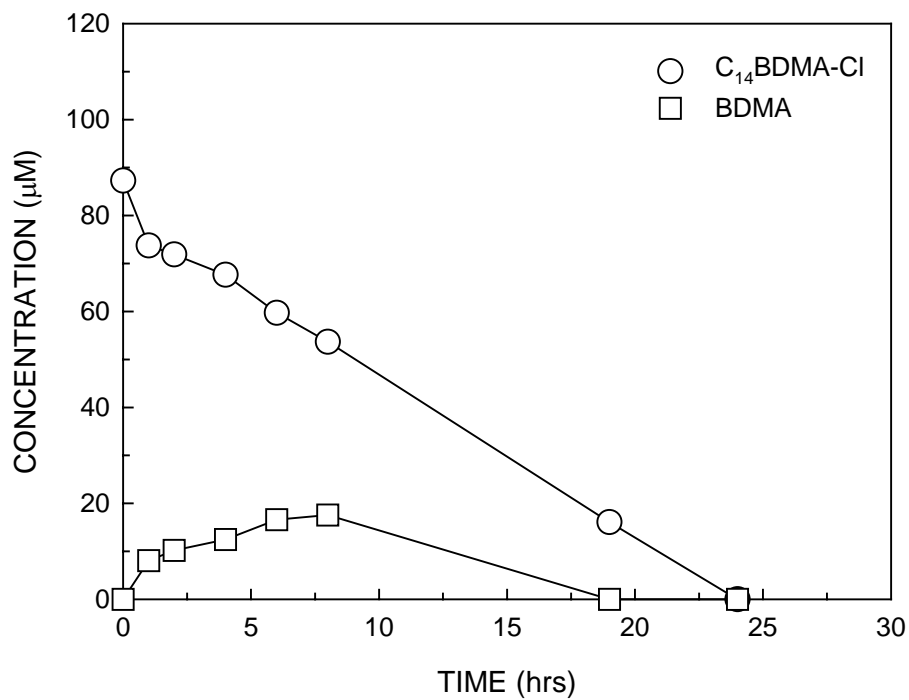


Figure 5.2. Time course of C₁₄BDMA-Cl transformation and formation and consumption of BDMA in the BAC enrichment culture amended with C₁₄BDMA-Cl

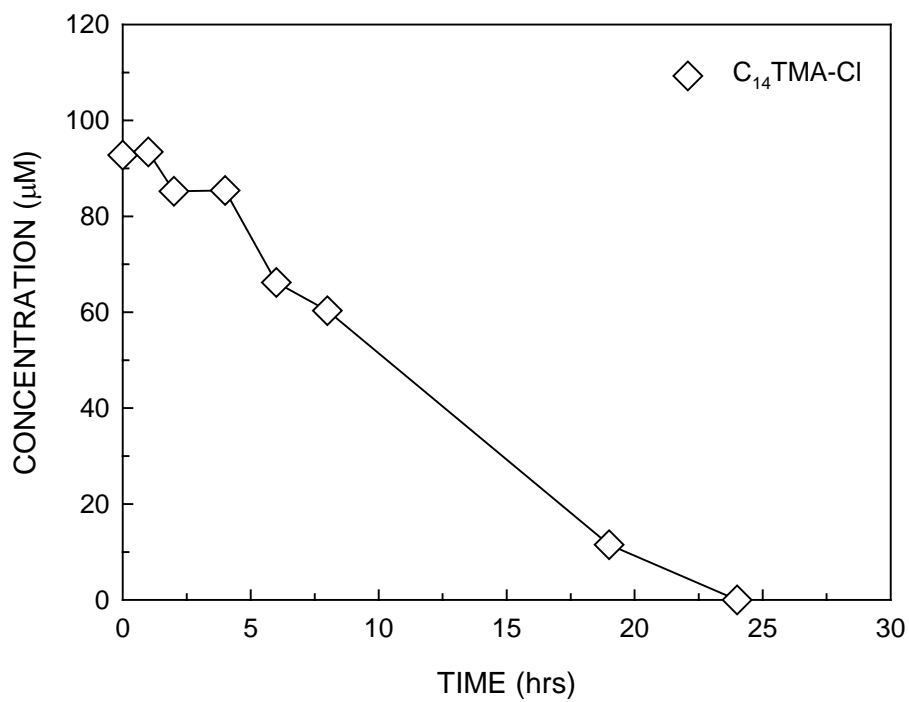


Figure 5.3. Time course of C₁₄TMA-Cl transformation in the BAC enrichment culture amended with C₁₄TMA-Cl for the first time

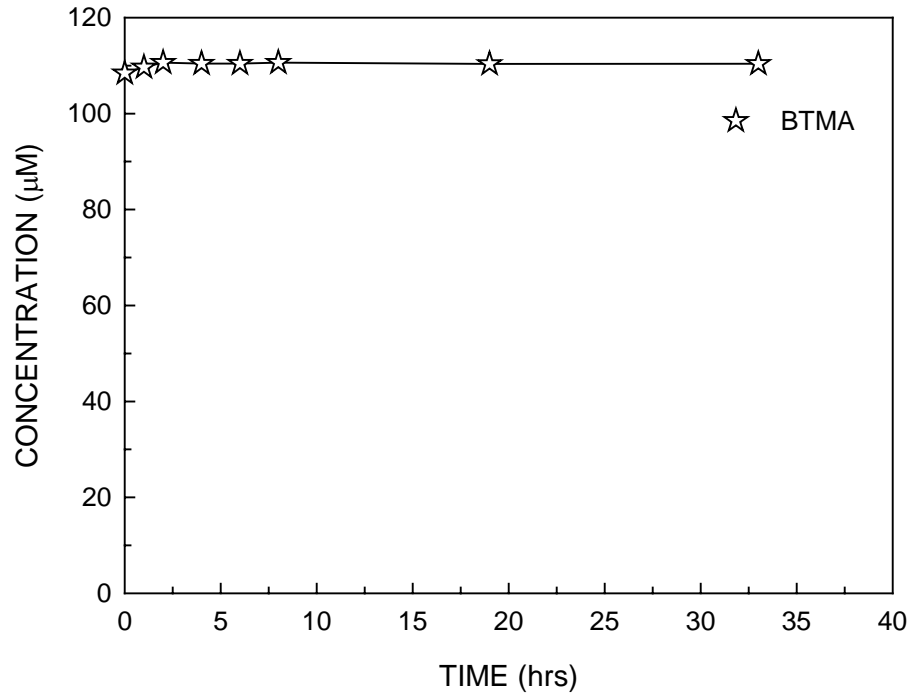


Figure 5.4. Time course of BTMA-Cl in the BAC enrichment culture amended with BTMA-Cl for the first time

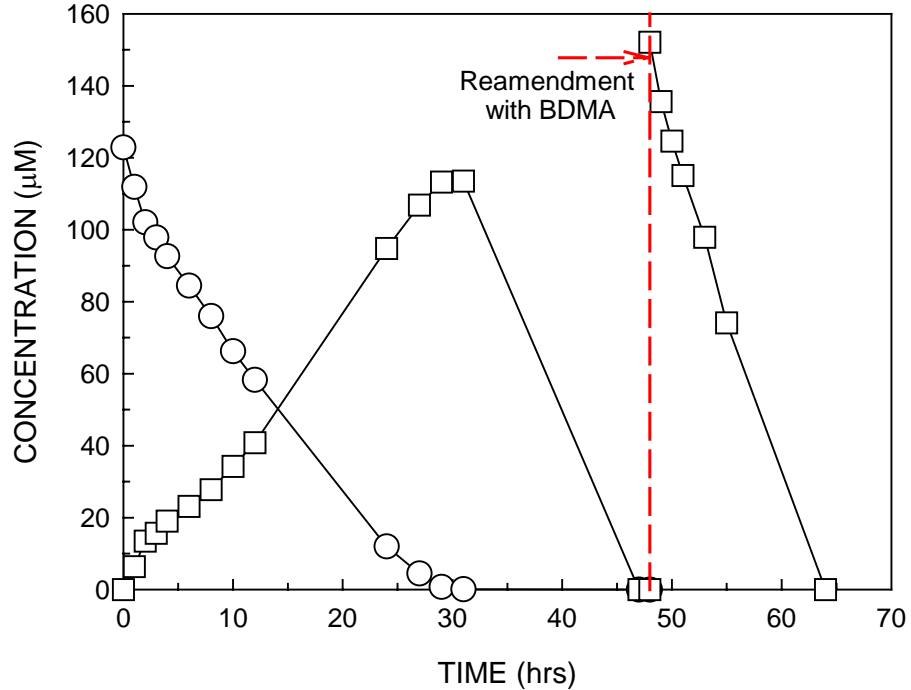


Figure 5.5. Time course of C_{14} BDMA-Cl transformation and formation and consumption of BDMA in a dilute BAC enrichment culture amended with C_{14} BDMA-Cl

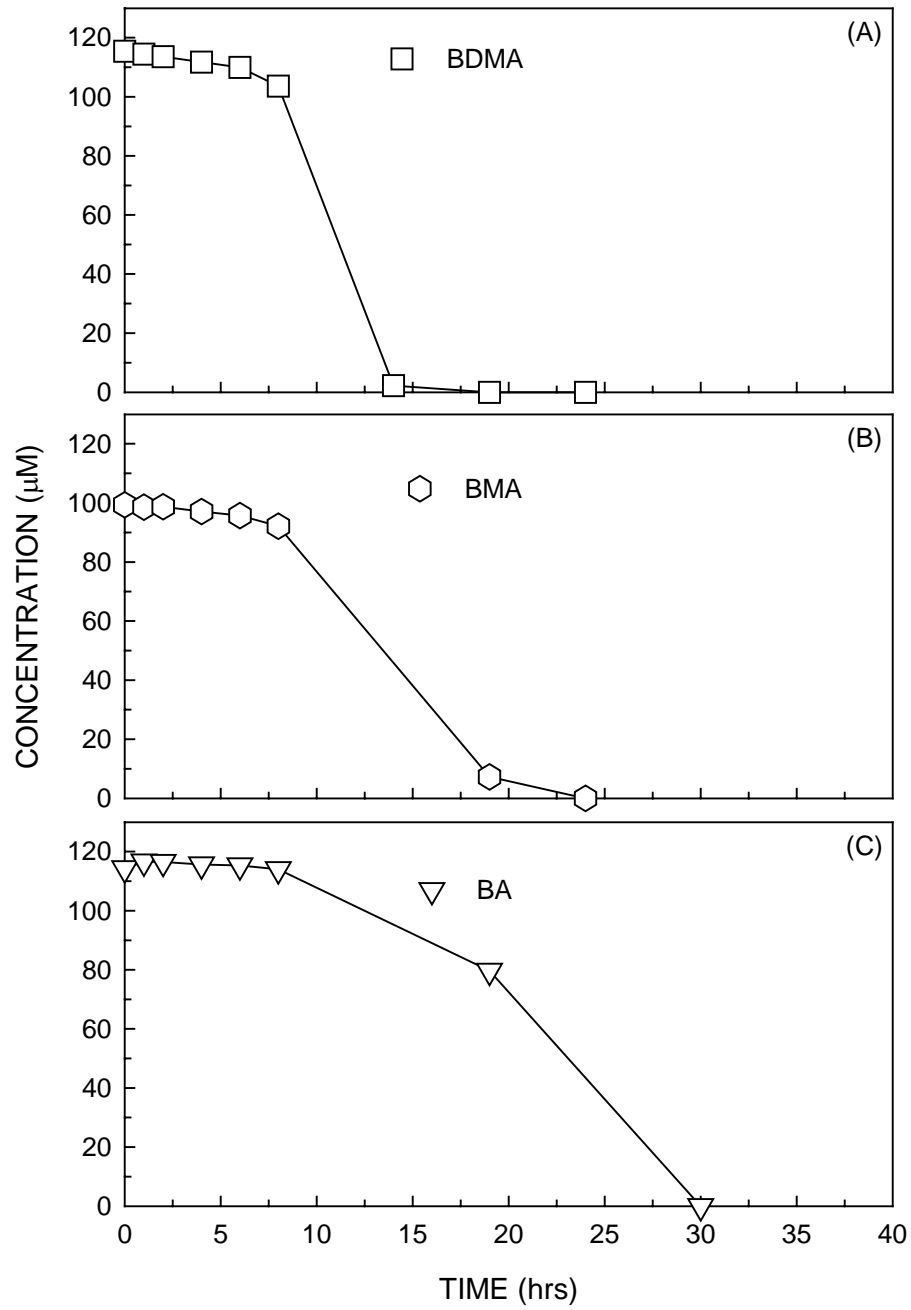


Figure 5.6. Time course of (A) BDMA, (B) BMA and (C) BA transformation in the BAC enrichment culture amended with BDMA, BMA and BA for the first time

biotransformation was achieved by different groups of microorganisms, i.e. C₁₄BDMA-Cl degraders and BDMA degraders.

The biotransformation of two potential BDMA transformation products reported by Patrauchan et al. (2003) which are BMA and BA, was also tested. Both compounds were degraded in 40 hours. In fact, the transformation was achieved after a longer lag than that observed for the BDMA transformation (Figure 5.6). Given also that none of these compounds was detected in the BDMA-amended culture (Figure 5.6A) and the C₁₄BDMA-Cl-amended culture (Figure 5.5), BMA and BA can not be the products of either C₁₄BDMA-Cl or BDMA biotransformation by the BAC enrichment culture.

The rate of C₁₄BDMA-Cl, C₁₄TMA-Cl, BDMA, BMA and BA transformation was determined in the culture series after the second amendment of the corresponding compound by using the Monod equation and applying non-linear regression fits to experimental data with the Igor Pro version 5.057 software package (WaveMetrics, Inc., Lake Oswego, OR). The biotransformation rate of each compound listed above was 6.9, 34.0, 26.8, 15.8 and 16.3 $\mu\text{M}/\text{hour}$, respectively. The biotransformation rate of C₁₄TMA-Cl (Figure 5.7A) was five-fold higher than the biotransformation rate of C₁₄BDMA-Cl (Figure 5.8), suggesting that substitution of the methyl group by a benzyl group decreases the biodegradation rate of a QAC due to steric hindrance resulting from the added hydrophobic benzyl moiety. In addition, the rate of BDMA biotransformation (Figure 5.7B) was two-fold higher than that of BMA (Figure 5.7C) and BA (Figure 5.7D) transformation.

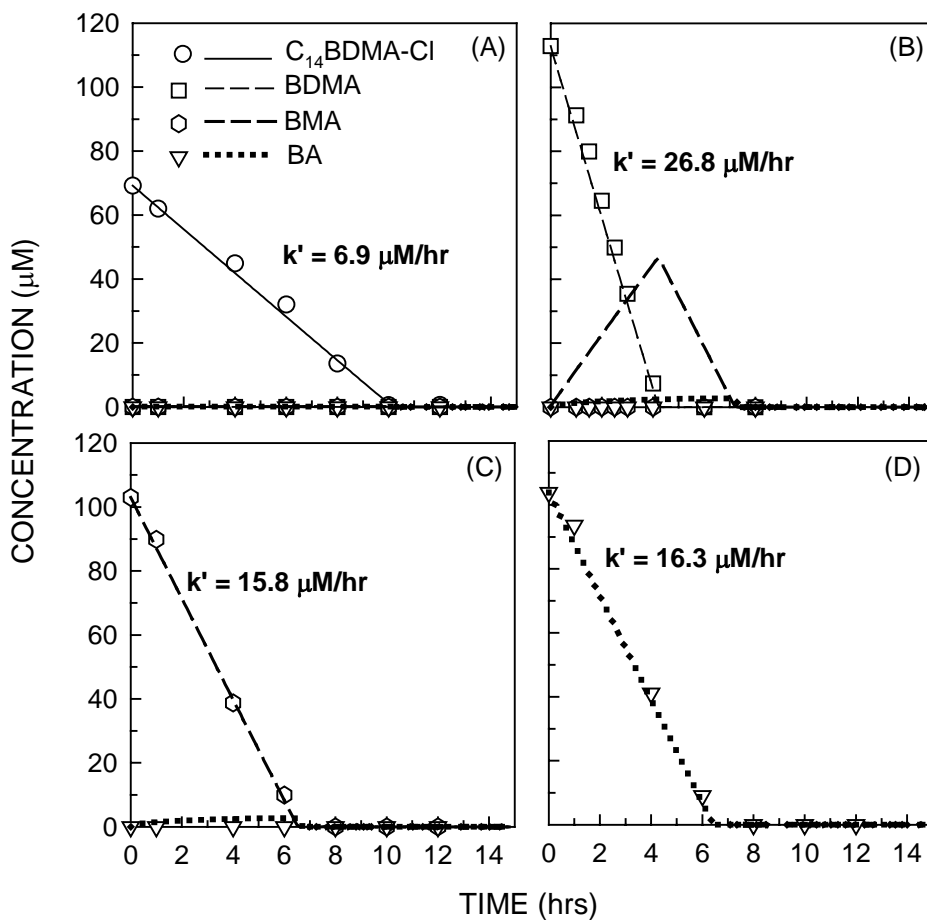


Figure 5.7. Time course of (A) C₁₄BDMA-Cl, (B) BDMA, (C) BMA and (D) BA biotransformation in the BAC enrichment culture and simulation of sequential C₁₄BDMA-Cl, BDMA and BMA transformation as proposed by Patrauchan et al. (2003) (symbols represent the experimental data whereas lines represent model simulations)

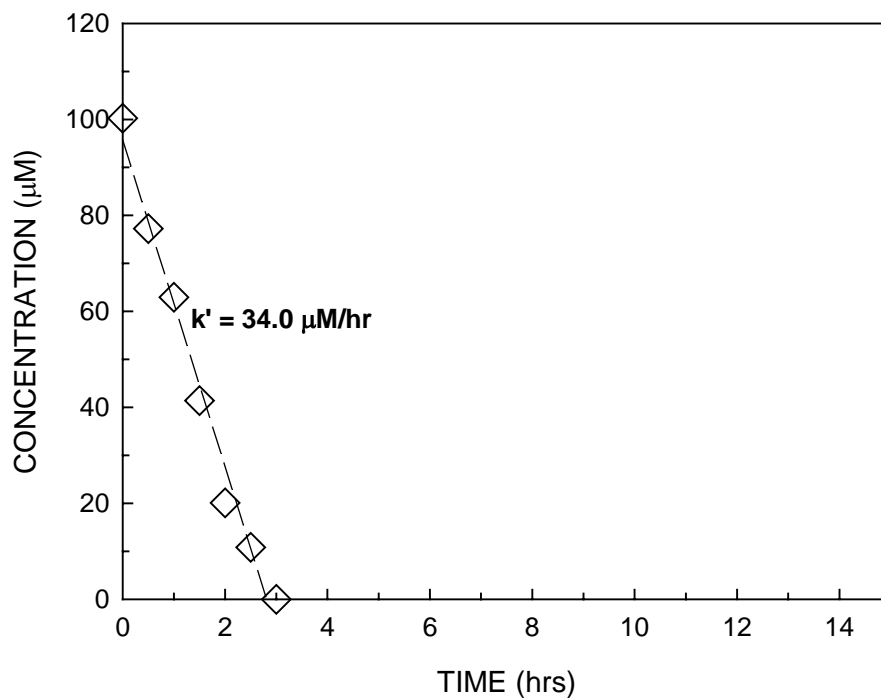


Figure 5.8. Time course and model simulation of C₁₄TMA-Cl transformation in the BAC enrichment culture

The biotransformation rate of individual compounds obtained in this assay was used to simulate the sequential biotransformation of C₁₄BDMA-Cl (C₁₄BDMA-Cl → BDMA → BMA → BA), BDMA (BDMA → BMA → BA) and BMA (BMA → BA) as suggested by Patrauchan et al. (2003) using the Monod model as given below.

$$\frac{dS_i}{dt} = \frac{k_{(i-1)}XS_{(i-1)}}{K_{S(i-1)} + S_{(i-1)}} - \frac{k_iXS_i}{K_{S_i} + S_i} \quad (\text{Equation 5.3})$$

In Equation 5.3, the first term is the accumulation rate, the second term is the production rate and the third term is the consumption rate. S represents the molar concentration of a compound (µM), t is the time (hours), k is the specific rate constant (µmoles/mg VSS-hour), X is the initial biomass concentration (mg VS/L), K_S is the half-

saturation concentration (μM), subscript (i-1) represents the reactant and i represents the product of each step of the sequential reaction. The simulations for each reaction were performed using the Igor Pro version 5.057 Ordinary Differential Equation (ODE) Toolbox (WaveMetrics, Inc., Lake Oswego, OR). The integration of the system of the coupled ODEs was performed using the Bulirsch-Stoer integration method (Stoer and Bulirsch, 2002).

The results of the simulations suggest that observing none of the potential $\text{C}_{14}\text{BDMA-Cl}$ biotransformation products (i.e., BDMA, BMA and BA), in the course of the $\text{C}_{14}\text{BDMA-Cl}$ biotransformation by the BAC enrichment culture is acceptable (Figure 5.7A) since the rate of utilization of these compounds was three- to four-fold higher than the rate of $\text{C}_{14}\text{BDMA-Cl}$ transformation, therefore the dealkylation reaction of $\text{C}_{14}\text{BDMA-Cl}$ was rate limiting. On the contrary, BMA had to be detected as a product during the biotransformation of BDMA, but in fact it was not detected. This result suggests that BMA is not a product of either $\text{C}_{14}\text{BDMA-Cl}$ or BDMA biotransformation. Therefore, $\text{C}_{14}\text{BDMA-Cl}$ biotransformation does not follow the scheme reported by Patrauchan et al. (2003) in the BAC enrichment culture.

Based on the results presented here, the proposed pathway of $\text{C}_{14}\text{BDMA-Cl}$ in the BAC enrichment culture is given in Figure 5.9. The $\text{C}_{14}\text{BDMA-Cl}$ biotransformation in the BAC enrichment culture involves a dealkylation step resulting in the formation of BDMA and tetradecanoate and BDMA is further transformed to dimethyl amine and benzoic acid by a debenzoylation step.

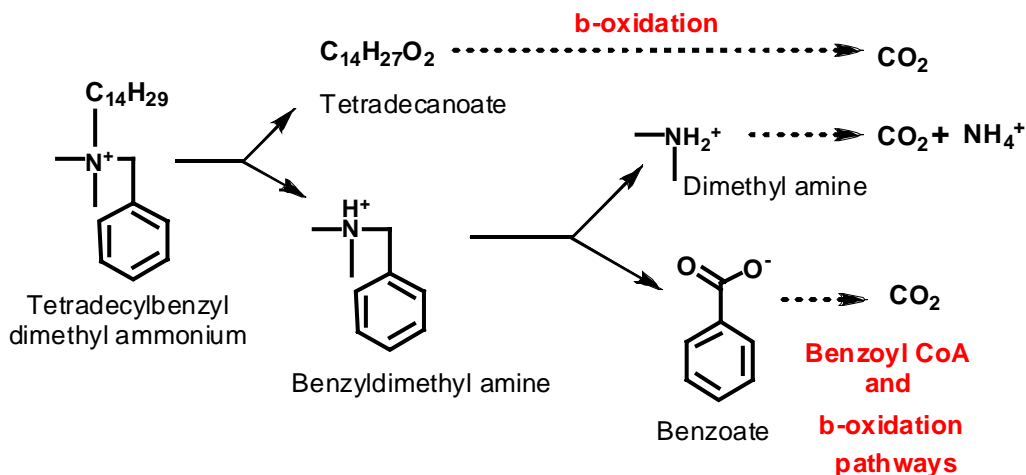


Figure 5.9. Proposed pathway of C₁₄BTMA-Cl biotransformation by the BAC enrichment culture

The biotransformation of the highly toxic C₁₄BDMA-Cl via the pathway demonstrated in this study or in the Patrauchan et al. (2003) study results in the formation of hydrophobic moieties such as BDMA, BMA and BA. The 15-minute acute EC₅₀ values of these potential C₁₄BDMA-Cl biotransformation products obtained using the Microtox® toxicity assay were 340±44, 257±92 and 224±87 μM, respectively. These results indicate that the toxicity of these products is at least 250-fold less than that of the parent compound. Therefore, aerobic biotransformation following the above-described pathway is a promising process because it reduces the serious environmental impacts associated with QACs.

5.3.3. Bacteria Community Composition Based on 16S rDNA Sequence Analysis

Biotransformation of QACs has been demonstrated in many studies using *Bacteria* isolates. However, none of these studies, which investigated the mineralization of QACs in mixed cultures, evaluated the microbial diversity in a QAC degrading culture.

Therefore, the objective of this part of the study was to evaluate the *Bacteria* community composition in the BAC enrichment culture which grows on BAC as the sole carbon and energy source.

The microbial diversity in the BAC enrichment culture was determined by 16S rDNA phylogenetic analysis of the clone library derived from the DNA extracted from the culture. A clone library was constructed representing a total of 47 *Bacteria* 16S rDNA clones. All clones were grouped according to the RFLP patterns. Rarefaction analysis was conducted to determine if a sufficient number of clones from the clone library were screened to estimate the diversity within the clone library sampled (Figure 5.10).

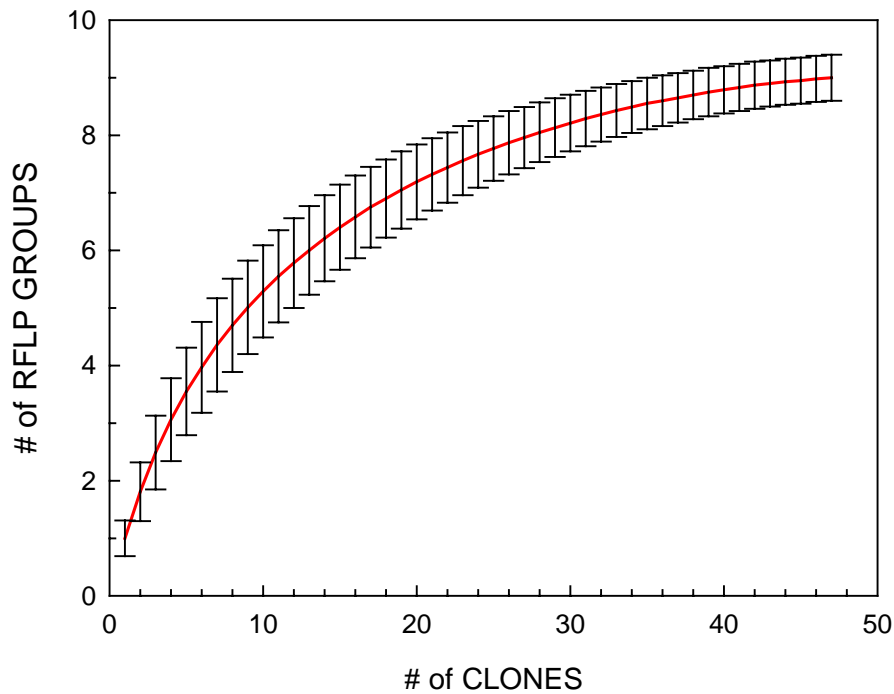


Figure 5.10. Rarefaction curve determined for different RFLP patterns of *Bacteria* 16S rDNA clones obtained from the BAC enrichment culture

The rarefaction curve did not reach saturation for the *Bacteria* rDNA library. Even though, additional sampling of the clones would be necessary to reveal the full extent of the diversity, several dominant RFLP groups were obtained. Therefore, the abundance of non-detected clones in the clone library was assumed to be much lower than the identified ones.

Analysis of the 47 rDNA *Bacteria* clones indicated a fair phylogenetic diversity in the clone library (Figure 5.11). A total of 9 distinct RFLP patterns were detected. All of the sequenced clones belonged to the Proteobacteria (Table 5.3). Of these, 98% were related to *Pseudomonas* genus of γ -Proteobacteria, including the most numerically dominant phylotype, BAC54, which is most similar to *Pseudomonas nitroreducens* (99% similarity) (Table 5.3). This phylotype comprised 36% of the total rDNA clone library. The other phylotypes, similar to BAC54, were BAC53, BAC106 and BAC37 and are closely related to *Pseudomonas sp.* WAI-21, *Pseudomonas sp.* Lin 2-2 and *Pseudomonas sp.* YG-1. The phylotypes that are listed above are designated as Group 1 (Figure 5.11) and are closely related to species that are capable of degrading simazine (*P. nitroreducens*, 99% similarity) (Hernandez et al., 2008), ethion (*P. sp.* strain WAI-21, 98% similarity) (Foster et al., 2004), pyrrolidine (*P. sp.* strain YG-1, 99% similarity) (Cho et al., 2002) and catechol (*P. sp.* strain Lin 2-2, 99% similarity). Given the abundance of Group 1, 60% of the total rDNA clone library, and the metabolic diversity of the phylotypes that belong to this group, the dealkylation and debenzoylation of C₁₄BDMA-Cl may be carried out by this group of bacteria in the BAC enrichment culture.

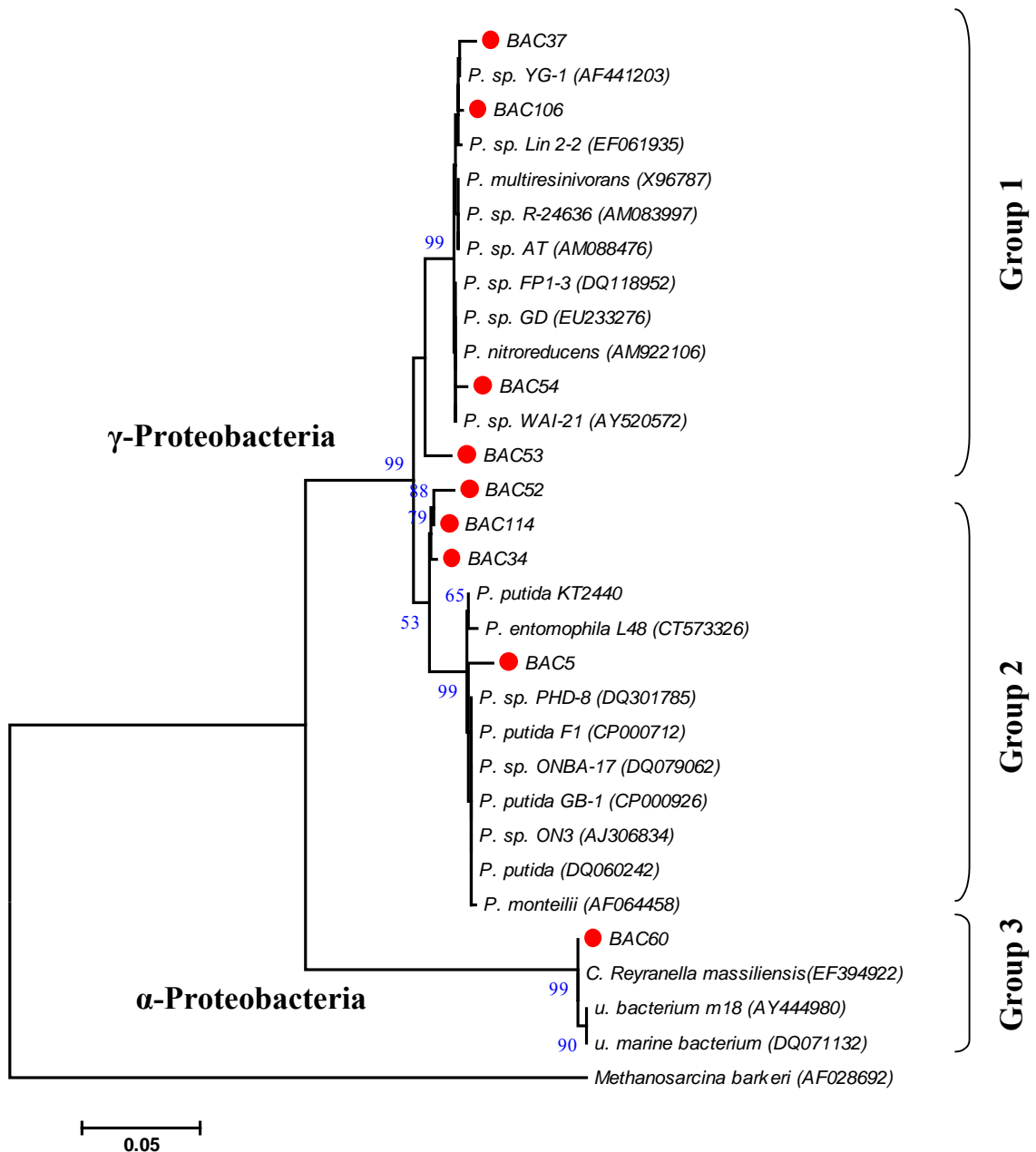


Figure 5.11. Phylogenetic tree of relationships of 16S rDNA clone sequences, as determined by distance Jukes-Cantor analysis, from BAC enrichment culture to selected cultured isolates and environmental clones. Bootstrap values represent 5000 replicates and only values greater than 50% are reported. The scale bar represents 0.05 substitutions per nucleotide position. *Methanosarcina barkeri* was used as the out group

Table 5.3. Representative bacterial clones sequenced from 16S rDNA clone library of the BAC enrichment culture

Phylogenic Group	Clone designation	# of clones	Sequence length (bp)	Nearest relative	Similarity (%)
γ -Proteobacteria	BAC54	17	1489	<i>P. nitroreducens</i>	99
	BAC53	6	1489	<i>P. sp.</i> WAI-21	98
	BAC37	3	1457	<i>P. sp.</i> YG-1	99
	BAC106	2	640	<i>P. sp.</i> Lin 2-2	99
	BAC52	9	1490	<i>P. sp.</i> ON3	98
	BAC5	5	1489	<i>P. putida</i> GB-1	99
	BAC114	2	1489	<i>P. putida</i> F1	98
	BAC34	2	1490	<i>P. putida</i> KT2440	99
	α -Proteobacteria	BAC60	1	1441	<i>C. Reyranella massiliensis</i>

The remaining γ -Proteobacteria lineage comprised 38% of the total rDNA clone library and was designated as Group 2. This group contained phylotypes BAC52, BAC5, BAC114 and BAC34, which were closely related to species that belong to the *Pseudomonas putida* group of genus *Pseudomonas*. BAC 5, BAC 114 and BAC 34 were closely related to *Pseudomonas putida* GB-1 (99% similarity), F-1 (98% similarity) and KT2240 (99% similarity) that are known for their ability to degrade various petroleum hydrocarbons such as alkanes, naphtalenes, toluene and xylenes. Therefore, Group 2 phylotypes may be present in the BAC enrichment culture due to their ability to metabolize hydrocarbon groups that are cleaved from BAC by Group 1 phylotypes.

A clone, BAC60, which was closely related to a recently discovered α -*Proteobacterium*, *Candidatus Reyranelia massiliensis* strain URTM1 (Pagnier et al., 2008) (99% similarity), was also identified in the 16S rDNA clone library. However the role of this phylotype in the BAC degradation was not speculated since the metabolic activity of the most related species, Strain URTM1, is not known.

The terminology and the logical sequence used, in part, in the interpretation of the results presented here were adapted from Martinez et al. (2006).

5.4. Summary

The biotransformation of C₁₄BDMA-Cl under aerobic conditions was investigated in a batch assay using an enrichment culture developed from a hydrocarbon-contaminated sediment and growing on benzalkonium chlorides. The kinetics and the mechanism of the biotransformation were also investigated. The biomass-normalized rate of C₁₄BDMA-Cl biotransformation was 0.09 μ moles/mg VSS-hour. The proposed C₁₄BDMA-Cl biotransformation pathway involved sequential dealkylation and debenzilation steps resulting in the cleavage of the alkyl and benzyl groups and formation of benzyl dimethyl amine and dimethyl amine, respectively. The composition of the *Bacteria* community in the BAC enrichment culture was determined by 16S rDNA phylogenetic analysis of the clone library derived from the DNA extracted from the culture. Although the full extent of *Bacteria* diversity in the 16S rDNA clone library was not revealed, numerous dominant RFLP groups were obtained. The vast majority of the sequenced clones (98% of the clone library) belonged to *Pseudomonas* genus of γ -*Proteobacteria* which suggests that *Pseudomonas* spp. was responsible for the degradation of BAC in the BAC enrichment culture.

CHAPTER 6

BIOTRANSFORMATION POTENTIAL OF QACS IN A MIXED METHANOGENIC CULTURE UNDER FERMENTATIVE/METHANOGENIC CONDITIONS

6.1. Introduction

Most uses of QACs lead to their release into wastewater treatment systems or directly into the environment. QACs have high affinity to adsorb onto suspended organic and inorganic solids thus adsorption outcompetes biodegradation in aerobic biological systems. As a result, QACs are transferred to anaerobic biological systems such as anaerobic digesters as a part of the waste activated sludge and aquatic sediments. It was reported that QAC concentrations may reach 4-50 mg/L in anaerobic digesters of sewage treatment plants. QAC concentrations may exceed these levels in biological treatment systems or aquatic sediments receiving direct discharges of industrial facilities, such as food processing that extensively use QACs. Although QAC degradation is energetically feasible ($\Delta G_r' = -5.4 \pm 0.3$ kJ/eq) under methanogenic conditions (Figure 6.1) based on standard reaction free energies, there is no evidence of mineralization of QACs under anaerobic conditions most likely because of the highly reduced nature of QAC structure as well as their low bioavailability and high toxicity. In spite of the fact that the presence of QACs in anaerobic treatment systems is inevitable, their fate and effect under anaerobic conditions have not been studied extensively. In addition, information on the effect of QACs on specific physiological groups participating in the complex anaerobic digestion process is presently lacking.

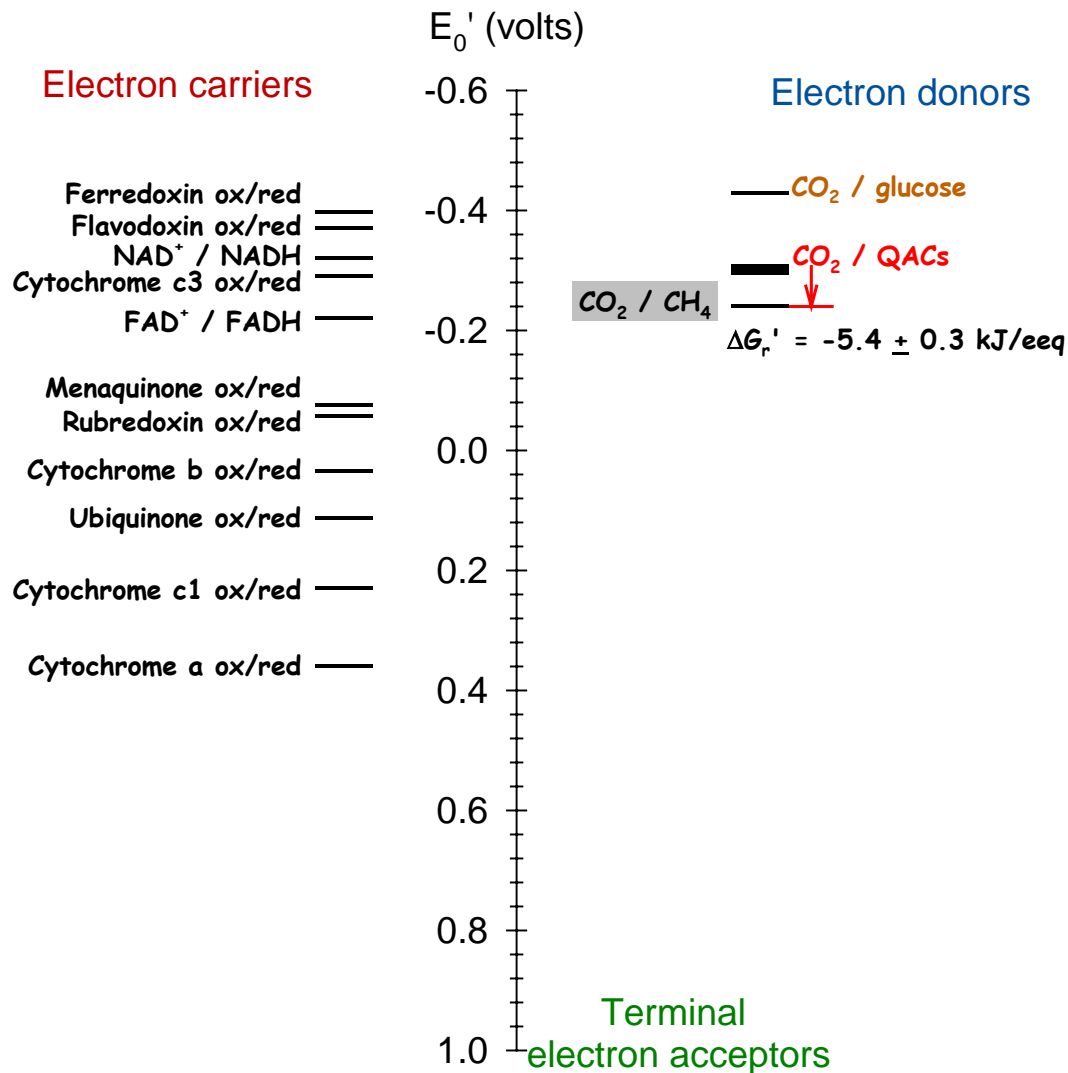


Figure 6.1. Schematic showing the positions of CO_2/QAC and $CO_2/methane$ redox couples on the electron tower and the standard free energy upon complete oxidation of QACs to CO_2 under methanogenic conditions (QACs represent monoalkonium, dialkonium and benzalkonium chlorides which have average half-reaction free energy equal to $28.9 \pm 3.5 \text{ kJ/eeq}$)

The objectives of the research reported in this chapter were to: (a) evaluate the potential inhibitory effect of selected QACs on acidogenesis and methanogenesis in a mixed, mesophilic (35°C) methanogenic culture; and (b) quantify the fate and phase distribution of the selected QACs in the same culture. Assays were conducted using serum bottles (batch) and a fed-batch reactor at a range of QAC concentrations.

6.2. Materials and Methods

6.2.1. Target Compounds

Vigilquat® (VQ) and its four active quaternary ammonium ingredients were used in this study. VQ (Alec C. Fergusson, Inc., Frazer, PA, USA) is comprised of four QACs and ethanol as follows (molecular formula, % w/w): benzalkonium chloride (C_n BDMA-Cl; 3%), didecyl dimethyl ammonium chloride (DC₁₀DMA-Cl; 1.35%), dioctyl dimethyl ammonium chloride (DC₈DMA-Cl; 0.9%), octyl decyl dimethyl ammonium chloride (DC₈₋₁₀DMA-Cl; 2.25%) and ethanol (1.5%). All individual QACs specified in the VQ formulation were defined in Chapter 3, section 3.2.1.

6.2.2. Mixed Methanogenic Culture

A mixed, methanogenic culture, developed with inoculum obtained from a mesophilic, municipal anaerobic digester and maintained fed-batch with a 35-d solids retention time at 35°C was used as seed in all assays reported here. The culture was fed with 8 g/L dextrin and 4 g/L peptone (in the feed) and anaerobic culture media described in Chapter 3. The culture was fed twice a week corresponding to an average organic loading rate of 0.34 g COD/L-day. The steady-state gas-phase methane and carbon dioxide concentration of this culture was 60.7±0.5% and 39.2±0.4% (mean ± standard deviation), respectively.

The steady-state total (TS) and volatile solids (VS) concentration of this culture was 6.9 ± 0.3 and 2.2 ± 0.1 g/L (mean \pm standard deviation), respectively.

6.2.3. Batch Inhibition Assay

A batch assay was performed to investigate the potential inhibitory effect of VQ, C_nBDMA-Cl, DC₁₀DMA-Cl, DC₈DMA-Cl and DC₈₋₁₀DMA-Cl on the mixed methanogenic culture. The assay was conducted in 160-mL serum bottles (100 mL liquid volume) sealed with rubber stoppers and aluminum crimps and flushed with helium gas for 15 min before any liquid addition. A sample of 80 mL of mixed liquor from the mixed methanogenic culture taken at the end of a 7-day feeding cycle was anaerobically transferred to each serum bottle along with 15 mL of culture media. A dextrin/peptone solution (D/P), which served as carbon/energy source, and QACs at desired concentrations were added and the total liquid volume was adjusted to 100 mL with deionized water (DI). The D/P COD in the bottles was 1200 mg/L. The first culture series included six bottles that were amended with VQ resulting in total QAC concentrations of 10, 15, 25, 37.5, 50 and 100 mg/L. The other four culture series were prepared with C_nBDMA-Cl, DC₁₀DMA-Cl, DC₈DMA-Cl or DC₈₋₁₀DMA-Cl, respectively. Each culture series had five bottles that were amended with individual QACs resulting in total QAC concentrations of 10, 25, 50, 75 and 100 mg/L. The QAC concentrations were selected according to literature reports, which state that QAC concentrations in anaerobic digesters may range from 4 to 10.5 mg/g-dry solids (ECETOC, 1993; Garcia et al., 1999). For our culture, which had 6.12 ± 0.02 g TS/L, this range corresponds to QAC concentrations from 25 to 65 mg/L. Based on the expectation that QACs will favor solids, their concentration range was increased to 100 mg/L. Two additional culture series were

prepared: seed blank and reference which consisted of only seed, culture media and DI water, and seed, culture media, DI water and D/P (1200 mg COD/L), respectively. Each culture series, including blank and reference, was prepared in triplicate. The initial pH in all culture series was 7.1 ± 0.1 . All culture series were incubated in the dark at 35°C and the bottles were agitated daily by hand. Throughout the incubation period, the total gas volume produced and its methane and carbon dioxide content were measured. At the end of the incubation period, the pH, volatile fatty acids (VFAs) concentrations, as well as the total and liquid phase QAC concentrations were measured. The total amount of methane and VFAs produced in each culture series throughout the incubation period was expressed in COD units. The COD processed as methane or VFAs was normalized relative to the total COD processed in the reference series and used to evaluate the inhibition of methanogenesis and acidogenesis in the culture series amended with QACs.

6.2.4. Phase Distribution Test

The phase distribution of QACs in the mixed methanogenic culture was evaluated at the end of the batch inhibition assay. The total and liquid phase concentration of QACs was determined as described in Chapter 3. The liquid phase concentration of QACs was measured after 15 minutes of centrifugation of mixed liquor samples at 2800 rpm. The supernatant was transferred to a test tube and the concentration of QACs was quantified as described in Chapter 3. QACs accumulate on solids through chemisorption (Neu, 1996). Although microbial cells possess limited adsorption sites for QACs, QACs form mixed-micelles or liposomes with microbial cells (Strevett et al., 2002). Adsorption isotherms such as Langmuir, that assume saturation of adsorption sites may not be applicable for QAC-biomass partitioning. The Freundlich isotherm which assumes that

there are multiple types of sorption sites acting in parallel, with each site type exhibiting a different sorption free energy and total site abundance, is therefore appropriate to simulate the adsorption of QACs on the biomass (Denyer and Maillard, 2002; Schwarzenbach et al., 2003).

The Freundlich adsorption isotherm equation is as follows: $q = K_F C^n$; where q is the QAC concentration on the biomass (mg QAC/g VS), C is the QAC concentration in the liquid phase (mg QAC/L), K_F is the capacity factor ((mg/g VS)(L/mg)ⁿ), and n is the Freundlich exponent. The QAC concentration on the biomass was determined by subtracting the QAC concentration in the liquid phase from the total concentration and normalizing it to the initial VS concentration in the bottles (1.93±0.12 g VS/L equal to 6.12±0.02 g TS/L). Experimentally determined data were fitted to the Freundlich isotherm equation and adsorption constants (K_F and n) determined by using non-linear regression.

6.2.5. Inhibition Assay Using an Anaerobic Fed-Batch Reactor

The potential inhibitory effect of VQ on the mixed methanogenic culture was further investigated in an anaerobic fed-batch reactor. This assay was performed in a 2.25-L glass reactor which was sealed and flushed with helium gas for 30 minutes. A sample of 1.5 L of the methanogenic culture at the end of a 7-day feeding cycle was transferred anaerobically to the reactor along with 250 mL of culture media. The reactor was maintained in the dark in a 35°C constant temperature room and its contents were mixed using a magnetic stirrer. Seven feeding cycles were performed with this reactor (Table 6.1), each lasting 7, 7, 32, 100, 11, 8 and 10 days, respectively. In each cycle, the reactor was fed with a D/P solution, resulting in an organic loading rate of 1.2 g COD/L-

Table 6.1. Feeding protocol of the fed-batch reactor used to assess the long-term effect of Vigilquat® on a mixed methanogenic culture

Feeding Cycle	Incubation Period (days)	Amendment ^a	Calculated QAC	Measured QAC
			Concentration in the Reactor (mg/L)	Concentration in the Reactor (mg/L)
1	7	D/P	0.0	0.0
2	7	D/P + VQ	15.0	-
3	32	D/P + VQ	30.0	-
4	100	D/P	30.0	30.0±0.1 ^b
5	11	D/P	30.0	-
6	8	D/P	30.0	-
7	10	D/P	30.0	31.9±1.8

^a D/P, dextrin/peptone solution; VQ, Vigilquat®

^b Mean ± standard deviation; *n* = 2

cycle. Vigilquat® was added at the beginning of the second and third cycles resulting in 15 and 30 mg/L of a total QAC concentration in the reactor, respectively. The VQ concentration was based on the results of the batch inhibition assay which indicated that VQ was not inhibitory at 15 mg/L but was inhibitory to methanogens at 30 mg/L. During the feeding cycles, the total gas production was recorded and gas analysis for methane and carbon dioxide was performed on samples directly taken from the reactor headspace. Liquid phase analyses for pH, VFAs and QACs were performed on mixed liquor samples drawn from the reactor.

6.3. Results and Discussion

6.3.1. Effect of QACs on Mixed Methanogenic Culture – Serum Bottle Assay

The inhibitory effect of QACs on the mixed methanogenic culture was assessed using five culture series amended with different QAC concentrations. For the first series, the effect of VQ was assessed and the incubation period was 98 days. The final pH in all culture series amended with VQ was between 7.0 and 7.3, which was close to the final pH value of 7.2 in the reference and seed cultures. Profiles of methane, net carbon dioxide, and COD conversion are given in Figures 6.2 and 6.4A, respectively. Long-term inhibition of methanogenesis was not observed at VQ concentrations of 10, 15, 25 and 37.5 mg/L (Figure 6.2A). All COD processed was completely converted to methane in these series (Figure 6.4A). Nevertheless, the inhibitory effect of VQ on the methanogenesis was noticeable at 25 and 37.5 mg/L for an incubation period equal to or less than 40 days (Figure 6.2A). Methane production was initially depressed in these series, but finally recovered after 20 and 40 days of incubation, respectively (Figure 6.2A). Nonetheless, methanogenesis was affected drastically in the series amended with an initial VQ concentration of 50 and 100 mg/L. The amount of methane produced in these series was noticeably lower than that of the reference (Figure 6.2A), whereas the net CO₂ production, which reflects the fermentative metabolic activity of the culture, was affected only in the series amended with an initial VQ concentration of 100 mg/L. Relative to the total COD processed in the reference series, about 34 and 3% of the total COD was converted to methane, whereas 68 and 72% was accumulated as VFAs in the 50 and 100 mg VQ/L series, respectively (Figure 6.4A). Note that values of COD processed exceeding 100% reflect experimental error/differences between the QAC-

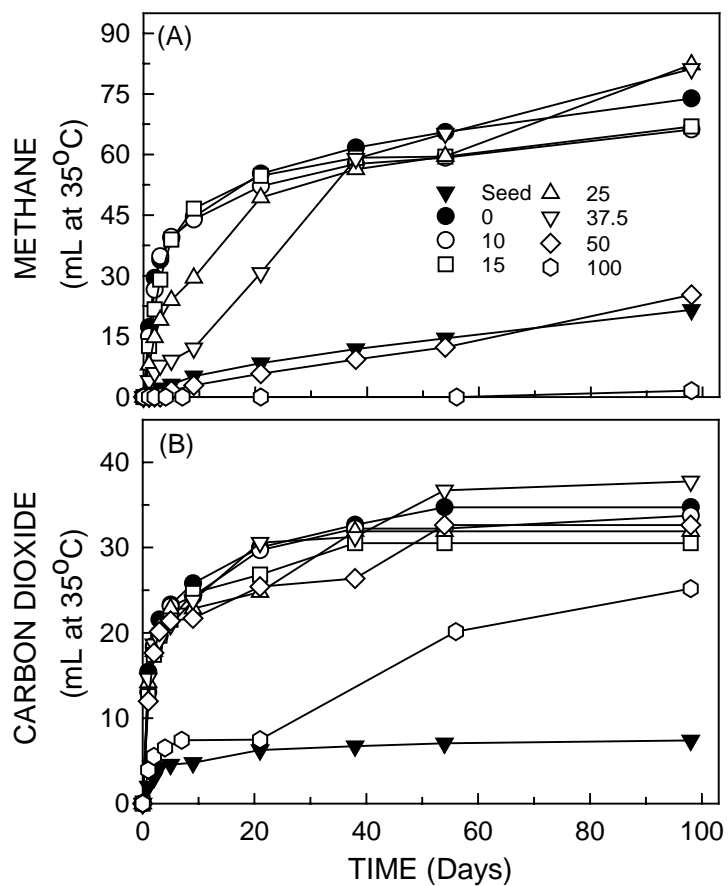


Figure 6.2. Methane (A) and carbon dioxide (B) production profiles during the batch inhibition assay with Vigilquat® at different concentrations (0-100 mg/L)

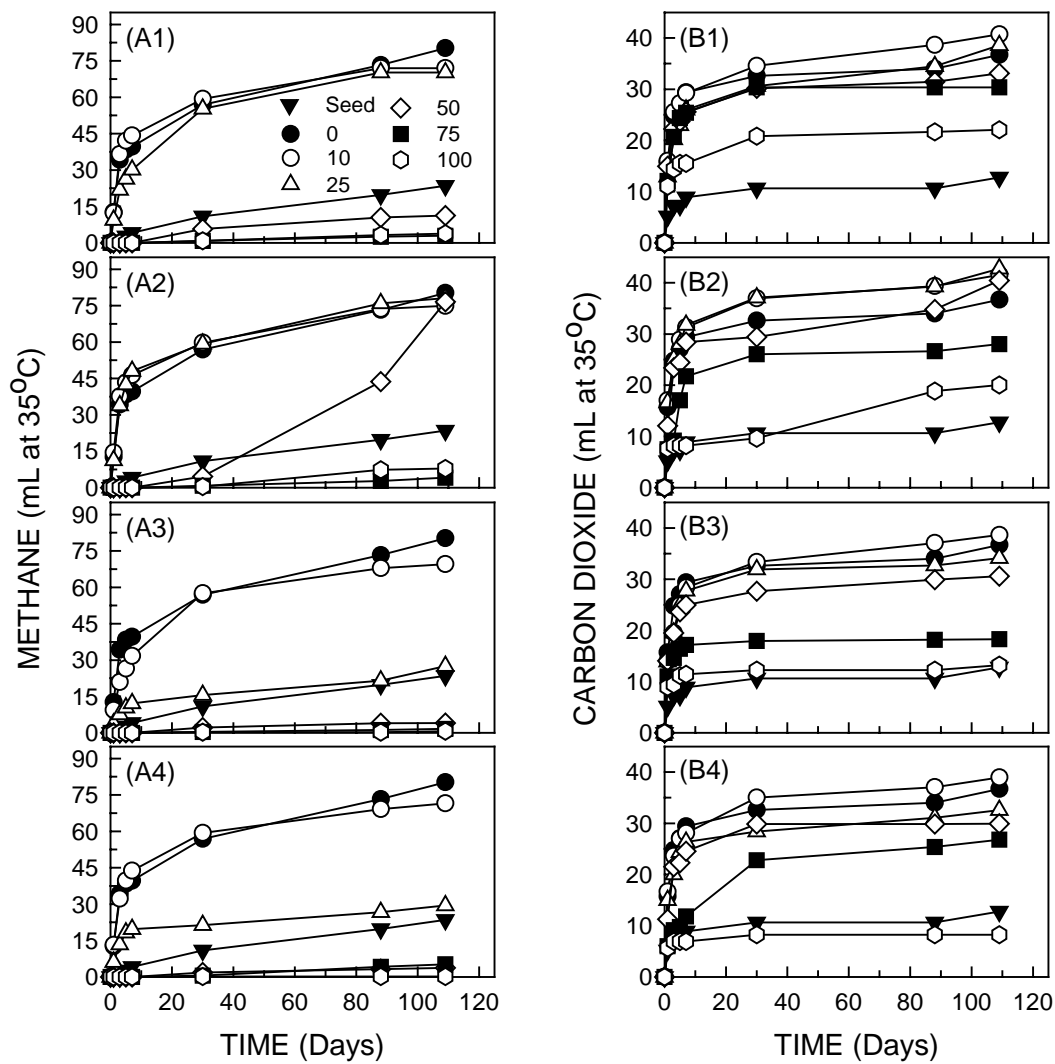


Figure 6.3. Methane (A) and carbon dioxide (B) production profiles during the batch inhibition assay with (1) C_n BDMA-Cl, (2) DC_{10} DMA-Cl, (3) DC_8 DMA-Cl, and (4) DC_{8-10} DMA-Cl at different concentrations (0-100 mg/L)

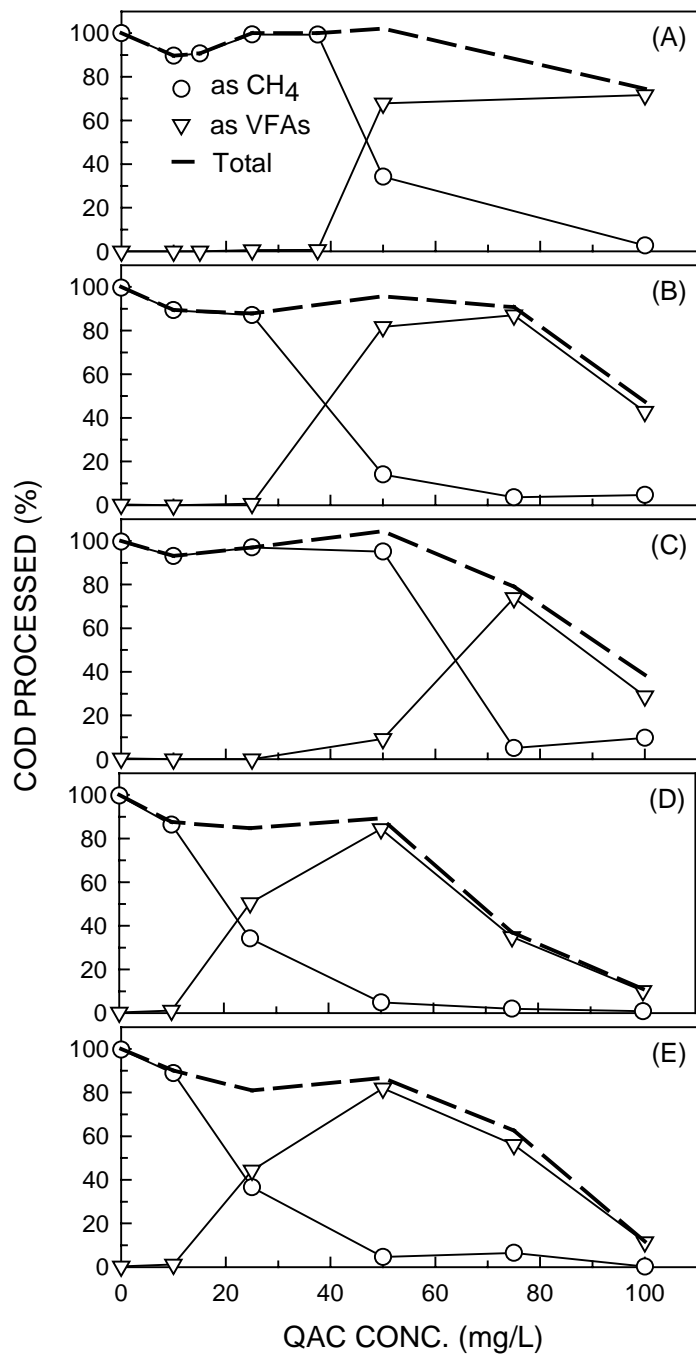


Figure 6.4. COD conversion profiles relative to the reference series during the batch inhibition assay with (A) Vigilquat®, (B) C_nBDMA-Cl, (C) DC₁₀DMA-Cl, (D) DC₈DMA-Cl, and (E) DC₈₋₁₀DMA-Cl at different concentrations (0-100 mg/L)

amended and the reference culture series. These results show that methanogenesis and acidogenesis had different susceptibilities to VQ. Thus, high concentrations of QAC result in the accumulation of VFAs and a decrease of the COD removal efficiency, which may affect the stability of an anaerobic digester.

The inhibitory effect of the four active QAC ingredients of VQ -- C_n BDMA-Cl, DC_{10} DMA-Cl, DC_8 DMA-Cl and DC_{8-10} DMA-Cl -- was assessed using four culture series amended with different QAC concentrations. Incubation for all four series lasted for 109 days. The final pH in all QAC-amended culture series varied between 6.8 and 7.3, which was close to the final pH value of 7.2 in the reference and seed cultures. Methane, net CO_2 , and COD conversion profiles in these series are shown in Figures 6.3 and 6.4, respectively and summaries including VFAs distribution for each QACs are given in Table 6.2 to 6.5. Long-term inhibition of methanogenesis was not observed in all series with 10 mg QAC/L (Figure 6.3A). On the other hand, short-term inhibition of methane production was observed in the series amended with 10 mg/L DC_8 DMA-Cl, but methane production recovered between 10 and 30 days of incubation (Figure 6.3A3). All COD processed was converted to methane in all series with 10 mg QAC/L, but accounted for $89\pm 3\%$ as compared to the reference series (Figure 6.4).

C_n BDMA-Cl and DC_{10} DMA-Cl had no long-term inhibitory effect on methanogenesis at 25 mg QAC/L (Fig. 6.3A1). At this QAC concentration, alkyl benzyl had a short-term inhibitory effect on methanogenesis, but methane production recovered between 10 and 30 days of incubation (Figure 6.3A1). In contrast, methane production was inhibited drastically at 25 mg QAC/L in the series amended with DC_8 DMA-Cl and DC_{8-10} DMA-Cl (Figure 6.3A3 and 6.3A4) and did not recover during the incubation

Table 6.2. COD utilization and products at the end of the incubation in mixed methanogenic culture amended with D/P and different initial C_nBDMA-Cl concentrations (10-100 mg/L)

Parameter	C _n BDMA-Cl (mg/L)				
	10	25	50	75	100
pH	7.1	7.1	6.9	6.9	7.0
Gas Composition (mL)					
Total Gas	117.1	112.2	49.6	38.1	32.0
CH ₄	72.0	70.2	11.2	2.9	3.7
CO ₂	40.7	38.6	33.1	30.4	22.1
VFAs (mg COD/L)					
Acetate	-*	12.7	887.9	718.9	528.1
Propionate	-	-	628.7	960.5	237.5
<i>iso</i> -Butyrate	-	-	-	-	6.5
<i>n</i> -Butyrate	-	-	140.4	96.5	100.3
<i>iso</i> -Valerate	-	-	-	-	-
<i>n</i> -Valerate	-	-	9.1	-	-
TOTAL	-	12.7	1666.1	1775.9	872.4
COD processed (%)					
VFAs	0	0.6	81.7	87.1	42.8
Methane	89.4	87.1	14.0	3.6	4.6
TOTAL	89.4	87.8	95.7	90.7	47.4

* Below the minimum detection limits given in Chapter 3

Table 6.3. COD utilization and products at the end of the incubation in mixed methanogenic culture amended with D/P and different initial DC₁₀DMA-Cl concentrations (10-100 mg/L)

Parameters	DC ₁₀ DMA-Cl (mg/L)				
	10	25	50	75	100
pH	7.1	7.1	7.1	6.8	6.9
Gas Composition (mL)					
Total Gas	120.3	121.2	115.4	36.7	35.9
CH ₄	75.0	78.1	76.6	4.1	7.8
CO ₂	41.5	42.8	40.5	28.0	20.0
VFAs (mg COD/L)					
Acetate	-*	-	-	592.6	335.9
Propionate	-	-	61.4	800.4	190.3
<i>iso</i> -Butyrate	-	-	-	-	-
<i>n</i> -Butyrate	-	-	128.2	114.2	61.1
<i>iso</i> -Valerate	-	-	-	-	-
<i>n</i> -Valerate	-	-	-	-	-
TOTAL	-	-	189.6	1507.2	587.3
COD processed (%)					
VFAs	0	0	9.3	73.9	28.8
Methane	93.1	97.0	95.1	5.1	9.7
TOTAL	93.1	97.0	104.4	79.0	38.5

* Below the minimum detection limits given in Chapter 3

Table 6.4. COD utilization and products at the end of the incubation in mixed methanogenic culture amended with D/P and different initial DC₈DMA-Cl concentrations (10-100 mg/L)

Parameter	DC ₈ DMA-Cl (mg/L)				
	10	25	50	75	100
pH	7.1	6.9	6.8	7.0	7.2
Gas Composition (mL)					
Total Gas	114.0	71.8	44.8	27.6	15.5
CH ₄	69.5	27.5	4.0	1.6	0.7
CO ₂	38.6	34.1	30.6	18.3	13.2
VFAs (mg COD/L)					
Acetate	24.1	846.6	855.0	432.9	95.7
Propionate	-*	74.0	730.0	225.7	73.3
<i>iso</i> -Butyrate	-	-	-	-	-
<i>n</i> -Butyrate	-	100.8	123.0	52.1	38.4
<i>iso</i> -Valerate	-	-	-	-	-
<i>n</i> -Valerate	-	7.9	12.3	-	-
TOTAL	24.1	1029.3	1720.3	710.7	207.3
COD processed (%)					
VFAs	1.2	50.5	84.4	34.9	10.2
Methane	86.4	34.2	4.9	2.0	0.8
TOTAL	87.5	84.7	89.3	36.9	11.0

* Below the minimum detection limits given in Chapter 3

Table 6.5. COD utilization and products at the end of the incubation in mixed methanogenic culture amended with D/P and different initial DC₈₋₁₀DMA-Cl concentrations (10-100 mg/L)

Parameter	DC ₈₋₁₀ DMA-Cl (mg/L)				
	10	25	50	75	100
pH	7.0	6.8	6.8	6.8	7.3
Gas Composition (mL)					
Total Gas	113.6	66.8	40.3	38.9	11.8
CH ₄	71.5	29.4	3.6	5.2	0.1
CO ₂	38.9	32.6	29.9	26.8	8.2
VFAs (mg COD/L)					
Acetate	24.0	754.2	668.5	502.4	158.3
Propionate	-*	54.5	788.0	560.3	39.9
<i>iso</i> -Butyrate	-	-	73.8	-	-
<i>n</i> -Butyrate	-	86.7	141.7	78.4	37.0
<i>iso</i> -Valerate	-	-	-	-	-
<i>n</i> -Valerate	-	8.1	-	-	-
TOTAL	24.0	903.5	1672.0	1141.1	235.2
COD processed (%)					
VFAs	1.2	44.3	82.0	56.0	11.5
Methane	88.8	36.6	4.6	6.5	0.2
TOTAL	90.0	80.9	86.6	62.5	11.7

* Below the minimum detection limits given in Chapter 3

period. On the other hand, the net CO₂ production was not affected in these series (Figure 6.3B3 and 6.3B4). VFAs accumulated in these series and resulted in 51 and 44% of the total COD added to the system (Figure 6.4D and 6.4E). The predominant VFAs were acetate and propionate. These results show that DC₈DMA-Cl, which has the shortest alkyl chain length as well as the highest CMC among all QACs tested in the present study, was the most inhibitory, which agrees with a similar conclusion drawn by Garcia et al. (1999).

All QACs had a drastic inhibitory effect on methanogenesis at concentrations of 50, 75 and 100 mg/L. C_nBDMA-Cl inhibited methanogenesis but, the net CO₂ production was not affected to the same extent at these concentrations (Figure 6.3A1 and 6.3B1). With increasing C_nBDMA-Cl concentration, 82, 87 and 43% of the total COD accumulated as VFAs (Figure 6.4B and Table 6.2) and recovery of methane production was not observed during the long-term incubation period (Fig. 6.3A1).

DC₁₀DMA-Cl inhibited methanogenesis at 50, 75 and 100 mg QAC/L, as well. However, methane production recovered between 80 and 100 days of incubation in the 50 mg QAC/L series. In contrast, recovery of methane production was not observed at 75 and 100 mg QAC/L (Figure 6.3A2). The net CO₂ production decreased at and above 75 mg/L DC₁₀DMA-Cl (Figure 6.3B2). About 95, 5 and 10% of the total COD was processed as methane and 9, 74 and 29% was processed and accumulated as VFAs at 50, 75 and 100 mg QAC/L, respectively (Figure 6.4C and Table 6.3).

DC₈DMA-Cl and DC₈₋₁₀DMA-Cl were more inhibitory than the other two QACs. Methanogenesis was totally inhibited at QAC concentrations of 50 mg/L and above (Figure 6.3A3 and 6.3A4). On the other hand, 84, 35 and 10% of total COD in the

DC₈DMA-Cl-amended and 82, 56 and 12% of total COD in the DC₈₋₁₀DMA-Cl - amended series was converted to VFAs and accumulated at 50, 75 and 100 mg QAC/L, respectively (Figure 6.4D and 6.4E and Table 6.4 and 6.5). Thus, with increasing DC₈DMA-Cl and DC₈₋₁₀DMA-Cl concentration above 50 mg/L, acidogenesis was severely inhibited and led to a very low COD conversion and removal.

Inhibition of methanogenesis by various types of QACs has been reported by other researchers. In a previous study, Garcia et al. (2000) reported that di(hydrogenated tallow) dimethyl ammonium chloride did not affect the methane production in an anaerobic culture below 200 mg/L concentration (Garcia et al., 2000). Hexadecyl trimethyl ammonium bromide at about 60 mg/L inhibited the biogas production in cultures inoculated with anaerobic digester sludge, however, gas production recovered after 2 weeks of lag period (Battersby and Wilson, 1989). In another study investigating the effect of alkyl chain length of QACs on anaerobic degradation concluded that the toxicity of QACs to methanogens decreased with increasing alkyl chain length at 20 and 40 mg/L (Garcia et al., 1999). These studies also showed that QACs were not degraded under methanogenic conditions.

The results of this study confirm that the inhibitory effect of QACs on the mixed methanogenic culture is negatively correlated with alkyl chain length or positively correlated with the CMC as described in Chapter 4. DC₈DMA-Cl was the most toxic among all tested QACs. Based on the results of the present study, the four QACs tested may be ranked as DC₈DMA-Cl, DC₈₋₁₀DMA-Cl, C_nBDMA-Cl and DC₁₀DMA-Cl in terms of decreasing toxicity. Moreover, methanogenesis was found to be more susceptible to QAC inhibition than acidogenesis. None of the QACs tested in this study

was biodegraded. The persistence of QACs in all series as well as their phase distribution determined at the end of the incubation period are discussed below.

6.3.2. Phase Distribution of QACs

The phase distribution of QACs was evaluated in all QAC-amended series at the end of the incubation period of the above-described QAC inhibition assay. Figure 6.5 shows the results from the QAC phase distribution test. For comparison, a 100% recovery line is drawn which shows the hypothetical distribution of an infinitely soluble substance and with zero adsorption to the solids. According to these results, all QACs were recovered by 100.9 ± 13.6 (mean \pm standard deviation, $n = 50$). Thus, all QACs were resistant to biodegradation under the methanogenic conditions applied in the present study. At a total QAC concentration of 10 mg/L, the fraction of QACs which accumulated on the solids ranged between 92 and 100%. However, the solid phase QAC fraction was between 28 and 75% at a total QAC concentration of 100 mg/L. It has been reported that in activated sludge, 95% of the QACs were adsorbed to particulate matter (Topping and Waters, 1982; Scott and Jones, 2000), which is similar to the results of the present study.

The adsorption of QACs in the methanogenic culture was simulated with the Freundlich isotherm equation and estimated parameter values (K_F and n) for VQ, alkyl benzyl, didecyl, dioctyl and octyl decyl are given in Table 6.6. According to these results, the affinity of individual QACs to adsorb on the biomass forms the following series in descending order: DC₁₀DMA-Cl, C_nBDMA-Cl, DC₈₋₁₀DMA-Cl and DC₈DMA-Cl. The adsorption affinity of VQ is between that of C_nBDMA-Cl and DC₈₋₁₀DMA-Cl. Since VQ is a mixture of four individual QACs and each QAC exhibits different adsorption affinity,

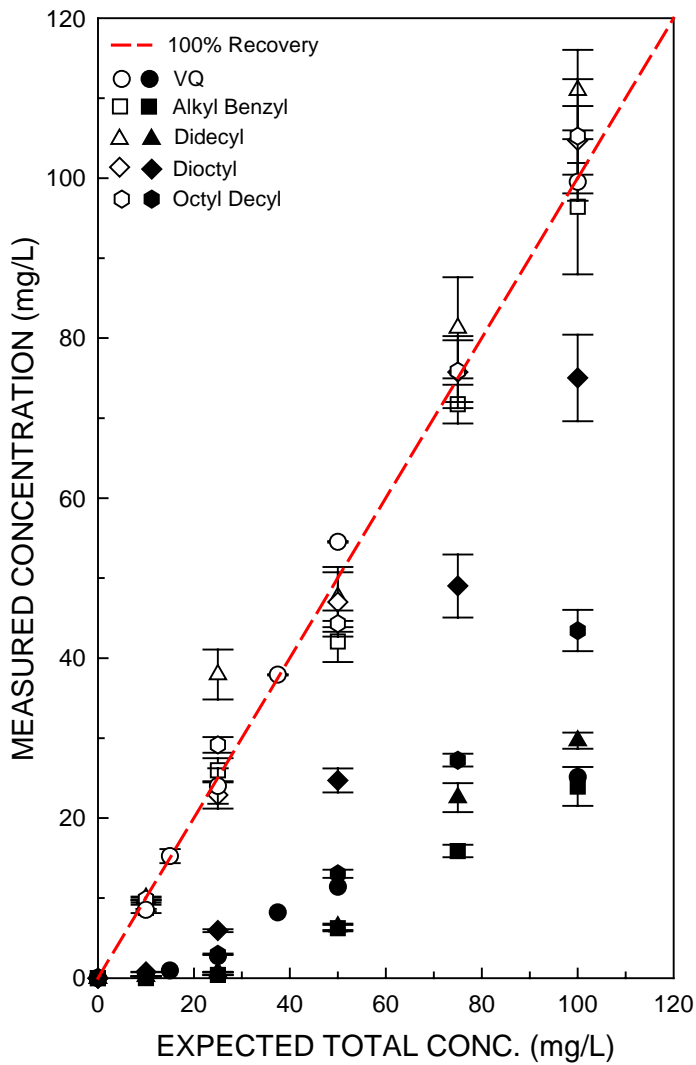


Figure 6.5. Phase distribution of Vigilquat®, C_nBDMA-Cl, DC₁₀DMA-Cl, DC₈DMA-Cl, and DC₈₋₁₀DMA-Cl in the mixed methanogenic culture (Error bars represent one standard deviation of the means; hollow and filled symbols represent total and liquid phase QAC concentrations, respectively)

Table 6.6. Freundlich adsorption isotherm constants for QAC phase distribution in a mixed methanogenic culture

QAC	K_F (mg/g VS)(L/mg) ⁿ	<i>n</i>	R ²
Vigilquat®	9.5±0.4 ^a	0.42±0.02 ^a	0.997
C _n BDMA-Cl	12.8±3.2	0.31±0.09	0.940
DC ₁₀ DMA-Cl	13.9±3.3	0.29±0.08	0.920
DC ₈ DMA-Cl	5.3±0.3	0.25±0.01	0.997
DC ₈₋₁₀ DMA-Cl	7.5±1.4	0.37±0.06	0.974

^a Mean ± standard error

the adsorption affinity of VQ represents the combined, overall affinity of the individual QACs in the mixture. As the alkyl chain length increases and CMC decreases, the affinity of QACs to adsorb on biomass increases, which is consistent with their relative hydrophobicity as described in Chapter 4. Recalling that adsorption of QACs on biomass is chemisorption and is driven by both charge interaction and hydrophobicity, our results agree with those of Cowan and White (1958) who assessed the adsorption of alkyl ammonium compounds with different alkyl chain length on the clay mineral montmorillonite (Cowan and White, 1958).

The adsorption capacity increased noticeably at total initial QAC concentrations above 50 mg/L in cultures amended with C_nBDMA-Cl and DC₁₀DMA-Cl (Figure 6.6). On the other hand, such an increase in adsorption capacity was not observed for the VQ, dioctyl and octyl decyl. Arrigler et al. (2005) reported that cetylpyridinium chloride

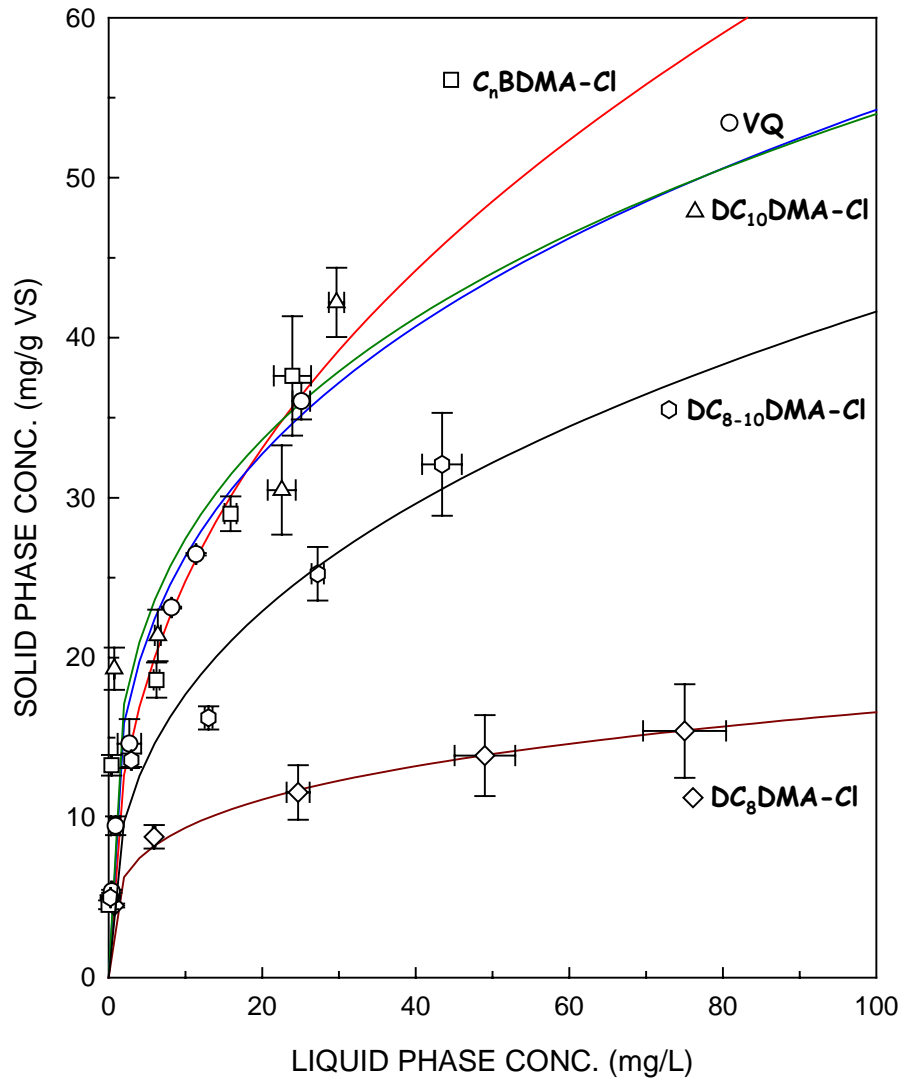


Figure 6.6. Freundlich adsorption isotherms for Vigilquat®, C_n BDMA-Cl, DC_{10} DMA-Cl, DC_8 DMA-Cl, and DC_{8-10} DMA-Cl at equilibrium (Error bars represents one standard deviation of the means; solid lines are model predictions)

(CPC), a C₁₆ QAC, caused disintegration of the lipid bi-layer after adsorption on the vesicle surface and formed lipid/CPC mixed micelles resulting in a sharp increase in adsorption capacity after solubilization of the membrane. In C_nBDMA-Cl and DC₁₀DMA-Cl amended cultures, cell lysis followed by the mixed micelle formation may have caused an increase in the adsorption capacity at 50 mg QAC/L and above.

6.3.3. Effect of QACs on Mixed Methanogenic Culture – Fed-Batch Reactor Assay

The effect of VQ on the mixed methanogenic culture was also investigated in a fed-batch reactor for an overall incubation period of 185 days. The pH of the culture varied between 6.9 and 7.2 during the incubation period. The gas production as well as the production and consumption of VFAs throughout the entire incubation period are shown in Figure 6.7.

Cycle 1 served as a reference cycle and the reactor was fed only with a D/P solution which resulted in a COD concentration of 1200 mg/L. During cycle 2, where the reactor was amended with both D/P (1200 mg COD/L) and VQ (15 mg/L total concentration), the methane and net CO₂ production was not affected and the trend was identical to the cycle 1 (Figure 6.7A). Thus, VQ at 15 mg/L total concentration was not inhibitory and the trend of methane production was similar to that observed in both cycle 1, as well as in the batch inhibition assay (Figure 6.2A).

The total VQ concentration was elevated to 30 mg/L and the reactor was fed with the same D/P solution in the third cycle. This VQ concentration was expected to be inhibitory to methanogenesis based on the results obtained from the batch inhibition assay (see Section 6.3.1 above). Significant inhibition of methanogenesis was observed in the fed-batch reactor at 30 mg VQ/L (total VQ concentration). About 50% of COD that

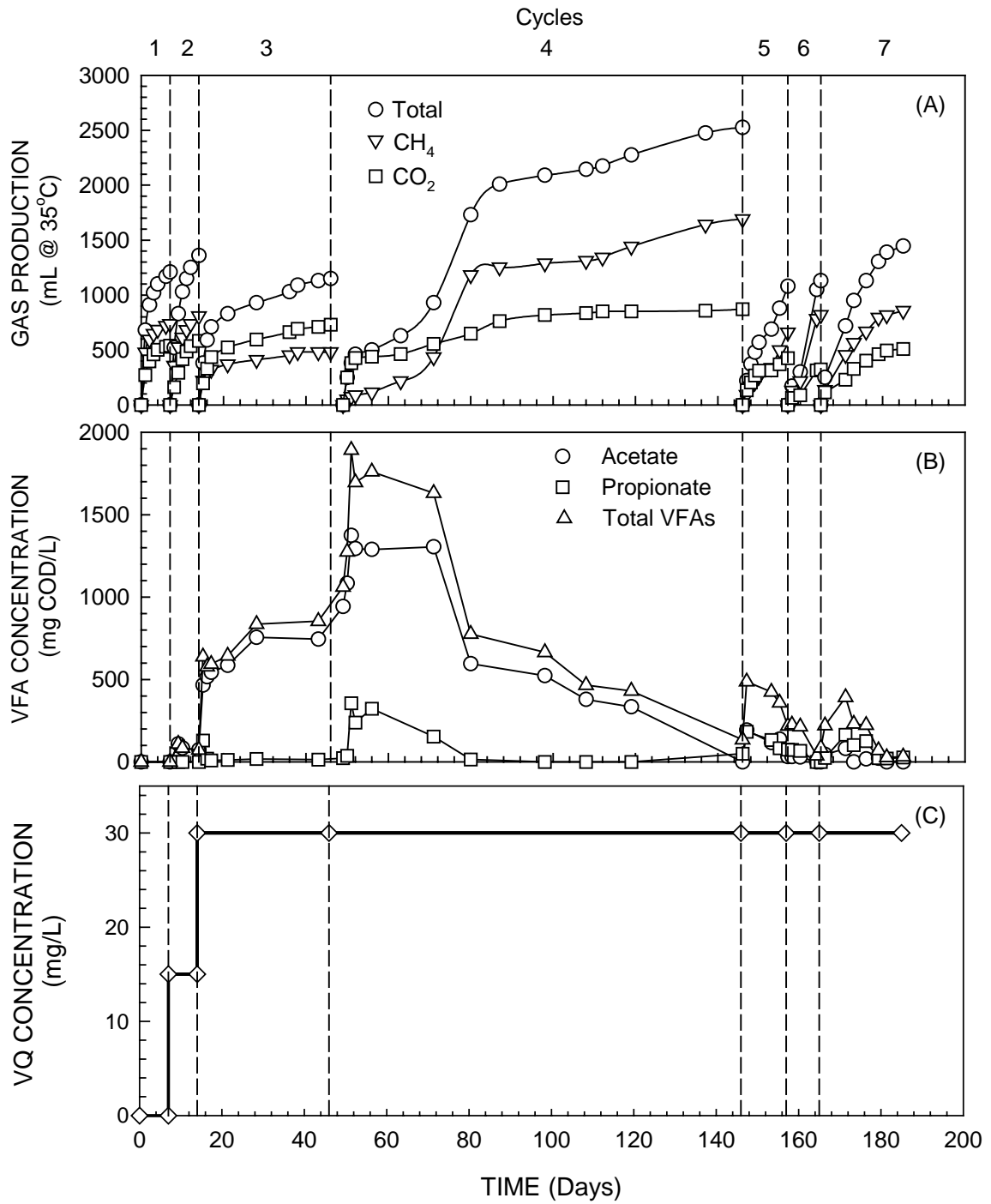


Figure 6.7. Gas production (A), VFA (B) and VQ (C) profiles in the fed-batch reactor

was ultimately converted to methane was processed in 1 day of incubation and methane production almost totally leveled off in subsequent days, indicating that the inhibitory effect of QACs on methanogenesis was time dependent. In other words, QACs require some time to reach their target sites of action and cause inhibition. VFAs, mainly acetate and propionate, accumulated and reached up to 854 mg COD/L, indicating that acidogenesis was still active at this total VQ concentration.

During the fourth feeding cycle, the total VQ concentration was maintained at 30 mg/L and the reactor fed with the D/P solution (1200 mg COD/L). The added COD was rapidly processed to VFAs which accumulated and reached about 2000 mg COD/L at day 51, while very low methane production was observed during this time. The VFAs were gradually depleted and converted to methane starting at 71 days of incubation, which corresponds to a significant increase in the methane production (Fig. 6.7). A similar pattern of methane production was observed during the batch inhibition assay in the culture series amended with VQ at 25 and 37.5 mg/L (see Section 6.3.1 above). Other studies which evaluated the inhibitory effect of QACs on the metabolic activity of either aerobic or anaerobic cultures at 10 to 60 mg/L QAC concentration, also observed transient inhibition and gradual recovery (Battersby and Wilson, 1989; Garcia et al., 1999; Garcia et al., 2000). At the end of the fourth cycle, 94% of the total COD was processed as methane and the methane and carbon dioxide content of the produced gas reached 67 and 35%, respectively. In order to achieve complete utilization of VFAs, the incubation period for cycle 4 was prolonged to 100 days.

For the remaining three cycles, the reactor was fed only with the D/P solution and the total VQ concentration remained stable at about 30 mg/L. All COD added to the

reactor in these three cycles was almost totally converted to methane and VFA accumulation was not observed at the end of these cycles. The recovery of methanogenesis in the latter four feeding cycles is attributed to the very low liquid-phase VQ concentration (< 3 mg/L), in spite of the fact that the total VQ concentration was maintained at 30 mg/L. As a result of the high VQ adsorption affinity for the biosolids, uninhibited methanogens were able to grow in the latter four feeding cycles, thus restoring methanogenesis in the reactor to pre-inhibition levels as recorded in cycle 1.

6.3.4. QAC Phase Distribution, Inhibition and Recalcitrance

The results of the present study show that QACs have high affinity to adsorb on the biosolids. DC₈DMA-Cl has the lowest affinity among all QACs tested and this affinity increases with increasing alkyl chain length. Relative to inhibition, it should be noted that DC₈DMA-Cl was the most inhibitory among all QACs tested and the extent of inhibition decreased as the alkyl chain length increased. Thus, the inhibitory effect of QACs was found to be inversely proportional to their adsorption affinity on the biomass or their hydrophobicity. However, methanogenesis recovered in less than 60 days in all culture series and fed-batch reactor amended with QACs less than 50 mg/L. The recovery of methanogenesis after a certain period of incubation may be the result of the high adsorption affinity of QACs for the biosolids, which in turn results in low liquid phase QAC concentration coupled with microbial growth and acclimation.

As mentioned above, QACs were more toxic to methanogens as compared to the acidogens in the mixed culture used in this study. The reasons may include: (i) Methanogens (Archaea) are structurally different than the acidogens (Bacteria). Methanogens have no outer membrane and their cell wall consists of a paracrystalline

surface layer (S-layer) composed of protein or glycoprotein (Madigan and Martinko, 2006). For this reason, QACs reach the cytoplasmic membrane of methanogens easily, and cause inhibition. (ii) The structure of the cytoplasmic membrane of methanogens is unique and contains either diether or tetraether lipids rather than ester lipids. Thus, the membrane of methanogens is more hydrophobic than that of bacteria, which makes methanogens more vulnerable to QACs. It has been reported that QAC-resistant microorganisms have a higher content of hydroxylated fatty acids in their membrane, which confers resistance by making their membrane less hydrophobic (Guerin-Mechin et al., 1999; Chapman, 2003). (iii) Energy generation by fermenters is largely based on substrate level phosphorylation, whereas methanogens generate ATP by using proton motive force (PMF). Thus, because QACs affect the PMF, they are more inhibitory to methanogens than to acidogens.

None of the QACs tested in this study was biodegraded. The recalcitrance of QACs (dimethyl QACs, $R_2Me_2N^+$) observed in the present study under methanogenic conditions may be related to the presence of the highly saturated and reduced form of the alkyl functional groups attached to the positively charged nitrogen atom as well as the low bioavailability and high toxicity of QACs.

6.4. Summary

The inhibitory effect and biotransformation potential of four QACs and VQ, a commercial sanitizer which is a mixture of the four QACs, was investigated at concentrations up to 100 mg/L using a mixed mesophilic methanogenic culture. Dextrin and peptone were used as the carbon and energy sources. A batch assay conducted at a range of QAC concentrations showed that all QACs tested in this study had short- or

long-term inhibitory effects on the mixed methanogenic culture at 25 mg/L and above. Methanogenesis was more sensitive to QAC inhibition than acidogenesis. The inhibitory impact of the individual QACs on the methanogenic activity decreased according to the following series: $DC_8DMA-Cl > DC_{8-10}DMA-Cl > C_nBDMA-Cl > DC_{10}DMA-Cl$. Thus, QACs with the shorter alkyl chain length are the most inhibitory. Adsorption of QACs on biomass was successfully simulated with the Freundlich isotherm equation. Analysis of the phase distribution of QACs between the liquid phase and the solid (biomass) phase resulted in the following series of decreased affinity of QACs for the biomass solids: $DC_{10}DMA-Cl > C_nBDMA-Cl > DC_{8-10}DMA-Cl > DC_8DMA-Cl$. Thus, the inhibitory effect of QACs is inversely proportional to their adsorption affinity on the biomass or their hydrophobicity. The inhibitory effect of Vigilquat® on the mixed methanogenic culture was also investigated in a fed-batch reactor fed with dextrin and peptone. Methanogens were inhibited when the total QAC concentration reached 30 mg/L and volatile fatty acids (VFAs) accumulated. However, methane production recovered in 57 days of incubation, and all VFAs were consumed, suggesting that a prolonged incubation period is necessary for the methanogens to overcome the transient inhibition at a relatively low QAC concentration. None of the QACs tested in this study was biodegraded under methanogenic conditions.

CHAPTER 7

**BIOTRANSFORMATION POTENTIAL OF DIDECYL DIMETHYL
AMMONIUM CHLORIDE AND BENZALKONIUM CHLORIDE IN
A MIXED METHANOGENIC CULTURE UNDER NITRATE
REDUCING CONDITIONS**

7.1. Introduction

The biotransformation potential along with the inhibitory effect of QACs in a mixed methanogenic culture have been described in Chapter 6. None of the QACs tested was degraded and all of them were inhibitory, especially to methanogenesis, at and above 50 mg/L. As it was also discussed in the previous chapter, biodegradation of QACs is energetically less feasible under methanogenic conditions than under aerobic and nitrate reducing conditions. This energetics barrier coupled with the low bioavailability and high toxicity of QACs may explain the recalcitrance of QACs under methanogenic conditions.

The mixed methanogenic culture used in this study is metabolically versatile. It mediates several other terminal electron accepting processes, such as denitrification, dissimilatory nitrate reduction to ammonia (DNRA) (Tugtas and Pavlostathis, 2007), and iron reduction. In view of the fact that several electron acceptors are always present in engineered and natural systems where the QACs are present, such as anoxic/anaerobic bioreactor of a wastewater treatment plant employing biological nutrient removal or an oil-field, respectively, the biotransformation potential of QACs under different electron accepting conditions should be taken into account. One such condition is nitrate

reduction. QAC degradation is energetically more favorable under nitrate reducing conditions than under methanogenic conditions yielding a standard reaction free energy equal to -101.1 ± 0.3 kJ/eq (Figure 7.1). Based on this fact, we explored the fate and effect of two QACs, i.e. didecyl dimethyl ammonium chloride (DC₁₀DMA-Cl) and benzalkonium chloride (C_nBDMA-Cl), in the mixed methanogenic culture under nitrate reducing conditions.

The specific objectives of the research reported in this chapter were to assess: (a) the potential inhibitory effect of DC₁₀DMA-Cl and C_nBDMA-Cl on nitrate reduction and the combined nitrate reduction and carbon utilization; and (b) the biotransformation potential of the selected QACs in a mixed, mesophilic methanogenic culture.

7.2. Materials and Methods

7.2.1. Target Compounds

Didecyl dimethyl ammonium chloride (DC₁₀DMA-Cl) and benzalkonium chloride (C_nBDMA-Cl), defined in Chapter 3, were used as the target QACs.

7.2.2. Mixed Methanogenic Culture

The mixed, methanogenic culture used in the experiments was previously described in Chapter 6. The TS and VS concentration of the culture at the time of this study was 6.9 ± 0.1 and 2.7 ± 0.1 g/L, respectively.

7.2.3. Batch Inhibition Assay

A batch assay was performed to investigate the effect of DC₁₀DMA-Cl and C_nBDMA-Cl on nitrate reduction in the mixed methanogenic culture. The assay was conducted in 160-mL serum bottles (100 ml liquid volume) sealed with rubber stoppers

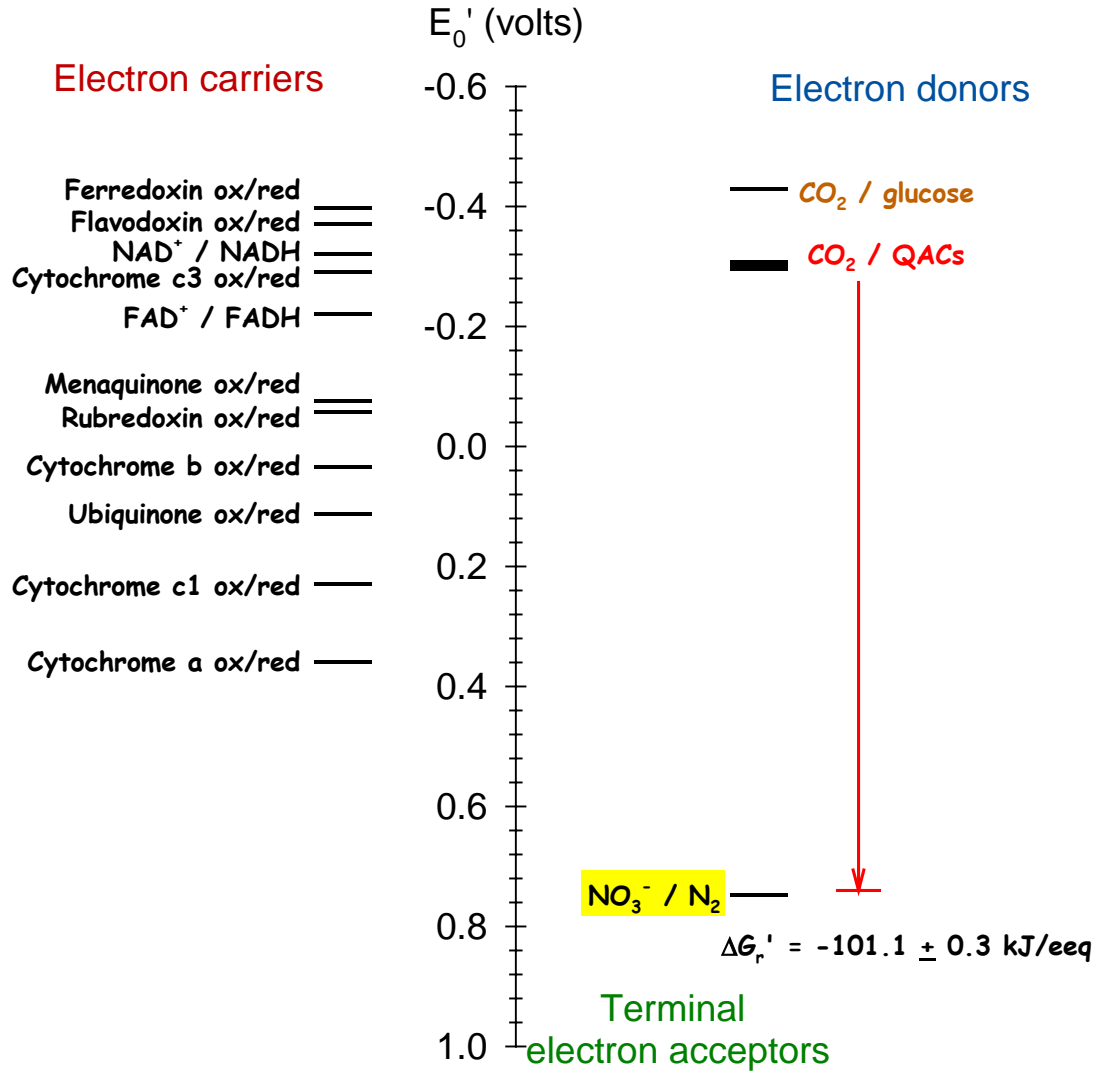


Figure 7.1. Schematic showing the positions of CO₂/QAC and NO₃⁻/N₂ redox couples on the electron tower and the standard free energy upon complete oxidation of QACs to CO₂ under nitrate reducing conditions (QACs represent monoalkonium, dialkonium and benzalkonium chlorides which have average half-reaction free energy equal to 28.9 ± 3.5 kJ/eeq)

and aluminum crimps and flushed with helium gas for 15 min before any liquid addition. A sample of 80 mL of the mixed methanogenic culture taken at the end of a 7-day feeding cycle was anaerobically transferred to each serum bottle along with 10 mL of culture media. Glucose, sodium nitrate and yeast extract solutions, and QAC at desired concentrations were added and the total liquid volume was adjusted to 100 mL with deionized (DI) water. The initial biomass, glucose, nitrate and yeast extract concentrations were 2.0 ± 0.1 g VSS/L, 750 mg/L (800 mg COD/L), 70 mg N/L and 20 mg/L, respectively. The assay included five culture series amended with QAC resulting in initial QAC concentrations of 10, 25, 50, 75 and 100 mg/L, and one culture was prepared without QAC (nitrate reference). Two additional culture series were prepared: seed blank and glucose reference, which consisted of only seed, culture media and DI water, and seed, culture media, DI water, glucose (750 mg/L) and yeast extract (20 mg/L), respectively. All culture series were prepared in triplicate. The initial pH in all cultures was 7.1 ± 0.1 . The cultures were incubated in the dark at 35°C and agitated daily by hand. Throughout the incubation period the total gas volume produced and its composition (i.e., methane, carbon dioxide, nitric oxide, nitrous oxide and dinitrogen), as well as nitrate, nitrite and VFAs were measured. At the end of the incubation period, the pH, VFAs, ammonia, soluble COD (sCOD), VSS, and the total and liquid phase QAC concentrations were measured.

7.2.4. Batch BAC Transformation Assays

Following the observation of a significant decrease of the C_nBDMA-Cl concentration in a mixed methanogenic culture under nitrate reducing conditions at an initial C_nBDMA-Cl concentration of 100 mg/L, three follow-up assays were set up in

160-mL serum bottles (100 mL liquid volume). The first assay was conducted in order to reproduce the C_nBDMA-Cl transformation achieved in the previous assay and to elucidate the transformation pathway under the same conditions described above. This assay included six replicate cultures amended with 5 mM NO₃⁻, 750 mg/L glucose, 20 mg/L yeast extract and 100 mg/L C_nBDMA-Cl. The second and third assays were performed to investigate the role of nitrate (NO₃⁻), nitrite (NO₂⁻) and nitric oxide (NO) on C_nBDMA-Cl transformation and to delineate whether the transformation was abiotic, biotic or biologically mediated. The second assay included four bottles, which were set up in helium flushed 160-mL serum bottles with autoclaved culture media, amended with 100 mg/L of BAC and 5 mM (in the liquid phase) of either NO₃⁻, NO₂⁻ or NO, respectively. The third assay was performed similarly to the second one but the mixed methanogenic culture was used as the seed without glucose and yeast extract amendment. All bottles were incubated in the dark at 35°C and were agitated daily by hand. Throughout the incubation period, the total gas volume produced and its methane, carbon dioxide, nitric oxide, nitrous oxide and dinitrogen content, as well as nitrate, nitrite, total BAC, its homologues and transformation products were measured.

7.2.5. Electron Equivalents Calculations

Electron equivalence calculations were performed at the end of the incubation period based on the electron donor electron equivalents (eeq) added and by accounting for each process, as follows: 4, 5, and 8 eeq/mol of nitrate reduced to nitrous oxide, dinitrogen, and ammonium, respectively; 8 eeq/mol methane produced; 0.125 eeq/g sCOD; and 0.177 eeq/g VSS (using C₅H₇O₂N as the empirical formula for VSS). The COD of liquid phase QAC (2.89 g COD/g C_nBDMA-Cl, and 2.92 g COD/ g DC₁₀DMA-

Cl) was subtracted from the sCOD values and the adsorbed QAC on biomass was subtracted from the measured VSS concentrations of each QAC-amended culture in order to estimate the QAC-free sCOD and VSS concentrations. The biomass-adsorbed BAC was calculated assuming that all BAC homologues have approximately the same sorption affinity for biomass and the weighted average molecular weight of the BAC mixture is 359.6 g/mole.

7.3. Results and Discussion

7.3.1. Didecyl Dimethyl Ammonium Chloride (DC₁₀DMA-Cl)

7.3.1.1. Effect of DC₁₀DMA-Cl on Nitrate Reduction

The assay testing the effect of DC₁₀DMA-Cl on nitrate reduction lasted 100 days. The final pH in all culture series amended with DC₁₀DMA-Cl was between 7.0 and 7.3, which was close to the final pH value of 7.0 and 7.2 in the glucose reference and seed blank cultures. Nitrate was rapidly converted to N₂ in the DC₁₀DMA-Cl-free, nitrate-reference culture (Figure 7.2A). Transient accumulation of N₂O was observed in the 10 and 25 mg/L DC₁₀DMA-Cl amended cultures, and was completely converted to N₂ in 50 and 90 days in these cultures, respectively (Figure 7.2B and 7.2C). Nitrogen balance calculations were based on initial and final nitrogen species taking into account the control (i.e., nitrate-free) culture series. As a result, about 32.1±1.9, 23.1±0.0 and 24.4±1.9% of the initially added NO₃⁻-N was converted to ammonia in the nitrate-reference, and the 10 and 25 mg DC₁₀DMA-Cl/L amended cultures, respectively (Figure 7.3). These data are consistent with previously reported results by Tugtas and Pavlostathis (2007) for the same methanogenic culture at a COD/N ratio of 11.

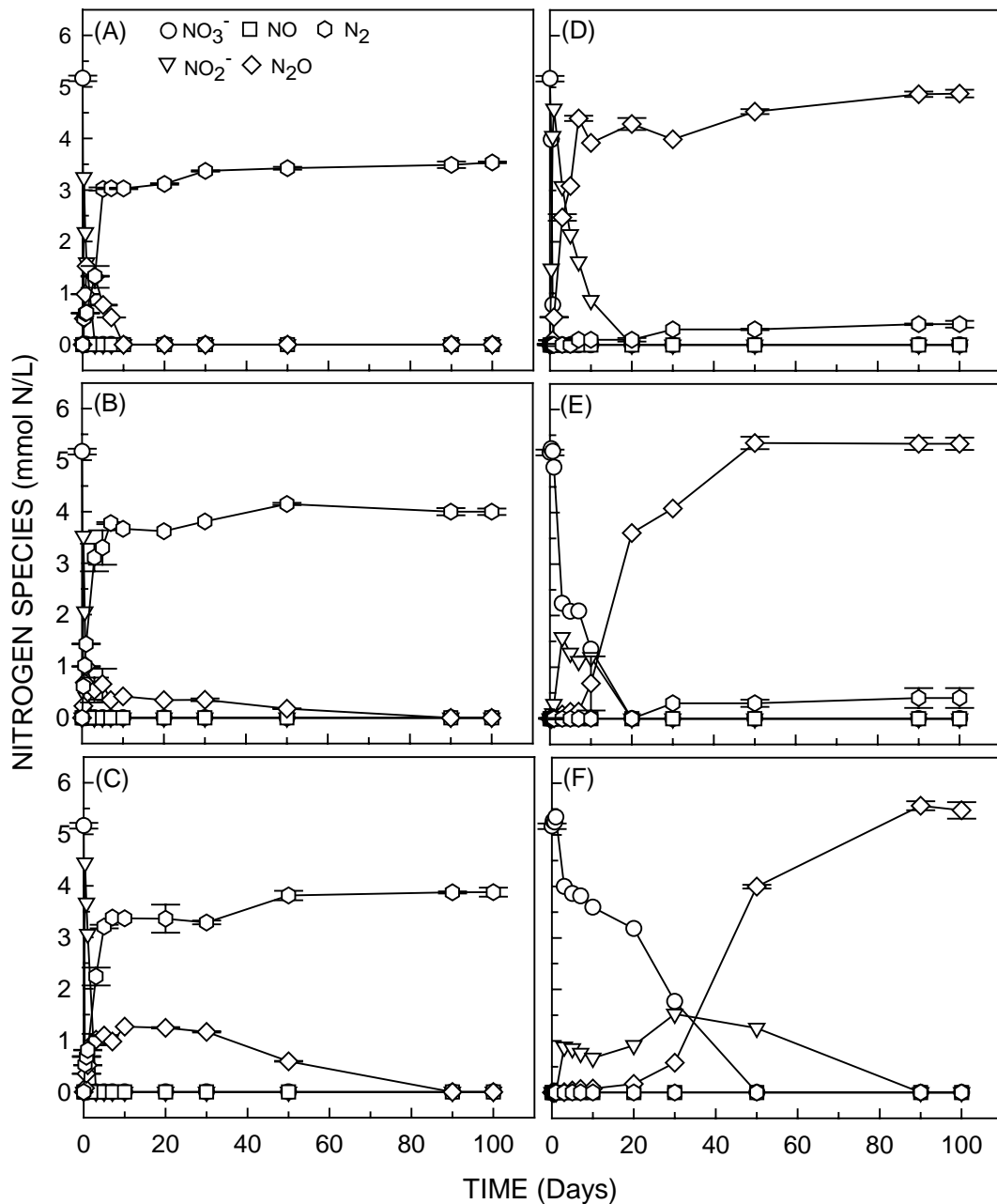


Figure 7.2. Production and consumption profiles of N oxides and N₂ in mixed methanogenic culture series amended with 750 mg/L glucose and 70 mg nitrate-N/L (5 mmol N/L) at (A) 0 (nitrate reference), (B) 10, (C) 25, (D) 50, (E) 75, and (F) 100 mg/L DC₁₀DMA-Cl during 100 days of incubation (Error bars represent one standard deviation of the means; *n* = 3)

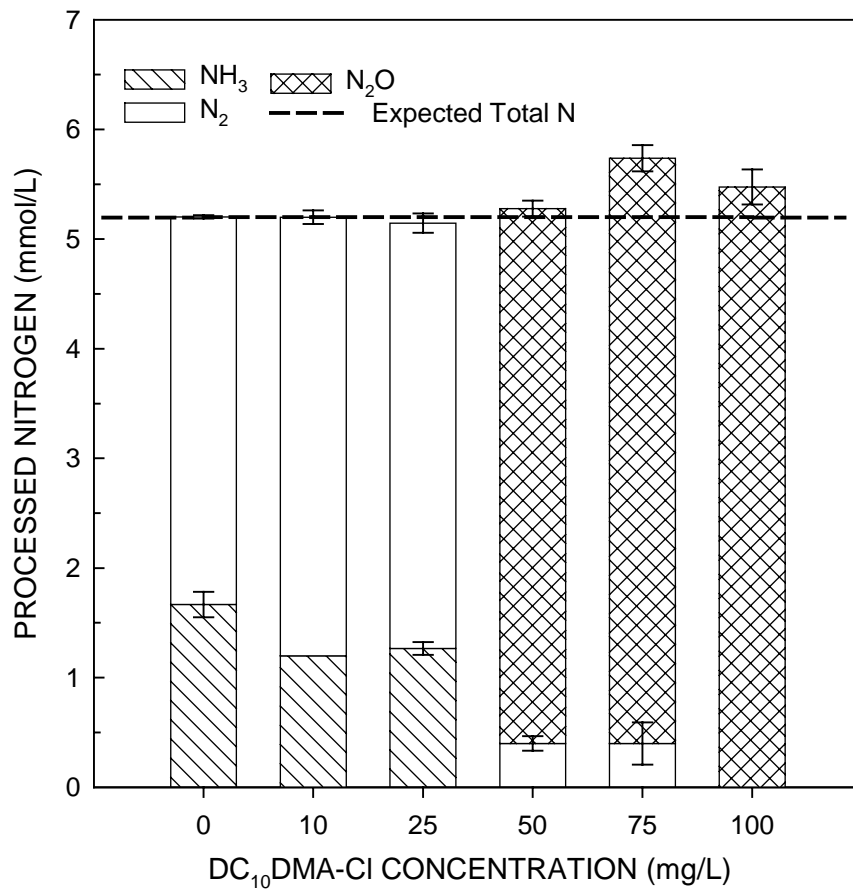


Figure 7.3. Distribution of nitrogen species at the end of the incubation period in mixed methanogenic culture series amended with 750 mg/L glucose, 70 mg nitrate-N/L (5 mmol N/L) and different DC₁₀DMA-Cl concentrations (0-100 mg/L) (Error bars represent one standard deviation of the means; $n = 3$)

The rate and pathway of nitrate reduction in the mixed methanogenic culture were affected at high DC₁₀DMA-Cl concentrations. Nitrate conversion to nitrite was inhibited resulting in a transient slow reduction rate and accumulation of nitrite in the 50, 75 and 100 mg DDAC/L amended cultures (Figure 7.2D, 7.2E, and 7.2F). Inhibition of nitrate reduction to nitrite by DC₁₀DMA-Cl was previously reported for a pure culture of *Bacillus licheniformis* (Seifert and Domka, 2005). All nitrate was utilized through the denitrification pathway since net ammonia production was not detected in these cultures at the end of the incubation. However, N₂O was the final product of nitrate reduction, which indicates that the final step of denitrification was noticeably inhibited at and above 50 mg/L DC₁₀DMA-Cl.

7.3.1.2. Effect of DC₁₀DMA-Cl on Electron Flow

The inhibitory effect of DC₁₀DMA-Cl on the same mixed, methanogenic culture and at a biomass concentration of 1.8±0.1 g VS/L, was previously described in Chapter 6. DC₁₀DMA-Cl had no long-term inhibitory effect on methanogenesis at 10 and 25 mg/L, but methanogenesis was inhibited at 50, 75 and 100 mg DC₁₀DMA-Cl /L. However, methane production recovered between 80 and 100 days of incubation in the 50 mg DC₁₀DMA-Cl/L series. In contrast, recovery of methane production was not observed at 75 and 100 mg DC₁₀DMA-Cl/L. In addition, the net CO₂ production decreased at and above 75 mg/L DC₁₀DMA-Cl, which was taken as an indication that fermentation was also inhibited at and above this DC₁₀DMA-Cl concentration. About 95, 5 and 10% of the total COD was processed as methane and 9, 74 and 29% was processed and accumulated as VFAs at 50, 75 and 100 mg DC₁₀DMA-Cl/L, respectively.

In the present study, among the nitrate amended cultures, methane formation was observed only in the DC₁₀DMA-Cl-free and the 10 mg DC₁₀DMA-Cl/L amended cultures. A transient slow methane production was followed by a faster rate and total methane reached the expected level in the DC₁₀DMA-Cl-free, nitrate-reference culture. However, methane formation was suppressed until N₂O was totally converted to N₂ in the culture amended with 10 mg DC₁₀DMA-Cl/L (Figures 7.2B and 4A). Thus, taking into account the results of our previous study (see Chapter 6) as summarized above, inhibition of methanogenesis at 25 and 50 mg DC₁₀DMA-Cl/L was due to N₂O accumulation. Inhibition of methanogenesis at 75 and 100 mg DC₁₀DMA-Cl/L was probably the result of the combined effect of DC₁₀DMA-Cl direct inhibition and that of N₂O. Fermentation was affected only at 75 and 100 mg DC₁₀DMA-Cl/L and resulted in a lower rate of VFAs production in these cultures (Figure 7.4B).

The net soluble COD concentration at the end of the incubation as compared to the glucose-reference culture was zero in the nitrate-reference and the 10 mg/L DC₁₀DMA-Cl amended cultures, whereas it was 550±83, 1469±65, 1499±37 and 1521±58 mg/L in the 25, 50, 75 and 100 mg/L DC₁₀DMA-Cl amended cultures, respectively. The soluble COD concentration in the 25 mg DC₁₀DMA-Cl/L cultures corresponded to the VFAs-COD. However, the soluble COD concentration was higher than the VFAs-COD in all cultures amended with DC₁₀DMA-Cl higher than 25 mg/L. At the end of the incubation period, glucose was not detected in these cultures. The VS concentration in the 50, 75 and 100 mg/L DC₁₀DMA-Cl amended cultures (1.24±0.04, 1.17±0.02 and 1.27±0.02 g VS/L, respectively) was significantly lower than that of the DC₁₀DMA-Cl -free, nitrate-reference (1.53±0.08 g VS/L) and was comparable with that

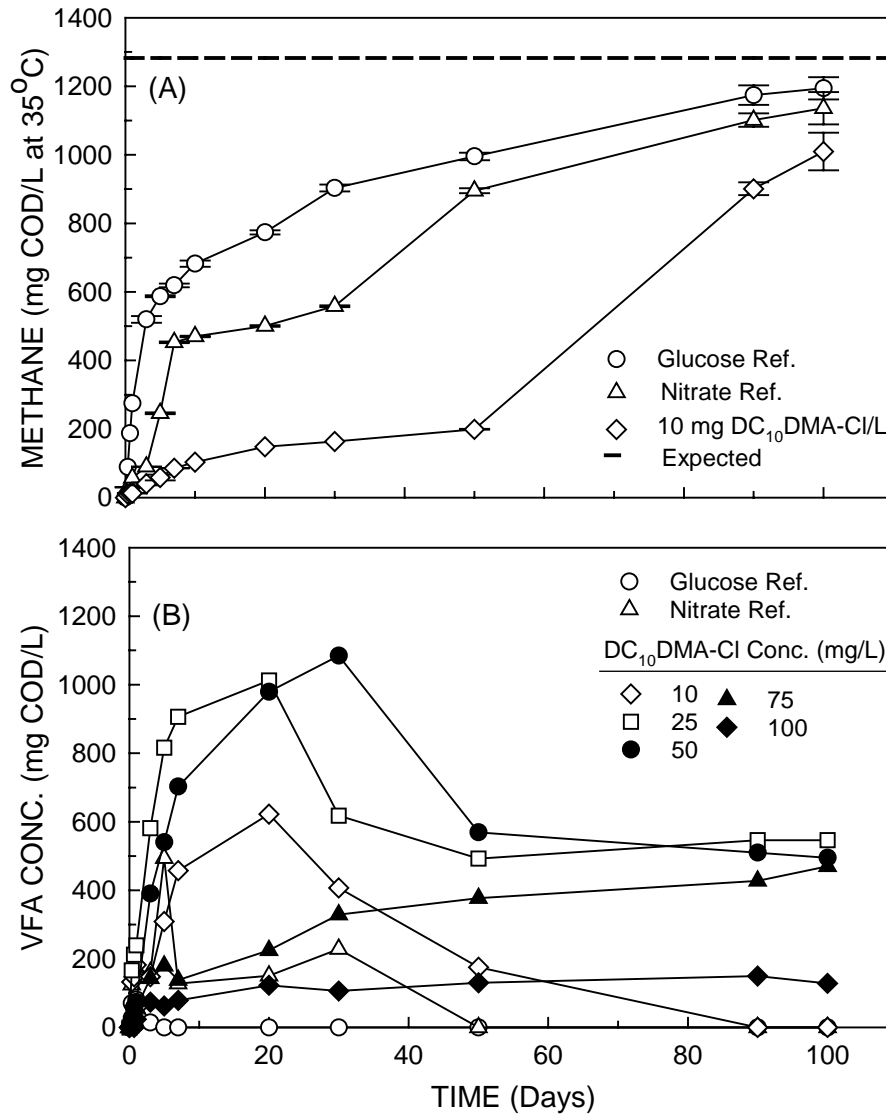


Figure 7.4. Profiles of (A) methane production in glucose and nitrate reference cultures and 10 mg DC₁₀DMA-Cl amended culture and (B) VFAs production and consumption in the mixed methanogenic cultures amended with 750 mg/L glucose and 70 mg nitrate-N/L at different DC₁₀DMA-Cl concentrations (0-100 mg/L) (Error bars represent one standard deviation of the means, $n = 3$)

of seed blank (1.28 ± 0.06 g VS/L). These results indicate that DC₁₀DMA-Cl suppressed microbial growth and caused cell lysis at and above 50 mg/L, which may be related to the high adsorption affinity of DC₁₀DMA-Cl for the biosolids, as mentioned below.

7.3.1.3. Phase Distribution of DC₁₀DMA-Cl

The total and aqueous phase DC₁₀DMA-Cl concentrations in all DC₁₀DMA-Cl - amended cultures were measured at the end of the incubation period. According to these results, DC₁₀DMA-Cl was recovered by $96.2 \pm 5.5\%$ (mean \pm standard deviation, $n = 15$). Thus, DC₁₀DMA-Cl was resistant to biodegradation in the mixed methanogenic culture under the conditions applied in the present study. The solid phase DC₁₀DMA-Cl fraction was 99.2 and 54.7% at a total DC₁₀DMA-Cl concentration of 10 and 100 mg/L, respectively (Figure 7.5). These data agree with values reported in Chapter 6 relative to the phase distribution of DC₁₀DMA-Cl in the same methanogenic culture and demonstrate the high adsorption affinity of DC₁₀DMA-Cl for biosolids.

7.3.2. Benzalkonium Chloride (C_nBDMA-Cl)

7.3.2.1. Effect of C_nBDMA-Cl on Nitrate Reduction

The assay testing the effect of C_nBDMA-Cl on nitrate reduction lasted 100 days. The final pH in all culture series amended with C_nBDMA-Cl was between 7.0 and 7.3, which was close to the final pH value of 7.0 and 7.2 in the glucose reference and seed blank cultures. Nitrate was rapidly converted to N₂ in the C_nBDMA-Cl -free, nitrate reference culture (Figure 7.6A). Transient accumulation of N₂O was observed in the 10 and 25 mg/L C_nBDMA-Cl amended cultures, and was completely converted to N₂ in 10 and 20 days in these cultures, respectively (Figure 7.6B and 7.6C). Nitrogen balance calculations

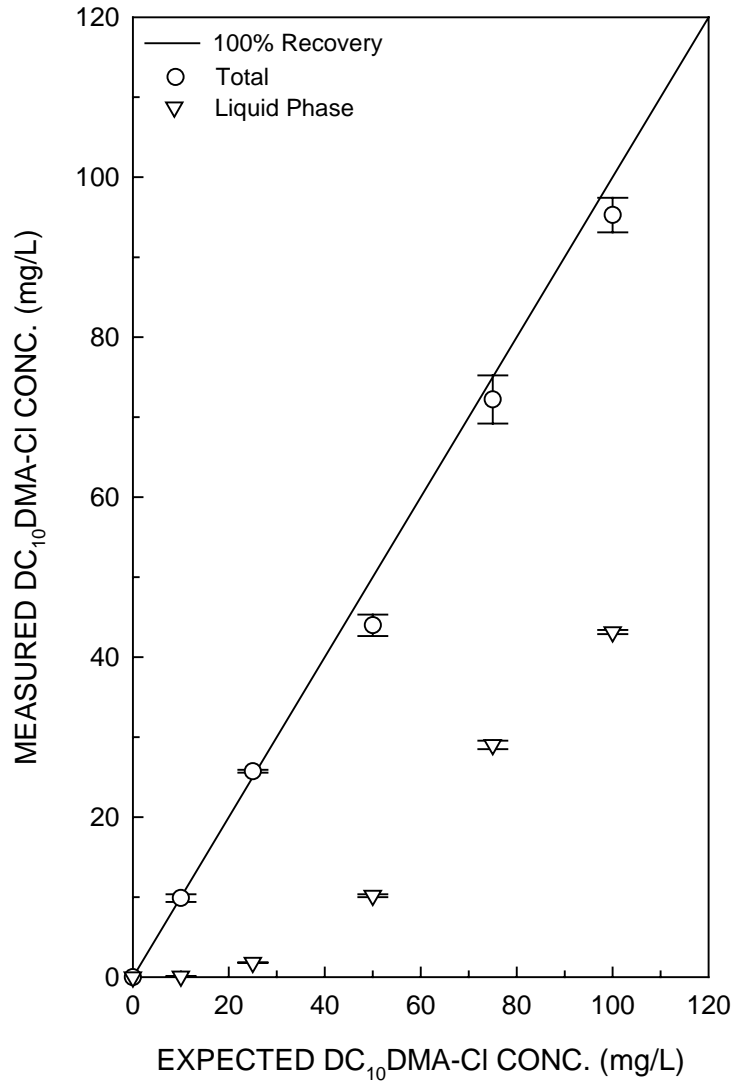


Figure 7.5. Phase distribution of DC₁₀DMA-Cl in mixed methanogenic culture series amended with DC₁₀DMA-Cl at different concentrations (0-100 mg/L) at the end of the incubation (Error bars represent one standard deviation of the means; $n = 3$)

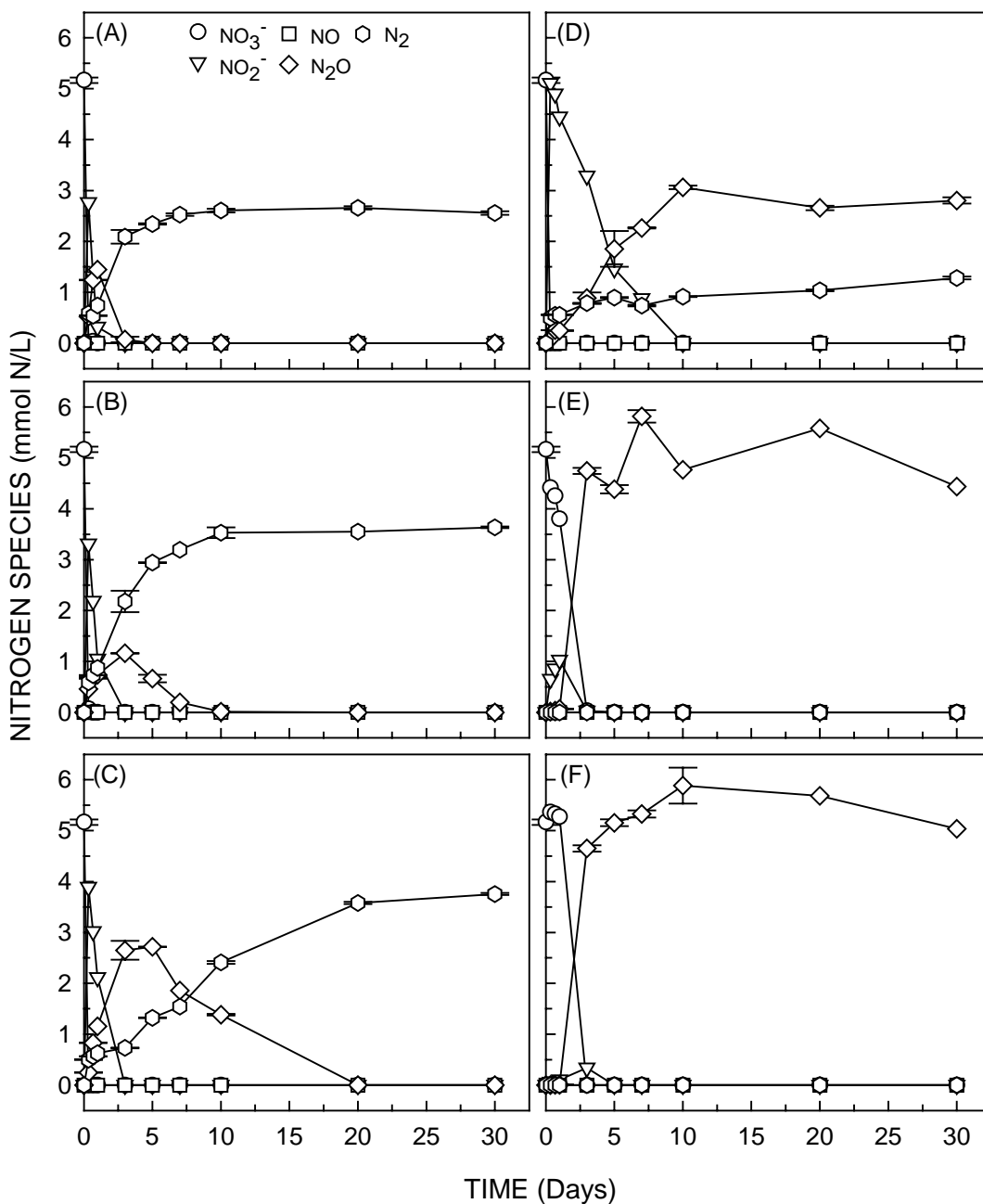


Figure 7.6. Production and consumption profiles of N oxides and N_2 in mixed methanogenic culture series amended with 750 mg/L glucose and 70 mg nitrate-N/L (5 mmol N/L) at (A) 0 (nitrate reference), (B) 10, (C) 25, (D) 50, (E) 75, and (F) 100 mg/L $\text{C}_n\text{BDMA-Cl}$ during 100 days of incubation (Error bars represent one standard deviation of the means; $n = 3$)

performed by taking into account the control (i.e., nitrate-free) culture series showed that 38.7 ± 4.5 , 20.6 ± 7.7 and $18.1 \pm 4.5\%$ of the initially added NO_3^- -N was converted to ammonia in the nitrate reference, and the 10 and 25 mg $\text{C}_n\text{BDMA-Cl/L}$ amended cultures, respectively (Figure 7.7). DNRA and denitrification occurred simultaneously in the mixed methanogenic culture and the extent of nitrate proportionation between these two nitrate reduction pathways in the absence of $\text{C}_n\text{BDMA-Cl}$ using glucose as the carbon and energy source was consistent with results reported above for the same methanogenic culture. However, the fraction of nitrate reduced via DNRA decreased with increasing $\text{C}_n\text{BDMA-Cl}$ concentration. A similar effect was described for $\text{DC}_{10}\text{DMA-Cl}$ in the previous section.

The extent and pathway of nitrate reduction in the mixed methanogenic culture were affected by $\text{C}_n\text{BDMA-Cl}$. As the $\text{C}_n\text{BDMA-Cl}$ concentration increased from 10 to 50 mg/L, nitrite conversion to NO and N_2O was inhibited resulting in a lower nitrite reduction rate and a transient accumulation of nitrite (Figure 7.6B, 7.6C and 7.6D). On the other hand, nitrate reduction to nitrite was inhibited resulting in a slow nitrate reduction rate and almost undetectable intermediate nitrite in the 75 and 100 mg $\text{C}_n\text{BDMA-Cl/L}$ amended cultures (Figure 7.6E and 7.6F). However, all N oxides were rapidly converted to N_2O in less than 5 days in these cultures. All nitrate was utilized through the denitrification pathway since net ammonia production was not detected in these cultures at the end of the incubation (Figure 7.7). However, N_2O was the final product of nitrate reduction, which indicates that the final step of denitrification was completely inhibited at and above 75 mg/L $\text{C}_n\text{BDMA-Cl}$ (Figure 7.6E and 7.6F) as described for $\text{DC}_{10}\text{DMA-Cl}$ in the previous section.

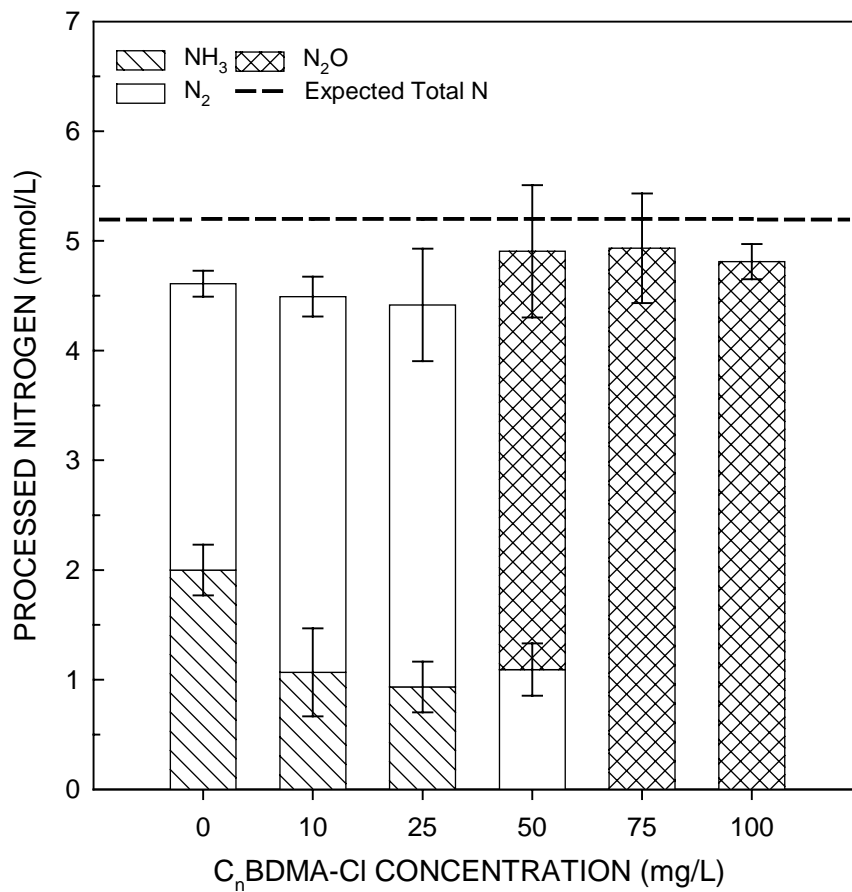


Figure 7.7. Distribution of nitrogen species at the end of the incubation period in mixed methanogenic culture series amended with 750 mg/L glucose, 70 mg nitrate-N/L (5 mmol N/L) and different C_nBDMA-Cl concentrations (0-100 mg/L) (Error bars represent one standard deviation of the means; $n = 3$)

The experiments conducted with DC₁₀DMA-Cl and C_nBDMA-Cl showed a similar inhibitory effect on nitrate reduction, that is DNRA was inhibited and denitrification was incomplete resulting in accumulation of nitrous oxide at and above 50 mg QAC/L. The major mode of action of QACs involves adsorption onto the cell surface and penetration into the cell through the periplasm and the cytoplasmic membrane. The nitrate and nitric oxide reductases, which convert NO₃⁻ to NO₂⁻ and NO to N₂O, respectively, are located in the cytoplasmic membrane, whereas the nitrite and nitrous oxide reductases, which reduce NO₂⁻ to NO and N₂O to N₂, respectively, are located in the periplasm (Zumft, 1997). Therefore, the latter two enzymes may be exposed to higher QAC concentrations than the ones located in the cytoplasmic membrane, which may explain why inhibition of these enzymes was more pronounced at high QAC concentrations in this study. Inhibition of nitrous oxide reductase by the QACs, which results in the accumulation of N₂O, is of particular concern since production of N₂O is undesirable because of its green house effect and its impact on global warming.

7.3.2.2. Effect of C_nBDMA-Cl on Electron Flow

Nitrate reduction, fermentation and methanogenesis are important terminal electron accepting microbial processes in natural systems such as aquatic sediments and are employed for the combined treatment of carbon- and nitrogen-bearing wastes in industrial wastewater treatment systems. As a result, in addition to the effect of C_nBDMA-Cl on nitrate reduction, we evaluated its effect on the overall electron flow in a mixed methanogenic culture. All cultures, except the seed blank, were amended with 100 meeq/L glucose. The seed used in each culture had unaccounted for biodegradable organics that yielded 49.9±2.1 meeq/L of methane. Electron equivalents consumed in

each process and residual sCOD and VSS in the various culture series are shown in Table 7.1.

Table 7.1. Electron equivalents balance in C_nBDMA-Cl -free and C_nBDMA-Cl -amended mixed methanogenic culture series^a

Culture Series	Process and Culture Component (meeq/L)					
	Denitrification	DNRA	Methanogenesis	sCOD	VSS	Total
Glucose Reference	NA ^b	NA	150.9±0.3	73.1±9.5	315.1±10.3	539.0±20.1
Nitrate Reference	13.1±0.6 ^c	16.0±1.9	142.2±7.4	74.0±11.5	310.7±15.2	555.9±36.6
10 mg BAC/L	17.1±0.9	8.5±3.2	133.5±6.1	66.5±5.6	305.9±12.6	531.6±28.4
25 mg BAC/L	17.4±2.6	7.5±1.9	82.4±19.1	99.2±10.1	300.8±15.4	507.3±49.0
50 mg BAC/L	22.0±0.9	0.0±0.0	3.7±0.3	234.2±30.1	211.7±5.4	471.6±36.9
75 mg BAC/L	20.9±0.8	0.0±0.0	3.6±0.2	260.0±43.2	192.7±22.2	477.2±66.3
100 mg BAC/L	21.0±0.3	0.0±0.0	4.4±0.6	300.2±1.1	216.9±11.6	542.4±13.6

^a At the end of the incubation period; all cultures were amended with 100 meeq/L glucose. ^b NA, not applicable. ^c Mean ± standard deviation ($n = 3$)

All biodegradable organics (150.9±0.3 meeq/L) were converted to methane in the glucose reference culture. The electron equivalents for nitrate reduction were 39.1±2.5, 25.6±4.1 and 24.9±4.5 meeq/L in the 0, 10 and 25 mg C_nBDMA-Cl/L amended cultures, respectively. The nitrate reference culture used more electron equivalents for nitrate reduction than the latter two cultures because the fraction of nitrate that was utilized through DNRA was higher than the fraction utilized by the cultures amended with 10 and 25 mg C_nBDMA-Cl /L, and the electron requirement for complete DNRA (8 eeq per mole NO₃⁻) is higher than that for complete denitrification (5 eeq per mole NO₃⁻). As soon as all the N oxides were utilized, the remaining electron equivalents were processed

to methane in these cultures (Figure 7.8A). The inhibitory effect of C_nBDMA-Cl on the same mixed, methanogenic culture at a biomass concentration of 1.8±0.1 g VS/L, was previously presented in Chapter 6. C_nBDMA-Cl did not inhibit the methanogenesis at 10 and 25 mg C_nBDMA-Cl/L, and the delay of methane formation was attributed to the transient formation of N oxides in these cultures. The biomass concentration in both reference cultures and the cultures amended with 10 and 25 mg C_nBDMA-Cl/L was almost the same.

In the cultures amended with 50, 75 and 100 mg C_nBDMA-Cl/L, nitrate was processed through partial denitrification to N₂O. Thus, the electron equivalents used for nitrate reduction in these cultures were less than in the nitrate reference culture and the cultures with low C_nBDMA-Cl concentrations. Methanogenesis was inhibited at these C_nBDMA-Cl concentrations and did not recover during the incubation period. The inhibitory effect of C_nBDMA-Cl on the same mixed methanogenic culture was previously described in Chapter 6. Thus, the inhibition of methanogenesis in these cultures was attributed to the combined effect of BAC and N oxides. Inhibition of methanogenesis resulted in a high concentration of sCOD in these cultures (Table 7.1). However, the concentration of sCOD at the end of the incubation was higher than at the beginning of the assay (glucose + unaccounted organics = ca. 150 meeq/L). The biomass concentration in these cultures was lower than in the references and the seed blank. Cationic surfactants like C_nBDMA-Cl are known to cause cell lysis at high concentrations by attacking the cell phospholipid bilayer, resulting in the release of intracellular material. Thus, growth inhibition and extensive cell lysis at high BAC concentrations resulted in low biomass and high sCOD concentrations in these cultures.

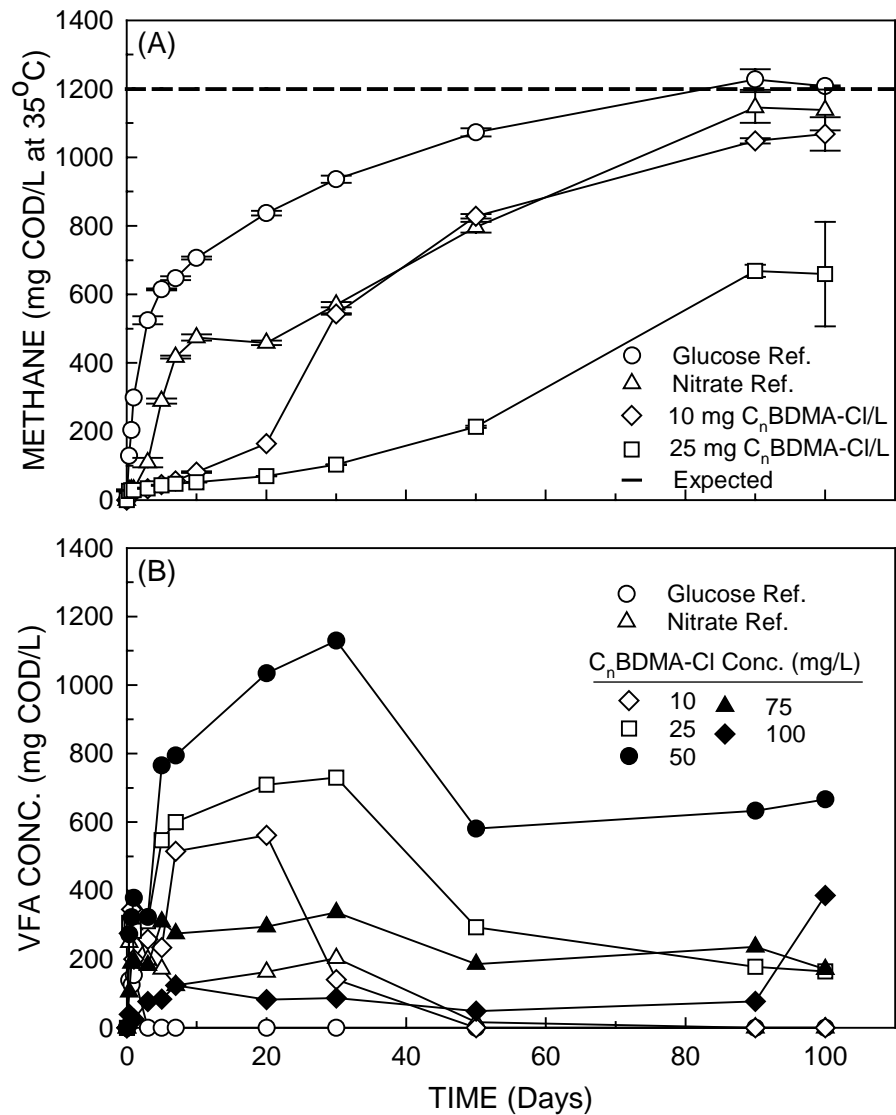


Figure 7.8. Profiles of (A) methane production in glucose and nitrate reference cultures and the cultures amended with 10 and 25 mg C_nBDMA-Cl, and (B) VFAs production and consumption in the mixed methanogenic cultures amended with 750 mg/L glucose and 70 mg nitrate-N/L at different C_nBDMA-Cl concentrations (0-100 mg/L) (Error bars represent one standard deviation of the means)

The major fraction of sCOD was VFAs, mainly acetate and propionate, in the culture with 50 mg C_nBDMA-Cl/L (Figure 7.8B). Glucose was not detected in this culture, which indicates that its fermentation was not inhibited at this C_nBDMA-Cl concentration (see Chapter 6). In the 75 mg C_nBDMA-Cl/L amended culture, a small portion of its sCOD was VFAs (21.3±0.9 meeq/L) and 43.0±4.3 meeq/L of glucose was not processed through acidogenic fermentation. Although C_nBDMA-Cl did not inhibit fermentation at this concentration as demonstrated in Chapter 6, the inhibition of fermentation reported in this study may be attributed to the combined effect of C_nBDMA-Cl and accumulation of N₂O in this culture. On the contrary, glucose was totally processed and converted to VFAs and unaccounted for alcohols and organic acids (observed in HPLC chromatograms) in the 100 mg C_nBDMA-Cl /L amended culture by the end of the incubation period (Figure 7.8B) in spite of the fact that C_nBDMA-Cl was expected to be inhibitory to fermentation at this concentration. The lack of glucose fermentation inhibition at 100 mg C_nBDMA-Cl/L, although it was inhibited at 75 mg C_nBDMA-Cl/L, is attributed to the transformation of C_nBDMA-Cl, which decreased the C_nBDMA-Cl concentration below its inhibitory concentration resulting in the recovery of fermentation, as discussed below.

7.3.2.3. Phase Distribution of C_nBDMA-Cl

The total and aqueous phase C_nBDMA-Cl concentrations in all C_nBDMA-Cl-amended cultures were measured at the end of the incubation period. C_nBDMA-Cl was recovered by 99.0±3.2% (mean ± standard deviation; *n* = 12) in all cultures except in the one amended with 100 mg C_nBDMA-Cl/L in which about 37% of C_nBDMA-Cl added was removed (Figure 7.9). This result also explains why glucose fermentation was not

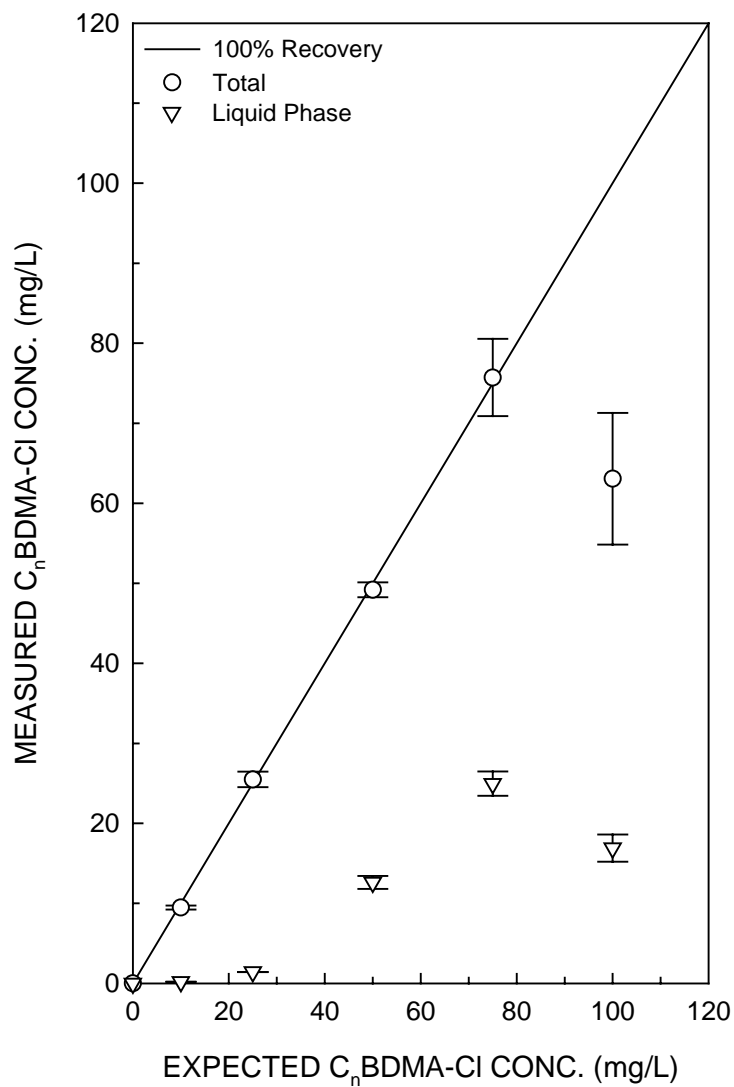


Figure 7.9. Phase distribution of C_nBDMA-Cl in mixed methanogenic culture series amended with C_nBDMA-Cl at different concentrations (0-100 mg/L) at the end of the incubation (Error bars represent one standard deviation of the means; $n = 3$)

inhibited at 100 mg C_nBDMA-Cl/L but was inhibited at 75 mg C_nBDMA-Cl/L. The solid phase C_nBDMA-Cl fraction was 98.0 and 67.0% at a total C_nBDMA-Cl concentration of 10 and 75 mg/L, respectively (Figure 7.9), which agrees with previously reported values relative to the phase distribution of C_nBDMA-Cl in the same methanogenic culture (Chapter 6), and demonstrates the high adsorption affinity of C_nBDMA-Cl for biosolids.

7.3.2.4. C_nBDMA-Cl Transformation

Upon the partial disappearance of C_nBDMA-Cl in the 100 mg C_nBDMA-Cl/L amended cultures, two assays were performed in order to replicate the C_nBDMA-Cl transformation under the same conditions and to identify potential products. In the first assay, the cultures in which partial C_nBDMA-Cl removal was reported were supplemented with 5 mM NO₃⁻, 750 mg/L glucose and 20 mg/L yeast extract in two consecutive cycles without C_nBDMA-Cl addition. In the first cycle, the C_nBDMA-Cl concentration decreased from 63.1±8.2 to 36.4±2.1 mg/L and all NO₃⁻ was converted to N₂O (5.0±0.1 mM N₂O-N expressed as liquid concentration) (Figure 7.10). In the second cycle, a statistically insignificant ($p = 0.54$) decrease in C_nBDMA-Cl concentration (33.9±2.0 mg/L at the end of the second cycle) was found and all NO₃⁻ was converted rapidly to N₂ (4.4±0.5 mM N₂-N expressed as liquid concentration) (Figure 7.10). These results suggest that the denitrification inhibition by C_nBDMA-Cl diminished as the C_nBDMA-Cl concentration decreased and/or was overcome by acclimation/adaptation of the culture to C_nBDMA-Cl during the prolonged incubation period, as discussed in Chapter 6. Moreover, the inhibition of denitrification may favor the transformation of C_nBDMA-Cl under the conditions applied in the present study, as discussed below.

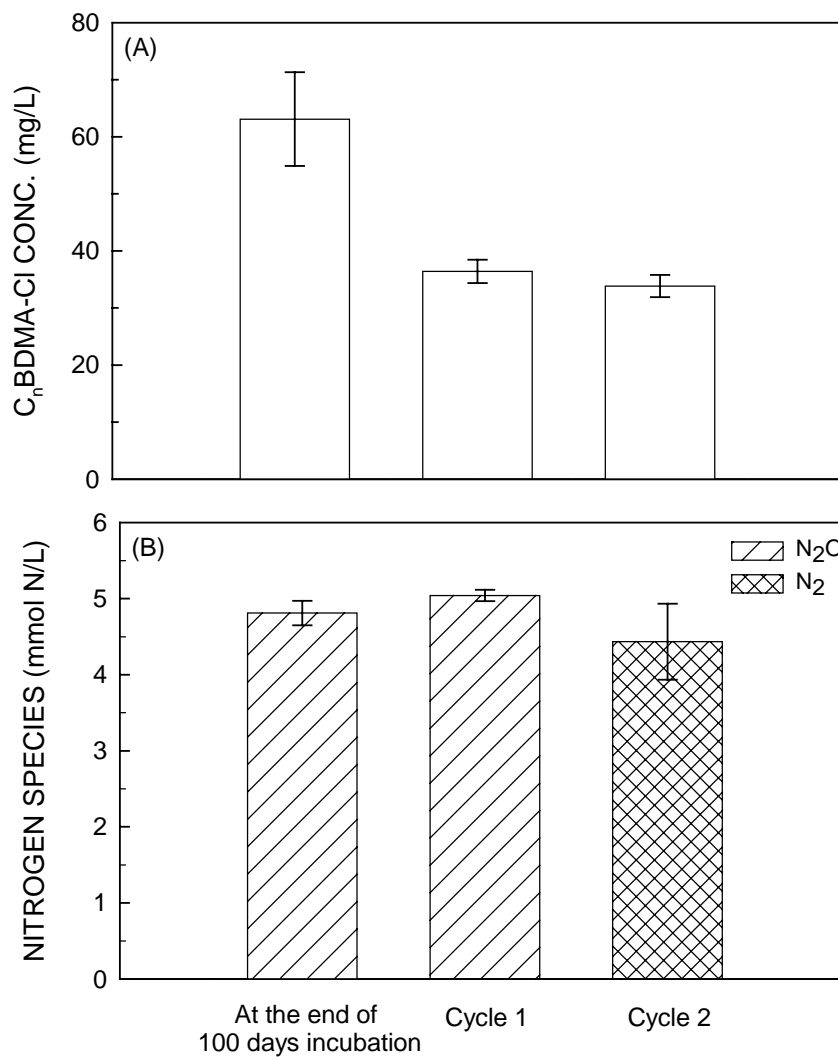


Figure 7.10. Concentrations of (A) C_nBDMA-Cl and (B) nitrogen species at the end of 100 days incubation, cycle 1 and cycle 2 (*See text*; Error bars represent one standard deviation of the means; $n = 3$)

In the second assay, lasting 63 days, six replicate cultures were prepared at 100 mg C_nBDMA-Cl/L as described above. The C_nBDMA-Cl concentration and headspace gas composition were followed during the course of the assay (Figure 7.11A). The C_nBDMA-Cl concentration decreased from 289.6±7.6 μM (104.1±2.7 mg/L) to 131.1±15.3 μM (47.2±5.5 mg/L) in less than 40 days, while almost all NO₃⁻ was converted to N₂O. When the nitrate reduction stopped, the C_nBDMA-Cl concentration leveled off at 110.3±16.9 μM (39.7±6.1 mg/L), which is consistent with the results of the previous two assays in the present study, suggesting that C_nBDMA-Cl was transformed during the denitrification process under the conditions applied in this assay.

At the end of the incubation period, samples taken from each culture were solvent extracted and analyzed for C_nBDMA-Cl and alkyl dimethyl amines by HPLC and LC-MS, respectively. Each C_nBDMA-Cl homologue (C₁₂BDMA-Cl, C₁₄BDMA-Cl and C₁₆BDMA-Cl) was transformed into its corresponding alkyl dimethyl amine (C₁₂DMA, C₁₄DMA and C₁₆DMA) at an equimolar concentration (Figure 7.11B). Degradation of the alkyl dimethyl amines was not observed, which may be attributed to their hydrophobicity resulting in limited bioavailability, toxicity or lack of appropriate microbial consortia. At the end of these assays, several questions were raised: (1) “Is C_nBDMA-Cl transformation a biotic or an abiotic reaction?”; (2) “What triggers the observed C_nBDMA-Cl transformation?”; and (3) “What is the C_nBDMA-Cl transformation mechanism?”.

In order to answer these questions, two additional assays were performed, lasting 87 days each. In the first assay, three culture series (all in triplicate) were set up at ca. 100 mg C_nBDMA-Cl/L and amended with 5 mM of either NO₃⁻, NO₂⁻ or NO, without any

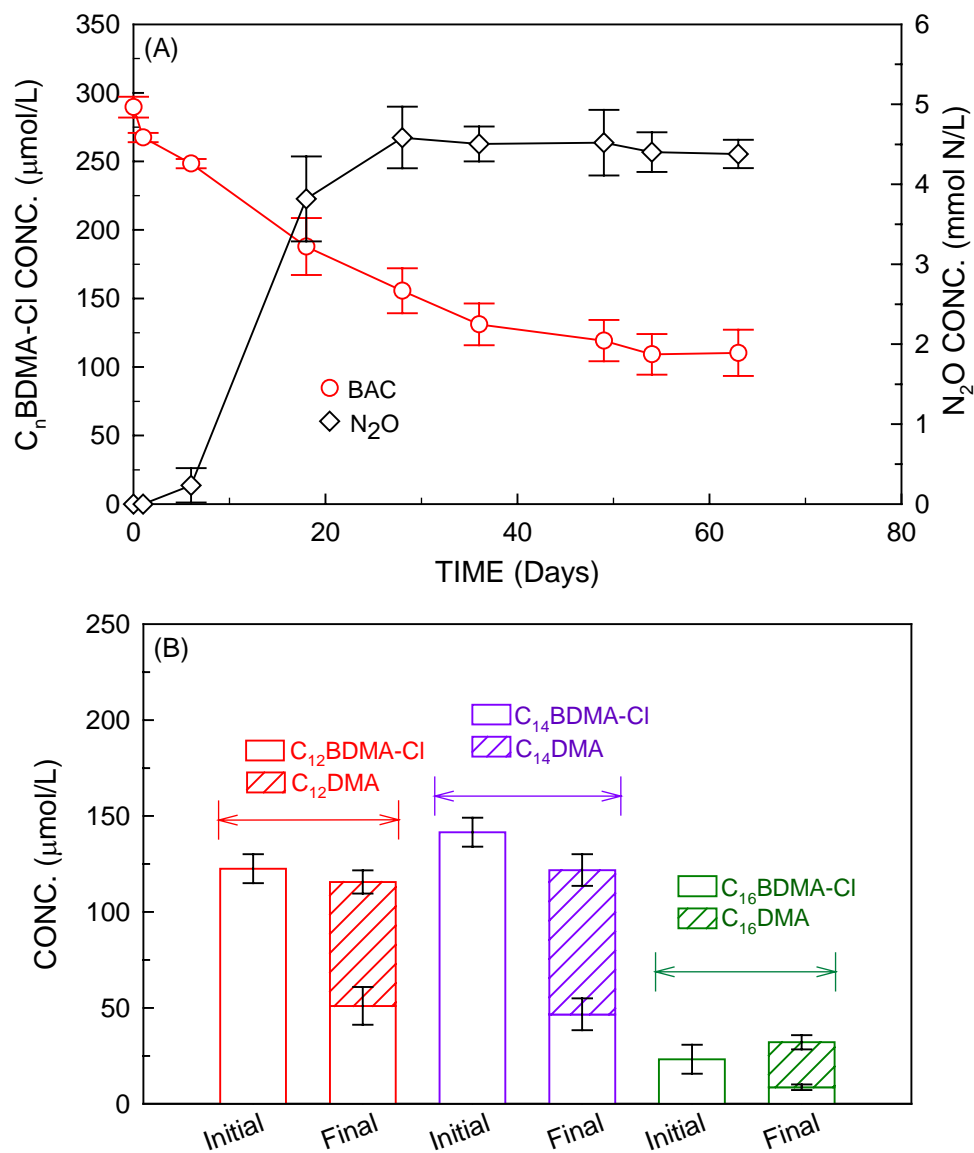


Figure 7.11. (A) Profiles of C_n BDMA-Cl consumption and N_2O formation during the incubation period and (B) distribution of C_n BDMA-Cl homologues and alkyl dimethyl amines at the first and last day of incubation in a mixed methanogenic culture amended with 750 mg/L glucose and 70 mg nitrate-N/L (5 mmol N/L) at 100 mg C_n BDMA-Cl/L (Error bars represent one standard deviation of the means; $n = 6$)

carbon and energy source. Control cultures without any N oxide or C_nBDMA-Cl were also prepared. The C_nBDMA-Cl concentration decreased from 356.9±3.8 μM (128.2±1.4 mg/L) to 153.1±3.6 μM (54.8±1.3 mg/L) (Figure 7.12A) during the incubation period and NO₃⁻ was totally converted to N₂O after a 10-day delay in the cultures amended with 5 mM NO₃⁻ (Figure 7.12B). NO₂⁻ was detected at a very low concentration during the incubation period. Similarly, the C_nBDMA-Cl concentration decreased from 358.8±5.7 μM (128.9±2.0 mg/L) to 110.4±3.3 μM (39.6±1.2 mg/L) (Figure 7.12A) and NO₂⁻ was totally converted to N₂O after a 10-day delay in the cultures amended with 5 mM NO₂⁻ (Figure 7.12C). The extent of C_nBDMA-Cl transformation in NO₂⁻ amended cultures was higher than in the NO₃⁻ amended cultures. The C_nBDMA-Cl concentration did not change in the N oxides free cultures (Figure 7.12A). N oxides were converted to N₂ in all cultures amended with 5 mM of NO₃⁻, NO₂⁻ or NO but not with C_nBDMA-Cl, which shows that these cultures used residual organics and/or sulfide during the denitrification process. This assay did not provide any evidence of whether the observed C_nBDMA-Cl transformation is biotic, but did show that C_nBDMA-Cl is transformed during NO₂⁻ reduction. Nitrate reduction to N₂O also supports C_nBDMA-Cl transformation since NO₂⁻ is an intermediate.

In the second assay, three triplicate abiotic reactors were set up at ca. 100 mg C_nBDMA-Cl/L with culture media and amended with 5 mM of either NO₃⁻, NO₂⁻ or NO. N oxide or C_nBDMA-Cl free controls were also prepared. The C_nBDMA-Cl concentration in the NO₂⁻ amended reactors decreased from 308.1±0.0 μM (110.1±0.0 mg/L) to 30.8±3.9 μM (10.8±1.4 mg/L) in 42 days (Figure 7.13). The C_nBDMA-Cl concentration did not change for the rest of the incubation period. Moreover, a slight but

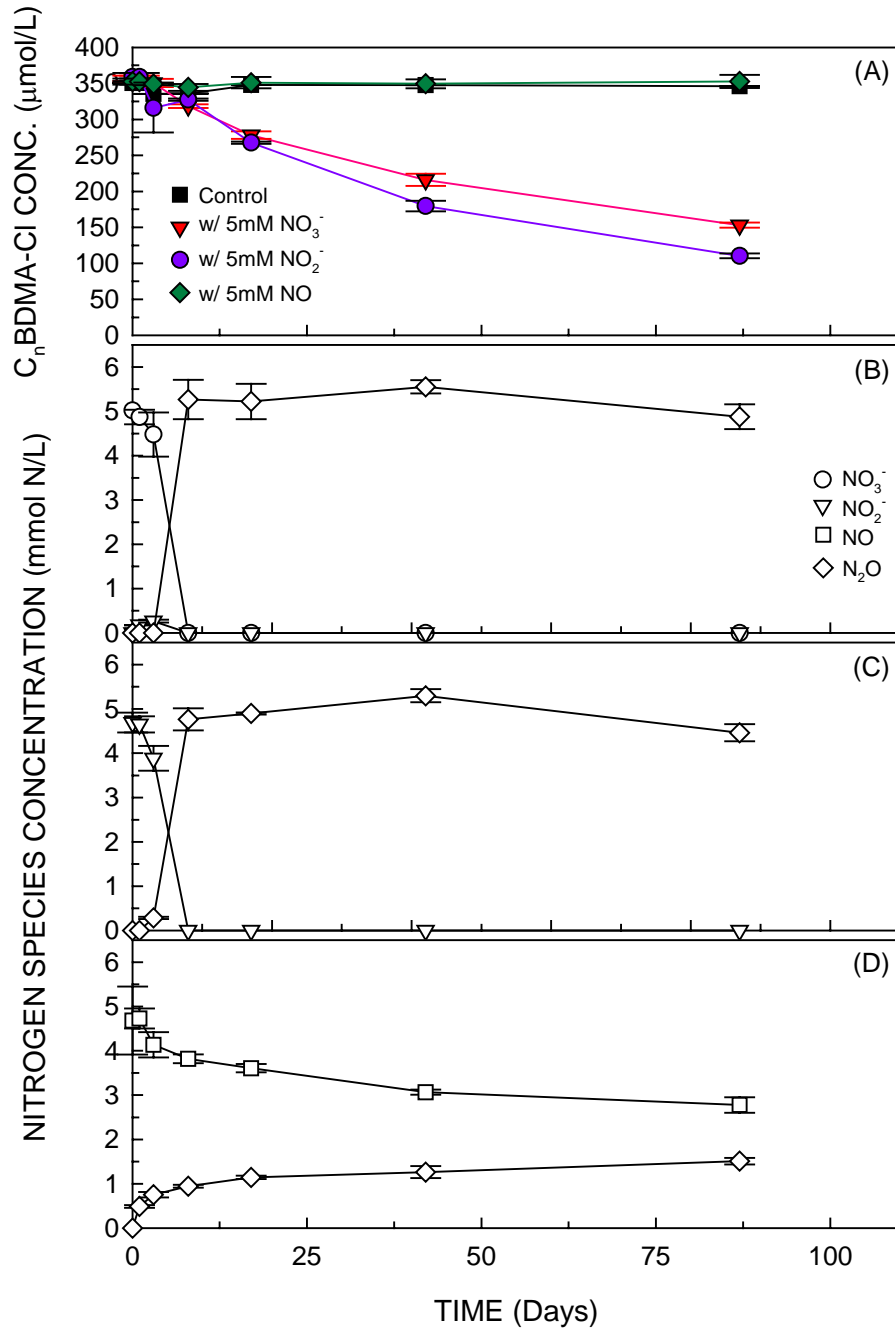


Figure 7.12. Profiles of (A) C_nBDMA-Cl in all test culture series and N oxides consumption and production in culture series amended with 100 mg/L C_nBDMA-Cl and 5 mmol N/L of (B) NO₃⁻, (C) NO₂⁻ and (D) NO, respectively (Error bars represent one standard deviation of the means; *n* = 3)

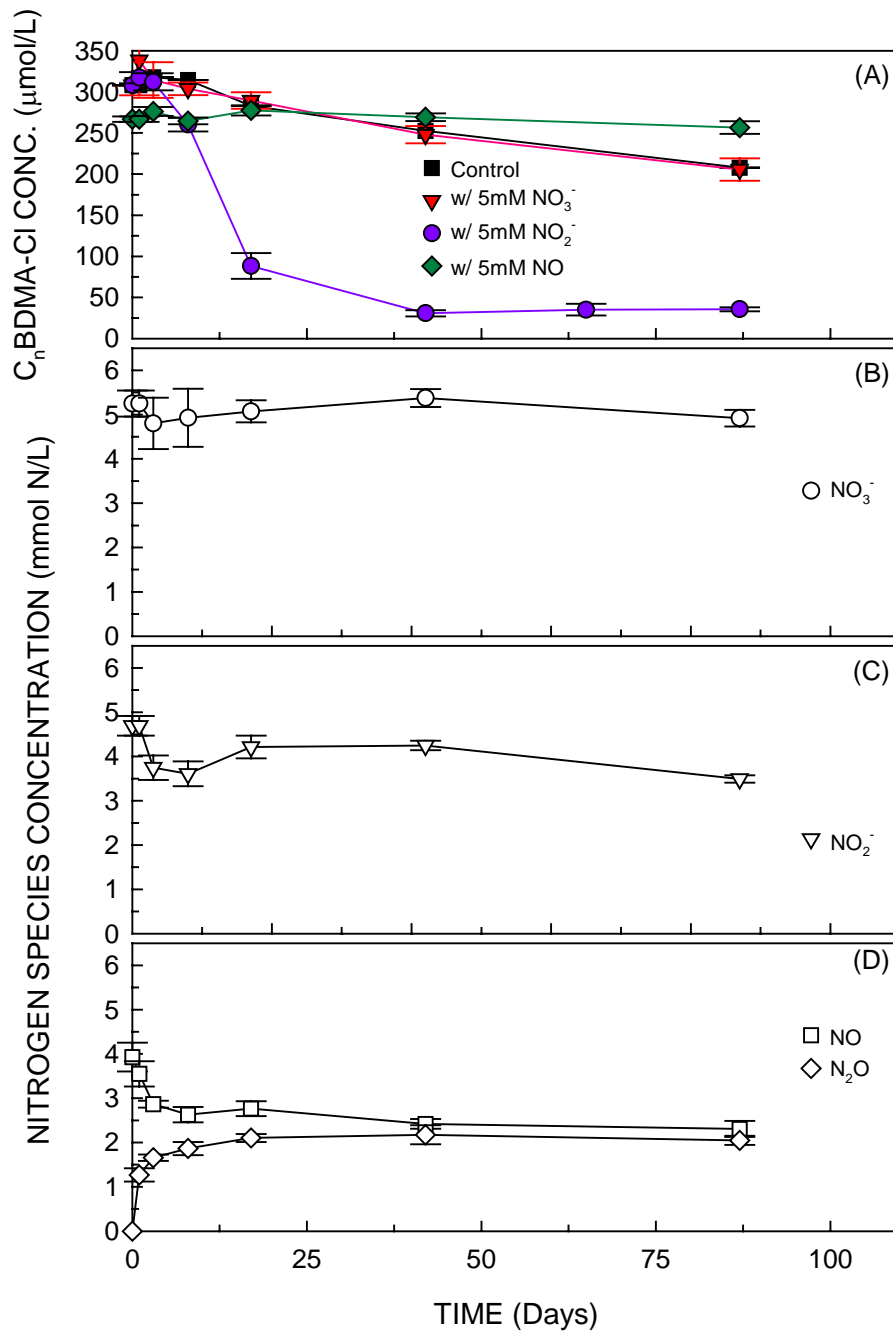


Figure 7.13. Profiles of (A) C_nBDMA-Cl in all abiotic controls and N oxides consumption and production in abiotic controls amended with 100 mg/L C_nBDMA-Cl and 5 mmol N/L of (B) NO₃⁻, (C) NO₂⁻ and (D) NO, respectively (Error bars represent one standard deviation of the means; *n* = 3)

statistically significant ($p = 0.023$) decrease in the NO_2^- concentration was observed, but NO_2^- reduction products were not detected (Figure 7.13C). $\text{C}_n\text{BDMA-Cl}$ removal in the rest of the N oxide amended reactors was comparable to that of the N oxide free reactor and not significant. $\text{C}_n\text{BDMA-Cl}$ transformation in the NO_2^- amended reactor followed the same pathway as in the cultures discussed above and yielded alkyl dimethyl amines (C_{12}DMA , C_{14}DMA and C_{16}DMA) (Figure 7.14). The sum of molar concentrations of $\text{C}_n\text{BDMA-Cl}$ homologues remaining and alkyl dimethyl amines produced was equal to the $\text{C}_n\text{BDMA-Cl}$ concentration added, which indicates that the alkyl dimethyl amines were stoichiometrically formed as a result of $\text{C}_n\text{BDMA-Cl}$ transformation under the conditions of the present study and that nitrite facilitates this transformation.

7.3.2.5. Mechanism of $\text{C}_n\text{BDMA-Cl}$ Transformation

Based on the above discussed results (Figure 7.14), the transformation of $\text{C}_n\text{BDMA-Cl}$ proceeded through the cleavage of the C-N bond between the benzyl and alkyl dimethyl amine groups of $\text{C}_n\text{BDMA-Cl}$, which is denoted as debenzylation hereafter. Three mechanisms that result in debenzylation of $\text{C}_n\text{BDMA-Cl}$ have been reported: pyrolysis (Criddle and Thomas, 1981; Ng et al., 1986; Haskins and Mitchell, 1991), Emde degradation (Brasen and Hauser, 1954; Smith and March, 2007), and modified Hofmann degradation (Suzuki et al., 1989; Ding and Liao, 2001). Debnylation of $\text{C}_n\text{BDMA-Cl}$ by pyrolysis takes place at temperatures above 200°C . A metallic catalyst, such as sodium amalgam (NaHg), is necessary for the debnylation of $\text{C}_n\text{BDMA-Cl}$ by Emde degradation. Conventional Hofmann degradation is a nucleophilic elimination reaction (E2 type) occurring at high temperatures ($> 80^\circ\text{C}$), resulting in dealkylation of QACs rather than debnylation, forming tertiary amines and alkenes.

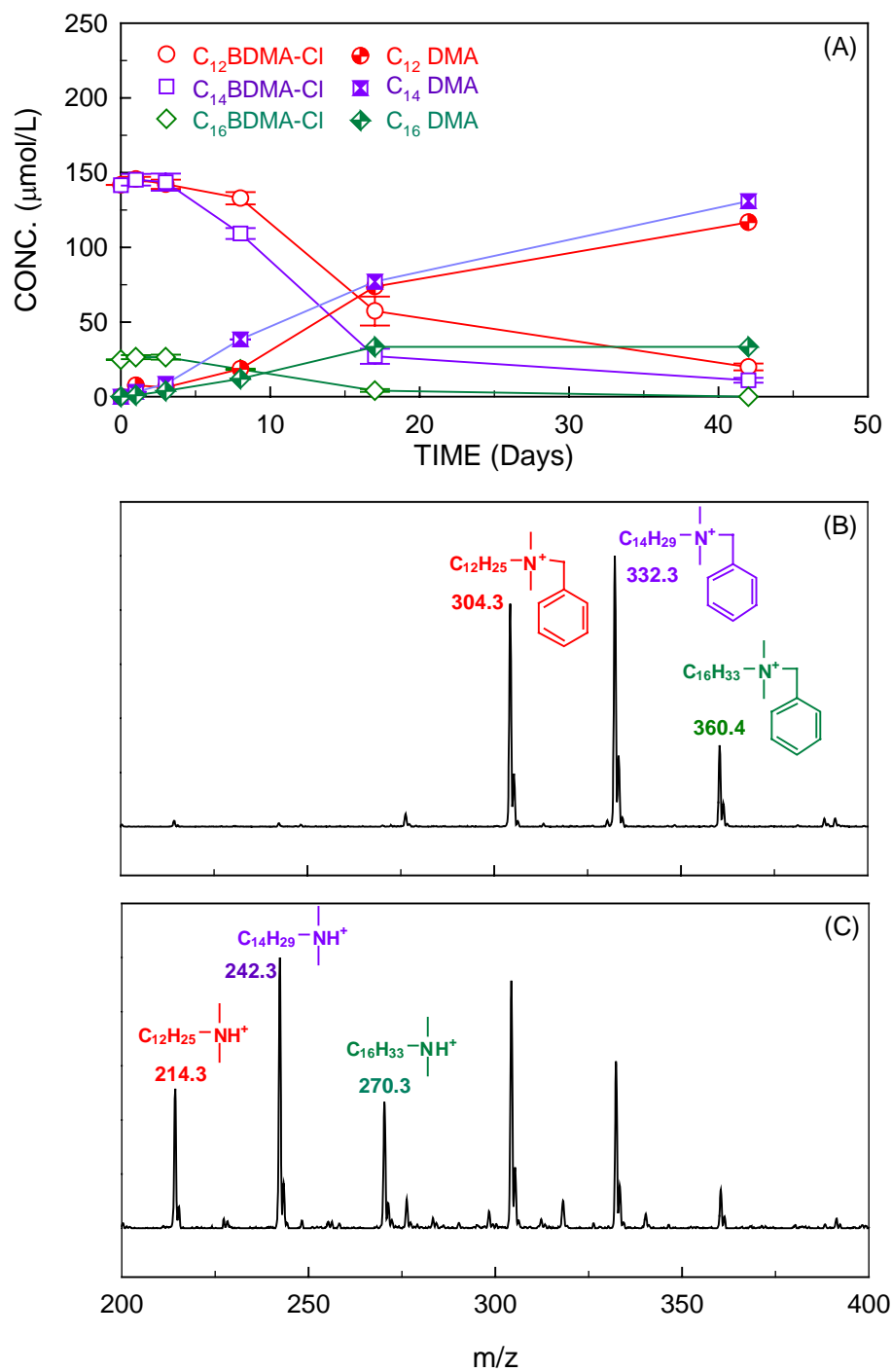


Figure 7.14. Profiles of (A) $\text{C}_n\text{BDMA-Cl}$ homologues and formation of alkyl dimethyl amines and mass spectra of total ion chromatograms of samples taken from the abiotic control amended with 5 mmol N/L of NO_2^- and 100 mg/L BAC after (B) 1 day and (C) 42 days of incubation

Debenzylation of C_nBDMA-Cl in the presence of a nucleophile, *tert*-butoxide, at low temperatures (between 0 and 40°C) was demonstrated. However, this reaction was more likely a nucleophilic substitution reaction rather than an elimination reaction, and was denoted as modified Hofmann degradation (Suzuki et al., 1989). It was also shown that predominance of elimination or substitution reactions over one another was temperature dependent as expected for nucleophilic reactions (Figure 7.15). C_nBDMA-Cl is transformed into alkyl dimethyl amines through a nucleophilic substitution at low temperatures ranging between 0 and 40°C and converted to alkenes and benzyl dimethyl amines through elimination at and above 80°C. Several studies have shown that a nucleophilic substitution reaction involving benzyl-containing QACs is a bimolecular substitution reaction (S_N2) and can occur in both protic and dipolar aprotic solvents with a broad range of nucleophiles such as *tert*-butoxide, thiophenoxide, thiophenol and thiocyanate (Ross et al., 1960; Ross et al., 1961; Kametani et al., 1969; Westaway and Poirier, 1975; Suzuki et al., 1989).

Nitrite is a *Lewis* base and an important environmental nucleophile. It can be classified as a strong nucleophile when the environmentally important nucleophiles are ranked according to their nucleophilicities, as follows (Schwarzenbach et al., 2003): ClO₄⁻ < H₂O < NO₃⁻ < F⁻ < SO₄²⁻, CH₃COO⁻ < Cl⁻ < HCO₃⁻, HPO₃²⁻ < NO₂⁻ < C₆H₅O⁻, Br⁻, OH⁻ < I⁻, CN⁻ < HS⁻, S₂O₃⁻, SO₃²⁻. The reaction of C_nBDMA-Cl and other QACs with nitrite, yielding tertiary amines such as alkyl dimethyl amines was demonstrated at acidic conditions and room temperature. These studies also demonstrated the nitrosation of the resulting tertiary amines to N-nitrosamines (Fiddler et al., 1972; Maduagwu, 1985).

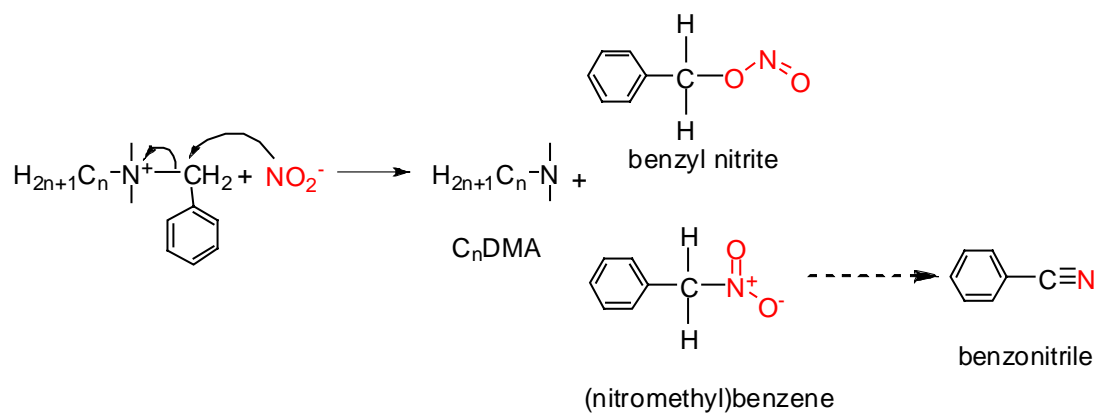


Figure 7.16. Proposed C_nBDMA-Cl transformation mechanism

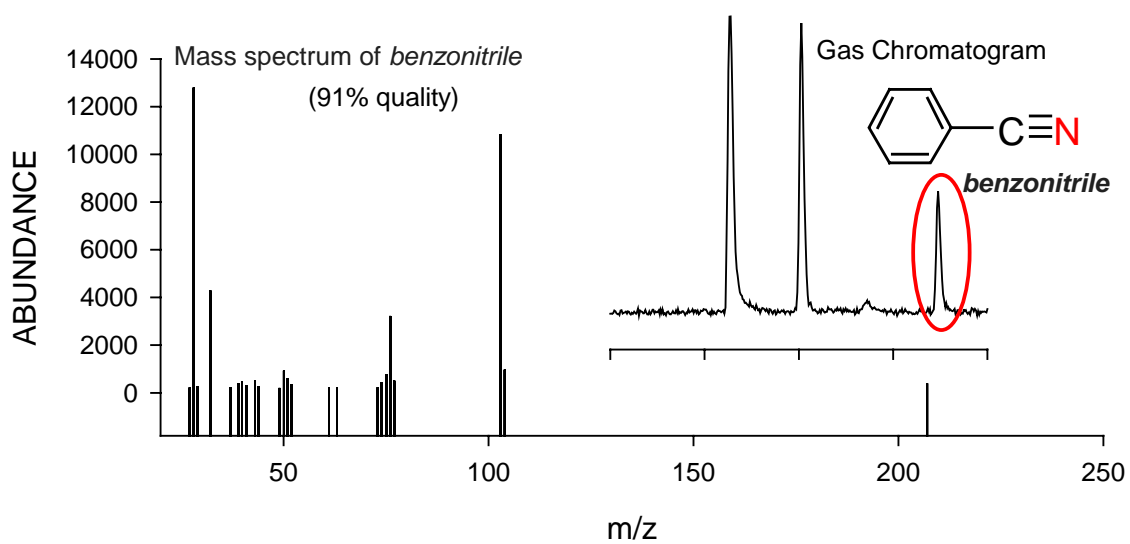


Figure 7.17. Gas chromatogram and total mass spectrum of the compound detected in the samples in which BAC was transformed, and identified as benzonitrile

In the present study, nitrite served as the nucleophile in both abiotic and biotic assays and facilitated the C_nBDMA-Cl transformation, which followed the same mechanism. Although nitrate is also a nucleophile, it did not result in the transformation of C_nBDMA-Cl in the abiotic assays. Nitrite is a stronger nucleophile than nitrate (Schwarzenbach et al., 2003). Therefore, the nucleophilicity of the nucleophile is an important factor in the transformation of C_nBDMA-Cl as expected for a bimolecular nucleophilic substitution reaction.

Nitrite was produced in all cultures amended with 5 mM NO₃⁻ and at different C_nBDMA-Cl concentrations (10-100 mg C_nBDMA-Cl/L). However, the C_nBDMA-Cl transformation was observed only at 100 mg C_nBDMA-Cl/L. C_nBDMA-Cl has a high adsorption affinity for biosolids, resulting in almost zero aqueous C_nBDMA-Cl concentration at very low total C_nBDMA-Cl concentrations (10 and 25 mg/L) and denitrification proceeded without a lag in all cultures except the one at 100 mg C_nBDMA-Cl/L. Consistent with S_N2 reactions, the rate and extent of C_nBDMA-Cl transformation were dependent on the concentration of both substrate and nucleophile (i.e., C_nBDMA-Cl and nitrite, respectively).

Nitrate and nitrite reduction was inhibited at 100 mg C_nBDMA-Cl/L for over 5 days (Figure 7.6F, 7.12B and 7.12C). After all N oxides were converted to N₂O and the aqueous C_nBDMA-Cl concentration dropped to 7.8 mg/L, its transformation stopped (Figure 7.11A and 7.12A). The aqueous C_nBDMA-Cl concentration was calculated using the equation: $[C_nBDMA-Cl_{Total}] = [C_nBDMA-Cl_{aq}] + 12.8 [C_nBDMA-Cl_{aq}]^{0.31} [VS]$ derived by using the Freundlich isotherm constants presented in Chapter 6 and using the VS concentration of 1.32 g/L measured in the 100 mg C_nBDMA-Cl/L amended cultures

at the end of the incubation period. The total amount of C_nBDMA-Cl transformed in the abiotic reactor was higher than the amount transformed in the culture amended with 5 mM NO₂⁻, since the aqueous C_nBDMA-Cl concentration was lower in the culture than in the abiotic reactor due to C_nBDMA-Cl adsorption on the biomass. In fact, the transformation of C_nBDMA-Cl ceased almost at the same aqueous C_nBDMA-Cl concentration, which was 7.8 and 10.8±1.4 mg/L in the biotic and abiotic reactors, respectively, demonstrating that the S_N2 reaction was rate limited at and below this C_nBDMA-Cl concentration range under the conditions of this study.

In spite of the fact that, both DC₁₀DMA-Cl and C_nBDMA-Cl have shown similar inhibitory effects on nitrate reduction and their phase distribution was almost identical in the mixed methanogenic culture, only C_nBDMA-Cl was transformed whereas DC₁₀DMA-Cl was recalcitrant. This phenomenon may be explained using the structural difference between these two molecules and the selectivity of nucleophilic reactions. Presence of the benzyl group in the C_nBDMA-Cl facilitates the nucleophilic substitution. The electron withdrawing property of the benzene ring coupled with the high electron affinity of the quaternary nitrogen makes the carbon, which connects benzene ring to the N, electron deficit. This electrophilic C, which has the lowest electrostatic potential charge among all the carbons in the C_nBDMA-Cl and DC₁₀DMA-Cl, has the highest affinity for a nucleophilic attack (Figure 7.18). On the other hand, transformation of DC₁₀DMA-Cl may be achieved at high temperatures by means of nucleophilic elimination of alkyl groups (Figure 7.15), in fact steric hindrance dictated by long-chain alkyl groups may affect the reaction.

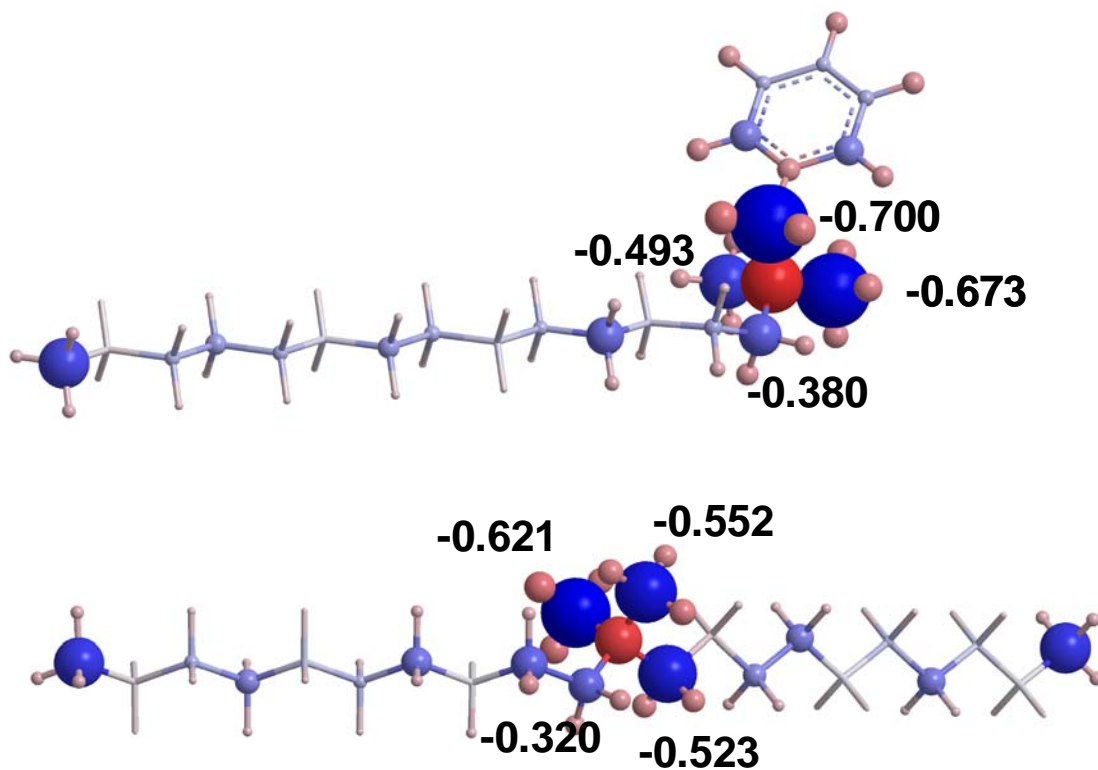


Figure 7.18. Electrostatic potential charges of the atoms of C₁₄BDMA-Cl and DC₁₀DMA-Cl calculated by using Austin Model 1 (AM1) method of MOPAC, a semi-empirical molecular orbital estimation program. Closed shell (restricted) was used as the wave function and water was selected as the solvent. The size of the atoms represent the magnitude, whereas color indicates the sign of the charges (red (+) and blue (-))

7.4. Summary

The effect of didecyl dimethyl ammonium chloride and benzalkonium chloride on nitrate reduction was investigated at concentrations up to 100 mg/L in a batch assay using a mixed, mesophilic (35°C) methanogenic culture. Glucose was used as the carbon and energy source and the initial nitrate concentration was 70 mg N/L. Dissimilatory nitrate reduction to ammonia (DNRA) and to dinitrogen (DNRN) were observed at QAC concentrations up to 25 mg/L. At and above 50 mg QAC/L, DNRA was inhibited and DNRN was incomplete resulting in accumulation of nitrous oxide. Long-term inhibition of methanogenesis and accumulation of volatile fatty acids were observed at and above 50 mg QAC/L. Over 96% of the added DC₁₀DMA-Cl was recovered from all cultures at the end of the 100-days incubation period, indicating that DC₁₀DMA-Cl did not degrade in the mixed methanogenic. On the other hand, over 99% of the added C_nBDMA-Cl was recovered from all cultures except the one amended with 100 mg C_nBDMA-Cl/L, in which 37% of the initially added C_nBDMA-Cl was transformed during the 100-days incubation period. Follow-up abiotic and biotic assays performed with 100 mg/L of C_nBDMA-Cl and 5 mM (in the liquid phase) of either nitrate, nitrite or nitric oxide, respectively, demonstrated that the C_nBDMA-Cl transformation was an abiotic reaction and followed the modified Hofmann degradation, i.e., a bimolecular nucleophilic substitution with nitrite, which was added directly or generated biologically from nitrate during denitrification. Alkyl dimethyl amines (tertiary amines) were produced at equimolar levels to the concentration of C_nBDMA-Cl transformed, but they were not further degraded.

This is the first report that demonstrates the effect of QACs on nitrate reduction and the transformation of a QAC, benzalkonium chloride, under nitrate reducing conditions.

CHAPTER 8

BIOTRANSFORMATION OF BENZALKONIUM CHLORIDE

UNDER FERMENTATIVE AND NITRATE REDUCING

CONDITIONS

8.1. Introduction

QACs contain saturated hydrocarbon moieties attached to a quaternary nitrogen. Under aerobic conditions, biotransformation of QACs is initiated by an attack of the alkyl moieties via *monooxygenase* enzymes (van Ginkel et al., 1992; van Ginkel, 1996). As a result of *monooxygenase* activity, QACs get activated and then used as energy and carbon source by the microorganisms. Bioactivation of highly saturated molecules under reduced conditions is difficult. Therefore, under anaerobic conditions, there is no evidence of mineralization of QACs that contain alkyl or benzyl groups (Battersby and Wilson, 1989; Federle and Schwab, 1992; Garcia et al., 1999, 2000). However, it was recently discovered that both aliphatic and aromatic hydrocarbons can be degraded under anoxic/anaerobic conditions by fumarate addition or oxygen-independent hydroxylation mechanisms (Heider et al., 1998; Spormann and Widdel, 2000; Van Hamme et al., 2003; Suflita et al., 2004; Davidova et al., 2005; Callaghan et al., 2006; Heider, 2007; Washer and Edwards, 2007; Winderl et al., 2007; Callaghan et al., 2008; Grundmann et al., 2008; Szaleniec et al., 2008). The activation of hydrocarbons via these mechanisms involves abstraction of a hydrogen atom from an electron deficit carbon of a hydrocarbon molecule followed by the integration of fumarate or hydroxyl anion to the molecule. These mechanisms are similar to the nucleophilic substitution mechanism discussed in

Chapter 7 in terms of the use of an electron deficit atom to initiate the reaction.

Therefore, biotransformation of QACs via the fumarate addition mechanism is promising under reduced conditions. Given the toxicity of QACs, the BAC enrichment culture, which is resistant to QACs and capable of QAC degradation under aerobic conditions, was used in this study to test the potential of QAC degradation under fermentative and nitrate reducing conditions.

The objective of the research reported here was to assess the biotransformation potential of C₁₄BDMA-Cl and, to the degree possible, elucidate the mechanism of BAC biotransformation in the BAC enrichment culture under fermentative and nitrate reducing conditions.

8.2. Materials and Methods

8.2.1. Batch C₁₄BDMA-Cl Biotransformation Assay

A batch biotransformation assay was performed to assess the biotransformation potential of C₁₄BDMA-Cl under fermentative and nitrate reducing conditions using the BAC enrichment culture described in Chapter 5. A sample of 1.5 L BAC enrichment culture collected at the end of the 7-day feeding cycle was centrifuged at 10,000 x g and the pellet was washed and resuspended in an equal volume (1.5 L) fresh autoclaved and deoxygenated culture media with a composition given in Chapter 3. The pH of the resuspended culture was adjusted to 7.0 with sodium bicarbonate.

The assay was conducted in 160-ml serum bottles (100 ml liquid volume) sealed with rubber stoppers and aluminum crimps and flushed with helium gas for 15 min before any liquid addition. A sample of 90 mL of the resuspended BAC enrichment culture was anaerobically transferred to each serum bottle. Fumarate, sodium nitrate and C₁₄BDMA-

Cl solutions were added and the total liquid volume was adjusted to 100 mL with deionized (DI) water. The initial biomass, fumarate, nitrate and C₁₄BDMA-Cl concentrations in the test culture were 80±3 mg VSS/L, 10 mM, 5 mM and 100 µM, respectively. The assay included four control culture series as follows: (1) fumarate-only culture, which contained seed and 10 mM fumarate; (2) C₁₄BDMA-Cl control culture, which contained seed and 100 µM C₁₄BDMA-Cl; (3) fumarate-control culture, which contained seed, 10 mM fumarate and 100 µM C₁₄BDMA-Cl; and (4) nitrate-control, which contained seed, 5 mM nitrate and 100 µM C₁₄BDMA-Cl. An autoclaved media control was also prepared using 90 mL autoclaved and deoxygenated culture media containing 10 mM fumarate, 5 mM nitrate and 100 µM C₁₄BDMA-Cl. The details of experimental matrix used in this assay are given in Table 8.1. All culture series and the media control were prepared in triplicate. The cultures were incubated in the dark at 22°C and agitated daily by hand. Throughout the incubation period, the total gas volume produced and its composition (i.e., carbon dioxide, nitric oxide, nitrous oxide and dinitrogen), as well as nitrate, nitrite, organic acids and C₁₄BDMA-Cl were measured as described in Chapter 3.

8.3. Results and Discussion

The biotransformation experiment performed to assess the biotransformation potential of C₁₄BDMA-Cl under fermentative and nitrate reducing conditions in the BAC enrichment culture lasted 85 days. C₁₄BDMA-Cl was not transformed in the media-control indicating that abiotic transformation of C₁₄BDMA-Cl by the chemicals present in the media is not possible (Figure 8.1). Therefore, transformation of C₁₄BDMA-Cl in the cultures, discussed below, was attributed to biological activity.

Table 8.1. Experimental matrix of culture series and controls used in the batch C_{14} BDMA-Cl biotransformation assay

Culture Series	C_{14} BDMA-Cl 100 μ M	NO_3^- 5 mM	Fumarate 10mM
Fumarate-only	-	-	+
C_{14} BDMA-control	+	-	-
Fumarate-control	+	-	+
Nitrate-control	+	+	-
Test	+	+	+
Media-control	+	+	+

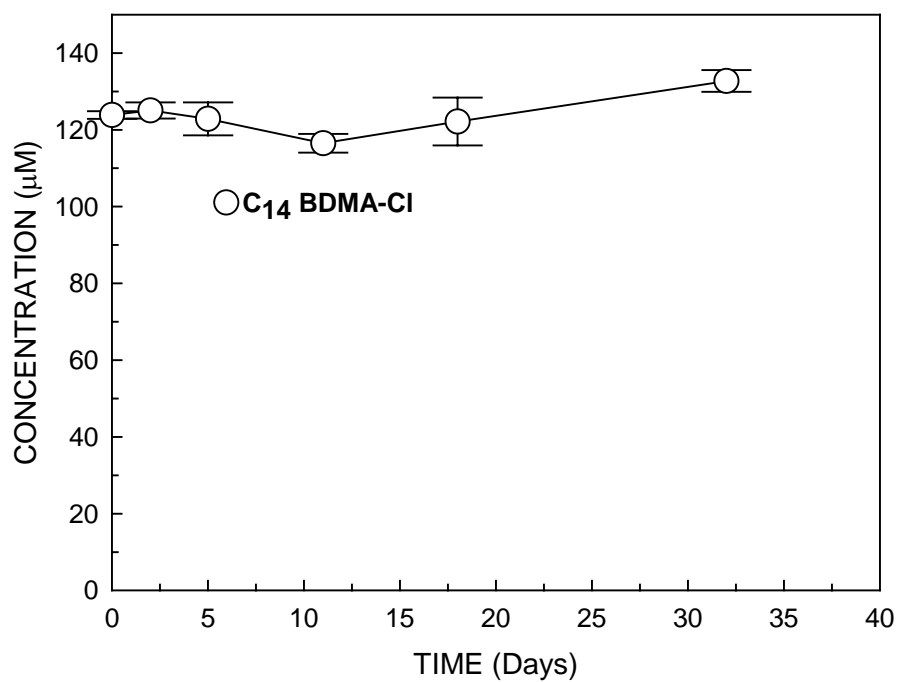


Figure 8.1. Profile of C_{14} BDMA-Cl in autoclaved culture media over the incubation period

Fumarate was disproportionated and utilized as both electron donor and acceptor in the fumarate-only culture. As an electron donor, fumarate was converted sequentially to malate, pyruvate, acetate and formate, whereas it was transformed to succinate as an electron acceptor (Figure 8.2A). At the end of 36 days, 10.5 mM fumarate (42 mM as carbon) amended to the fumarate-only culture was recovered as 0.1 mM malate (0.3 mM as carbon), 6.5 mM succinate (26.2 mM as carbon), 2.9 mM acetate (5.9 mM as carbon), 7.4 mM formate (7.4 mM as carbon) and 1.1 mM propionate (3.2 mM as carbon) (Figure 8.2B). The sequence of the metabolites in the BAC enrichment culture under fermentative conditions is consistent with the pathway (Figure 8.3) described previously by Zaunmuller et al. (2006).

On the other hand, fumarate was converted only to malate at equimolar levels in the fumarate-control culture in the presence of C₁₄BDMA-Cl (Figure 8.4 Cycle-1). While fumarate was being utilized, all C₁₄BDMA-Cl was converted to a hypothetical homologous compound identified during the HPLC analysis and defined as fumarate added C₁₄BDMA or (2R)-2-((dimethyl(tetradecyl)ammonio) (phenyl)methyl)succinate (abbreviated as C₁₄BDMA^{*}, hereafter). The proposed reaction resulting in the transformation of C₁₄BDMA to C₁₄BDMA^{*} is given in Figure 8.5. However, C₁₄BDMA^{*} was not utilized throughout the incubation period (Figure 8.4, Cycle-1, 50 days).

When 5 mM nitrate was added to the fumarate-control culture, about 40% of C₁₄BDMA^{*} was utilized as nitrate was converted to dinitrogen (Figure 8.4, Cycle-2). Trace amounts of succinate were observed only when C₁₄BDMA^{*} was degraded in the fumarate-control culture, indicating that succinate formed was the product of C₁₄BDMA^{*} transformation rather than the result of fumarate fermentation. On the contrary,

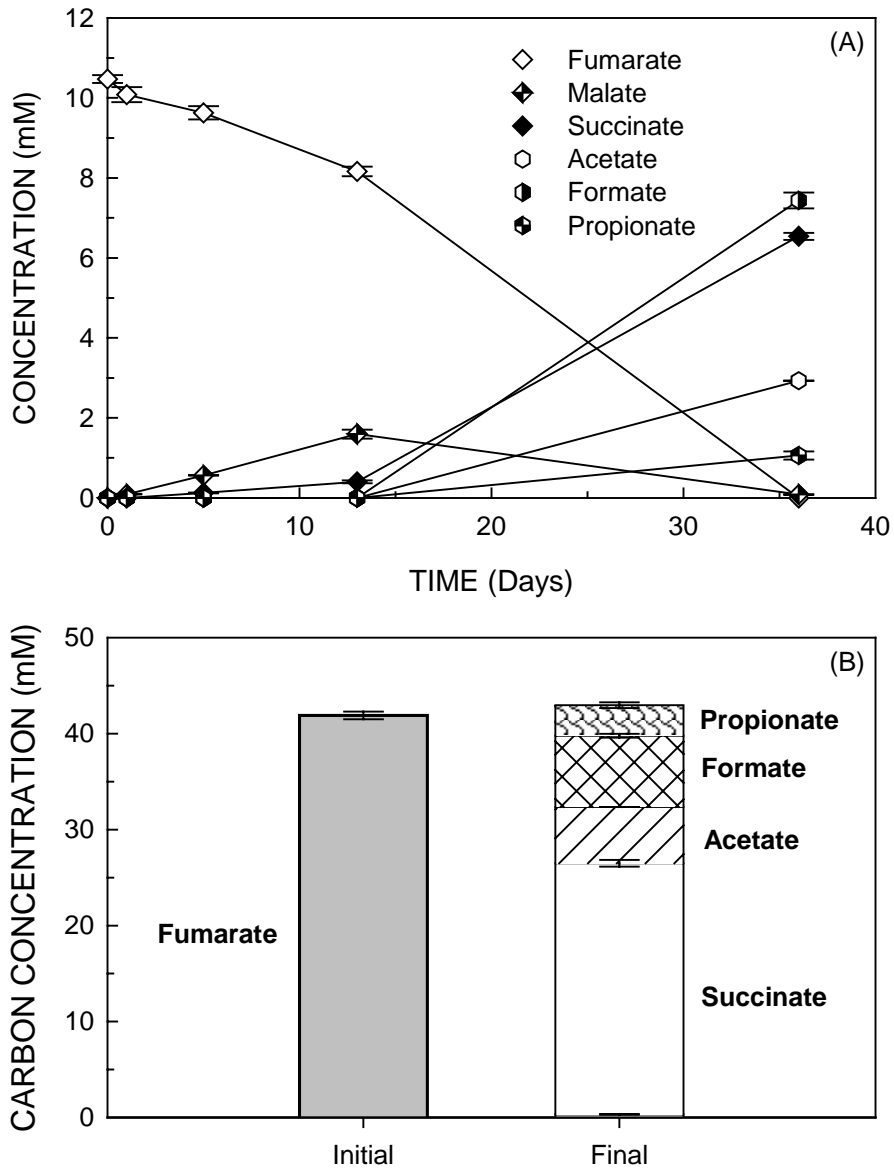


Figure 8.2. (A) Time course of fumarate metabolism and (B) distribution of organic acids in the fumarate-only culture at the beginning and the end of the incubation period

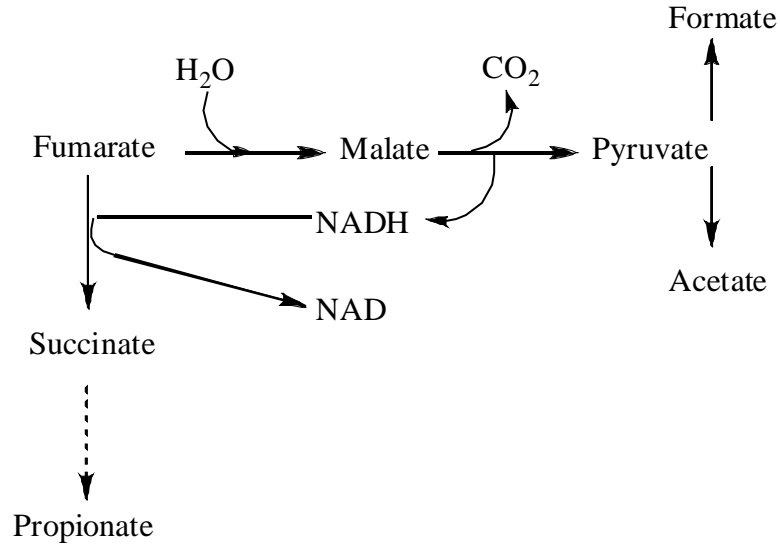


Figure 8.3. Fumarate disproportionation pathway described previously by Zaunmuller et al. (2006)

$C_{14}BDMA$ was not utilized in the $C_{14}BDMA$ -control and nitrate-control cultures suggesting that $C_{14}BDMA$ was neither fermented nor utilized as an electron donor (Figure 8.6 and Figure 8.7) in the absence of fumarate.

All $C_{14}BDMA$ was converted to $C_{14}BDMA^*$ within five days in the test culture containing fumarate, nitrate and $C_{14}BDMA$ (Figure 8.8C Cycle-1 and Figure 8.9). $C_{14}BDMA$ was converted to $C_{14}BDMA^*$ faster in the test culture than in the fumarate-control culture. Fumarate conversion was also faster in the test culture than in the fumarate-control (Figure 8.8B, Cycle-1). These results show that the $C_{14}BDMA$ transformation was coupled to fumarate metabolism. About 40% of the $C_{14}BDMA^*$ formed was utilized as nitrate was converted to dinitrogen (Figure 8.8A Cycle-1). Further $C_{14}BDMA^*$ transformation was achieved as the culture was amended with nitrate in two consecutive cycles (Figure 8.8 Cycle-2 and 3).

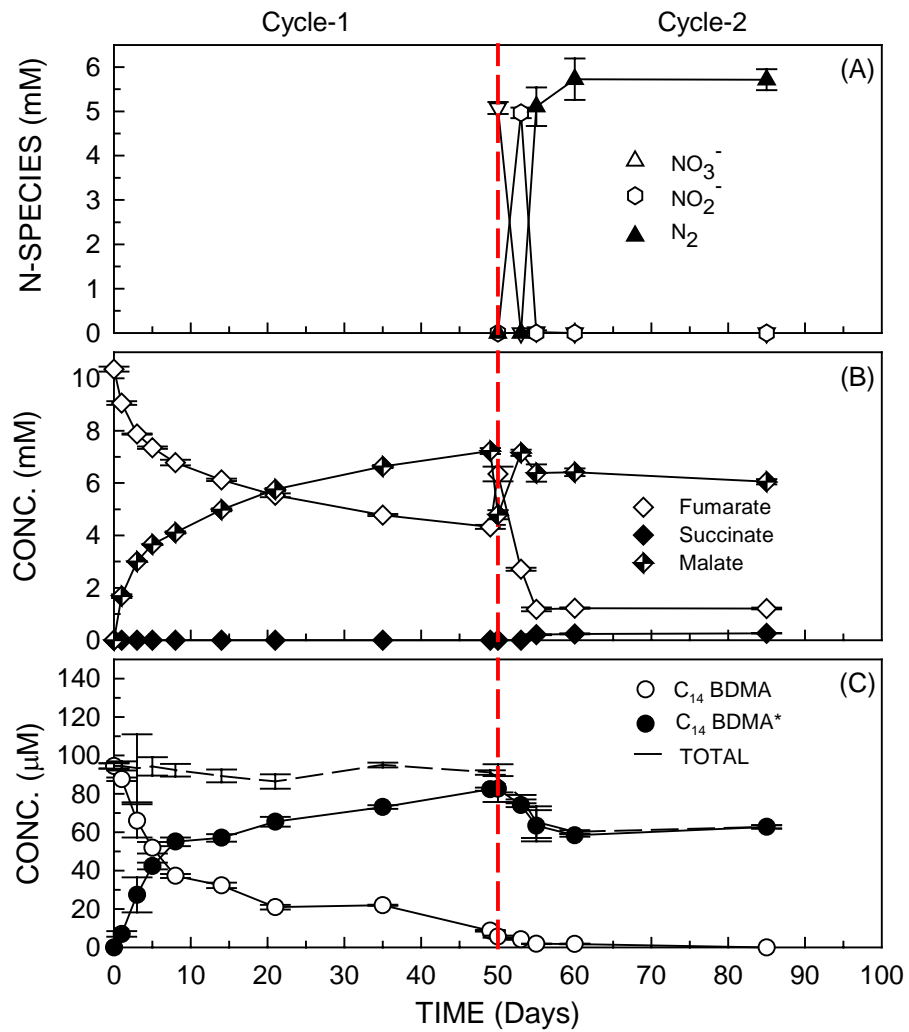


Figure 8.4. Time course of (A) nitrate reduction, (B) fumarate fermentation and (C) C_{14}BDMA transformation in the fumarate-control culture before (Cycle-1) and after (Cycle-2) nitrate (5 mM) addition

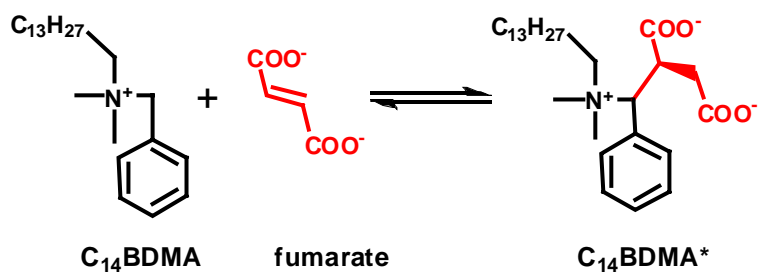


Figure 8.5. Proposed mechanism of fumarate addition to C₁₄BDMA

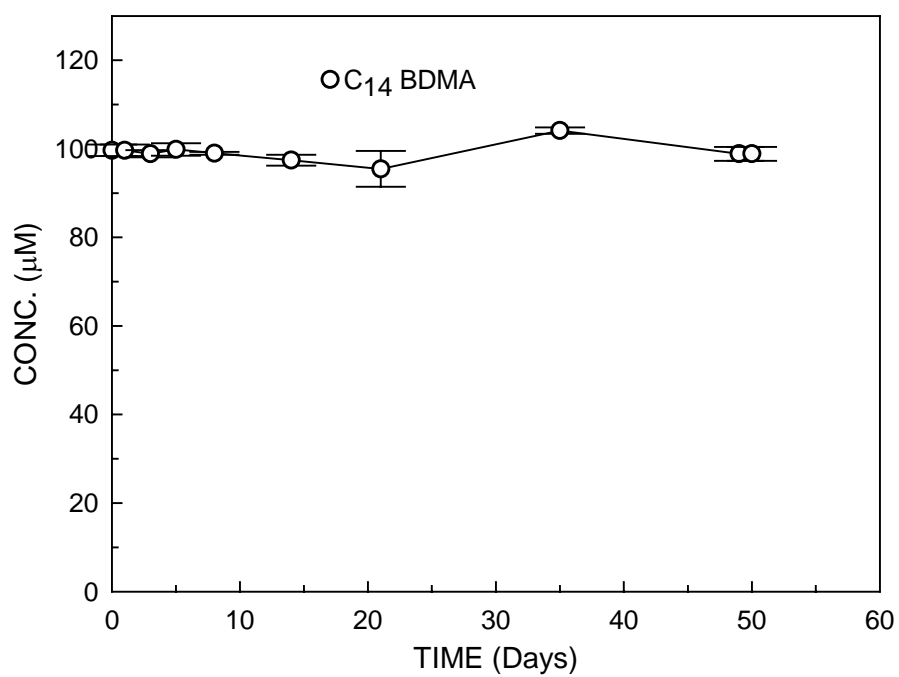


Figure 8.6. Profile of C₁₄BDMA in the C₁₄BDMA-control culture

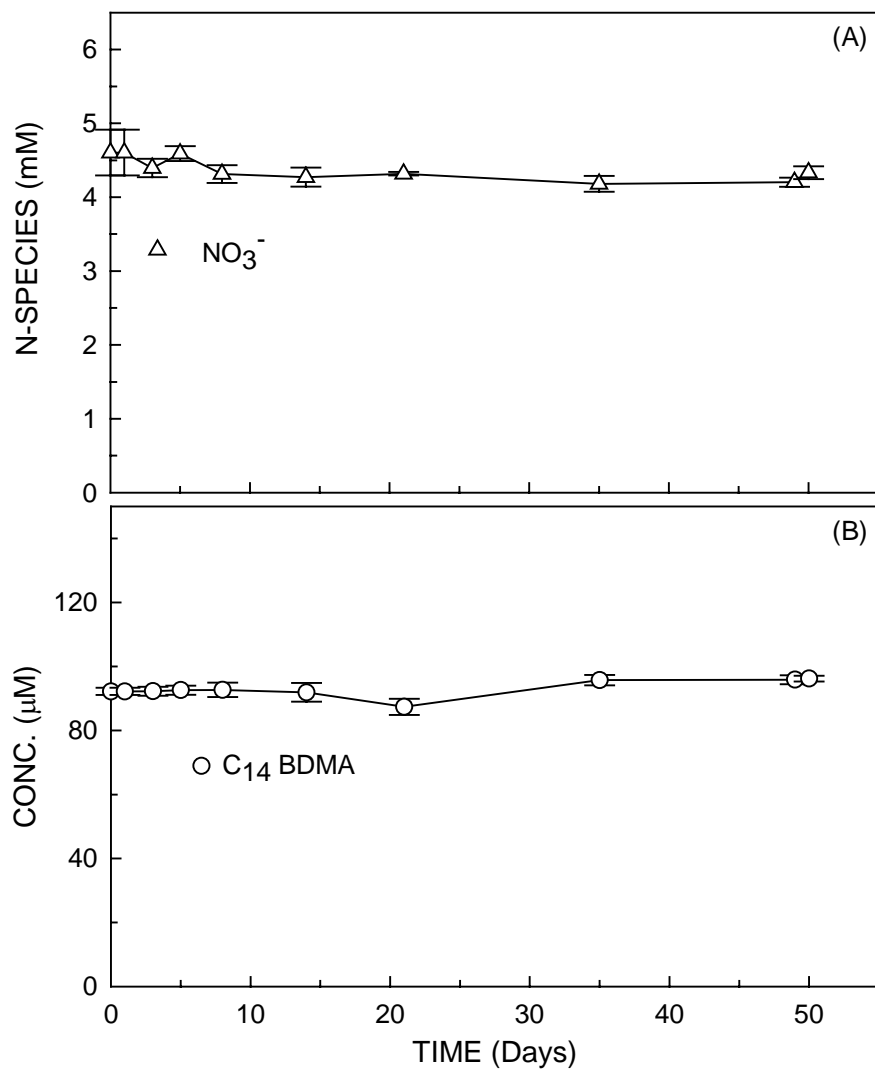


Figure 8.7. Profiles of (A) nitrate and (B) C₁₄BDMA in the nitrate-control culture

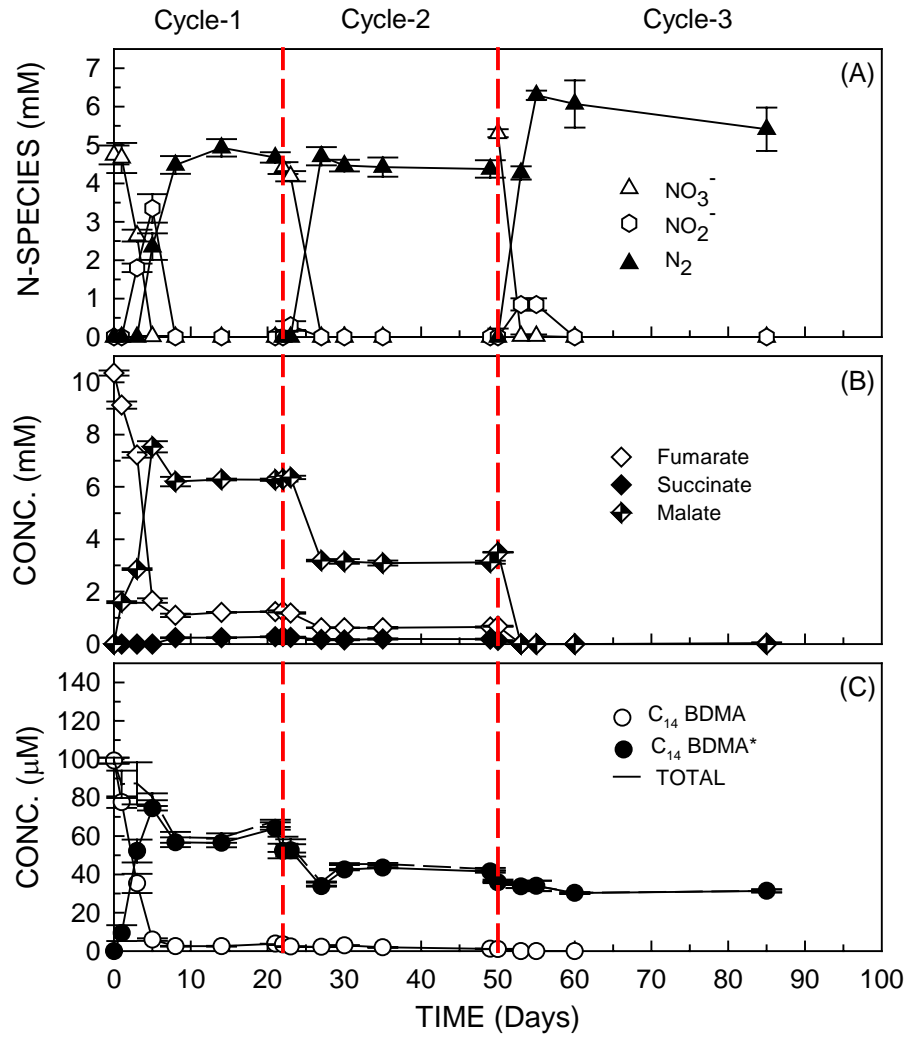


Figure 8.8. Time course of (A) nitrate reduction, (B) fumarate fermentation and (C) C_{14}BDMA transformation in the test culture at three nitrate amendment cycles

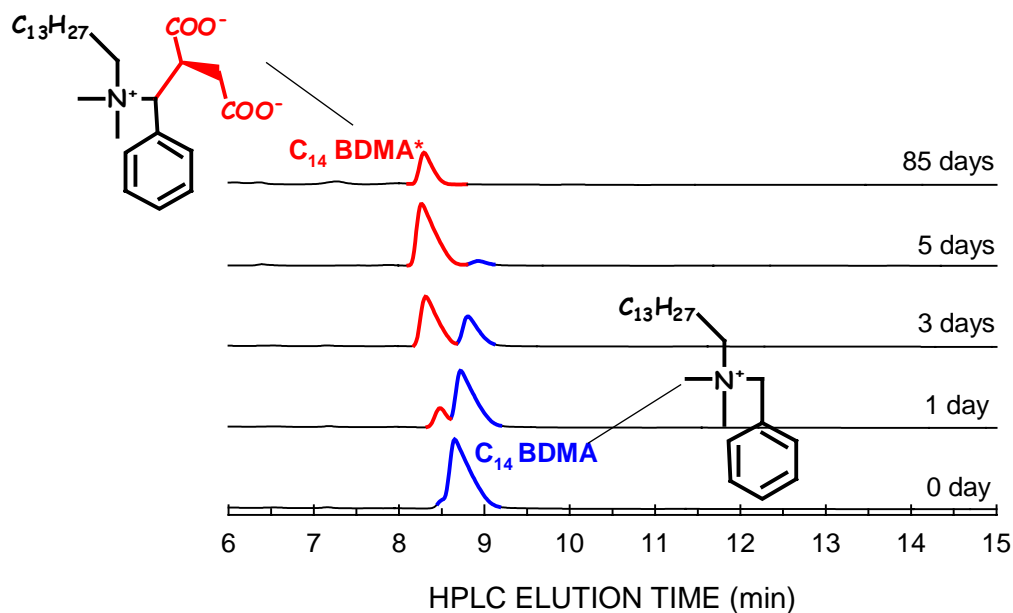


Figure 8.9. HPLC chromatograms showing the time course of C_{14} BDMA transformation in the BAC enrichment culture under nitrate reducing conditions

Given the inhibitory effect of benzalkonium chlorides on fermentation and nitrate reduction discussed in previous chapters at the concentrations similar to those used in the assays described here, the biotransformation mechanism presented above may be evolved to compensate for the inhibitory effect of C_{14} BDMA on the metabolic activity in the BAC enrichment culture under fermentative and nitrate reducing conditions.

The C_{14} BDMA biotransformation mechanism presented here is the first ever report to document QAC transformation under fermentative and nitrate reducing conditions. However, the pathway of complete mineralization of BAC, which is initiated by the fumarate addition and partially described here, under fermentative and anoxic conditions has to be elucidated further by using advanced instrumental analysis, enzymatic assays, and molecular biology tools.

8.4. Summary

The biotransformation of C₁₄BDMA-Cl under fermentative and nitrate reducing conditions was investigated in a batch assay using an enrichment culture developed from a hydrocarbon contaminated sediment and subsisting on benzalkonium chlorides. The transformation of C₁₄BDMA-Cl was achieved only during fumarate fermentation. In the presence of fumarate, C₁₄BDMA-Cl was transformed completely to a homologous structure which was defined as fumarate added C₁₄BDMA (C₁₄BDMA*) while the fumarate was converted to an equimolar concentration of malate. C₁₄BDMA* was not further degraded during the fumarate fermentation. The formation of C₁₄BDMA* was faster when fumarate was added along with nitrate. C₁₄BDMA* was also utilized while nitrate was being converted to dinitrogen. The C₁₄BDMA transformation under nitrate reducing conditions was therefore proposed to be initiated with the activation of C₁₄BDMA with fumarate addition resulting in the formation of C₁₄BDMA*. The resulting product was utilized and may be completely mineralized via a pathway which is under investigation.

CHAPTER 9

CONCLUSIONS AND RECOMMENDATIONS

9.1. Conclusions

The study presented here assessed the fate and toxicity of quaternary ammonium compounds as well as their inhibitory effects and biotransformation potential under aerobic, anoxic and anaerobic conditions in biological systems.

Nine QACs, belonging to three groups -- monoalkonium, dialkonium and benzalkonium chlorides -- were selected as the target QACs based on their consumption rate, frequency of occurrence in engineered and natural biological systems, and molecular structure. The critical micelle concentration, which reflects the ionic and hydrophobic properties of QACs, was determined for each QAC and used as a descriptor to develop quantitative structure-activity relationships to express their sorption affinity for biosolids and their Microtox® toxicity. All QACs tested had a high sorption affinity for biosolids. QACs with low CMCs had a higher adsorption affinity for biosolids than QACs with relatively high CMCs suggesting that QACs with high CMCs are more mobile than the ones with low CMCs. On the contrary, QACs with high CMCs were more toxic than the ones with lower CMCs. The acute Microtox® toxicity was as follows in descending order: C₁₂TMA-Cl > DC₈DMA-Cl > C₁₄TMA-Cl > DC₈₋₁₀DMA-Cl > C₁₆TMA-Cl > DC₁₀DMA-Cl > C₁₂BDMA-Cl > C₁₄BDMA-Cl > C₁₆BDMA-Cl. The combination of these two factors, i.e., sorption and toxicity, results in a serious environmental impact problem, that is, QACs which are more mobile and more (bio)available are more toxic.

The presence of counter-ions (anions) had no significant effect on the QAC toxicity, but NOM decreased the QAC toxicity.

Biotransformation of QACs is energetically feasible under aerobic conditions. Bioassays performed to investigate the biotransformation potential of benzalkonium chloride under aerobic conditions by an enrichment culture revealed that BAC biotransformation proceeds with sequential dealkylation and debenzoylation steps resulting in the separation of the alkyl and benzyl groups and the formation of benzyl dimethyl amine, and dimethyl amine, respectively. The resulting biotransformation products were at least 250-fold less toxic than the BAC. Microbial community analysis of the mixed culture that carried out BAC degradation suggested that the main species were members of the genus *Pseudomonas*.

Although QACs biodegradation is energetically feasible under methanogenic conditions, none of the QACs tested in this study was degraded under methanogenic conditions in long-term batch assays. QACs had short- or long-term inhibitory effects on a mixed methanogenic culture at 25 mg/L and above. Methanogenesis was more sensitive to QAC inhibition than acidogenesis. The inhibitory impact of the individual QACs on the methanogenic activity decreased according to the following series: DC₈DMA-Cl > DC₈₋₁₀DMA-Cl > C_nBDMA-Cl > DC₁₀DMA-Cl. Thus, QACs with the shorter alkyl chain length are the most inhibitory. Phase distribution analysis of QACs between the liquid phase and the solid (biomass) phase resulted in the following series of decreased affinity for the biosolids: DC₁₀DMA-Cl > C_nBDMA-Cl > DC₈₋₁₀DMA-Cl > DC₈DMA-Cl. Thus, the inhibitory effect of QACs is inversely proportional to their adsorption affinity on the biomass or their hydrophobicity. The highly reduced structure of QACs, combined with

their low bioavailability and inhibitory effects, play an important role in their recalcitrance in biological systems under methanogenic conditions.

Assays performed using the same mixed methanogenic culture mentioned above under nitrate reducing conditions showed that QACs were inhibitory to the nitrate reduction processes. DNRA was inhibited and DNRN was incomplete resulting in the accumulation of nitrous oxide at and above 50 mg QAC/L. BAC was transformed abiotically to alkyl dimethyl amines via the modified Hofmann degradation, a bimolecular nucleophilic substitution with nitrite.

BAC degradation was also demonstrated in bioassays performed using the mixed, BAC enrichment culture mentioned above under fermentative and nitrate reducing conditions. In the presence of fumarate, BAC was transformed completely to a homologue structure which, based on LC/MS analysis was presumed to be succinyl-benzalkonium (SBA), while fumarate was converted to an equimolar malate concentration. SBA was not further degraded during the fumarate fermentation and in the absence of nitrate reduction. In contrast, SBA formation was faster when fumarate was supplemented along with nitrate and SBA was utilized while nitrate was converted to dinitrogen. The BAC transformation pathway under nitrate reducing conditions was therefore proposed to be initiated with the activation of BAC with fumarate addition, and proportionation of SBA to benzylsuccinyl-CoA which was utilized via the benzoyl-CoA pathway and alkyl dimethyl amine which was subjected to sequential fumarate additions and transformation via β -oxidation. Note that the discovery of BAC transformation by the above mentioned two reactions, i.e., modified Hofmann degradation and fumarate

addition, is the first ever report to document QAC transformation under anoxic/anaerobic conditions and delineate the transformation pathways, at least the initial, activation steps.

9.2. Potential Applications of the Study Outcomes

This research showed the potential impacts of QACs along with the physical, chemical and biological processes that determine the fate of QACs in engineered and natural biological systems. Such information may facilitate the development of strategies to mitigate adverse effects of QACs and to aid industry, as well as state and federal regulatory agencies in the development of sound policies and risk assessment strategies.

The outcomes of this research may be used for the specific applications listed below:

- (1) The physical/chemical properties, such as CMC and especially K_{ow} , of nine QACs representing three QAC groups determined in this study may be used in developing read-across database for the prediction of physical/chemical properties of other QACs in the cationic surfactant category. The log K_{ow} estimation method that was described in this study can be integrated to EPISuite or other property estimation/QSAR modeling tools as an alternative method to accurately estimate the partitioning coefficients.
- (2) The QSARs developed for nine QACs may be used to evaluate the fate and toxicity of these compounds more precisely, which then can be utilized in decision making on (re)registration, evaluation, authorization or restriction of QACs through REACH, U.S. EPA, and OECD HPV challenge programs.
- (3) Individual QACs were found to behave differently both in terms of the degree of partitioning on solids as well as in terms of their inhibitory effect on biological treatment systems. This information may be used in the selection of mixtures of individual QACs in

industrial applications by assessing the tradeoff between sanitation efficiency and their impact on the treatment of QAC-bearing wastewaters.

(4) Bioremediation of hydrocarbon contaminated soils and sediments is problematic due to the low solubility and bioavailability of these contaminants. Surfactant enhanced remediation strategies have been developed to mitigate this problem. However, the toxicity of the surfactants used and their recalcitrance are major factors which restrict their application of such strategies. Here, we described the biodegradation of QACs, which are cationic surfactants, under both aerobic and anoxic/anaerobic conditions by a microbial population including species which are closely related to the most common hydrocarbon degrading species and developed from a hydrocarbon contaminated sediment. The biodegradability of QACs demonstrated in this study may be used as the acceptance criteria to verify their potential use as the surfactants of choice in the surfactant-enhanced remediation of hydrocarbon contaminated sites.

(5) This research showed a strong evidence of biodegradation potential of QACs in biological systems under aerobic, anoxic and anaerobic conditions. It is known that biological treatment of QAC-bearing wastewaters is problematic. However, the information presented here can be used to develop alternative treatment strategies for QAC-bearing wastewaters. For instance, selectors which receive high concentrations of QACs and therefore enrich for QAC-tolerant and degrading microorganisms may be employed before the waste stream is introduced to sensitive biological treatment units (e.g., nitrification/denitrification). Attached growth (i.e., biofilm) biological treatment systems can also be employed in the treatment of QAC-bearing wastewaters. These systems contain high biomass concentrations which may reduce the inhibitory effects of

QACs due to their high adsorption affinity. The biofilm formation results in a layered microbial community development, which may protect the sensitive but metabolically important microorganisms from QAC inhibition, and a redox gradient (aerobic to anaerobic), which may facilitate the complete degradation of QACs via multiple transformation mechanisms described in this study under aerobic, anoxic and anaerobic conditions.

9.3. Recommendations

The QSAR approach presented in this study may be deployed to investigate the fate and toxicity of other QACs such as pyridinium chlorides which have promising new applications (e.g., ionic liquid as organic solvent replacement or phase transfer catalyst), which will dominate the market in the future.

Given the antimicrobial properties of QACs, microbes that subsist on QACs have to also have developed resistance mechanisms. Such antimicrobial resistance mechanisms and their mobility need to be further investigated in the mixed, BAC enrichment culture using modern molecular biology/proteomics tools in order to fully understand the actual or potential human health risks resulting from chronic QAC pollution.

The abiotic QAC transformation mechanism via the nucleophilic substitution reaction may further be investigated to identify other environmentally relevant nucleophiles that may play a role in QAC transformation. Moreover, the effect of physical and chemical factors such as pH, temperature and reduction potential on the abiotic QAC transformation mechanism may be explored. The anaerobic ammonium oxidation (ANAMMOX) process, which converts ammonium to dinitrogen utilizing nitrite as an electron acceptor, may be investigated as an alternative pathway of QAC

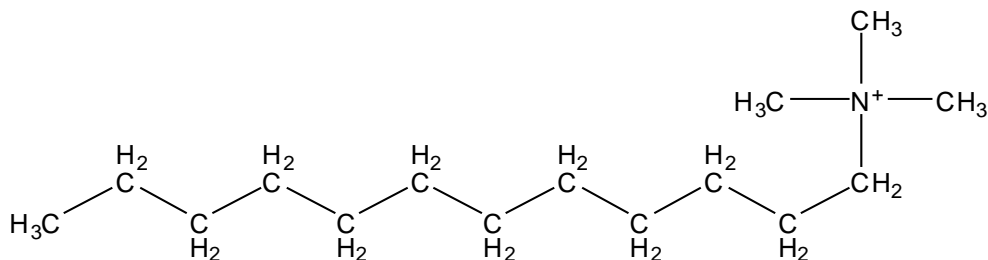
transformation via nucleophilic substitution. In case QAC transformation via ANAMMOX is achieved, the interaction and competition between the nitrite involving abiotic and biotic mechanisms should be investigated using stable isotope probes.

BAC transformation via the fumarate addition mechanism was proposed in this study, but further, more conclusive evidence is necessary. The positive identification of important metabolites, such as SBA, needs to be made using advanced instrumental analysis. Isolation of microorganisms capable of anaerobic BAC degradation and performing enzymatic assays may assist in the elucidation of the pathway proposed in this study. Moreover, similar bioassays described in this study may be performed using pure cultures of known anaerobic hydrocarbon degrading microorganisms such as *Azoarcus* EbN1 and *Thauera aromatica*.

Complete mineralization of QACs under aerobic conditions described in this study was not achieved under anoxic and anaerobic conditions. Therefore, biotransformation of QACs and their anoxic and anaerobic transformation products leading the complete mineralization of QACs should be investigated under alternating anoxic and aerobic conditions.

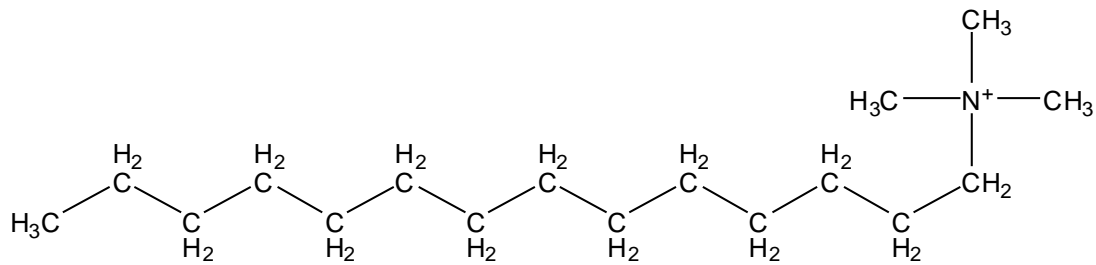
APPENDIX A

CALCULATION OF LOG K_{ow} VALUES OF QACS USING THE HANSCH AND LEO METHOD



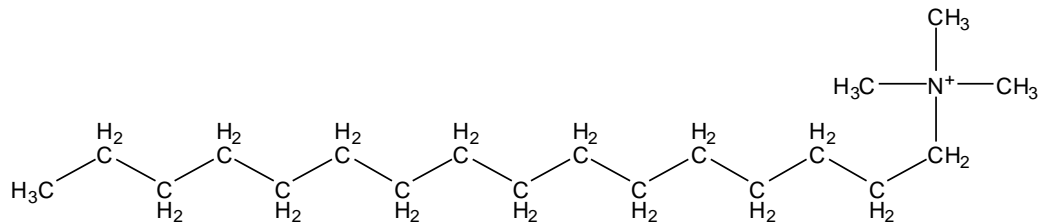
Dodecyltrimethyl ammonium chloride (C₁₂TMA-Cl)

Fragment/Bond Factor	Contribution	# of Fragments	Total Contribution
f N ⁺	-3.40	1	-3.40
f Cl ⁻	0.06	1	0.06
f CH ₃	0.89	4	3.56
f CH ₂	0.66	11	7.26
f C ₇ H ₇	2.51	0	0.00
F _{bx+1}	-0.90	4	-3.60
F _{bx+2}	-0.60	1	-0.60
F _{bx+3}	-0.45	1	-0.45
F _{bx+4}	-0.35	1	-0.35
F _{bx+5}	-0.30	1	-0.30
F _{bx+6≤}	-0.27	7	-1.89
logK _{ow}			0.24
Exp. logK _{ow}			0.36±0.07



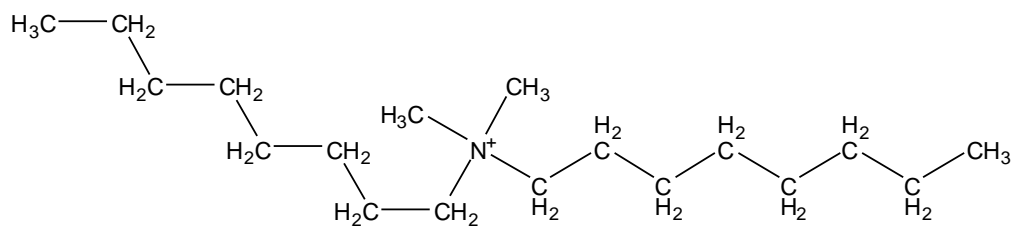
Tetradecyltrimethyl ammonium chloride (C₁₄TMA-Cl)

Fragment/Bond Factor	Contribution	# of Fragments	Total Contribution
f N ⁺	-3.40	1	-3.40
f Cl ⁻	0.06	1	0.06
f CH ₃	0.89	4	3.56
f CH ₂	0.66	13	8.58
f C ₇ H ₇	2.51	0	0.00
F _{bx+1}	-0.90	4	-3.60
F _{bx+2}	-0.60	1	-0.60
F _{bx+3}	-0.45	1	-0.45
F _{bx+4}	-0.35	1	-0.35
F _{bx+5}	-0.30	1	-0.30
F _{bx+6≤}	-0.27	9	-2.43
logK _{ow}			1.07
Exp. logK _{ow}			0.70±0.05



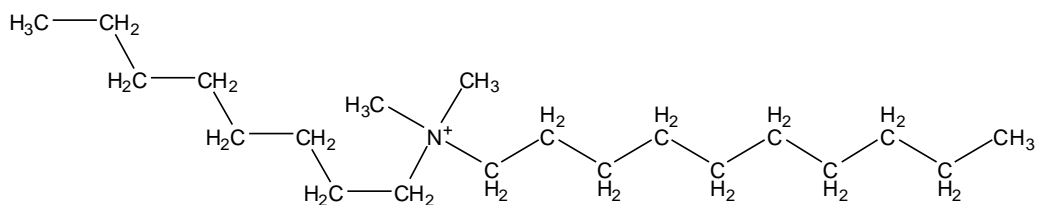
Hexadecyltrimethyl ammonium chloride (C₁₆TMA-Cl)

Fragment/Bond Factor	Contribution	# of Fragments	Total Contribution
f N ⁺	-3.40	1	-3.40
f Cl ⁻	0.06	1	0.06
f CH ₃	0.89	4	3.56
f CH ₂	0.66	15	9.90
f C ₇ H ₇	2.51	0	0.00
F _{bx+1}	-0.90	4	-3.60
F _{bx+2}	-0.60	1	-0.60
F _{bx+3}	-0.45	1	-0.45
F _{bx+4}	-0.35	1	-0.35
F _{bx+5}	-0.30	1	-0.30
F _{bx+6≤}	-0.27	11	-2.97
logK _{ow}			1.85
Exp. logK _{ow}			1.50±0.06



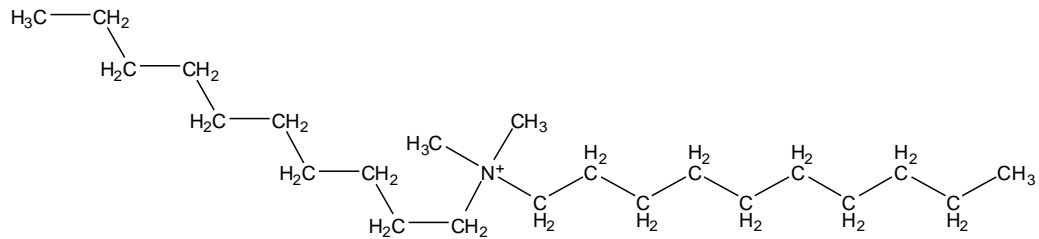
Diocetyltrimethyl ammonium chloride (DC₈DMA-Cl)

Fragment/Bond Factor	Contribution	# of Fragments	Total Contribution
$f \text{ N}^+$	-3.40	1	-3.40
$f \text{ Cl}^-$	0.06	1	0.06
$f \text{ CH}_3$	0.89	4	3.56
$f \text{ CH}_2$	0.66	14	9.24
$f \text{ C}_7\text{H}_7$	2.51	0	0.00
$F_{\text{bx}+1}$	-0.90	4	-3.60
$F_{\text{bx}+2}$	-0.60	2	-1.20
$F_{\text{bx}+3}$	-0.45	2	-0.90
$F_{\text{bx}+4}$	-0.35	2	-0.70
$F_{\text{bx}+5}$	-0.30	2	-0.60
$F_{\text{bx}+6 \leq}$	-0.27	6	-1.62
$\log K_{\text{ow}}$			0.84
Exp. $\log K_{\text{ow}}$			0.28±0.22



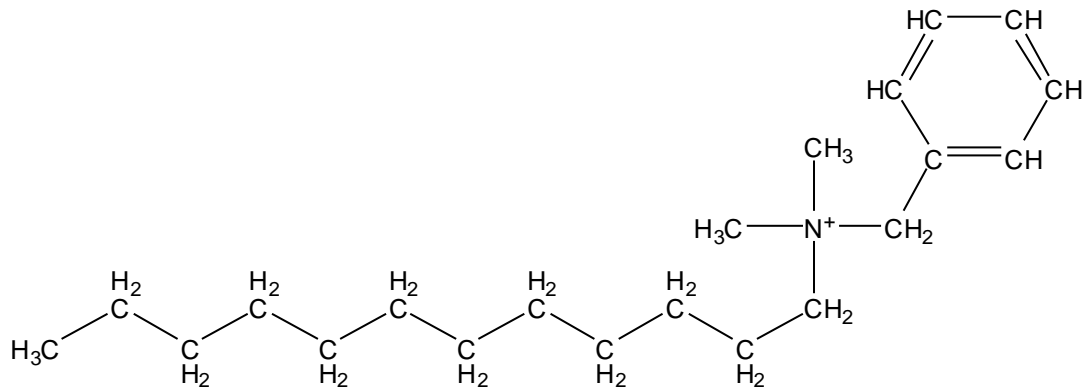
Octyldecyldimethyl ammonium chloride (DC₈₋₁₀DMA-Cl)

Fragment/Bond Factor	Contribution	# of Fragments	Total Contribution
f N ⁺	-3.40	1	-3.40
f Cl ⁻	0.06	1	0.06
f CH ₃	0.89	4	3.56
f CH ₂	0.66	16	10.56
f C ₇ H ₇	2.51	0	0.00
F _{bx+1}	-0.90	4	-3.60
F _{bx+2}	-0.60	2	-1.20
F _{bx+3}	-0.45	2	-0.90
F _{bx+4}	-0.35	2	-0.70
F _{bx+5}	-0.30	2	-0.60
F _{bx+6≤}	-0.27	8	-2.16
logK _{ow}			1.62
Exp. logK _{ow}			1.54±0.06



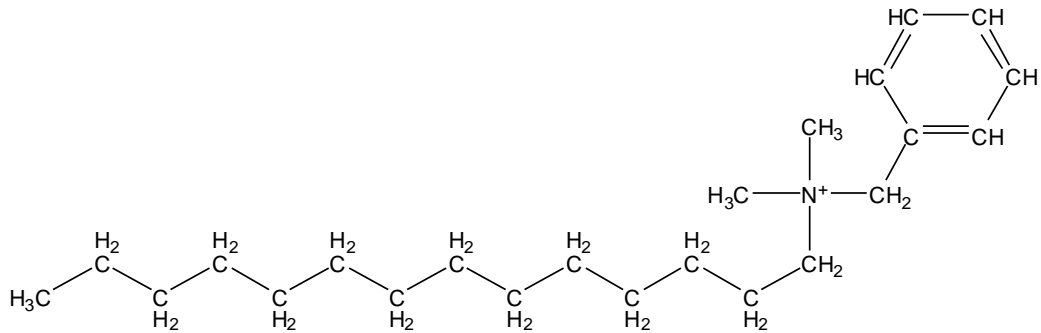
Didecyltrimethyl ammonium chloride (DC₁₀DMA-Cl)

Fragment/Bond Factor	Contribution	# of Fragments	Total Contribution
f N ⁺	-3.40	1	-3.40
f Cl ⁻	0.06	1	0.06
f CH ₃	0.89	4	3.56
f CH ₂	0.66	18	11.88
f C ₇ H ₇	2.51	0	0.00
F _{bx+1}	-0.90	4	-3.60
F _{bx+2}	-0.60	2	-1.20
F _{bx+3}	-0.45	2	-0.90
F _{bx+4}	-0.35	2	-0.70
F _{bx+5}	-0.30	2	-0.60
F _{bx+6≤}	-0.27	10	-2.70
logK _{ow}			2.40
Exp. logK _{ow}			2.56±0.01



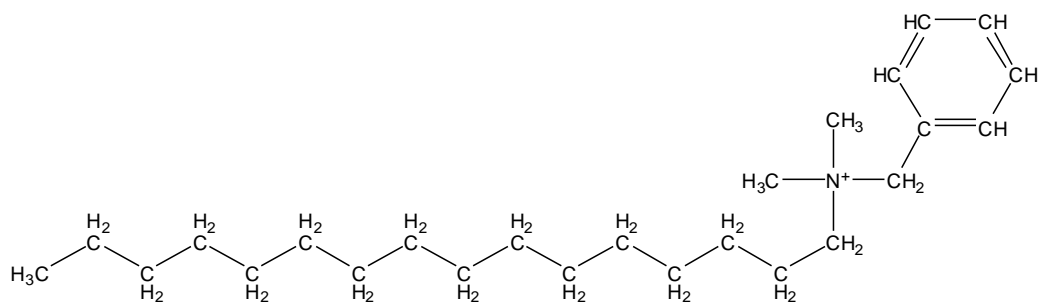
Dodecylbenzyltrimethyl ammonium chloride (C₁₂BDMA-Cl)

Fragment/Bond Factor	Contribution	# of Fragments	Total Contribution
f N ⁺	-3.40	1	-3.40
f Cl ⁻	0.06	1	0.06
f CH ₃	0.89	3	2.67
f CH ₂	0.66	11	7.26
f C ₇ H ₇	2.51	1	2.51
F _{bx+1}	-0.90	3	-2.70
F _{bx+2}	-0.60	1	-0.60
F _{bx+3}	-0.45	1	-0.45
F _{bx+4}	-0.35	1	-0.35
F _{bx+5}	-0.30	1	-0.30
F _{bx+6≤}	-0.27	14	-3.78
logK _{ow}			0.92
Exp. logK _{ow}			0.59±0.04



Tetradecylbenzyltrimethyl ammonium chloride (C₁₄BDMA-Cl)

Fragment/Bond	Contribution	# of Fragments	Total Contribution
f N ⁺	-3.40	1	-3.40
f Cl ⁻	0.06	1	0.06
f CH ₃	0.89	3	2.67
f CH ₂	0.66	13	8.58
f C ₇ H ₇	2.51	1	2.51
F _{bx+1}	-0.90	3	-2.70
F _{bx+2}	-0.60	1	-0.60
F _{bx+3}	-0.45	1	-0.45
F _{bx+4}	-0.35	1	-0.35
F _{bx+5}	-0.30	1	-0.30
F _{bx+6≤}	-0.27	16	-4.32
logK _{ow}			1.70
Exp. logK _{ow}			1.67±0.02

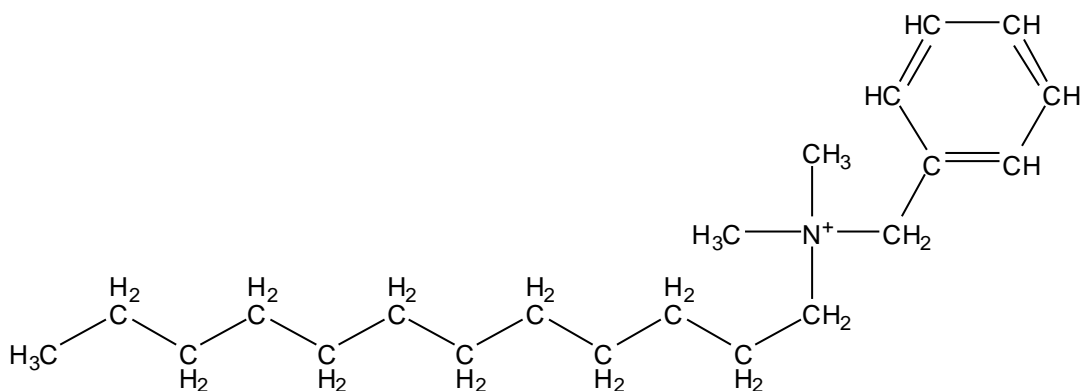


Hexadecylbenzyltrimethyl ammonium chloride (C₁₆BDMA-Cl)

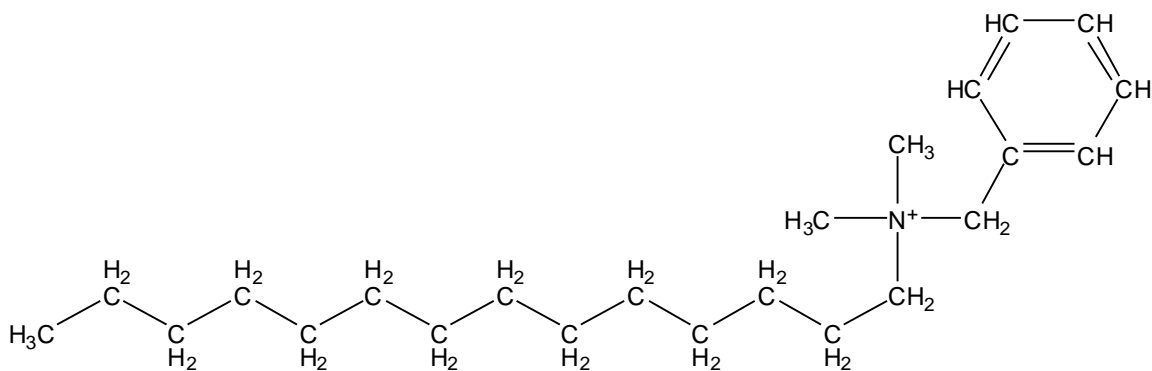
Fragment/Bond Factor	Contribution	# of Fragments	Total Contribution
f N ⁺	-3.40	1	-3.40
f Cl ⁻	0.06	1	0.06
f CH ₃	0.89	3	2.67
f CH ₂	0.66	15	9.90
f C ₇ H ₇	2.51	1	2.51
F _{bx+1}	-0.90	3	-2.70
F _{bx+2}	-0.60	1	-0.60
F _{bx+3}	-0.45	1	-0.45
F _{bx+4}	-0.35	1	-0.35
F _{bx+5}	-0.30	1	-0.30
F _{bx+6≤}	-0.27	18	-4.86
logK _{ow}			2.48
Exp. logK _{ow}			2.97±0.03

APPENDIX B

GIBB'S FREE FORMATION ENERGY OF QACS

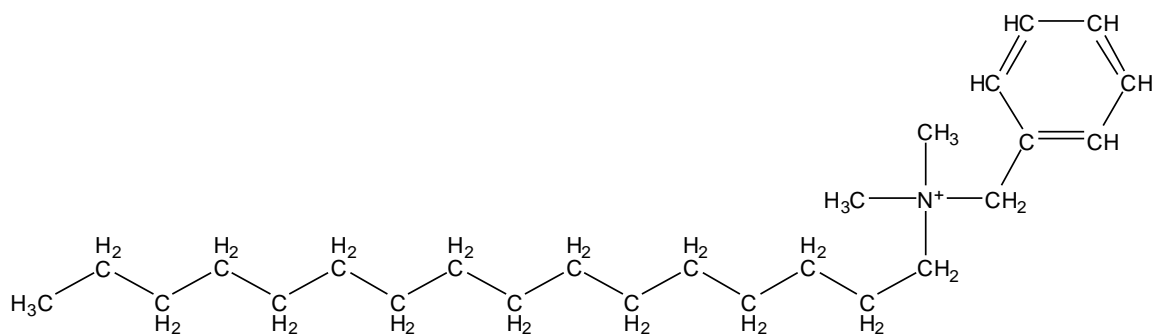


Group/Correction	# of occurrence	Contribution (kcal/mol)	Total contribution (kcal/mol)
Origin	1	-24.7	-24.7
Aromatic ring	1	-6.0	-6.0
-CH ₃	3	8.5	25.5
-CH ₂ -	12	1.7	20.4
>N ⁺ <	1	8.9	8.9
>CH- benzene	5	8.6	43.0
>C- benzene	1	1.1	1.1
ΔG_f⁰			68.2 kcal/mol 285.4 kJ/mol



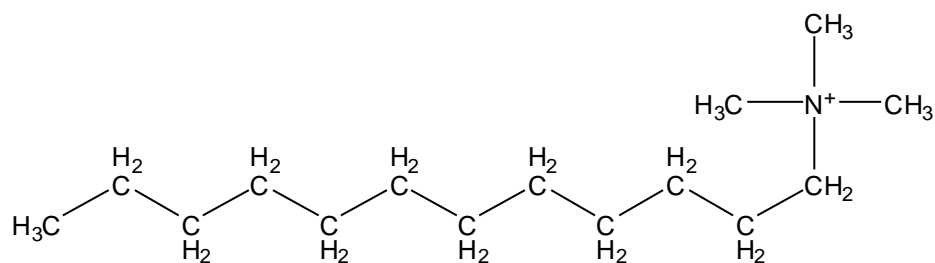
Benzyltetradecyldimethyl ammonium

Group/Correction	# of occurrence	Contribution (kcal/mol)	Total contribution (kcal/mol)
Origin	1	-24.7	-24.7
Aromatic ring	1	-6.0	-6.0
-CH ₃	3	8.5	25.5
-CH ₂ -	14	1.7	23.8
>N ⁺ <	1	8.9	8.9
>CH- benzene	5	8.6	43.0
>C- benzene	1	1.1	1.1
ΔG_f°			71.6 kcal/mol 299.6 kJ/mol



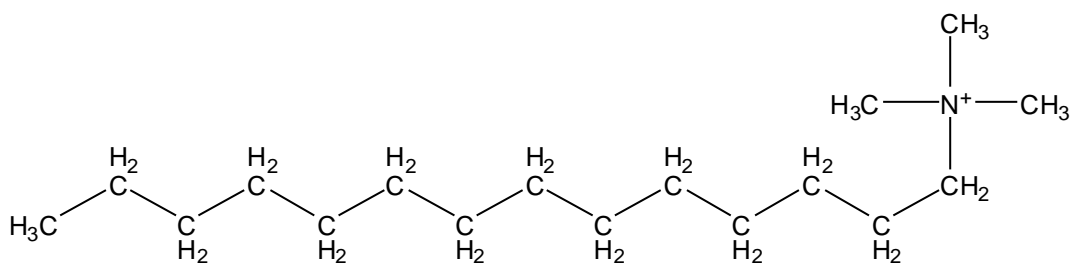
Benzylhexadecyldimethyl ammonium

Group/Correction	# of occurrence	Contribution (kcal/mol)	Total contribution (kcal/mol)
Origin	1	-24.7	-24.7
Aromatic ring	1	-6.0	-6.0
-CH ₃	3	8.5	25.5
-CH ₂ -	16	1.7	27.2
>N ⁺ <	1	8.9	8.9
>CH- benzene	5	8.6	43.0
>C- benzene	1	1.1	1.1
ΔG_f°			75.0 kcal/mol 313.8 kJ/mol



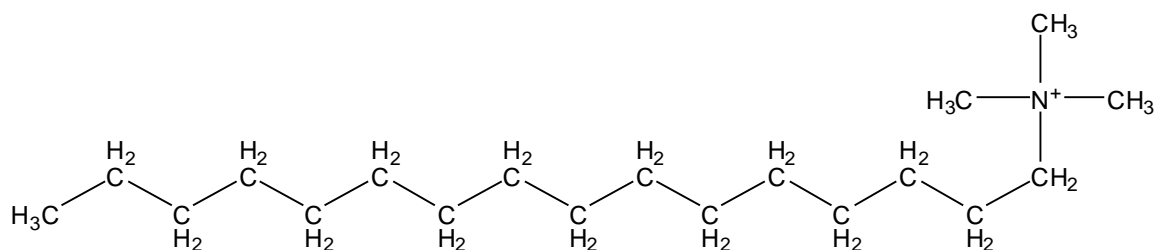
Dodecyltrimethyl ammonium

Group/Correction	# of occurrence	Contribution (kcal/mol)	Total contribution (kcal/mol)
Origin	1	-24.7	-24.7
-CH ₃	4	8.5	34.0
-CH ₂ -	11	1.7	18.7
>N ⁺ <	1	8.9	8.9
ΔG_f⁰			36.9 kcal/mol 154.4 kJ/mol



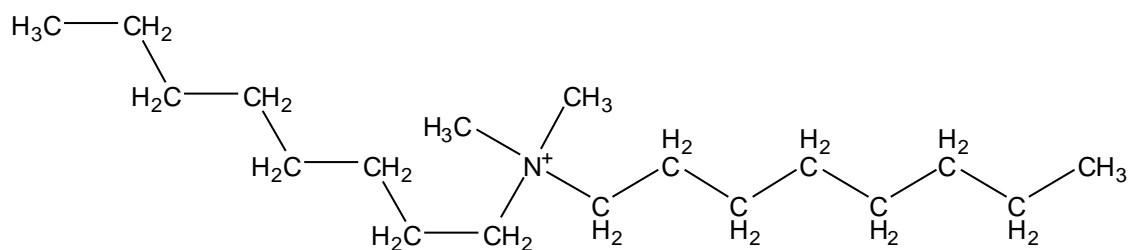
Tetradecyltrimethyl ammonium

Group/Correction	# of occurrence	Contribution (kcal/mol)	Total contribution (kcal/mol)
Origin	1	-24.7	-24.7
-CH ₃	4	8.5	34.0
-CH ₂ -	13	1.7	22.1
>N ⁺ <	1	8.9	8.9
ΔG_f⁰			40.3 kcal/mol 168.6 kJ/mol



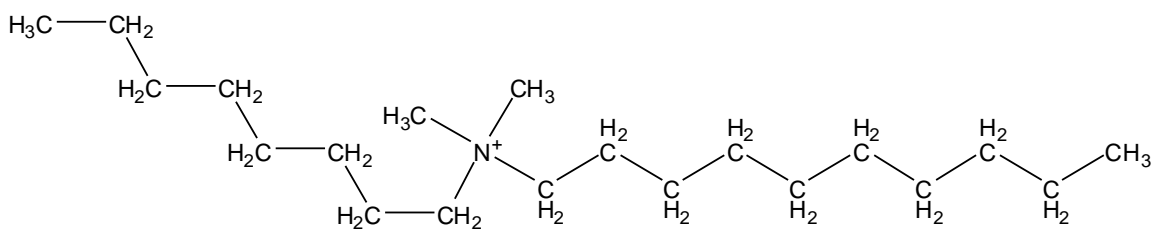
Hexadecyltrimethyl ammonium

Group/Correction	# of occurrence	Contribution (kcal/mol)	Total contribution (kcal/mol)
Origin	1	-24.7	-24.7
-CH ₃	4	8.5	34.0
-CH ₂ -	15	1.7	25.5
>N ⁺ <	1	8.9	8.9
ΔG_f⁰			43.7 kcal/mol 182.8 kJ/mol



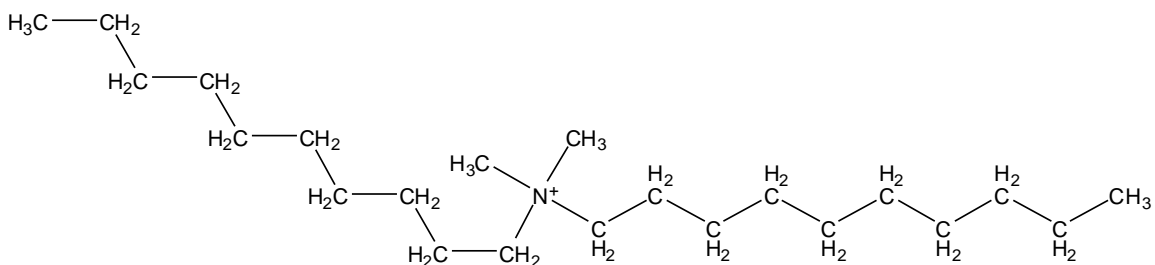
Diocyltrimethyl ammonium

Group/Correction	# of occurrence	Contribution (kcal/mol)	Total contribution (kcal/mol)
Origin	1	-24.7	-24.7
-CH ₃	4	8.5	34.0
-CH ₂ -	14	1.7	23.8
>N ⁺ <	1	8.9	8.9
ΔG_f⁰			42.0 kcal/mol 175.7 kJ/mol



Octyldecyl dimethyl ammonium

Group/Correction	# of occurrence	Contribution (kcal/mol)	Total contribution (kcal/mol)
Origin	1	-24.7	-24.7
-CH ₃	4	8.5	34.0
-CH ₂ -	16	1.7	27.2
>N ⁺ <	1	8.9	8.9
ΔG_f°			45.4 kcal/mol 190.0 kJ/mol



Didecyl dimethyl ammonium

Group/Correction	# of occurrence	Contribution (kcal/mol)	Total contribution (kcal/mol)
Origin	1	-24.7	-24.7
-CH ₃	4	8.5	34.0
-CH ₂ -	18	1.7	30.6
>N ⁺ <	1	8.9	8.9
$\Delta G_f^{0'}$			48.8 kcal/mol 204.2 kJ/mol

REFERENCES

- Altschul, S. F., Gish, W., Miller, W., Myers, E. W., and Lipman, D. J.** 1990. Basic local alignment search tool. *J. Mol. Biol.* **215**:403-410.
- Battersby, N. S., and Wilson, V.** 1989. Survey of the anaerobic biodegradation potential of organic chemicals in digesting sludge. *Appl. Environ. Microbiol.* **55**:433-439.
- Bay, D. C., Rommens, K. L., and Turner, R. J.** 2008. Small multidrug resistance proteins: A multidrug transporter family that continues to grow. *Biochim. Biophys. Acta-Biomem.* **1778**:1814-1838.
- Bayer Corporation.** 2003. Benzyltrimethylammonium chloride (U.S. EPA Document No. 201-14845B).
- Bergstrom, K.** 2001. Cationic Surfactants: Cationic surfactants in paper processing. *In* K. Holmberg (ed.), *Handbook of Applied Surface and Colloid Chemistry*, vol. 1. John Wiley & Sons, Ltd, West Sussex, England.
- Boethling, R. S.** 1994. Environmental aspects of cationic surfactants. *In* J. Cross and E. J. and Singer (ed.), *Cationic Surfactants: Analytical and Biological Evaluation*, vol. 53. Marcel Dekker, Inc. , New York, USA.
- Boll, M., Fuchs, G., and Heider, J.** 2002. Anaerobic oxidation of aromatic compounds and hydrocarbons. *Curr. Opin. Chem. Biol.* **6**:604-611.
- Boyd, S. A., Lee, J. F., and Mortland, M. M.** 1988. Attenuating organic contaminant mobility by soil modification. *Nature* **333**:345-347.
- Brasen, W. R., and Hauser, C. R.** 1954. Hemimellitene - Benzene, 1,2,3-trimethyl. *Org. Synth.* **34**:56-57.
- Callaghan, A. V., Gieg, L. M., Kropp, K. G., Suflita, J. M., and Young, L. Y.** 2006. Comparison of mechanisms of alkane metabolism under sulfate-reducing conditions among two bacterial isolates and a bacterial consortium. *Appl. Environ. Microbiol.* **72**:4274-4282.
- Callaghan, A. V., Wawrik, B., Chadhain, S. M. N., Young, L. Y., and Zylstra, G. J.** 2008. Anaerobic alkane-degrading strain AK-01 contains two alkylsuccinate synthase genes. *Biochem. Biophys. Res. Commun.* **366**:142-148.
- Ceccarelli, D., Salvia, A. M., Sami, J., Cappuccinelli, P., and Colombo, M. M.** 2006. New cluster of plasmid-located class 1 integrons in *Vibrio cholerae* O1 and a *dfrA15* cassette -containing integron in *Vibrio parahaemolyticus* isolated in Angola. *Antimicrob. Agents Chemother.* **50**:2493-2499.

- Chapman, J. S.** 2003. Biocide resistance mechanisms. *Int. Biodeterior. Biodegrad.* **51**:133-138.
- Cho, Y.-G., Bae, H.-S., Yoon, J.-H., Park, Y.-H., Lee, J. M., and Lee, S.-T.** 2002. Isolation and characterization of a novel *Pseudomonas sp.*, strain YG1, capable of degrading pyrrolidine under denitrifying conditions. *FEMS Microbiol. Lett.* **211**:111-115.
- Clara, M., Scharf, S., Scheffknecht, C., and Gans, O.** 2007. Occurrence of selected surfactants in untreated and treated sewage. *Water Res.* **41**:4339-4348.
- Colores, G. M., Macur, R. E., Ward, D. M., and Inskip, W. P.** 2000. Molecular analysis of surfactant-driven microbial population shifts in hydrocarbon-contaminated soil. *Appl. Environ. Microbiol.* **66**:2959-2964.
- Comité Europeen Des Agents De Surface Et De Leurs Intermediaires Organiques (CESIO).** 2004. 6th World Surfactants Congress, Berlin, Germany.
- Corwell, R. K.** 2006. EstimateS: Statistical estimation of species richness and shared species from samples. Version 8. <http://purl.aclcl.org/estimates> (Accessed September 2008).
- Coschigano, P. W., Wehrman, T. S., and Young, L. Y.** 1998. Identification and analysis of genes involved in anaerobic toluene metabolism by strain T1: Putative role of a glycine free radical. *Appl. Environ. Microbiol.* **64**:1650-1656.
- Cowan, C. T., and White, D.** 1958. The mechanism of exchange reactions occurring between sodium montmorillonite and various n-primary aliphatic amine salts. *Trans. Faraday Soc.* **54**:691-697.
- Criddle, W. J., and Thomas, J.** 1981. Pyrolysis-gas chromatography of quaternary ammonium salts in aqueous solution. *J. Anal. Appl. Pyrolysis* **2**:361-368.
- Davidova, I. A., Gieg, L. M., Nanny, M., Kropp, K. G., and Suflita, J. M.** 2005. Stable isotopic studies of n-alkane metabolism by a sulfate-reducing bacterial enrichment culture. *Appl. Environ. Microbiol.* **71**:8174-8182.
- Dean-Raymond, D., and Alexander, M.** 1977. Bacterial metabolism of quaternary ammonium compounds. *Appl. Environ. Microbiol.* **33**:1037-1041.
- Denyer, S. P., and Maillard, J. Y.** 2002. Cellular impermeability and uptake of biocides and antibiotics in Gram-negative bacteria. *J. Appl. Microbiol.* **92**:35S-45S.
- Dery, M.** 2001. Cationic Surfactants: The synthesis and manufacture of cationic surfactants. *In* K. Holmberg (ed.), *Handbook of Applied Surface and Colloid Chemistry*, vol. 1. John Wiley & Sons, Ltd, West Sussex, England.

- Ding, W. H., and Liao, Y. H.** 2001. Determination of alkylbenzyltrimethylammonium chlorides in river water and sewage effluent by solid phase extraction and gas chromatography mass spectrometry. *Anal. Chem.* **73**:36-40.
- Dominguez, A., Fernandez, A., Gonzalez, N., Iglesias, E., and Montenegro, L.** 1997. Determination of critical micelle concentration of some surfactants by three techniques. *J. Chem. Educ.* **74**:1227-1231.
- Drobeck, H. P.** 1994. Current topics on the toxicity of cationic surfactants. *In* J. Cross and E. J. and Singer (ed.), *Cationic Surfactants: Analytical and Biological Evaluation*, vol. 53. Marcel Dekker, Inc. , New York, USA.
- Dubois-Brissonnet, F., Malgrange, C., Guerin-Mechin, L., Heyd, B., and Leveau, J. Y.** 2001. Changes in fatty acid composition of *Pseudomonas aeruginosa* ATCC 15442 induced by growth conditions: consequences of resistance to quaternary ammonium compounds. *Microbios* **106**:97-110.
- Eaton, A. D., Clesceri, L. S., Rice, E. W., Greenberg, A. E., and Franson, M. A. H. (ed.)**. 2005. *Standard Methods for the Examination of Water and Wastewater*, 21 ed. American Public Health Association, American Water Works Association, and Water Environment Federation, Washington, DC.
- Ellis, L. B. M., Hershberger, C. D., and Wackett, L. P.** 2000. The University of Minnesota Biocatalysis/Biodegradation Database: microorganisms, genomics and prediction. *Nucleic Acids Res.* **28**:377-379.
- European Center for Ecotoxicology and Toxicology of Chemicals (ECTOC).** 1993. DHTDMC: Aquatic and Terrestrial Hazard Assessment. European Center for Ecotoxicological and Toxicological Safety Assessment of Chemicals, Brussels, Belgium.
- Federle, T. W., and Schwab, B. S.** 1992. Mineralization of surfactants in anaerobic sediments of a Laundromat wastewater pond. *Water Res.* **26**:123-127.
- Fernandez, P., Alder, A. C., Suter, M. J. F., and Giger, W.** 1996. Determination of the quaternary ammonium surfactant ditallowdimethylammonium in digested sludges and marine sediments by supercritical fluid extraction and liquid chromatography with postcolumn ion-pair formation. *Anal. Chem.* **68**:921-929.
- Fernandez, P., Valls, M., Bayona, J. M., and Albaiges, J.** 1991. Occurrence of cationic surfactants and related products in urban coastal environments. *Environ. Sci. Technol.* **25**:547-550.
- Ferrer, I., and Furlong, E. T.** 2001. Identification of alkyl dimethylbenzylammonium surfactants in water samples by solid-phase extraction followed by ion trap LC/MS and LC/MS/MS. *Environ. Sci. Technol.* **35**:2583-2588.

- Ferrer, I., and Furlong, E. T.** 2002. Accelerated solvent extraction followed by on-line solid-phase extraction coupled to ion trap LC/MS/MS for analysis of benzalkonium chlorides in sediment samples. *Anal. Chem.* **74**:1275-1280.
- Fiddler, W., Wasserman, A. E., Pensaben, J. W., and Doerr, R. C.** 1972. Formation of N-Nitrosodimethylamine from Naturally Occurring Quaternary Ammonium Compounds and Tertiary Amines. *Nature* **236**:307-&.
- Foster, L. J. R., Kwan, B. H., and Vancov, T.** 2004. Microbial degradation of the organophosphate pesticide, Ethion. *FEMS Microbiol. Lett.* **240**:49-53.
- Gaillon, L., Lelievre, J., and Gaboriaud, R.** 1999. Counterion effects in aqueous solutions of cationic surfactants: Electromotive force measurements and thermodynamic model. *J. Colloid Interface Sci.* **213**:287-297.
- Garcia, M. T., Campos, E., Sanchez-Leal, J., and Comelles, F.** 2006. Sorption of alkyl benzyl dimethyl ammonium compounds by activated sludge. *J. Dispersion Sci. Technol.* **27**:739-744.
- Garcia, M. T., Campos, E., Sanchez-Leal, J., and Comelles, F.** 2004. Structure-activity relationships for sorption of alkyl trimethyl ammonium compounds on activated sludge. *Tenside Surfact. Deterg.* **41**:235-239.
- Garcia, M. T., Campos, E., Sanchez-Leal, J., and Ribosa, I.** 1999. Effect of the alkyl chain length on the anaerobic biodegradability and toxicity of quaternary ammonium based surfactants. *Chemosphere* **38**:3473-3483.
- Garcia, M. T., Campos, E., Sanchez-Leal, J., and Ribosa, I.** 2000. Anaerobic degradation and toxicity of commercial cationic surfactants in anaerobic screening tests. *Chemosphere* **41**:705-710.
- Garcia, M. T., Ribosa, I., Guindulain, T., Sanchez-Leal, J., and Vives-Rego, J.** 2001. Fate and effect of monoalkyl quaternary ammonium surfactants in the aquatic environment. *Environ. Pollut.* **111**:169-175.
- Gaze, W. H., Abdousslam, N., Hawkey, P. M., and Wellington, E. M. H.** 2005. Incidence of class 1 integrons in a quaternary ammonium compound-polluted environment. *Antimicrob. Agents Chemother.* **49**:1802-1807.
- Geftic, S. G., Heymann, H., and Adair, F. W.** 1979. 14 year survival of *Pseudomonas cepacia* in a salts solution preserved with benzalkonium chloride. *Appl. Environ. Microbiol.* **37**:505-510.
- Gerhardt, P., Murray, R. G. E., Wood, W. A., and Krieg, N. R.** 1994. *Methods for General and Molecular Bacteriology.* American Society for Microbiology, Washington DC, USA.

- Gibson, J., and Harwood, C. S.** 2002. Metabolic diversity in aromatic compound utilization by anaerobic microbes. *Annu. Rev. Microbiol.* **56**:345-369.
- Gilbert, P., and Moore, L. E.** 2005. Cationic antiseptics: diversity of action under a common epithet. *J. Appl. Microbiol.* **99**:703-715.
- Giolando, S. T., Rapaport, R. A., Larson, R. J., Federle, T. W., Stalmans, M., and Masscheleyn, P.** 1995. Environmental fate and effects of DEEDMAC - A new rapidly biodegradable cationic surfactant for use in fabric softeners. *Chemosphere* **30**:1067-1083.
- Gonzalez-Perez, A., Czapkiewicz, J., Del Castillo, J. L., and Rodriguez, J. R.** 2001. Micellar properties of long-chain alkyldimethylbenzylammonium chlorides in aqueous solutions. *Colloids Surf.* **193**:129-137.
- Grundmann, O., Behrends, A., Rabus, R., Amann, J., Halder, T., Heider, J., and Widdel, F.** 2008. Genes encoding the candidate enzyme for anaerobic activation of n-alkanes in the denitrifying bacterium, strain HxN1. *Environ. Microbiol.* **10**:376-385.
- Guerin-Mechin, L., Dubois-Brissonnet, F., Heyd, B., and Leveau, J. Y.** 1999. Specific variations of fatty acid composition of *Pseudomonas aeruginosa* ATCC 15442 induced by quaternary ammonium compounds and relation with resistance to bactericidal activity. *J. Appl. Microbiol.* **87**:735-742.
- Guerin-Mechin, L., Dubois-Brissonnet, F., Heyd, B., and Leveau, J. Y.** 2000. Quaternary ammonium compound stresses induce specific variations in fatty acid composition of *Pseudomonas aeruginosa*. *Int. J. Food Microbiol.* **55**:157-159.
- Gustavsson, B.** 2001. Cationic Surfactants: Cationic surfactants in agricultural formulations. *In* K. Holmberg (ed.), *Handbook of Applied Surface and Colloid Chemistry*, vol. 1. John Wiley & Sons, Ltd, West Sussex, England.
- Hall, R. M., and Collis, C. M.** 1998. Antibiotic resistance in gram-negative bacteria: the role of gene cassettes and integrons. *Drug Resistance Updates* **1**:109-119.
- Hansch, C., and Leo, A.** 1979. Substituent constants for correlation analysis in chemistry and biology. John Wiley & Sons, Inc., Toronto, Canada.
- Hansch, C., Leo, A., and Hoekman, D. H.** 1995. Exploring QSAR. American Chemical Society, Washington, DC.
- Haskins, N. J., and Mitchell, R.** 1991. Thermal degradation of some benzyltrialkylammonium salts using pyrolysis-gas chromatography mass spectrometry. *Analyst* **116**:901-903.
- Heider, J.** 2007. Adding handles to unhandy substrates: anaerobic hydrocarbon activation mechanisms. *Curr. Opin. Chem. Biol.* **11**:188-194.

- Heider, J., Spormann, A. M., Beller, H. R., and Widdel, F.** 1998. Anaerobic bacterial metabolism of hydrocarbons. *FEMS Microbiol. Rev.* **22**:459-473.
- Hernandez, M., Villalobos, P., Morgante, V., Gonzalez, M., Reiff, C., Moore, E., and Seeger, M.** 2008. Isolation and characterization of a novel simazine-degrading bacterium from agricultural soil of central Chile, *Pseudomonas* sp. MHP41. *FEMS Microbiol. Lett.* **286**:184-190.
- Hiemenz, P. C., and Rajagopalan, R.** 1997. Principles of colloid and surface chemistry, 3rd ed. Marcel Dekker, Inc., Basel, NY.
- Higgins, D., Thompson, J., Gibson, T., Thompson, J. D., Higgins, D. G., and Gibson, T. J.** 1994. CLUSTAL W: improving the sensitivity of progressive multiple sequence alignment through sequence weighting, position-specific gap penalties and weight matrix choice. *Nucleic Acids Res.* **22**:4673-4680.
- Himo, F.** 2002. Catalytic mechanism of benzylsuccinate synthase, a theoretical study. *J. Phys. Chem. B* **106**:7688-7692.
- Himo, F.** 2005. C-C bond formation and cleavage in radical enzymes, a theoretical perspective. *Biochimica Et Biophysica Acta-Bioenergetics* **1707**:24-33.
- HMSO.** 1981. Analysis of Surfactants in Waters, Wastewaters and Sludges, Methods for the Examination of Waters and Associated Materials, SCA, Her Majesty's Stationery Office, London, UK.
- Hoey, M.** 2001. Cationic Surfactants: Cationic surfactants in organoclays. *In* K. Holmberg (ed.), *Handbook of Applied Surface and Colloid Chemistry*, vol. 1. John Wiley & Sons, Ltd, West Sussex, England.
- Hou, B. K., Wackett, L. P., and Ellis, L. B. M.** 2003. Microbial pathway prediction: A functional group approach. *J. Chem. Inf. Comput. Sci.* **43**:1051-1057.
- Huang, J. Z., O'Toole, P. W., Shen, W., Amrine-Madsen, H., Jiang, X. H., Lobo, N., Palmer, L. A., Voelker, L., Fan, F., Gwynn, M. N., and McDevitt, D.** 2004. Novel chromosomally encoded multidrug efflux transporter MdeA in *Staphylococcus aureus*. *Antimicrob. Agents Chemother.* **48**:909-917.
- Ishikawa, S., Matsumura, Y., Yoshizako, F., and Tsuchido, T.** 2002. Characterization of a cationic surfactant-resistant mutant isolated spontaneously from *Escherichia coli*. *J. Appl. Microbiol.* **92**:261-268.
- Ismail, Z. Z., Tezel, U., and Pavlostathis, S. G.** 2008. Adsorption of quaternary ammonium compounds on municipal biosolids. *Water Res.* **(Submitted)**.
- Jalali-Heravi, M., and Konouz, E.** 2003. Multiple linear regression modeling of the critical micelle concentration of alkyltrimethylammonium and alkylpyridinium salts. *Journal Of Surfactants And Detergents* **6**:25-30.

- Josephson, J.** 2006. The micro "Resistome". *Environ. Sci. Technol.* **40**:6531-6534.
- Kaech, A., and Egli, T.** 2001. Isolation and characterization of a *Pseudomonas putida* strain able to grow with trimethyl-1,2-dihydroxy-propyl-ammonium as sole source of carbon, energy and nitrogen. *Syst. Appl. Microbiol.* **24**:252-261.
- Kametani, T., Kigasawa, K., Hiiragi, M., Wagatsum.N, and Wakisaka, K.** 1969. Novel debenzoylation of quaternary ammonium salts with thiophenol. *Tetrahedron Lett.*:635-&.
- Kim, S. G., Bae, H. S., and Lee, S. T.** 2001. A novel denitrifying bacterial isolate that degrades trimethylamine both aerobically and anaerobically via two different pathways. *Arch. Microbiol.* **176**:271-277.
- King, G. M.** 1984. Metabolism Of Trimethylamine, Choline, And Glycine Betaine By Sulfate-Reducing And Methanogenic Bacteria In Marine-Sediments. *Appl. Environ. Microbiol.* **48**:719-725.
- Knox, W. E., Auerbach, V. H., Zarudnaya, K., and Spirtes, M.** 1949. The Action Of Cationic Detergents On Bacteria And Bacterial Enzymes. *J. Bacteriol.* **58**:443-452.
- Kopecky, F.** 1996. Micellization and other associations of amphiphilic antimicrobial quaternary ammonium salts in aqueous solutions. *Pharmazie* **51**:135-144.
- Kreuzinger, N., Fuerhacker, M., Scharf, S., Uhl, M., Gans, O., and Grillitsch, B.** 2007. Methodological approach towards the environmental significance of uncharacterized substances-quaternary ammonium compounds as an example. *Desalination* **215**:209-222.
- Krieger, C. J., Roseboom, W., Albracht, S. P. J., and Spormann, A. M.** 2001. A stable organic free radical in anaerobic benzylsuccinate synthase of *Azoarcus* sp strain T. *J. Biol. Chem.* **276**:12924-12927.
- Kroon, A. G. M., and van Ginkel, C. G.** 2001. Complete mineralization of dodecyldimethylamine using a two-membered bacterial culture. *Environ. Microbiol.* **3**:131-136.
- Kummerer, K., Eitel, A., Braun, U., Hubner, P., Daschner, F., Mascart, G., Milandri, M., Reinthaler, F., and Verhoef, J.** 1997. Analysis of benzalkonium chloride in the effluent from European hospitals by solid-phase extraction and high-performance liquid chromatography with post-column ion-pairing and fluorescens detection. *J. Chromatogr. A* **774**:281-286.
- Larson, R. J., and Schaeffer, S. L.** 1982. A Rapid Method for Determining the Toxicity of Chemicals to Activated-Sludge. *Water Res.* **16**:675-680.
- Leal, J. S., Gonzalez, J. J., Kaiser, K. L. E., Palabrica, V. S., Comelles, F., and**

- Garcia, M. T.** 1994. On the toxicity and biodegradation of cationic surfactants. *Acta Hydroch. Hydrob.* **22**:13-18.
- Lewis, M. A.** 1991. Chronic And Sublethal Toxicities Of Surfactants To Aquatic Animals - A Review And Risk Assessment. *Water Res.* **25**:101-113.
- Lianos, P., Lang, J., and Zana, R.** 1983. Fluorescence probe study of the effect of concentration on the state of aggregation of dodecylalkyldimethylammonium bromides and dialkyldimethylammonium chlorides in aqueous solution. *J. Colloid Interface Sci.* **91**:276-279.
- Liffourrena, A. S., Lopez, F. G., Salvano, M. A., Domenech, C. E., and Lucchesi, G. I.** 2008. Degradation of tetradecyltrimethylammonium by *Pseudomonas putida* A ATCC 12633 restricted by accumulation of trimethylamine is alleviated by addition of Al³⁺ ions. *J. Appl. Microbiol.* **104**:396-402.
- Loughlin, M. F., Jones, M. V., and Lambert, P. A.** 2002. *Pseudomonas aeruginosa* cells adapted to benzalkonium chloride show resistance to other membrane-active agents but not to clinically relevant antibiotics. *J. Antimicrob. Chemother.* **49**:631-639.
- Maduagwu, E. N.** 1985. Nitrosation of quaternary ammonium compounds invivo in the Wistar rat. *Xenobiotica* **15**:1061-1068.
- Maillard, J. Y.** 2002. Bacterial target sites for biocide action. *J. Appl. Microbiol.* **92**:16S-27S.
- Maillard, J. Y.** 2007. Bacterial resistance to biocides in the healthcare environment: should it be of genuine concern? *J. Hosp. Infect.* **65**:60-72.
- Martinez, R. J., Mills, H. J., Story, S., and Sobczyk, P. A.** 2006. Prokaryotic diversity and metabolically active microbial populations in sediments from an active mud volcano in the Gulf of Mexico. *Environ. Microbiol.* **8**:1783-1796.
- Martinez-Carballo, E., Gonzalez-Barreiro, C., Sitka, A., Kreuzinger, N., Scharf, S., and Gans, O.** 2007. Determination of selected quaternary ammonium compounds by liquid chromatography with mass spectrometry. Part II. Application to sediment and sludge samples in Austria. *Environ. Pollut.* **146**:543-547.
- Martinez-Carballo, E., Sitka, A., Gonzalez-Barreiro, C., Kreuzinger, N., Furhacker, M., Scharf, S., and Gans, O.** 2007. Determination of selected quaternary ammonium compounds by liquid chromatography with mass spectrometry. Part I. Application to surface, waste and indirect discharge water samples in Austria. *Environ. Pollut.* **145**:489-496.
- Merino, F., Rubio, S., and Perez-Bendito, D.** 2003. Solid-phase extraction of amphiphiles based on mixed hemimicelle/admicelle formation: Application to the

concentration of benzalkonium surfactants in sewage and river water. *Anal. Chem.* **75**:6799-6806.

- Meylan, W. M., and Howard, P. H.** 1995. Atom fragment contribution method for estimating octanol-water partition-coefficients. *J. Pharm. Sci.* **84**:83-92.
- Nagai, K., Murata, T., Ohta, S., Zenda, H., Ohnishi, M., and Hayashi, T.** 2003. Two different mechanisms are involved in the extremely high-level benzalkonium chloride resistance of a *Pseudomonas fluorescens* strain. *Microbiol. Immunol.* **47**:709-715.
- Nalecz-Jawecki, G., Grabinska-Sota, E., and Narkiewicz, P.** 2003. The toxicity of cationic surfactants in four bioassays. *Ecotoxicol. Environ. Saf.* **54**:87-91.
- Neill, A. R., Grime, D. W., and Dawson, R. M. C.** 1978. Conversion Of Choline Methyl-Groups Through Trimethylamine Into Methane In Rumen. *Biochem. J.* **170**:529-535.
- Neu, T. R.** 1996. Significance of bacterial surface-active compounds in interaction of bacteria with interfaces. *Microbiol. Rev.* **60**:151-166.
- Ng, L. K., Hupe, M., and Harris, A. G.** 1986. Direct gas chromatographic method for determining the homolog composition of benzalkonium chlorides. *J. Chromatogr.* **351**:554-559.
- Nishihara, T., Okamoto, T., and Nishiyama, N.** 2000. Biodegradation of didecyldimethylammonium chloride by *Pseudomonas fluorescens* TN4 isolated from activated sludge. *J. Appl. Microbiol.* **88**:641-647.
- Nishiyama, N., and Nishihara, T.** 2002. Biodegradation of dodecyltrimethylammonium bromide by *Pseudomonas fluorescens* F7 and F2 isolated from activated sludge. *Microbes Environ.* **17**:164-169.
- Nishiyama, N., Toshima, Y., and Ikeda, Y.** 1995. Biodegradation of alkyltrimethylammonium salts in activated sludge. *Chemosphere* **30**:593-603.
- Nye, J. V., Guerin, W. F., and Boyd, S. A.** 1994. Heterotrophic activity of microorganisms in soils treated with quaternary ammonium compounds. *Environmental Science & Technology* **28**:944-951.
- Organization for Economic Co-operation and Development (OECD).** 2006. Section 1: Physical-Chemical properties - Test No. 123: Partition Coefficient (1-Octanol/Water): Slow-Stirring Method OECD Guidelines for the Testing of Chemicals. Organization for Economic Co-operation and Development.
- Organization for Economic Co-operation and Development (OECD).** 2008. OECD Application Toolbox.

- Pagnier, I., Raoult, D., and La Scola, B.** 2008. Isolation and identification of amoeba-resisting bacteria from water in human environment by using an *Acanthamoeba* polyphaga co-culture procedure. *Environ. Microbiol.* **10**:1135-1144.
- Partridge, S. R., Brown, H. J., and Hall, R. A.** 2002. Characterization and movement of the class 1 integron known as Tn2521 and Tn1405. *Antimicrob. Agents Chemother.* **46**:1288-1294.
- Patrauchan, M. A., and Oriel, P. J.** 2003. Degradation of benzyldimethylalkylammonium chloride by *Aeromonas hydrophila* sp K. *J. Appl. Microbiol.* **94**:266-272.
- Poole, K.** 2002. Mechanisms of bacterial biocide and antibiotic resistance. *J. Appl. Microbiol.* **92**:55S-64S.
- Poole, K.** 2005. Efflux-mediated antimicrobial resistance. *J. Antimicrob. Chemother.* **56**:20-51.
- Pruden, A., Pei, R. T., Storteboom, H., and Carlson, K. H.** 2006. Antibiotic resistance genes as emerging contaminants: Studies in northern Colorado. *Environ. Sci. Technol.* **40**:7445-7450.
- Pruesse, E., Quast, C., Knittel, K., Fuchs, B. M., Ludwig, W., Peplies, J., and Glockner, F. O.** 2007. SILVA: a comprehensive online resource for quality checked and aligned ribosomal RNA sequence data compatible with ARB. *Nucl. Acids Res.* **35**:7188-7196.
- Putman, M., van Veen, H. W., and Konings, W. N.** 2000. Molecular properties of bacterial multidrug transporters. *Microbiol. Mol. Biol. Rev.* **64**:672-693.
- Qin, Y., Zhang, G. Y., Kang, B. A., and Zhao, Y. M.** 2005. Primary aerobic biodegradation of cationic and amphoteric surfactants. *Journal of Surfactants and Detergents* **8**:55-58.
- Reynolds, L., Blok, J., Demorsier, A., Gerike, P., Wellens, H., and Bontinck, W. J.** 1987. Evaluation of the Toxicity of Substances to Be Assessed for Biodegradability. *Chemosphere* **16**:2259-2277.
- Rittmann, B. E., and McCarty, P. L.** 2001. *Environmental Biotechnology: Principles and Applications*. McGraw-Hill, Boston.
- Roberts, D. W., and Costello, J.** 2003. QSAR and mechanism of action for aquatic toxicity of cationic surfactants. *QSAR* **22**:220-225.
- Rodriguez, J. R., Gonzalez-Perez, A., Del Castillo, J. L., and Czapkiewicz, J.** 2002. Thermodynamics of micellization of alkyl dimethylbenzylammonium chlorides in aqueous solutions. *J. Colloid Interface Sci.* **250**:438-443.

- Ross, S. D., Finkelstein, M., and Petersen, R. C.** 1960. Rates, products and salt effects in the reactions of benzyldimethylanilinium ion with ethoxide ion in ethanol. *J. Am. Chem. Soc.* **82**:5335-5339.
- Ross, S. D., Finkelstein, M., and Petersen, R. C.** 1961. Changes in reaction order due to ion association in the reaction of benzyldimethylanilinium ion and thiocyanate Ion. *J. Am. Chem. Soc.* **83**:4853-4858.
- Saitou, N., and Nei, M.** 1987. The neighbor-joining method: A new method for reconstructing phylogenetic trees. *Mol. Biol. Evol.* **4**:406-425.
- Schluter, A., Szczepanowski, R., Puhler, A., and Top, E. M.** 2007. Genomics of IncP-1 antibiotic resistance plasmids isolated from wastewater treatment plants provides evidence for a widely accessible drug resistance gene pool. *FEMS Microbiol. Rev.* **31**:449-477.
- Schmitt, T. M.** 1994. Environmental Analysis. *In* J. Cross and E. J. Singer (ed.), *Analysis of Surfactants*, 2 ed, vol. 96. Marcel Dekker, Inc., New York, USA.
- Schwarzenbach, R. P., Gschwend, P. M., and Imboden, D. M.** 2003. *Environmental Organic Chemistry*, 2 ed. John Wiley & Sons, Inc., Hoboken, NJ.
- Scott, M. J., and Jones, M. N.** 2000. The biodegradation of surfactants in the environment. *Biochim. Biophys. Acta-Biomembranes* **1508**:235-251.
- Seifert, K., and Domka, F.** 2005. Inhibiting effect of surfactants and heavy metal ions on the denitrification process. *Polish Journal of Environmental Studies* **14**:87-93.
- Sikkema, J., Debont, J. A. M., and Poolman, B.** 1995. Mechanisms of Membrane Toxicity of Hydrocarbons. *Microbiol. Rev.* **59**:201-222.
- Singer, R. S., Ward, M. P., and Maldonado, G.** 2006. Opinion - Can landscape ecology untangle the complexity of antibiotic resistance? *Nature Rev. Microbiol.* **4**:943-952.
- Smith, K., Gemmell, C. G., and Hunter, I. S.** 2008. The association between biocide tolerance and the presence or absence of *qac* genes among hospital-acquired and community-acquired MRSA isolates. *J. Antimicrob. Chemother.* **61**:78-84.
- Smith, M. B., and March, J.** 2007. *March's Advanced Organic Chemistry: Reactions, mechanisms, and structure*, 6 ed. John Wiley & Sons, Inc., Hoboken, NJ.
- Spormann, A. M., and Widdel, F.** 2000. Metabolism of alkylbenzenes, alkanes, and other hydrocarbons in anaerobic bacteria. *Biodegradation* **11**:85-105.
- Steichen, D. S.** 2001. Cationic Surfactants. *In* K. Holmberg (ed.), *Handbook of Applied Surface and Colloid Chemistry*, vol. 1. John Wiley & Sons, Ltd, West Sussex, England.

- Stoer, J., and Bulirsch, R.** 2002. Introduction to Numerical Analysis. Springer, New York.
- Strevett, K., Davidova, I., and Suflita, J. M.** 2002. A comprehensive review of the screening methodology for anaerobic biodegradability of surfactants. *Rev. Environ. Sci. Biotechnol.* **1**:143-167.
- Suflita, J. M., Davidova, I. A., Gieg, L. M., Nanny, M., and Prince, R. C.** 2004. Anaerobic hydrocarbon biodegradation and the prospects for microbial enhanced energy production, p. 283-305, *Petroleum Biotechnology: Developments and Perspectives*, vol. 151. Elsevier Science Bv, Amsterdam.
- Sun, H. F., Takata, A., Hata, N., Kasahara, I., and Taguchi, S.** 2003. Transportation and fate of cationic surfactant in river water. *J. Environ. Monitor.* **5**:891-895.
- Sutterlin, H., Alexy, R., and Kummerer, K.** 2008. The toxicity of the quaternary ammonium compound benzalkonium chloride alone and in mixtures with other anionic compounds to bacteria in test systems with *Vibrio fischeri* and *Pseudomonas putida*. *Ecotoxicol. Environ. Saf.* **71**:498-505.
- Sutterlin, H., Trittler, R., Bojanowski, S., Stadbauer, E. A., and Kummerer, K.** 2007. Fate of benzalkonium chloride in a sewage sludge low temperature conversion process investigated by LC-LC/ESI-MS/MS. *Clean* **35**:81-87.
- Suzuki, S., Nakamura, Y., Kaneko, M., Mori, K., and Watanabe, Y.** 1989. Analysis of benzalkonium chlorides by gas chromatography. *J. Chromatogr.* **463**:188-191.
- Syracuse Research Corporation.** 2007. Estimation Program Interface Suite (EPISuite) v. 3.20, Syracuse, NY.
- Szaleniec, M., Witko, M., and Heider, J.** 2008. Quantum chemical modelling of the C-H cleavage mechanism in oxidation of ethylbenzene and its derivatives by ethylbenzene dehydrogenase. *Journal of Molecular Catalysis a-Chemical* **286**:128-136.
- Tabata, A., Nagamune, H., Maeda, T., Murakami, K., Miyake, Y., and Kourai, H.** 2003. Correlation between resistance of *Pseudomonas aeruginosa* to quaternary ammonium compounds and expression of outer membrane protein OprR. *Antimicrob. Agents Chemother.* **47**:2093-2099.
- Takenaka, S., Tonoki, T., Taira, K., Murakami, S., and Aoki, K.** 2007. Adaptation of *Pseudomonas sp* strain 7-6 to quaternary ammonium compounds and their degradation via dual pathways. *Appl. Environ. Microbiol.* **73**:1797-1802.
- Tamura, K., Dudley, J., Nei, M., and Kumar, S.** 2007. MEGA4: Molecular Evolutionary Genetics Analysis (MEGA) software version 4.0. *Mol. Biol. Evol.* **24**:1596-1599.

- Tang, D.** 2001. Cationic Surfactants: Cationic surfactants in personal care. *In* K. Holmberg (ed.), Handbook of Applied Surface and Colloid Chemistry, vol. 1. John Wiley & Sons, Ltd, West Sussex, England.
- Tezel, U., Pierson, J. A., and Pavlostathis, S. G.** 2006. Fate and effect of quaternary ammonium compounds on a mixed methanogenic culture. *Water Res.* **40**:3660-3668.
- Tezel, U., Pierson, J. A., and Pavlostathis, S. G.** 2007. Effect of polyelectrolytes and quaternary ammonium compounds on the anaerobic biological treatment of poultry processing wastewater. *Water Res.* **41**:1334-1342.
- Thauer, R. K., Jungermann, K., and Decker, K.** 1977. Energy conservation in chemotrophic anaerobic bacteria *Bacteriol. Rev.* **41**:100-180.
- Tiedink, J.** 2001. Cationic Surfactants: Cationic surfactants in biocides. *In* K. Holmberg (ed.), Handbook of Applied Surface and Colloid Chemistry, vol. 1. John Wiley & Sons, Ltd, West Sussex, England.
- Topping, B. W., and Waters, J.** 1982. The monitoring of cationic surfactants in sewage treatment plants. *Tenside Detergents* **19**:164-169.
- Tubbing, D. M. J., and Admiraal, W. I. M.** 1991. Inhibition of Bacterial and Phytoplanktonic Metabolic-Activity in the Lower River Rhine by Ditolowdimethylammonium Chloride. *Appl. Environ. Microbiol.* **57**:3616-3622.
- Tugtas, A. E., and Pavlostathis, S. G.** 2007. Effect of sulfide on nitrate reduction in mixed methanogenic cultures. *Biotechnol. Bioeng.* **97**:1448-1459.
- Tugtas, A. E., and Pavlostathis, S. G.** 2007. Electron donor effect on reduction pathway and kinetics in a mixed methanogenic culture. *Biotechnol. Bioeng.* **98**:756-763.
- U.S. Environmental Protection Agency.** 2006. High Production Volume Challenge Program. U.S. EPA Office of Pollution Prevention and Toxics, Washington, DC. (<http://www.epa.gov/chemrtk/pubs/general/hazchem.htm>) (Accessed January 2007).
- U.S. Environmental Protection Agency.** 2006. Reregistration eligibility decision for alkyl dimethyl benzyl ammonium chloride (ADBAC).
- Utsunomiya, A., Watanuki, T., Matsushita, K., and Tomita, I.** 1997. Toxic effects of linear alkylbenzene sulfonate, quaternary alkylammonium chloride and their complexes on *Dunaliella* sp. and *Chlorella pyrenoidosa*. *Environ. Toxicol. Chem.* **16**:1247-1254.
- Valls, M., Bayona, J. M., Albaiges, J.** 1989. Use of trialkylamines as an indicator of urban sewage in sludges, coastal waters and sediments. *Nature* **337**:722-724.

- van Beilen, J. B., and Funhoff, E. G.** 2005. Expanding the alkane oxygenase toolbox: new enzymes and applications. *Curr. Opin. Biotechnol.* **16**:308-314.
- van Ginkel, C. G.** 1996. Complete degradation of xenobiotic surfactants by consortia of aerobic microorganisms. *Biodegradation* **7**:151-164.
- van Ginkel, C. G.** 2004. Biodegradation of cationic surfactants. *In* U. Zoller (ed.), *Handbook of Detergents Part B: Environmental Impact*, vol. 121. Marcel Dekker, Inc., New York, USA.
- van Ginkel, C. G., and Kolvenbach, M.** 1991. Relations between the Structure of Quaternary Alkyl Ammonium-Salts and Their Biodegradability. *Chemosphere* **23**:281-289.
- van Ginkel, C. G., Vandijk, J. B., and Kroon, A. G. M.** 1992. Metabolism of hexadecyltrimethylammonium chloride in *Pseudomonas* Strain-B1. *Appl. Environ. Microbiol.* **58**:3083-3087.
- Van Hamme, J. D., Singh, A., and Ward, O. P.** 2003. Recent advances in petroleum microbiology. *Microbiol. Mol. Biol. Rev.* **67**:503-549.
- Ventullo, R. M., and Larson, R. J.** 1986. Adaptation of aquatic microbial communities to quaternary ammonium compounds. *Appl. Environ. Microbiol.* **51**:356-361.
- Wackett, L. P., and Ellis, L. B. M.** 1999. Predicting biodegradation. *Environ. Microbiol.* **1**:119-124.
- Washer, C. E., and Edwards, E. A.** 2007. Identification and expression of benzylsuccinate synthase genes in a toluene-degrading methanogenic consortium. *Appl. Environ. Microbiol.* **73**:1367-1369.
- Weber, D. J., Rutala, W. A., and Sickbert-Bennett, E. E.** 2007. Outbreaks associated with contaminated antiseptics and disinfectants. *Antimicrob. Agents Chemother.* **51**:4217-4224.
- Wee, V. T.** 1984. Determination Of Cationic Surfactants In Wastewater And River Water. *Water Res.* **18**:223-225.
- Wee, V. T., and Kennedy, J. M.** 1982. Determination of Trace Levels of Quaternary Ammonium-Compounds in River Water by Liquid-Chromatography with Conductometric Detection. *Anal. Chem.* **54**:1631-1633.
- Westaway, K. C., and Poirier, R. A.** 1975. Isotope effects in nucleophilic substitution reactions. I. The mechanism of the reaction of phenylbenzyltrimethylammonium ion with thiophenoxide ion. *Canadian Journal of Chemistry-Revue Canadienne De Chimie* **53**:3216-3226.

- Widdel, F., and Rabus, R.** 2001. Anaerobic biodegradation of saturated and aromatic hydrocarbons. *Curr. Opin. Biotechnol.* **12**:259-276.
- Winderl, C., Schaefer, S., and Lueders, T.** 2007. Detection of anaerobic toluene and hydrocarbon degraders in contaminated aquifers using benzylsuccinate synthase (bssA) genes as a functional marker. *Environ. Microbiol.* **9**:1035-1046.
- World Health Organization (WHO).** 2000. WHO Annual Report on Infectious Disease: Overcoming Antimicrobial Resistance. Geneva, Switzerland. (<http://www.who.int/infectious-disease-report/2000>).
- Xue, Y. Y., Hieda, Y., Saito, Y., Nomura, T., Fujihara, J., Takayama, K., Kimura, K., and Takeshita, H.** 2004. Distribution and disposition of benzalkonium chloride following various routes of administration in rats. *Toxicol. Lett.* **148**:113-123.
- Yang, J.** 2007. Fate and Effect of Alkyl Benzyl Dimethyl Ammonium Chloride in Mixed Aerobic and Nitrifying Cultures. MS Thesis. Georgia Institute of Technology, Atlanta, GA.
- Ying, G. G.** 2006. Fate, behavior and effects of surfactants and their degradation products in the environment. *Environ. Int.* **32**:417-431.
- Ying, G.-G.** 1999. Distribution, behavior, fate, and effects of surfactants and their degradation products in the environment. *In* U. Zoller (ed.), Handbook of Detergents Part B: Environmental Impact, vol. 121. Marcel Dekker, Inc., New York, USA.
- Zachwieja, J.** 2001. Cationic Surfactants: Cationic surfactants in fabric softening. *In* K. Holmberg (ed.), Handbook of Applied Surface and Colloid Chemistry, vol. 1. John Wiley & Sons, Ltd, West Sussex, England.
- Zumft, W. G.** 1997. Cell biology and molecular basis of denitrification. *Microbiol. Mol. Biol. Rev.* **61**:533-616.

VITA

The author was born in Luleburgaz, Turkey on October 14, 1978. In 2001, he graduated with *Summa Cum Laude* from Middle East Technical University, where he received the bachelor's degree in Environmental Engineering. In 2003 he received his Master's degree in Environmental Engineering from the same university. The author worked on the treatment of gaseous trichloroethylene by sequential biotic and abiotic removal mechanisms under supervisions of Dr. Goksel N. Demirer and Dr. Sibel Uludag-Demirer. After completing his Master's degree in 2003, he joined Dr. Pavlostathis' research group in the School of Civil and Environmental Engineering at the Georgia Institute of Technology in Atlanta, GA, USA. He performed research on the fate and effect of quaternary ammonium compounds in biological systems, anaerobic digestion of municipal sludges and occurrence and anaerobic biotransformation of nitrosamines in the biological treatment systems. The author received his Ph. D. degree in May 2009.